

Copyright
by
Christopher Scott Williams
2011

**The Thesis Committee for Christopher Scott Williams
Certifies that this is the approved version of the following thesis:**

**Strut-and-Tie Model
Design Examples for Bridges**

**APPROVED BY
SUPERVISING COMMITTEE:**

Supervisor:

Oguzhan Bayrak

Wassim M. Ghannoum

**Strut-and-Tie Model
Design Examples for Bridge**

by

Christopher Scott Williams, B.S.

Thesis

Presented to the Faculty of the Graduate School of

The University of Texas at Austin

in Partial Fulfillment

of the Requirements

for the Degree of

Master of Science in Engineering

The University of Texas at Austin

December 2011

Dedication

To my mom and dad for their never-ending support

Acknowledgements

Many individuals deserve much gratitude for their contributions to this thesis. First, I would like to express deep appreciation to my advisor, Dr. Oguzhan Bayrak, for his insight and advice that continuously pointed me in the right direction. His experience and knowledge offered during our countless discussions resulted in the best solutions for the matters at hand. Not only has he contributed to the project and this thesis, his efforts have undoubtedly pushed me to become a better engineer and will continue to affect me throughout my future career.

The work presented in this thesis was funded by the Texas Department of Transportation. My gratitude extends to those at TxDOT who have made this project possible. The Project Director, Dean Van Landuyt, deserves much appreciation for his recommendations that benefitted this thesis. The time and input offered by John Vogel is also worthy of many thanks.

My endless gratitude must be expressed to Dean Deschenes for his significant contributions to the content and quality of this thesis. He was always willing to go above and beyond the call of duty to offer his time and ideas. I have unquestionably gained knowledge and improved my technical writing skills due to his input. I also thank Dr. Wassim Ghannoum for sacrificing his time to contribute to this thesis. Furthermore, my fellow students at Ferguson Structural Engineering Laboratory deserve thanks for always being available to bounce ideas around and for simply creating a friendly atmosphere at the lab, maintaining a healthy balance between the advancement of knowledge and much needed socialization. I also send my gratitude to FSEL staff members Barbara Howard and Jessica Harbison for ensuring the lab always functioned smoothly.

Too much appreciation could never be expressed to my loving family. My mother and father have always supported me 100 percent as I pursue my goals. Their lifestyle and work ethic have set the standard toward which I can strive. They have exemplified the meaning of true success, contentment found only in God. I also thank

my sister, Ali, for her encouragement and for keeping a close relationship with me despite the distance. Additionally, I must express gratitude to my friends in Austin, those who have become part of my Austin family. I could always count on them for prayers and support through the toughest and busiest moments of my graduate life.

Most importantly, I would like to thank God for leading me and helping me find success in my studies. He gives me the true reason to strive forward day by day. Blessings I have seen in my life while in Austin have been more than coincidence. Ultimately, all thanks goes to Him.

Abstract

Strut-and-Tie Model Design Examples for Bridges

Christopher Scott Williams, M.S.E.

The University of Texas at Austin, 2011

Supervisor: Oguzhan Bayrak

Strut-and-tie modeling (STM) is a versatile, lower-bound (i.e. conservative) design method for reinforced concrete structural components. Uncertainty expressed by engineers related to the implementation of existing STM code specifications as well as a growing inventory of distressed in-service bent caps exhibiting diagonal cracking was the impetus for the Texas Department of Transportation (TxDOT) to fund research project 0-5253, D-Region Strength and Serviceability Design, and the current implementation project (5-5253-01). As part of these projects, simple, accurate STM specifications were developed. This thesis acts as a guidebook for application of the proposed specifications and is intended to clarify any remaining uncertainties associated with strut-and-tie modeling. A series of five detailed design examples feature the application of the STM specifications. A brief overview of each design example is provided below. The examples are prefaced with a review of the theoretical background and fundamental design process of STM (Chapter 2).

- Example 1: Five-Column Bent Cap of a Skewed Bridge
This design example serves as an introduction to the application of STM. Challenges are introduced by the bridge's skew and complicated loading pattern. A clear procedure for defining relatively complex nodal geometries is presented.
- Example 2: Cantilever Bent Cap
A strut-and-tie model is developed to represent the flow of forces around a frame corner subjected to closing loads. The design and detailing of a curved-bar node at the outside of the frame corner is described.
- Example 3a: Inverted-T Straddle Bent Cap (Moment Frame)
An inverted-T straddle bent cap is modeled as a component within a moment frame. Bottom-chord (ledge) loading of the inverted-T necessitates the use of local STMs to model the flow of forces through the bent cap's cross section.
- Example 3b: Inverted-T Straddle Bent Cap (Simply Supported)
The inverted-T bent cap of Example 3a is designed as a member that is simply supported at the columns.
- Example 4: Drilled-Shaft Footing
Three-dimensional STMs are developed to properly model the flow of forces through a deep drilled-shaft footing. Two unique load cases are considered to familiarize the designer with the development of such models.

Table of Contents

List of Tables	xv
List of Figures.....	xvi
Chapter 1. Introduction.....	1
1.1 Background	1
1.2 Project Objective and Scope	3
1.3 Organization.....	3
Chapter 2. Introduction to Strut-and-Tie Modeling	6
2.1 Overview	6
2.2 Discontinuity Regions of Beams	6
2.3 Overview of Strut-and-Tie Modeling	9
2.3.1 <i>Fundamentals of Strut-and-Tie Modeling</i>	9
2.3.2 <i>Prismatic and Bottle-Shaped Struts</i>	11
2.3.3 <i>Strut-and-Tie Model Design Procedure</i>	11
2.4 Separate B- and D-Regions.....	15
2.5 Define Load Case.....	15
2.6 Analyze Structural Component.....	16
2.7 Develop Strut-and-Tie Model	17
2.7.1 <i>Overview of Strut-and-Tie Model Development</i>	17
2.7.2 <i>Determine Geometry of Strut-and-Tie Model</i>	17
2.7.3 <i>Create Efficient and Realistic Strut-and-Tie Models –</i> <i>Rules of Thumb</i>	21
2.7.4 <i>Analyze Strut-and-Tie Model</i>	22
2.8 Proportion Ties.....	26
2.9 Perform Nodal Strength Checks	26
2.9.1 <i>Hydrostatic Nodes versus Non-Hydrostatic Nodes</i>	26
2.9.2 <i>Types of Nodes</i>	27
2.9.3 <i>Proportioning CCT Nodes</i>	28
2.9.4 <i>Proportioning CCC Nodes</i>	29

2.9.5	<i>Proportioning CTT Nodes</i>	34
2.9.6	<i>Designing Curved-Bar Nodes</i>	36
2.9.7	<i>Calculating Nodal Strengths</i>	37
2.9.8	<i>Special Consideration – Back Face of CCT/CTT Nodes</i>	44
2.10	Proportion Crack Control Reinforcement.....	45
2.11	Provide Necessary Anchorage for Ties.....	48
2.12	Perform Shear Serviceability Check.....	49
2.12.1	<i>Special Note – Shear Serviceability Check</i>	51
2.13	Summary	52
Chapter 3.	Proposed Strut-and-Tie Modeling Specifications	54
3.1	Introduction.....	54
3.2	Overview of TxDOT Project 0-5253	54
3.2.1	<i>Deep Beam Database</i>	54
3.2.2	<i>Experimental Program</i>	55
3.2.3	<i>Objectives and Corresponding Conclusions</i>	57
3.3	Proposed Strut-and-Tie Modeling Specifications	62
3.3.1	<i>Overview of Proposed Specifications</i>	62
3.3.2	<i>Updates to the TxDOT Project 0-5253 Specifications as a Result of the Current Implementation Project (5-5253-01)</i>	62
3.3.3	<i>Proposed Revisions to the AASHTO LRFD Bridge Design Specifications</i>	64
3.4	Summary	81
Chapter 4.	Example 1: Five-Column Bent Cap of a Skewed Bridge	82
4.1	Synopsis.....	82
4.2	Design Task	82
4.2.1	<i>Bent Cap Geometry</i>	82
4.2.2	<i>Determine the Loads</i>	87
4.2.3	<i>Determine the Bearing Areas</i>	91
4.2.4	<i>Material Properties</i>	94
4.3	Design Procedure.....	95

4.4 Design Calculations	95
4.4.1 Step 1: Analyze Structural Component	95
4.4.2 Step 2: Develop Strut-and-Tie Model	96
4.4.3 Step 3: Proportion Longitudinal Ties	101
4.4.4 Step 4: Perform Nodal Strength Checks	102
4.4.5 Step 5: Proportion Stirrups in High Shear Regions	123
4.4.6 Step 6: Proportion Crack Control Reinforcement	128
4.4.7 Step 7: Provide Necessary Anchorage for Ties	129
4.4.8 Step 8: Perform Shear Serviceability Check.....	132
4.5 Reinforcement Layout	135
4.6 Comparison of STM Design to Sectional Design.....	138
4.7 Summary	140
Chapter 5. Example 2: Cantilever Bent Cap.....	142
5.1 Synopsis	142
5.2 Design Task	142
5.2.1 Bent Cap Geometry.....	142
5.2.2 Determine the Loads	145
5.2.3 Determine the Bearing Areas.....	147
5.2.4 Material Properties.....	150
5.3 Design Procedure.....	151
5.4 Design Calculations	151
5.4.1 Step 1: Analyze Structural Component	151
5.4.2 Step 2: Develop Strut-and-Tie Models.....	153
5.4.3 Step 3: Proportion Vertical Tie and Crack Control Reinforcement	160
5.4.4 Step 4: Proportion Longitudinal Ties	162
5.4.5 Step 5: Perform Nodal Strength Checks	163
5.4.6 Step 6: Provide Necessary Anchorage for Ties	175
5.4.7 Step 7: Perform Shear Serviceability Check.....	176
5.5 Reinforcement Layout	177

5.6 Summary	179
Chapter 6. Example 3a: Inverted-T Straddle Bent Cap (Moment Frame).....	181
6.1 Synopsis	181
6.2 Design Task	181
6.2.1 Bent Cap Geometry.....	181
6.2.2 Determine the Loads	184
6.2.3 Determine the Bearing Areas.....	187
6.2.4 Material Properties.....	187
6.2.5 Inverted-T Terminology.....	187
6.3 Design Procedure	188
6.4 Design Calculations	189
6.4.1 Step 1: Analyze Structural Component and Develop Global Strut-and-Tie Model.....	189
6.4.2 Step 2: Develop Local Strut-and-Tie Models.....	195
6.4.3 Step 3: Proportion Longitudinal Ties	199
6.4.4 Step 4: Proportion Hanger Reinforcement/Vertical Ties	200
6.4.5 Step 5: Proportion Ledge Reinforcement	203
6.4.6 Step 6: Perform Nodal Strength Checks	206
6.4.7 Step 7: Proportion Crack Control Reinforcement.....	223
6.4.8 Step 8: Provide Necessary Anchorage for Ties	225
6.4.9 Step 9: Perform Other Necessary Checks.....	227
6.4.10 Step 10: Perform Shear Serviceability Check.....	227
6.5 Reinforcement Layout	229
6.6 Summary	232
Chapter 7. Example 3b: Inverted-T Straddle Bent Cap (Simply Supported)	233
7.1 Synopsis	233
7.2 Design Task	233
7.2.1 Bent Cap Geometry.....	233
7.2.2 Determine the Loads	235

7.2.3 Determine the Bearing Areas.....	237
7.2.4 Material Properties.....	237
7.3 Design Procedure.....	237
7.4 Design Calculations.....	238
7.4.1 Step 1: Develop Global Strut-and-Tie Model.....	238
7.4.2 Step 2: Develop Local Strut-and-Tie Models.....	242
7.4.3 Step 3: Proportion Longitudinal Ties.....	246
7.4.4 Step 4: Proportion Hanger Reinforcement/Vertical Ties.....	246
7.4.5 Step 5: Proportion Ledge Reinforcement.....	250
7.4.6 Step 6: Perform Nodal Strength Checks.....	250
7.4.7 Step 7: Proportion Crack Control Reinforcement.....	259
7.4.8 Step 8: Provide Necessary Anchorage for Ties.....	259
7.4.9 Step 9: Perform Other Necessary Checks.....	261
7.4.10 Step 10: Perform Shear Serviceability Check.....	262
7.5 Reinforcement Layout.....	263
7.6 Comparison of Two STM Designs – Moment Frame and Simply Supported.....	266
7.7 Serviceability Behavior of Existing Field Structure.....	267
7.8 Summary.....	269
Chapter 8. Example 4: Drilled-Shaft Footing.....	271
8.1 Synopsis.....	271
8.2 Design Task.....	271
8.2.1 Drilled-Shaft Footing Geometry.....	271
8.2.2 First Load Case.....	273
8.2.3 Second Load Case.....	273
8.2.4 Material Properties.....	274
8.3 Design Procedure.....	274
8.4 Design Calculations (First Load Case).....	275
8.4.1 Step 1: Determine the Loads.....	275
8.4.2 Step 2: Analyze Structural Component.....	279

8.4.3 Step 3: Develop Strut-and-Tie Model	280
8.4.4 Step 4: Proportion Ties	288
8.4.5 Step 5: Perform Strength Checks	291
8.4.6 Step 6: Proportion Shrinkage and Temperature Reinforcement	295
8.4.7 Step 7: Provide Necessary Anchorage for Ties	296
8.5 Design Calculations (Second Load Case).....	300
8.5.1 Step 1: Determine the Loads.....	300
8.5.2 Step 2: Analyze Structural Component	302
8.5.3 Step 3: Develop Strut-and-Tie Model	303
8.5.4 Step 4: Proportion Ties	307
8.5.5 Step 5: Perform Strength Checks	310
8.5.6 Step 6: Proportion Shrinkage and Temperature Reinforcement	310
8.5.7 Step 7: Provide Necessary Anchorage for Ties	310
8.6 Reinforcement Layout	312
8.7 Summary	318
Chapter 9. Summary and Concluding Remarks.....	320
9.1 Summary	320
9.2 Concluding Remarks.....	322
References.....	325
Vita	329

List of Tables

Table 2.1:	Concrete efficiency factors, v	40
Table 3.1:	Filtering of the deep beam database of TxDOT Project 0-5253 (from Birrcher et al., 2009)	55
Table 5.1:	Bearing sizes and effective bearing areas for each beam/girder.....	150
Table 7.1:	Comparison of the two STM designs (moment frame versus simply supported)	266
Table 7.2:	Comparison of diagonal cracking strength to service shear (two STM designs).....	267

List of Figures

Figure 1.1: Strut-and-tie model for a beam	2
Figure 2.1: Stress trajectories within B- and D-regions of a flexural member (adapted from Birrcher et al., 2009)	6
Figure 2.2: (a) One-panel (arch action); (b) two-panel (truss action) strut-and-tie models for deep beam region (adapted from Birrcher et al., 2009)	8
Figure 2.3: Struts, ties, and nodes within a strut-and-tie model	10
Figure 2.4: Prismatic and bottle-shape struts within a strut-and-tie model (adapted from Birrcher et al., 2009)	11
Figure 2.5: Strut-and-tie model design procedure	14
Figure 2.6: Linear stress distribution assumed at the interface of a B-region and a D-region	17
Figure 2.7: Placement of the longitudinal ties and prismatic struts within a strut-and-tie model	19
Figure 2.8: Elastic stress distribution and corresponding strut-and-tie model for cantilever bent cap of Chapter 5	20
Figure 2.9: Choosing optimal strut-and-tie model based on number and lengths of ties (adapted from MacGregor and Wight, 2005)	21
Figure 2.10: Using the least number of vertical ties (and truss panels) as possible	22
Figure 2.11: Steps for the development of a strut-and-tie model	25
Figure 2.12: Nodal proportioning techniques - hydrostatic versus non- hydrostatic nodes (adapted from Birrcher et al., 2009)	27
Figure 2.13: Three types of nodes within a strut-and-tie model (adapted from Birrcher et al., 2009)	28
Figure 2.14: Geometry of a CCT node (adapted from Birrcher et al., 2009)	28
Figure 2.15: CCC node – (a) original geometry of the STM; (b) adjacent struts resolved together; (c) node divided into two parts; (d) final nodal geometry	30
Figure 2.16: Geometry of a CCC node (adapted from Birrcher et al., 2009)	31
Figure 2.17: Optimizing the height of the strut-and-tie model (i.e. the moment arm, jd)	33
Figure 2.18: Determination of available length of vertical tie connecting two smeared nodes (adapted from Wight and Parra-Montesinos, 2003)	36

Figure 2.19: Curved-bar node at the outside of a frame corner (adapted from Klein, 2008)	37
Figure 2.20: Determination of triaxial confinement factor, m (from ACI 318-08).....	39
Figure 2.21: Concrete efficiency factors, ν (node illustrations).....	41
Figure 2.22: Stresses within a bottle-shaped strut.....	43
Figure 2.23: Stress condition at the back face of a CCT node – (a) bond stress resulting from the anchorage of a developed tie; (b) bearing stress applied from an anchor plate or headed bar; (c) interior node over a continuous support	45
Figure 2.24: Web reinforcement within effective strut area (adapted from Birrcher et al., 2009).....	47
Figure 2.25: Available development length for ties (adapted from Birrcher et al., 2009)	48
Figure 2.26: Diagonal cracking load equation with experimental data (from Birrcher et al., 2009).....	51
Figure 3.1: Scaled comparison of deep beams (from Birrcher et al., 2009)	56
Figure 3.2: Elevation view of test setup for TxDOT Project 0-5253 (from Birrcher et al., 2009).....	57
Figure 4.1: Plan and elevation views of five-column bent cap (left)	84
Figure 4.2: Plan and elevation views of five-column bent cap (right).....	85
Figure 4.3: Transverse slab sections for forward and back spans	86
Figure 4.4: Factored loads acting on the bent cap (excluding self-weight)	88
Figure 4.5: Assumed location of girder loads	89
Figure 4.6: Determining when to combine loads – (a) Combine loads together; (b) keep loads independent.....	90
Figure 4.7: Assumed square area for the columns	91
Figure 4.8: Effective bearing area considering effect of bearing seat.....	92
Figure 4.9: Assumed bearing areas for girder loads – (a) single girder load; (b) two girder loads that have been combined.....	94
Figure 4.10: Strut-and-tie model for the five-column bent cap.....	97
Figure 4.11: Determining the location of the top and bottom chords of the STM	98
Figure 4.12: Orientation of diagonal members – (a) incorrect; (b) correct.....	99
Figure 4.13: Minimizing number of truss panels – (a) efficient; (b) inefficient	100
Figure 4.14: Modeling flow of forces near Column 2 – (a) efficient/realistic; (b) inefficient/unrealistic.....	101

Figure 4.15: Determination of triaxial confinement factor, m , at Column 4.....	104
Figure 4.16: Node JJ – (a) from STM; (b) with resolved struts	107
Figure 4.17: Node JJ subdivided into two parts	107
Figure 4.18: Node JJ – right nodal subdivision.....	110
Figure 4.19: Node JJ – left nodal subdivision	112
Figure 4.20: Adjusting the angle of Strut P/JJ due to the subdivision of Node JJ.....	113
Figure 4.21: Node P shown with Node JJ and Strut P/JJ	114
Figure 4.22: Node R	116
Figure 4.23: Node Q.....	117
Figure 4.24: Node EE – (a) from STM and (b) with resolved struts and subdivided into three parts.....	119
Figure 4.25: Node EE.....	120
Figure 4.26: Nodes V and NN and Strut V/NN	122
Figure 4.27: Determination of the available length for Tie L/FF (adapted from Wight and Parra-Montesinos, 2003).....	124
Figure 4.28: Limiting the assumed available lengths for ties to prevent overlap	126
Figure 4.29: (a) Available length for Tie P/II; (b) required spacing for Tie P/II extended to the column	127
Figure 4.30: Anchorage of bottom chord reinforcement at Node NN	130
Figure 4.31: Anchorage of top chord reinforcement at Node V	132
Figure 4.32: Diagonal cracking load equation with experimental data and the normalized service shear for two regions of the bent cap (adapted from Birrcher et al., 2009)	134
Figure 4.33: Reinforcement details – elevation (design per proposed STM specifications)	136
Figure 4.34: Reinforcement details – cross-sections (design per proposed STM specifications).....	137
Figure 4.35: Reinforcement details near Column 4 – (a) STM design; (b) sectional design	139
Figure 5.1: Plan and elevation views of cantilever bent cap (simplified geometry).....	144
Figure 5.2: Plan and elevation views of cantilever bent cap (detailed geometry).....	144
Figure 5.3: Factored loads acting on the bent cap (excluding self-weight) – (a) from each beam/girder; (b) resolved loads.....	146
Figure 5.4: Adding factored self-weight to the superstructure loads	147

Figure 5.5: Effective bearing areas considering effect of bearing seats (elevation)	149
Figure 5.6: Effective bearing areas considering effect of bearing seats (plan)	149
Figure 5.7: Linear stress distribution at the boundary of the D-region	152
Figure 5.8: Strut-and-tie model for the cantilever bent cap – Option 1	154
Figure 5.9: Strut-and-tie model for the cantilever bent cap – Option 2	155
Figure 5.10: Modeling compressive forces within the column – (a) single strut; (b) two struts	157
Figure 5.11: Determining the vertical position of Node E	159
Figure 5.12: Node E	164
Figure 5.13: Node B	166
Figure 5.14: Node C	169
Figure 5.15: Stresses acting at a curved bar (adapted from Klein, 2008)	173
Figure 5.16: Bend radius, r_b , at Node A	174
Figure 5.17: Anchorage of longitudinal bars at Node C	175
Figure 5.18: Reinforcement details – elevation (design per proposed STM specifications)	178
Figure 5.19: Reinforcement details – Section A-A (design per proposed STM specifications)	178
Figure 5.20: Reinforcement details – Section B-B (design per proposed STM specifications)	179
Figure 6.1: Plan and elevation views of inverted-T bent cap	183
Figure 6.2: Factored superstructure loads acting on the bent cap	184
Figure 6.3: Factored loads acting on the global strut-and-tie model for the inverted-T bent cap (moment frame case)	186
Figure 6.4: Defining hanger and ledge reinforcement	188
Figure 6.5: Bent divided into D-regions and B-regions	188
Figure 6.6: Global strut-and-tie model for the inverted-T bent cap (moment frame case)	190
Figure 6.7: Analysis of moment frame – factored superstructure loads	191
Figure 6.8: Analysis of moment frame – factored superstructure loads and tributary self-weight	194
Figure 6.9: Local strut-and-tie model at Beam Line 1 (moment frame case) ...	196
Figure 6.10: Comparing the local strut-and-tie models (moment frame case)....	198
Figure 6.11: Available lengths for hanger reinforcement – plan and elevation views	201

Figure 6.12: Available lengths for ledge reinforcement.....	204
Figure 6.13: Dimension a_f	205
Figure 6.14: Top portion of ledge reinforcement carries force in Tie C_sF_s	206
Figure 6.15: Illustration of struts and nodes within the inverted-T bent cap	206
Figure 6.16: Node G (moment frame case).....	208
Figure 6.17: Determination of triaxial confinement factor, m , for Node G	210
Figure 6.18: Node C (moment frame case)	212
Figure 6.19: Node C – left nodal subdivision (moment frame case)	214
Figure 6.20: Node C – right nodal subdivision (moment frame case)	215
Figure 6.21: Node K (moment frame case).....	217
Figure 6.22: Bend radius, r_b , at Node F (moment frame case).....	221
Figure 6.23: Node C_s of local STM at Beam Line 1 (moment frame case)	222
Figure 6.24: Anchorage of bottom chord reinforcement at Node G	225
Figure 6.25: Anchorage of ledge reinforcement at Node C_s	226
Figure 6.26: Reinforcement details – elevation (design per proposed STM specifications – moment frame case).....	230
Figure 6.27: Reinforcement details – cross-sections (design per proposed STM specifications – moment frame case).....	231
Figure 7.1: Plan and elevation views of inverted-T bent cap.....	234
Figure 7.2: Factored superstructure loads acting on the bent cap	235
Figure 7.3: Factored loads acting on the global strut-and-tie model for the inverted-T bent cap (simply supported case)	236
Figure 7.4: Global strut-and-tie model for the inverted-T bent cap (simply supported case)	239
Figure 7.5: Determining the location of the top chord of the global STM.....	241
Figure 7.6: Local strut-and-tie model at Beam Line 1 (simply supported case)	243
Figure 7.7: Comparing the local strut-and-tie models (simply supported case)	245
Figure 7.8: Diagonal strut inclinations (greater than 25 degrees)	247
Figure 7.9: Vertical tie widths	248
Figure 7.10: Node P (simply supported case)	251
Figure 7.11: Node E – resolved struts (simply supported case).....	253
Figure 7.12: Node E – refined geometry (simply supported case).....	255
Figure 7.13: Node C (simply supported case).....	256
Figure 7.14: Anchorage of bottom chord reinforcement at Node H	260

Figure 7.15: Reinforcement details – elevation (design per proposed STM specifications – simply supported)	264
Figure 7.16: Reinforcement details – cross-sections (design per proposed STM specifications – simply supported case)	265
Figure 7.17: Existing field structure (inverted-T straddle bent cap) – (a) Upstation; (b) Downstation	269
Figure 8.1: Plan and elevation views of drilled-shaft footing	272
Figure 8.2: Factored load and moment of the first load case	273
Figure 8.3: Factored load and moment of the second load case.....	274
Figure 8.4: Developing an equivalent force system from the applied force and moment.....	276
Figure 8.5: Linear stress distribution over the column cross section and the locations of the loads comprising the equivalent force system (first load case).....	277
Figure 8.6: Assumed reinforcement layout of the column section.....	278
Figure 8.7: Applied loading and drilled-shaft reactions (first load case).....	280
Figure 8.8: Strut-and-tie model for the drilled-shaft footing – axonometric view (first load case).....	281
Figure 8.9: Strut-and-tie model for the drilled-shaft footing – plan view (first load case).....	282
Figure 8.10: Determining the location of the bottom horizontal ties of the STM	283
Figure 8.11: Potential positions of Nodes A and D (and Strut AD).....	284
Figure 8.12: Alternative strut-and-tie model for the first load case	288
Figure 8.13: Spacing of bottom mat reinforcement	290
Figure 8.14: Anchorage of bottom mat reinforcement.....	298
Figure 8.15: Anchorage of vertical ties – unknown available length.....	299
Figure 8.16: Factored load and moment of the second load case.....	300
Figure 8.17: Linear stress distribution over the column cross section and the locations of the loads comprising the equivalent force system (second load case)	301
Figure 8.18: Applied loading and drilled-shaft reactions (second load case)	303
Figure 8.19: Strut-and-tie model for the drilled-shaft footing – axonometric view (second load case)	304
Figure 8.20: Determining the location of the top horizontal ties of the STM (second load case)	305
Figure 8.21: Shrinkage and temperature reinforcement considered to carry the tie force	308

Figure 8.22: Assumed reinforcement layout of the drilled shafts	309
Figure 8.23: Anchorage of top mat reinforcement	311
Figure 8.24: Anchorage of Ties FL and GM (drilled-shaft reinforcement)	312
Figure 8.25: Reinforcement details – anchorage of vertical ties	313
Figure 8.26: Reinforcement details – elevation view (main reinforcement).....	314
Figure 8.27: Reinforcement details – elevation view (shrinkage and temperature reinforcement).....	315
Figure 8.28: Reinforcement details – Section A-A (main reinforcement).....	316
Figure 8.29: Reinforcement details – Section A-A (shrinkage and temperature reinforcement).....	316
Figure 8.30: Reinforcement details – plan view (bottom mat reinforcement)	317
Figure 8.31: Reinforcement details – plan view (top mat reinforcement)	318

Chapter 1. Introduction

1.1 BACKGROUND

Strut-and-tie modeling (STM) is a versatile, lower-bound (i.e. conservative) design method for reinforced concrete structural components. STM is most commonly used to design regions of structural components disturbed by a load and/or geometric discontinuity. Load and geometric discontinuities cause a nonlinear distribution of strains to develop within the surrounding region. As a result, plane sections can no longer be assumed to remain plane within the region disturbed by the discontinuity. Sectional design methodologies are predicated on traditional beam theory, including the assumption that plane sections remain plane, and are not appropriate for application to disturbed regions, or D-regions. The design of D-regions must therefore proceed on a regional, rather than a sectional, basis. STM provides the means by which this goal can be accomplished.

When designing a D-region using STM, the complex flow of forces through a structural component is first simplified into a truss model, known as a strut-and-tie model. A basic two-dimensional strut-and-tie model consists of concrete compression members (i.e. struts) and steel tension members (i.e. ties) interconnected within a single plane, as shown in Figure 1.1. In this figure, struts are denoted by dashed lines, while ties are denoted by solid lines. Complexity introduced by loading, boundary conditions, and/or component geometry may occasionally necessitate the development of a three-dimensional strut-and-tie model. The completed model is used by the designer to proportion and anchor the primary reinforcement, and ensure that the concrete has sufficient strength to resist the applied loads.

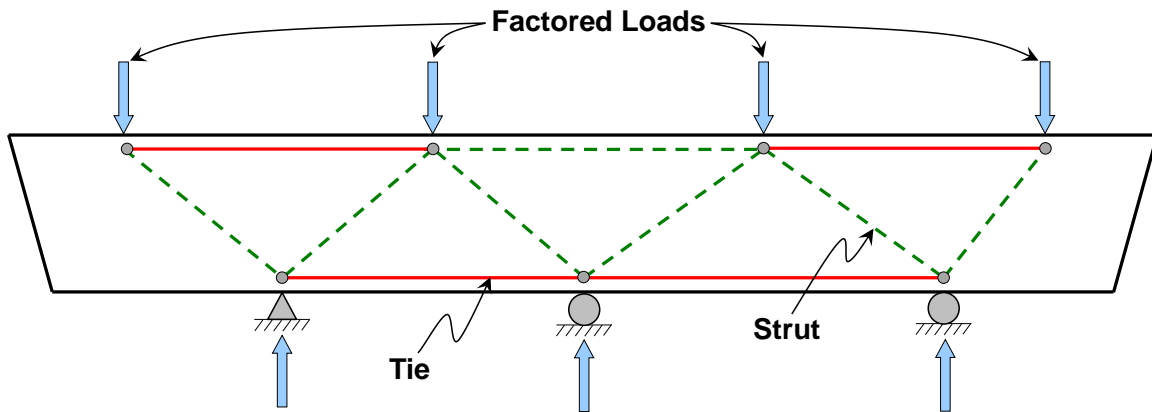


Figure 1.1: Strut-and-tie model for a beam

Strut-and-tie modeling can be applied to any structural component with any loading and support conditions. This versatility of STM is a source of both clarity and confusion. STM has lent clarity and led to safe designs in cases where the application of sectional design methods is overly complicated or even questionable (e.g. dapped beam ends). However, the numerous engineering judgments required to design structural components using STM (including the development of strut-and-tie models) have proven to be a continuing source of confusion for design practitioners. Uncertainty related to the implementation of strut-and-tie modeling has in fact been the primary roadblock to the routine application of the STM provisions introduced into the AASHTO LRFD Bridge Design Specifications in 1994 and the ACI 318: Building Code Requirements for Structural Concrete in 2002.

In response to the concerns expressed by design engineers and a growing inventory of distressed in-service bent caps exhibiting diagonal cracking, the Texas Department of Transportation (TxDOT) funded research project 0-5253, D-Region Strength and Serviceability Design. This project provided unprecedented insights into the safe, serviceable design of D-regions using strut-and-tie modeling. The researchers of TxDOT Project 0-5253 conducted a total of 37 tests on specimens that were some of the largest beams ever tested in the history of shear research. Existing STM code provisions were then calibrated and refined based upon the experimental results and a

complementary database of 142 tests from the literature. Upon implementation, the recommendations made by the researches of TxDOT Project 0-5253 will result in the simplest, most accurate strut-and-tie modeling provisions to date. Proposed changes to the AASHTO LRFD Bridge Design Specifications (2008) were included in Birrcher et al. (2009), the final report of TxDOT Project 0-5253. This document is referenced extensively herein.

1.2 PROJECT OBJECTIVE AND SCOPE

To facilitate adoption of the recommendations made by TxDOT Project 0-5253, the Texas Department of Transportation funded the creation of this guidebook under implementation project 5-5253-01. The primary objective of this guidebook is to clarify any remaining uncertainties associated with strut-and-tie modeling. To that end, the design examples included in this guidebook are prefaced with a review of the theoretical background and fundamental design process of strut-and-tie modeling. A subsequent series of detailed design examples explained in a step-by-step manner feature the application of the state-of-the-art STM design recommendations found in the TxDOT Project 0-5253 report and other reliable sources. Within these examples, clear and reasonable explanations are given for overcoming the challenges of STM design. This guidebook is intended to serve as a designer's primary reference material in the application of strut-and-tie modeling to bridge components.

1.3 ORGANIZATION

The concepts and design examples presented within this guidebook are organized to progressively build the knowledge and confidence of engineers new to strut-and-tie modeling. With that said, the designer should feel free to directly reference the most relevant design example after reviewing the introduction to STM (the STM primer) in Chapter 2. A brief overview of each chapter/example is provided here as a quick and easy reference:

- Chapter 2. Introduction to Strut-and-Tie Modeling
This chapter serves as a primer for designers who are new to strut-and-tie modeling. The fundamental concepts that form the basis of STM are first introduced. Then, the design tasks of the STM procedure are described in a step-by-step manner.
- Chapter 3. Proposed Strut-and-Tie Modeling Specifications
A brief overview of the work completed during TxDOT Project 0-5253 is presented. Each task of the research program is summarized, and the corresponding conclusions are described. The proposed STM specifications developed as part of project 0-5253 and the current implementation project (5-5253-01) are then provided.
- Chapter 4. Example 1: Five-Column Bent Cap of a Skewed Bridge
The first of five design examples is presented in this chapter. Challenges are introduced by the bridge's skew and complicated loading pattern. These issues are resolved so that a simple, realistic strut-and-tie model can be developed. A procedure for defining relatively complicated nodal geometries is also provided.
- Chapter 5. Example 2: Cantilever Bent Cap
For this design example, an STM is developed to model the flow of forces around a frame corner subjected to closing loads. Additionally, the detailing of a curved-bar node at the outside of the frame corner is described (see Section 5.4.5).
- Chapter 6. Example 3a: Inverted-T Straddle Bent Cap (Moment Frame)
The design of an inverted-T straddle bent cap is demonstrated in Chapters 6 and 7. The bent cap is assumed to be a component within a moment frame in Chapter 6. Within these two chapters, the concept of a three-dimensional STM is introduced in order to determine the necessary steel within the ledge of the inverted-T.
- Chapter 7. Example 3b: Inverted-T Straddle Bent Cap (Simply Supported)
The same inverted-T bent cap introduced in Chapter 6 is designed as a member that is simply supported at the columns.

- Chapter 8. Example 4: Drilled-Shaft Footing

The final design example presents the development of fairly complicated three-dimensional STMs. Two load cases are considered in order to familiarize the designer with the development of such models.

- Chapter 9. Summary and Concluding Remarks

The final chapter includes a summary of the most important points of the strut-and-tie modeling design procedure and the defining features of each design example. The designer is provided with rules of thumb and/or valuable comments for each step of the STM procedure.

Chapter 2. Introduction to Strut-and-Tie Modeling

2.1 OVERVIEW

The material presented within this chapter serves to (1) familiarize the design engineer with the basic concepts of strut-and-tie modeling (STM) and (2) provide the skills necessary to work through the five design examples included in this guidebook. To begin, the localized effect of a load or geometric discontinuity on beam behavior is examined and the concept of a disturbed region, or D-region, is described. The remainder of the chapter highlights the utility of strut-and-tie modeling for the design of D-regions and is accompanied by a thorough description of the STM design tasks.

2.2 DISCONTINUITY REGIONS OF BEAMS

Strut-and-tie modeling is primarily used for the design of D-regions (“D” standing for discontinuity or disturbed) that occur in the vicinity of load or geometric discontinuities. In Figure 2.1, the applied load and support reactions are discontinuities that “disturb” the regions of the member near the locations where they act. Frame corners, dapped ends, openings, and corbels are examples of geometric discontinuities that correspond to the existence of D-regions.

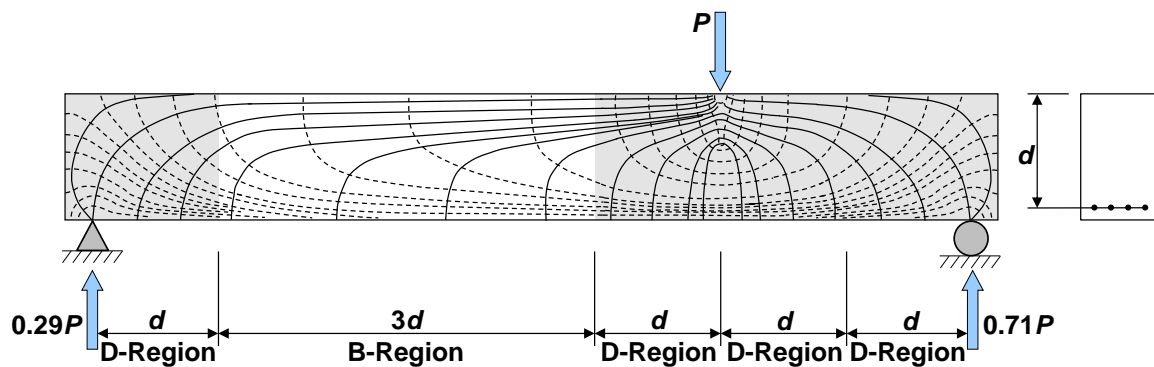


Figure 2.1: Stress trajectories within B- and D-regions of a flexural member (adapted from Birrcher et al., 2009)

B-regions (“B” standing for beam or Bernoulli) occur between D-regions, as shown in Figure 2.1. Plane sections are assumed to remain plane within B-regions

according to the primary tenets of beam theory, implying that a linear distribution of strains occurs through the member depth. The beam is therefore dominated by sectional behavior, and design can proceed on a section-by-section basis (i.e. sectional design). For the flexural design of a B-region, the compressive stresses (represented by solid lines in Figure 2.1) are conventionally assumed to act over a rectangular stress block, while the tensile stresses (represented by dashed lines) are assumed to be carried by the longitudinal steel reinforcement.

The distribution of strains through the member depth in D-regions is nonlinear, and the assumptions that underlie the sectional design procedure are therefore invalidated. According to St. Venant's principle, an elastic stress analysis indicates that a linear distribution of stress can be assumed at about one member depth from a load or geometric discontinuity. In other words, a nonlinear stress distribution exists within one member depth from the location where the discontinuity is introduced (Schlaich et al., 1987). D-regions are therefore assumed to extend approximately a distance d from the applied load and support reactions in Figure 2.1, where the member depth, d , is defined as the distance between the extreme compression fiber and the primary longitudinal reinforcement.

In general, a region of a structural member is assumed to be dominated by nonlinear behavior when the shear span, a , is less than about 2 or 2.5 times the member depth, d (i.e. $a < 2d$ to $2.5d$). The shear span, a , is defined as the distance between the applied load and the support in simple members. The distance between the applied load and right support in Figure 2.1 is only twice the member depth. The right shear span is therefore entirely composed of D-regions and will be dominated by nonlinear behavior, often referred to as deep beam behavior in recognition of the relatively short nature of the shear span in comparison to the member depth. Members expected to exhibit such behavior are commonly referred to as deep beams or deep members. Deep beam regions require the use of strut-and-tie modeling as discussed below. In Figure 2.1, the distance between the applied load and the left support is five times the member depth. Although the left shear span includes D-regions, it will be dominated by sectional behavior and can

therefore be designed using sectional methods. Of course, the actual transition from sectional behavior to deep beam behavior is gradual, but applying St. Venant's principle to determine the behavior of each region of a member results in a reasonable estimation.

The behavior of a deep beam can be described by considering the load transfer mechanism between the applied load and the support. The behavior of the deep beam region in Figure 2.1 is likely dominated by a combination of arch action and truss action between the load, P , and the right support. In the development of a strut-and-tie model, the arch action, or direct load transfer, can be represented by the diagonal concrete strut (dashed line) shown in Figure 2.2(a). The tension member, or tie, necessary to equilibrate the thrust of the diagonal strut is denoted by the solid line along the bottom of the beam in Figure 2.2(a). In an alternative strut-and-tie model, the truss action, or indirect load transfer, is represented by the two-panel truss model that includes a vertical tie, as shown in Figure 2.2(b).

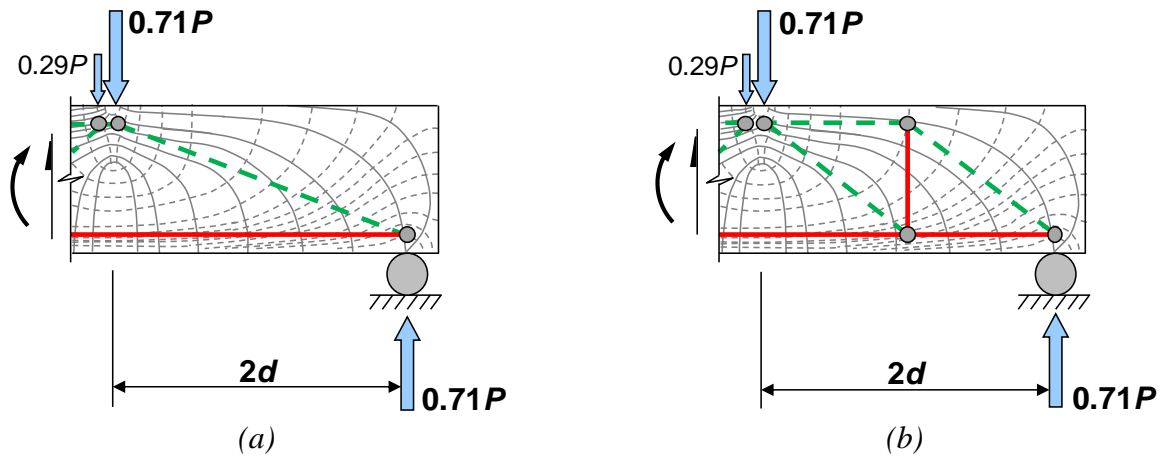


Figure 2.2: (a) One-panel (arch action); (b) two-panel (truss action) strut-and-tie models for deep beam region (adapted from Birrcher et al., 2009)

The versatility of strut-and-tie modeling allows it to be used for the design of any D-region and accommodate various load cases and load transfer mechanisms. Implementation of the STM design procedure presented in the following sections will result in safe, serviceable structures.

2.3 OVERVIEW OF STRUT-AND-TIE MODELING

2.3.1 Fundamentals of Strut-and-Tie Modeling

The principles that form the basis of strut-and-tie modeling ensure that the resulting structural design is conservative (i.e. is a lower-bound design). An STM design adheres to these principles if (1) the truss model is in equilibrium with external forces and (2) the concrete element has enough deformation capacity to accommodate the assumed distribution of forces (Schlaich et al., 1987). Proper anchorage of the reinforcement is an implicit requirement of the latter condition. Additionally, the compressive forces in the concrete as indicated by an analysis of the strut-and-tie model must not exceed the factored concrete strengths, and the tensile forces within the STM must not exceed the factored tie capacities. If all of the requirements above are satisfied, application of the STM procedure will result in a conservative design (i.e. lower-bound design).

Every STM consists of three components: struts, ties, and nodes. A basic STM representing the flow of forces through a simply supported beam is depicted in Figure 2.3. After calculating the external reactions and defining the geometry of the STM, the member forces of the truss model are calculated from statics. The compression members are referred to as *struts*, and the tension members are referred to as *ties*. Strut and ties are denoted by dashed lines and solid lines, respectively, in Figure 2.3 and throughout this guidebook. The struts and ties intersect at regions referred to as *nodes*. Due to the concentration of stresses from intersecting truss members, the nodes are the most highly stressed regions of a structural member.

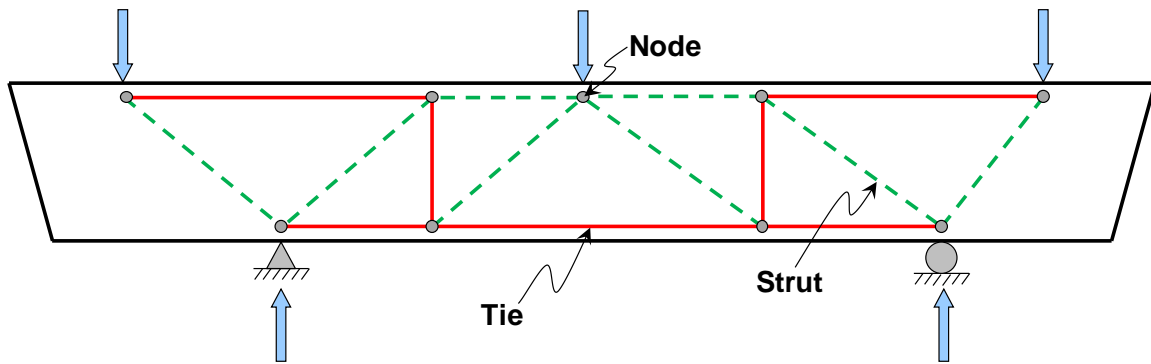


Figure 2.3: Struts, ties, and nodes within a strut-and-tie model

When developing an STM, the locations of the struts and ties should ideally be based upon the flow of forces indicated by an elastic analysis. Placing the struts and ties in accordance with the elastic flow of forces ensures a safe design with minimal cracking at service load levels (Bergmeister et al., 1993). Further discussion concerning the placement of struts and ties is provided in Section 2.7.

A strut-and-tie model can ultimately be tailored to any geometry and stress distribution that may be encountered in the design of D-regions. This versatility is simultaneously viewed as a primary advantage as well as a major challenge of the application of STM. The flexibility with which strut-and-tie modeling can be applied often leads to uncertainties and confusion for the designer: no one “correct” STM exists for any particular structure. If the principles required to achieve a lower-bound solution are satisfied, however, the engineer can be assured that a safe design will result. The desire to minimize uncertainties and formulate consistent STM design procedures within a design office is, nevertheless, understood. This guidebook is therefore meant to assist engineers with developing such procedures that can be applied to the design of structural components of highway bridges.

For further explanation of the theoretical background of STM, the reader is encouraged to reference the TxDOT Project 0-5253 report (Birrcher et al., 2009).

2.3.2 Prismatic and Bottle-Shaped Struts

Struts can either be defined as prismatic or bottle-shaped depending on the uniformity of the stress fields in which they are located. As illustrated in Figure 2.4, prismatic struts are concentrated in regions where stresses are fairly uniform, such as the region at the top of a member in positive bending. Bottle-shaped struts are located in regions where the compressive stresses are able to spread laterally. Diagonal struts within a beam are bottle-shaped. The spreading of the compressive stresses produces tensile stresses transverse to the strut, causing diagonal cracks to form within the member. These tensile stresses reduce the efficiency of the concrete that comprises the strut. Orthogonal reinforcement is provided in the vicinity of bottle-shaped struts to carry the tensile forces, strengthen the strut, and control the bursting cracks that tend to develop. Although bottle-shaped struts are often idealized as prismatic struts, as illustrated in Figure 2.4, the effects of the transverse tensile stresses must not be overlooked.

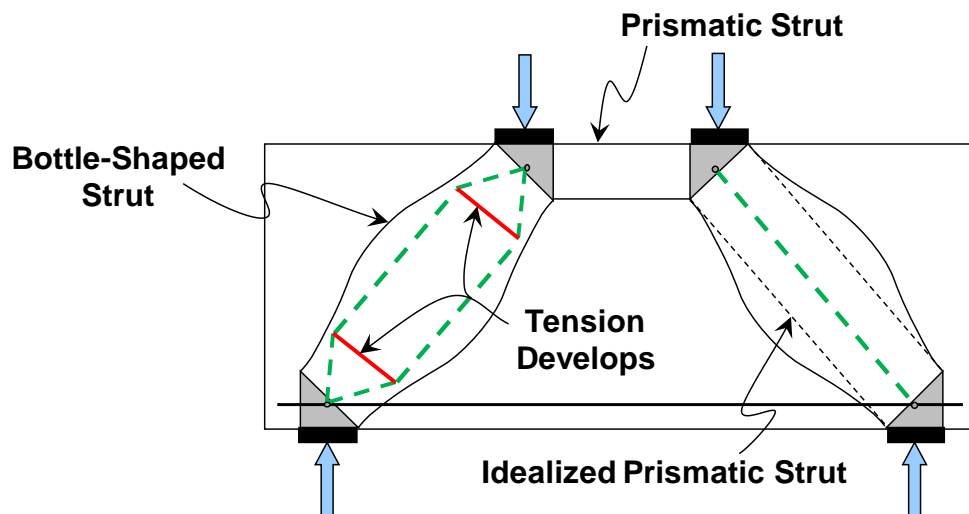


Figure 2.4: Prismatic and bottle-shape struts within a strut-and-tie model (adapted from Birrcher et al., 2009)

2.3.3 Strut-and-Tie Model Design Procedure

A list of the steps typically followed when designing a deep structural component using the STM procedure is provided below. The procedure is based on the application

of the STM specifications that were developed as a part of TxDOT Project 0-5253 and the current implementation project (5-5253-01). The proposed specifications as well as a brief overview of the work completed during project 0-5253 are presented in Chapter 3. The STM procedure provided below is generally followed in the design examples of Chapters 4 through 8 but is adapted to the particular design scenarios as necessary. While each step of the procedure will be independently described in the sections that follow, the designer should note that the steps are sometimes performed simultaneously. The STM procedure is presented in a flow-chart format in Figure 2.5.

1. Separate B- and D-regions – Determine which regions of the structural component are expected to exhibit deep beam behavior or if the entire component should be designed using STM.
2. Define load case – Calculate the factored loads acting on the structural component, and if necessary, make simplifying assumptions to develop a load case that can be applied to a reasonable STM.
3. Analyze structural component – Solve for the structural component's support reactions assuming linear elastic behavior.
4. Develop strut-and-tie model – Position struts and ties to represent the actual flow of forces within the structural component, and determine the forces in the struts and ties.
5. Proportion ties – Specify the reinforcement needed to carry the force in each tie.
6. Perform nodal strength checks – Define the geometries of the critical nodes, and ensure the strength of each face is adequate to resist the applied forces determined from the analysis of the STM.
7. Proportion crack control reinforcement – Specify the required crack control reinforcement to restrain diagonal cracks formed by the transverse tensile stresses of bottle-shaped struts.
8. Provide necessary anchorage for ties – Ensure reinforcement is properly anchored at the nodal regions.

9. Perform shear serviceability check – If serviceability is a concern, compare the internal shear forces due to service loads to the estimated diagonal cracking load calculated from the equation proposed in the TxDOT Project 0-5253 report.

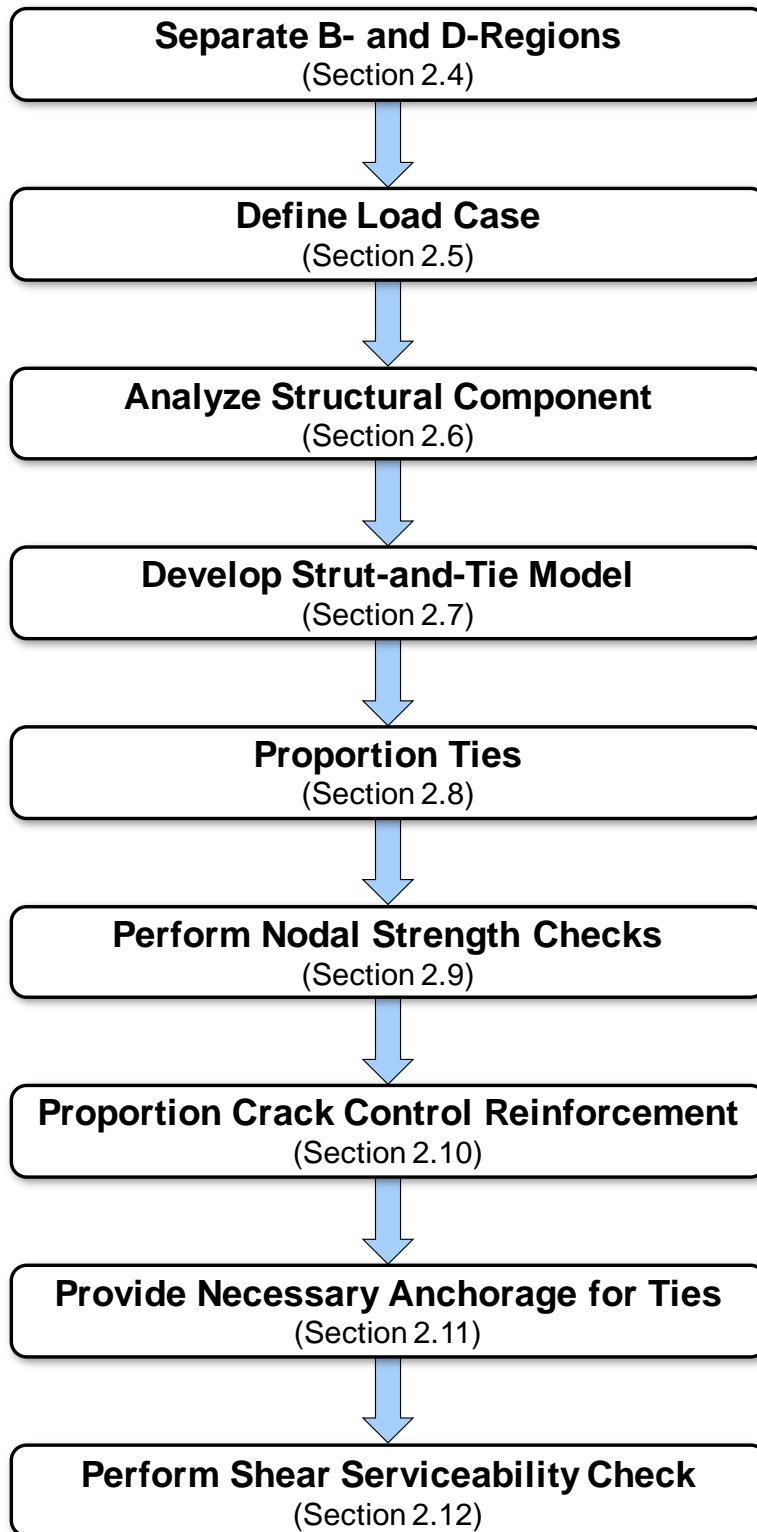


Figure 2.5: Strut-and-tie model design procedure

2.4 SEPARATE B- AND D-REGIONS

The first step in the STM design process is to divide the structure into B- and D-regions using St. Venant's principle. If the structure consists of only D-regions, the STM design process should be used to design the structure in its entirety. If the structure contains both D- and B-regions, the portions of the structure expected to exhibit deep beam behavior (as described in Section 2.2) should be designed using the STM procedure. Portions of the structure expected to be dominated by sectional behavior can be designed using the sectional design approach. However, if only a small portion of the structure is a B-region, the designer may decide that using strut-and-tie modeling for the entire structure is reasonable and will result in a suitable design. The STM design specifications presented in Chapter 3 have been calibrated to minimize the discrepancy between the sectional and STM design procedures when the a/d ratio is such that a member's behavior is transitioning from deep beam to sectional behavior (i.e. near an a/d ratio of 2).

2.5 DEFINE LOAD CASE

The next step of the design procedure is to define the loads that will be applied to the nodes of the strut-and-tie model. The designer should first determine the critical load cases that should be considered. Each load case (e.g. each location of the live load) will create a unique set of forces in the struts and ties of the STM, causing the locations of the critical regions of the STM to change. An analysis of the strut-and-tie model, therefore, should be performed for each critical load case. In some instances, the geometry of the STM must be modified when a new load case is applied (see the design of the drilled-shaft footing in Chapter 8). At other times, however, the geometry can remain the same for various load cases. After the factored loads and moments are applied to the structure for a particular load case, the designer should determine if a feasible STM can be developed for the loading. Modifications may be necessary to produce a loading for which an STM can be developed. Some examples of such modifications are listed as follows:

- A moment acting on the structure must be replaced by a couple or an equivalent set of forces since moments cannot be applied to a truss model.
- Point loads acting on the structure at a very close proximity to each other may be resolved together to simplify the development of the strut-and-tie model. The decision whether or not to combine loads together is left to the discretion of the designer.
- A distributed load acting on the structure must be divided into a set of point loads that act at the nodes of the STM since distributed loads cannot be applied to a truss model. The self-weight of the structure must be applied to the STM in this manner.

Oftentimes, determining how the loads will be applied to the strut-and-tie model is carried out simultaneously with the development of the STM, as will be demonstrated in Chapters 6 and 7.

2.6 ANALYZE STRUCTURAL COMPONENT

During this step of the design procedure, the forces acting at the boundaries of the D-region under consideration are determined. Knowledge of these boundary forces are (1) used to define the geometry of the strut-and-tie model and are (2) applied to the STM to determine the forces carried by the struts and ties. For each load case, the factored loads should first be applied to the structural component, and an overall linear elastic analysis of the component should be performed to determine the support reactions. If the structural component consists of both a B-region and a D-region and only part of the component will be designed using strut-and-tie modeling, the internal forces and moment within the B-region should be applied at the boundary of the D-region. A linear elastic distribution of stress can be assumed at the interface between the B- and D-regions as shown in Figure 2.6. This stress distribution is used to determine the forces applied to the STM at the B-region/D-region interface (see the design examples of Chapters 5, 6, and 8). The location of this interface is determined by using St. Venant's principle as

described in Section 2.4. The factored loads and boundary forces are then applied to the D-region under consideration to develop and analyze the strut-and-tie model.

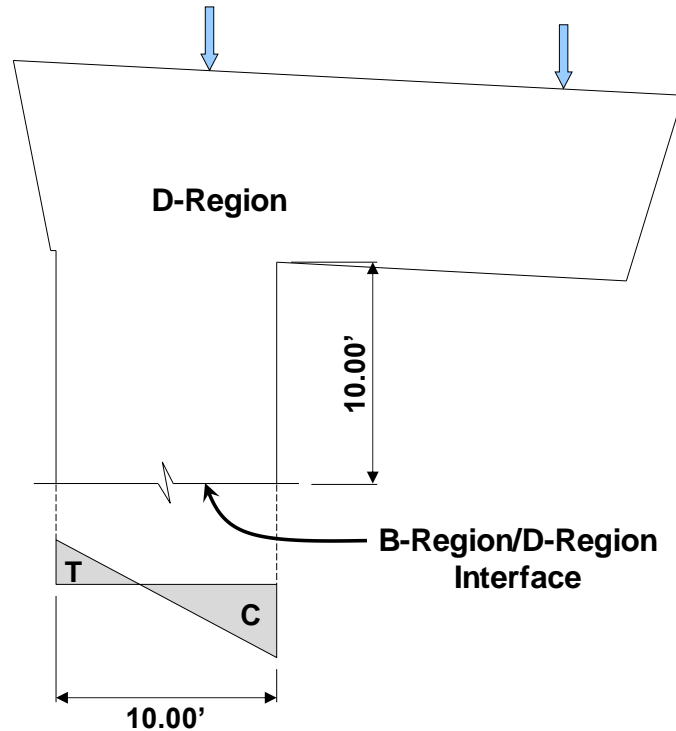


Figure 2.6: Linear stress distribution assumed at the interface of a B-region and a D-region

2.7 DEVELOP STRUT-AND-TIE MODEL

2.7.1 Overview of Strut-and-Tie Model Development

The development of a strut-and-tie model is typically performed in a two-step process. First, the geometry of the STM is determined using knowledge of the locations of the applied loads and boundary forces. Second, the STM is analyzed to determine the forces in the struts and ties. Detailed guidance for this process is provided in the following sections.

2.7.2 Determine Geometry of Strut-and-Tie Model

In the development of the strut-and-tie model, the placement of the struts and ties should be representative of the elastic flow of forces within the structural component

(Bergmeister et al., 1993; Schlaich et al., 1987). The designer has a few options for determining the proper orientation of the struts and tie: (1) use the locations of the applied loads and boundary forces to develop a logical load path represented by the struts and ties, (2) follow the known cracking pattern of the structure being designed if such information is available (MacGregor and Wight, 2005), or (3) perform a linear elastic finite element analysis to visualize the flow of forces in the component and place the struts and ties accordingly.

The ties represent the reinforcement within the structure. Each tie must therefore be positioned to correspond with the centroid of the bars that will be provided to carry the force in the tie. For example, ties representing the longitudinal reinforcement along the bottom of a beam (see Figure 2.7) should be placed at the centroid of this reinforcement considering the cover that will be provided from the bottom of the member to the bars.

The prismatic struts within beams, such as the horizontal struts along the top of the member in Figure 2.7, are positioned based upon either (1) the depth, a , of the rectangular compression stress block as determined from a typical flexural analysis or (2) the optimal height of the strut-and-tie model, h_{STM} . If the first option is used, the struts are placed at the centroid of the stress block (i.e. $a/2$ from the top surface of the beam in Figure 2.7). For the second option, the prismatic struts are positioned to optimize the height of the STM to increase the efficiency of the strut-and-tie model (i.e. provide a larger moment arm, jd). This method is demonstrated in Chapters 5 and 7.

After the longitudinal ties and prismatic struts are positioned, the remaining members of the STM are placed considering the elastic flow of forces within the structure.

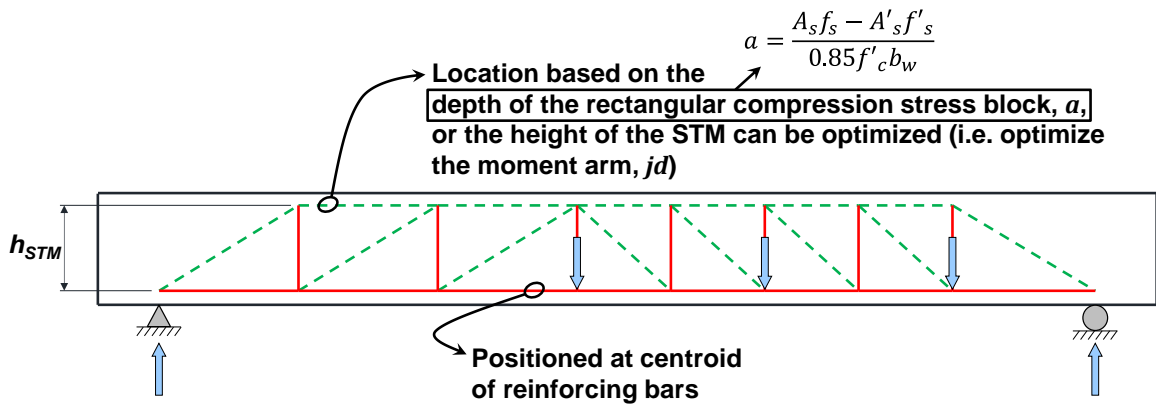


Figure 2.7: Placement of the longitudinal ties and prismatic struts within a strut-and-tie model

The STM for the cantilever bent cap that will be designed in Chapter 5 is shown in Figure 2.8. The development of this STM was based upon the locations of the applied loads and D-region boundary forces. No prior knowledge of cracking patterns or elastic stress fields influenced the modeling process. For illustrative purposes, the STM was superimposed upon the result of a linear elastic finite element analysis (see Figure 2.8). The placement of the struts and ties are seen to follow the general pattern of the compressive and tensile stress fields. The development of a feasible STM can typically be based on reasonable assumptions without the extra effort of a more complex analysis.

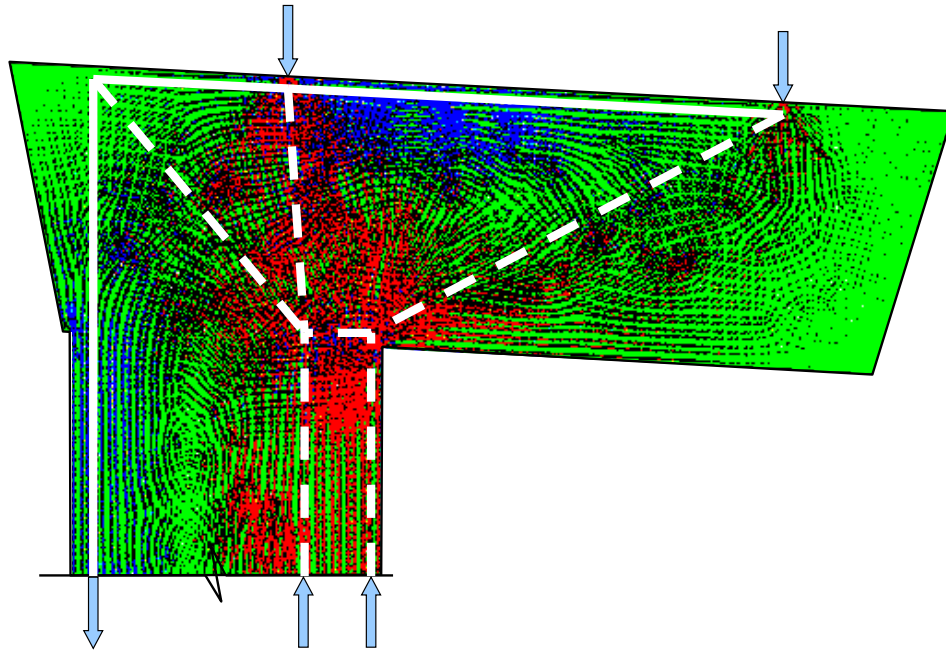


Figure 2.8: Elastic stress distribution and corresponding strut-and-tie model for cantilever bent cap of Chapter 5

In the final geometry of the STM, the angle between a strut and a tie entering the same node must not be less than 25 degrees. As the angle between the strut and tie decreases, both tensile and compressive forces act within the same vicinity of the STM, an undesired and unrealistic scenario. By avoiding this situation, the 25-degree limit prevents excessive strain in the reinforcement and mitigates wide crack openings. The importance of this 25-degree rule cannot be overstressed.

Several valid STMs can often be developed for the particular structure and load case under consideration. Schlaich et al. (1987) remind the designer “that there are no unique or absolute optimum solutions” and that there is “ample room for subjective decisions.” The designer is, nevertheless, reminded (refer back to Section 2.3.1) that the strut-and-tie model design will be conservative if the STM satisfies equilibrium with external forces and the concrete has enough deformation capacity to allow the distribution of forces as assumed by the STM. Because the reinforcement layout of the final design depends on the chosen strut-and-tie model, the forces within the structure

will tend to flow along the paths assumed by the STM. Although developing a model that *exactly* follows the elastic flow of forces within the structure is not required, selecting the STM that best represents the natural elastic stress distribution minimizes the likelihood of service cracks. Deviation from the elastic flow of forces increases the risk of serviceability cracking.

2.7.3 Create Efficient and Realistic Strut-and-Tie Models – Rules of Thumb

The strut-and-tie model featuring the fewest and shortest ties is typically the most efficient and realistic model for the particular structural component and load case under consideration. Loads tend to flow along a path that will minimize deformations. In reinforced concrete structures, the concrete struts (large, mildly stressed areas) will generally transfer force in compression with less deformation than the reinforcement in tension (small, highly stressed areas) (Schlaich et al., 1987). As illustrated in Figure 2.9, the forces will naturally flow along the paths of the STM on the left because it has fewer ties and closely matches the flow of stresses given by an elastic analysis (MacGregor and Wight, 2005).

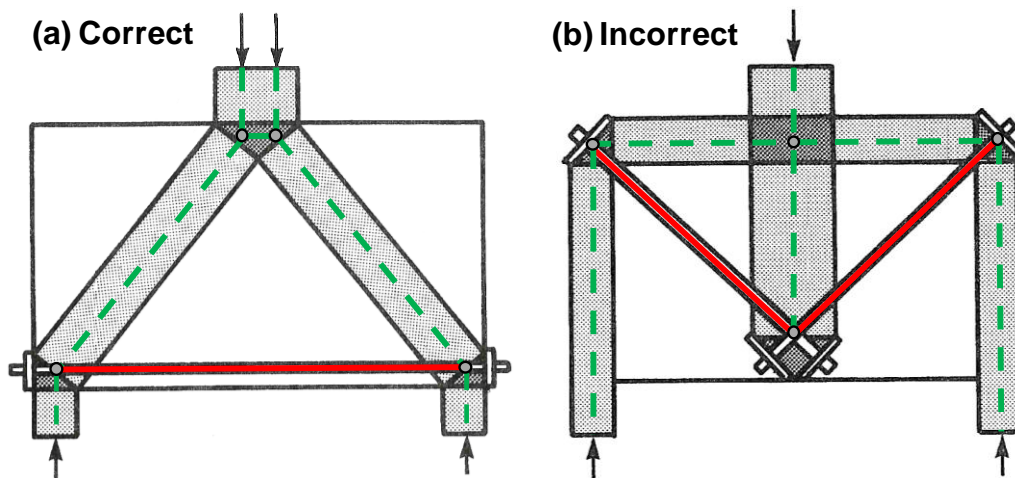


Figure 2.9: Choosing optimal strut-and-tie model based on number and lengths of ties (adapted from MacGregor and Wight, 2005)

Similarly, the least possible number of vertical ties should be used when modeling a beam. In other words, the STM should include the least number of truss panels as

possible while still satisfying the 25-degree rule between the struts and ties entering the same node. Efficient and inefficient methods for modeling a simply supported beam are depicted in Figure 2.10. To satisfy the 25-degree rule, the least number of truss panels that can be provided between the applied load and the support is two, as shown on the left side of the beam. Two more vertical ties than necessary are used to model the flow of forces on the right side of the beam. On this side, enough reinforcement will need to be provided to carry the forces in the three 50-kip ties; only the reinforcement required to carry the force in one 50-kip tie is needed on the left side. The model used on the left side of the beam is therefore much more efficient since less reinforcement is needed and the resulting design is still safe.

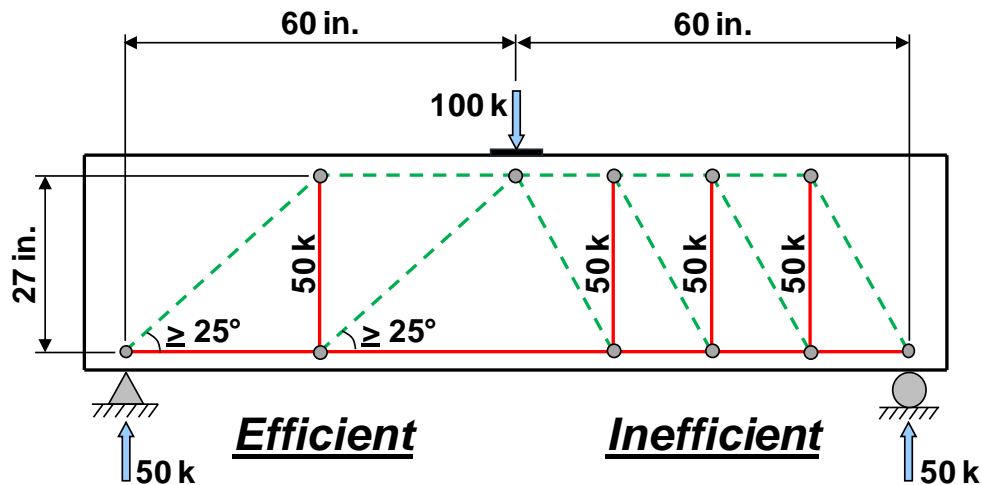


Figure 2.10: Using the least number of vertical ties (and truss panels) as possible

2.7.4 Analyze Strut-and-Tie Model

The forces in the struts and ties of the STM are determined by first applying the factored external loads, support reactions, and any other boundary forces to the STM at the nodes. The member forces are then calculated using statics (i.e. method of joints or method of sections). This approach is valid for statically determinate structures as well as statically indeterminate structures with redundant supports (see Figure 2.11).

Modeling a structure using an *internally* statically indeterminate STM (i.e. an STM with redundant struts/ties that cannot be solved via the method of joint or the

method of sections) creates uncertainties since the relative stiffnesses of the struts and ties affect the member forces of the truss model. Concerning statically indeterminate strut-and-tie models, Brown et al. (2006) state the following:

[I]t is preferable to have a truss model that is statically determinate. A determinate truss will require only equilibrium to determine the forces in each member. An indeterminate model will require some estimate of the member stiffnesses. It is difficult to estimate accurately the stiffness of the elements within a strut-and-tie model due to the complex geometry. Struts are in general not prismatic, and could display non-linear material behavior. The exact cross-sectional area of a strut is accurately known only at the location where the strut is influenced by an external bearing area. At other locations the geometry is not clearly defined. Consequently the stiffness will be difficult to assess.

Research has shown that neglecting the relative stiffnesses of the members in *internally* statically indeterminate STMs can result in conservative designs (Kuchma et al., 2008, 2011); more research is needed to confirm that this principle can be applied to all D-regions. Various methods have been proposed for the determination of the force distributions within statically indeterminate STMs as noted in Ashour and Yang (2007), Leu et al. (2006), and *fib* (2008). Since designers are expected to be able to model most of the D-regions within structural components of highway bridges by using *internally* statically determinate STMs, these methods are not expected to be needed for the design of bridge components similar to those presented in the following chapters. Even though some of the structures considered in the design examples included in this guidebook have redundant supports, all of the STMs are *internally* statically determinate. The assumed relative stiffnesses of the struts and ties are therefore inconsequential if the method of analysis described above is followed.

The steps for the development of a strut-and-tie model are shown pictorially in Figure 2.11. In this figure and throughout this guidebook, negative force values within the strut-and-tie model denote compression (struts) while positive force values denote tension (ties). After an appropriate STM is developed and the forces in the struts and ties

are calculated by satisfying equilibrium, the required amount of reinforcement can be determined and the adequacy of the nodal strengths can be checked.

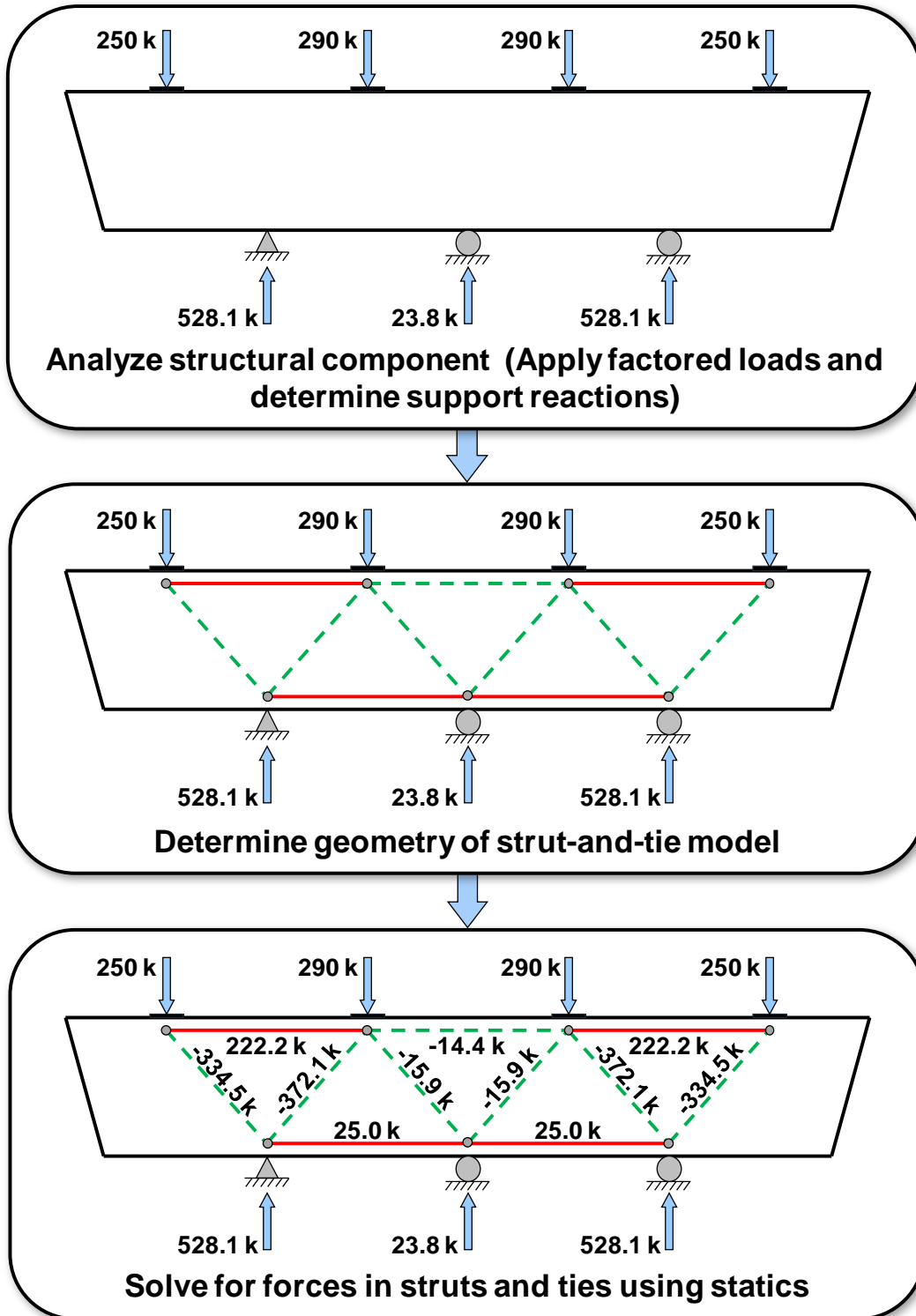


Figure 2.11: Steps for the development of a strut-and-tie model

2.8 PROPORTION TIES

Using the strut-and-tie model that was developed, the next step in the design process is to proportion the ties. The area of reinforcement provided for each tie in the STM should be sufficient to carry the calculated tie force without surpassing the yield strength of the steel. In a conventionally reinforced structure, the area of reinforcement needed for a tie, A_{st} , is determined from the following equation:

$$A_{st} = \frac{F_u}{\phi f_y} \quad (2.1)$$

where F_u is the factored force in the tie, f_y is the yield strength of the steel, and ϕ is the resistance factor of 0.9 according to AASHTO LRFD (2010). Please recall that the centroid of the bars must coincide with the position of the tie within the STM.

2.9 PERFORM NODAL STRENGTH CHECKS

For this step of the design process, each node is checked to ensure that it has adequate strength to resist the imposed forces without crushing the concrete. Nodes are the most highly stressed regions of a structural component because stresses from multiple struts and/or ties must be equilibrated within a small volume of concrete.

Much of the information within this section has been adapted from the TxDOT Project 0-5253 report.

2.9.1 Hydrostatic Nodes versus Non-Hydrostatic Nodes

The geometry of each node must be defined prior to conducting the strength checks. Nodes can be proportioned in two ways: (1) as hydrostatic nodes or (2) as non-hydrostatic nodes. Hydrostatic nodes are proportioned in a manner that causes the stresses applied to each face to be equal. Non-hydrostatic nodes, however, are proportioned based on the origin of the applied stress. For example, the faces of a non-hydrostatic node may be sized to match the depth of the equivalent rectangular compression stress block of a flexural member or may be based upon the desired location of the longitudinal reinforcement (see Figure 2.12). This proportioning technique allows

the geometry of the nodes to closely correspond to the actual stress concentrations at the nodal regions. In contrast, the use of hydrostatic nodes can sometimes result in unrealistic nodal geometries and impractical reinforcement layouts as shown in Figure 2.12. Thus, non-hydrostatic nodes are preferred in design and are used throughout this guidebook.

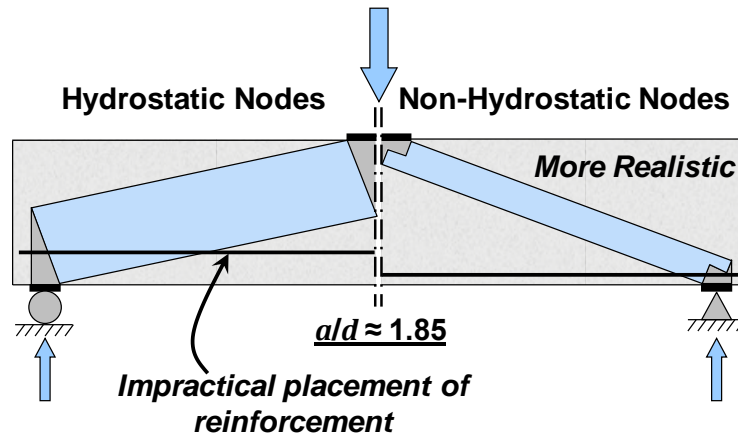


Figure 2.12: Nodal proportioning techniques - hydrostatic versus non-hydrostatic nodes (adapted from Birrcher et al., 2009)

2.9.2 Types of Nodes

Three types of nodes can exist within an STM. These three types are defined below, and an example of each type is given in Figure 2.13. Within the nodal designations, “C” stands for compression and “T” stands for tension.

- CCC: nodes where only struts intersect
- CCT: nodes where tie(s) intersect in only one direction
- CTT: nodes where ties intersect in two different directions

Struts are often resolved together to reduce the number of members intersecting at a node.

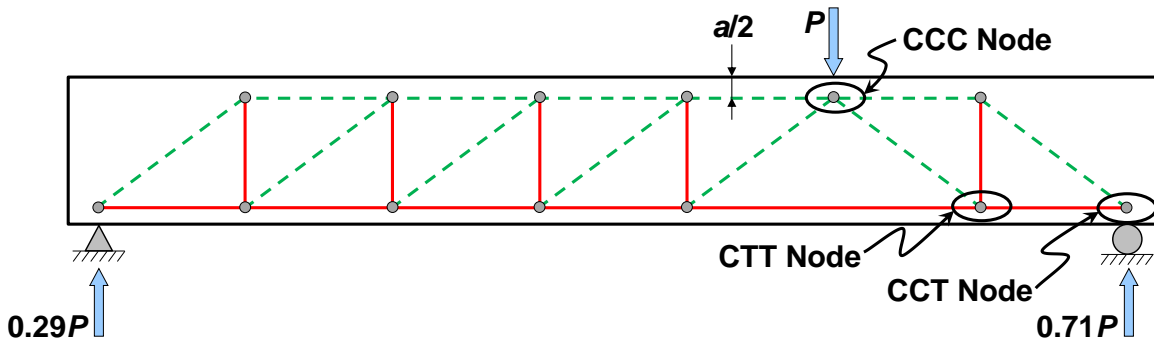


Figure 2.13: Three types of nodes within a strut-and-tie model (adapted from Birrcher et al., 2009)

2.9.3 Proportioning CCT Nodes

The CCT node labeled in Figure 2.13 is shown in-detail in Figure 2.14. The length of the *bearing face*, l_b , corresponds to the dimension of the bearing plate. The length of the *back face*, w_t , is defined by the width of the tie that represents the longitudinal reinforcement in the member. The value of w_t shown in Figure 2.14 is taken as twice the distance from the bottom of the beam to the centroid of the longitudinal steel (i.e. the location of the tie representing this steel).

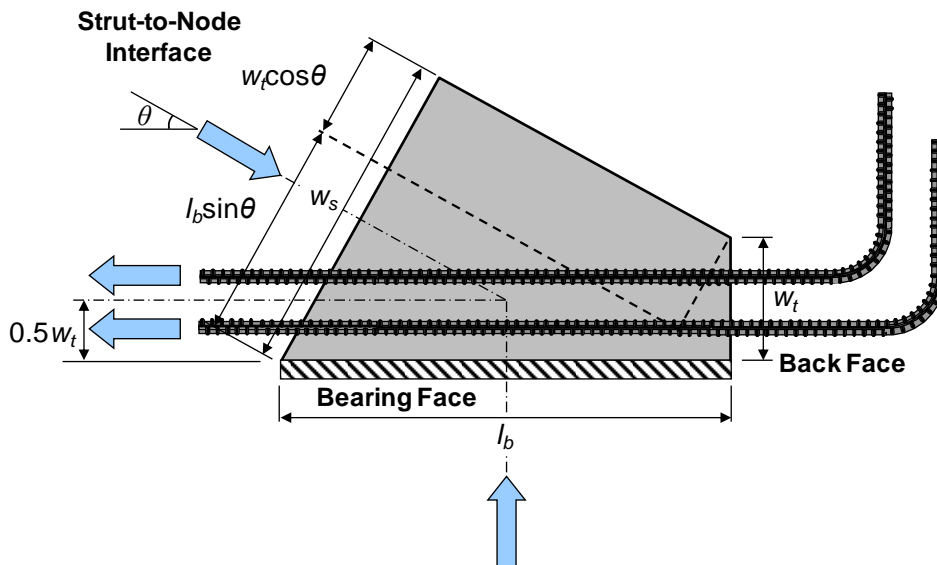


Figure 2.14: Geometry of a CCT node (adapted from Birrcher et al., 2009)

The *strut-to-node interface* is the face where the diagonal strut enters the node. This face is perpendicular to the axis of the diagonal strut. The length of the strut-to-node interface, w_s , depends on the angle, θ , that defines the orientation of this diagonal strut (shown in Figure 2.14). From the geometry of the node, the following equation for w_s is derived:

$$w_s = l_b \sin\theta + w_t \cos\theta \quad (2.2)$$

where:

- l_b = length of the bearing face (in.)
- w_t = length of the back face (in.)
- θ = angle of the diagonal strut measured from the longitudinal axis

2.9.4 Proportioning CCC Nodes

A couple adjustments must be made to the CCC node in Figure 2.13 before its geometry can be defined. First, adjacent struts are resolved together to reduce the number of forces acting on the node. The node is then divided into two parts since diagonal struts enter the node from both the right and the left.

The struts that intersect at the CCC node are shown in Figure 2.15(a). To simplify the nodal geometry, adjacent struts are resolved together, resulting in the diagonal struts presented in Figure 2.15(b). The compressive forces F_1 and F_2 have been resolved together to form the force F_R ; similarly, the two struts on the left have also been combined.

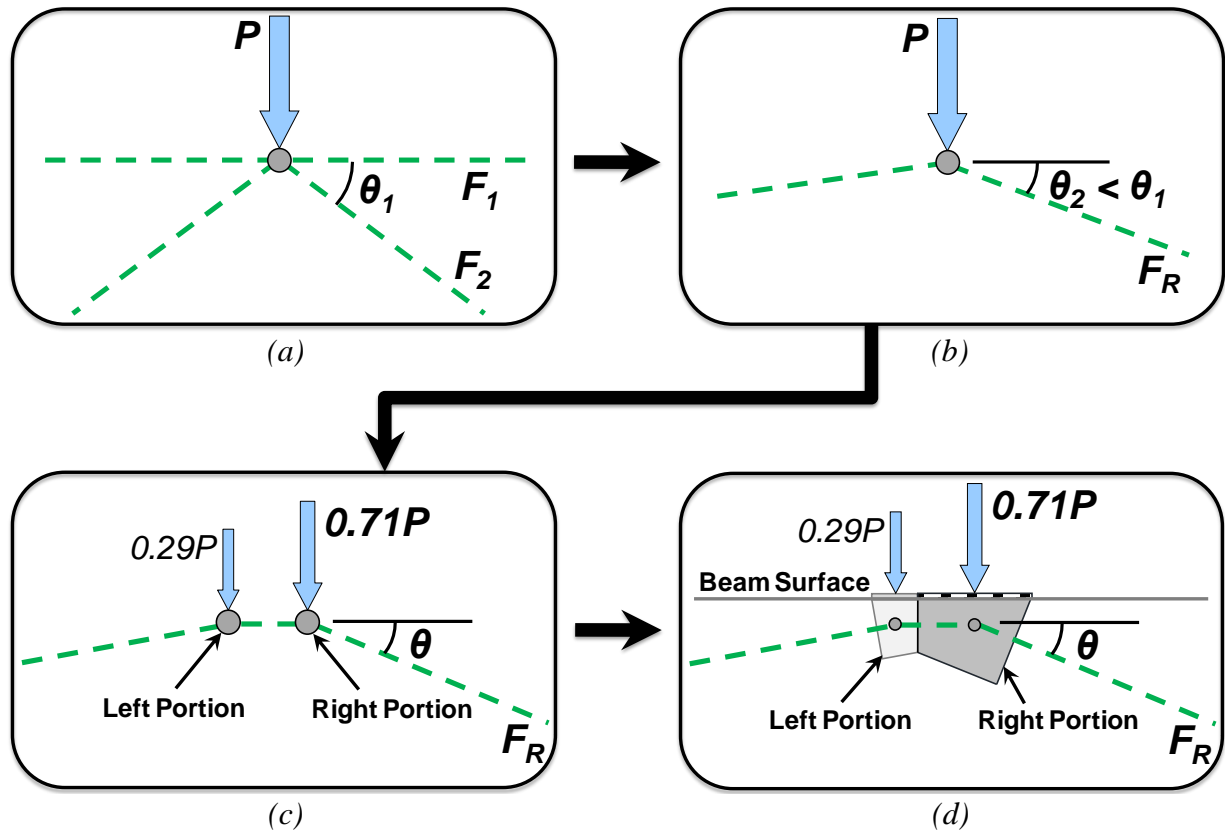


Figure 2.15: CCC node – (a) original geometry of the STM; (b) adjacent struts resolved together; (c) node divided into two parts; (d) final nodal geometry

A node is divided into two parts when diagonal struts enter the node from both sides (i.e. from both the right and left), as in Figure 2.15(b). The CCC node is divided based on the percentage of the applied load, P , that travels to each support. This division of the node results in the left and right portions of the node shown in Figure 2.15(c). Since 71 percent of the applied load flows to the right support, the load acting on the right portion of the node is 71 percent of P ; $0.29P$ acts on the left portion of the node.

The geometry of the CCC node can now be defined. The nodal geometry is shown in Figure 2.15(d) and is duplicated in Figure 2.16 with detailed dimensions. Only the deep beam region located to the right of the applied load will be designed using strut-and-tie modeling. The corresponding portion (i.e. right portion) of the CCC node is therefore of primary interest. Since 71 percent of load P acts on the right portion of the

node, this portion of the node occupies 71 percent of the total bearing length, l_b . The length of the bearing face of the right portion is therefore taken as $0.71l_b$.

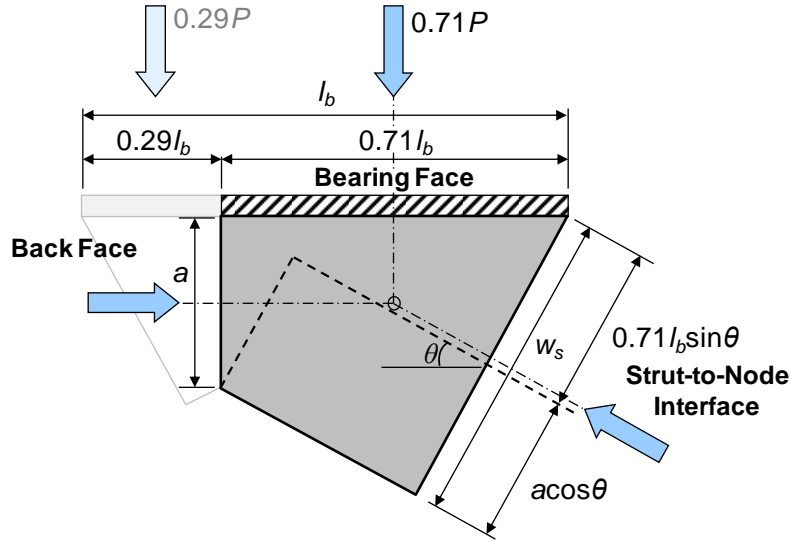


Figure 2.16: Geometry of a CCC node (adapted from Birrcher et al., 2009)

The length of the back face, a , is often taken as the depth of the rectangular compression stress block determined from a flexural analysis. Using this method, the value of a for a rectangular section is determined from the following calculation:

$$a = \frac{A_s f_s - A_s' f_s'}{0.85 f_c' b_w} \quad (2.3)$$

where:

- A_s = area of tension reinforcement (in.²)
- A_s' = area of compression reinforcement (in.²)
- f_s = stress in tension reinforcement (ksi)
- f_s' = stress in compression reinforcement (ksi)
- f_c' = specified compressive strength of concrete (ksi)
- b_w = width of member's web (in.)

Although a traditional flexural analysis is not valid in a D-region due to the nonlinear variation of strains, defining a using the equation above is conservative, and the assumption is well-established in practice.

Another option for determining the length of the back face, a , is to optimize the height of the strut-and-tie model (i.e. the moment arm, jd). After the optimal height of the STM is determined, the distance from the top surface of the member to the top chord of the STM is defined as $a/2$ (refer to Figure 2.13). This method is used in the design examples of Chapters 5 and 7 and is also demonstrated in Tjhin and Kuchma (2002). The concept of determining the optimal height of the STM is illustrated in Figure 2.17. If the moment arm, jd , is too small, the full depth of the member will not be utilized and the design will be less efficient than what could be achieved. If jd is too large, the length of the back face of the CCC node, a , will be too small, causing the imposed forces to act over a small area. The back face, therefore, will not have adequate strength to resist these forces. If the length jd is optimized, efficient use of the member depth is achieved. In this case, the factored force acting on the back face will be about equal to its design strength.

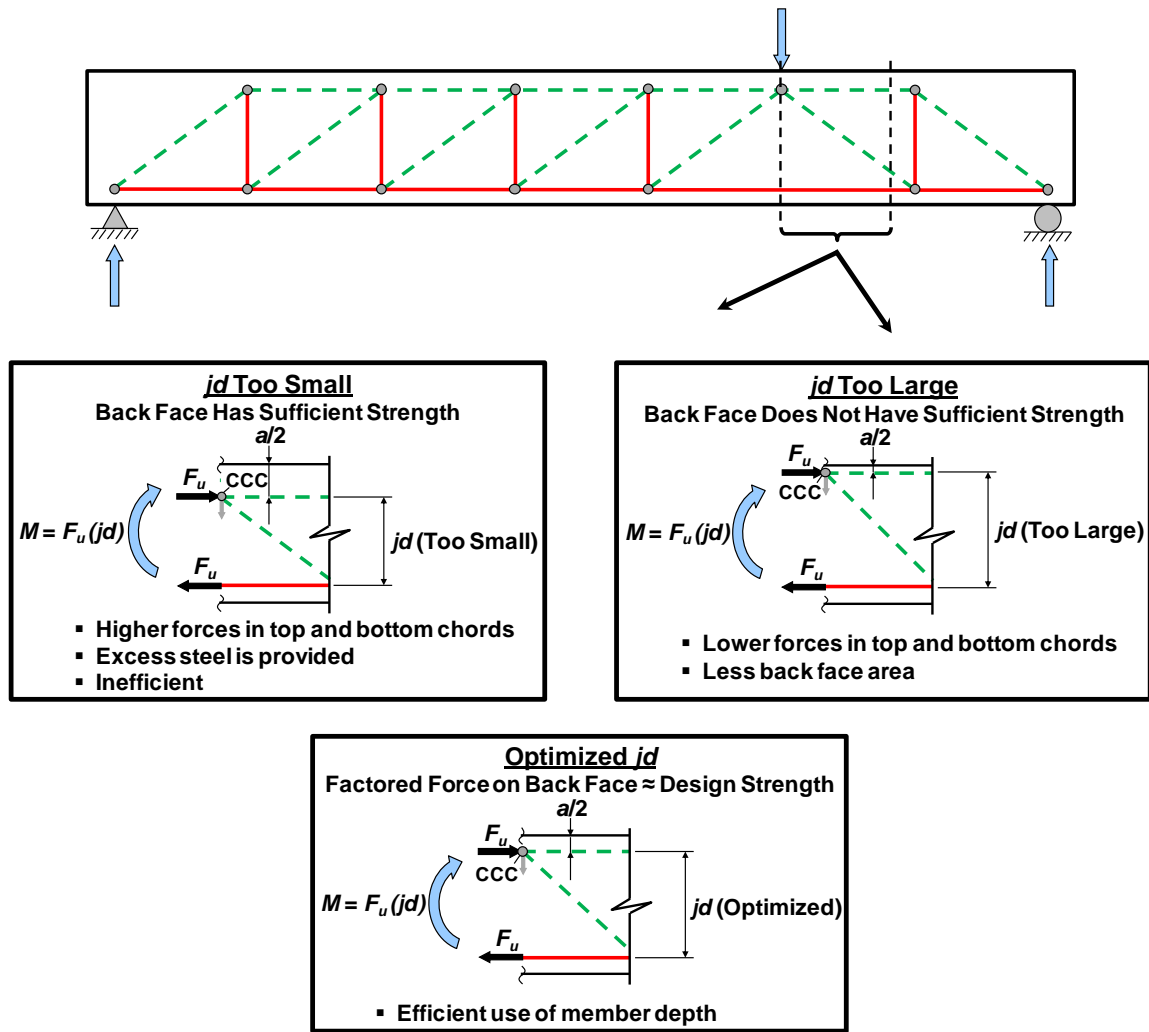


Figure 2.17: Optimizing the height of the strut-and-tie model (i.e. the moment arm, jd)

The length of the strut-to-node interface, w_s , is determined from the same equation used to find the value of w_s for a CCT node except the variable w_t is replaced with a . Thus, the expression for w_s becomes:

$$w_s = l_b \sin \theta + a \cos \theta \quad (2.4)$$

where:

- l_b = length of the bearing face (in.)
- a = length of the back face (in.)
- θ = angle of the diagonal strut measured from the longitudinal axis

The angle θ is shown in Figure 2.16. For the right portion of the node depicted in this figure, the value of l_b is actually taken as $0.71l_b$ in the equation above.

2.9.5 Proportioning CTT Nodes

CTT nodes within a strut-and-tie model, such as the node denoted in Figure 2.13, can often be classified as *smeared nodes*. Smeared nodes do not have a geometry that can be clearly defined by a bearing plate or by geometric boundaries of the structural member. The CTT node labeled in Figure 2.13 does not abut a bearing surface. The node's geometry, therefore, cannot be fully defined (i.e. the extents of the nodal region are unknown). The diagonal strut entering the node is able to disperse, or smear, over a large volume of concrete, and its force is transferred to several stirrups. Schlaich et al. (1987) stated that smeared nodes are not critical and that "a check of concrete stresses in smeared nodes is unnecessary". As a result of the research conducted as part of TxDOT Project 0-5253, the proposed STM specifications provided in Chapter 3 explicitly state that *singular nodes*, or nodes with clearly defined geometries, are critical while smeared nodes do not need to be checked. The reader should note that, at times, CCC and CCT nodes can also be classified as smeared nodes.

Although many CTT nodes that are encountered are smeared, exceptions do occur when the geometry of a CTT node must be defined. An inverted-T bent cap loaded on its ledge (i.e. the bottom chord of the STM) exemplifies such an exception. The CTT nodes located along the bottom chord of the STM for an inverted-T have geometries that can be defined and are therefore considered to be singular nodes. Such CTT nodes with defined geometries are proportioned using the same technique described for CCT nodes in

Section 2.9.3. Please refer to Chapters 6 and 7 for the design of an inverted-T bent cap with singular CTT nodes along the bottom chord of the STM.

To determine the stirrup reinforcement necessary to carry the force in a vertical tie extending from a smeared CTT node, the width of the tie must be determined. In other words, the designer must define the length over which the vertical reinforcement carrying the tie force may be practically distributed. Referring to Figure 2.13, the vertical tie at the right end of the beam extends between two smeared nodes (i.e. the smeared CTT node previously discussed and a smeared CCT node). Concentrating the reinforcement in a small region near the centroid of this vertical tie is impractical and unrealistic. To estimate a feasible width for a tie connecting two smeared nodes, a proportioning technique recommended by Wight and Parra-Montesinos (2003) is used. The tie width, or the available length, l_a , over which the stirrups considered to carry the force in the tie can be spread, is indicated in Figure 2.18. The diagonal struts extending from both the load and the support are assumed to spread to form the fan shapes shown in this figure. The stirrups engaged by the fan-shaped struts are included in the vertical tie. A demonstration of the use of this proportioning technique can be found in Section 4.4.5 of the first design example.

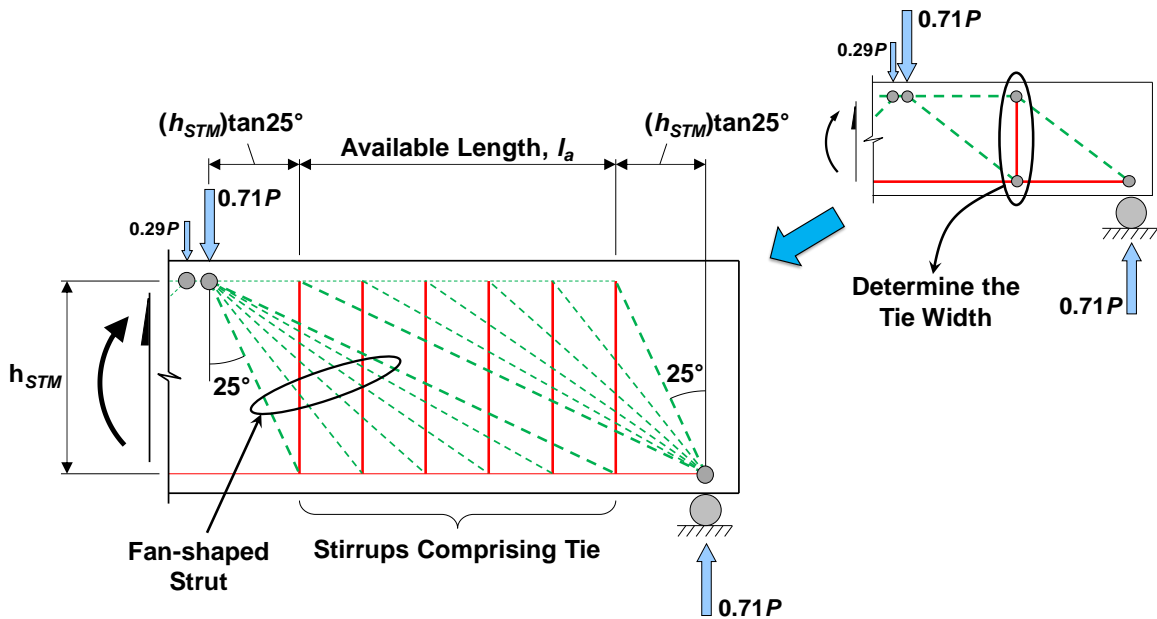


Figure 2.18: Determination of available length of vertical tie connecting two smeared nodes (adapted from Wight and Parra-Montesinos, 2003)

2.9.6 Designing Curved-Bar Nodes

One specialized type of CTT node is referred to as a curved-bar node and is illustrated in Figure 2.19. This example of a curved-bar node occurs at the outside of a frame corner. The continuous reinforcing bars that are bent around the corner resist the closing moment caused by the applied loads. This bend region of the bars is represented by two ties that are equilibrated by a diagonal strut, as shown in Figure 2.19 (Klein, 2008, 2011). The design of such a node requires two criteria to be satisfied. First, the specified bend radius, r_b , must be large enough to ensure that the radial compressive stress imposed by the diagonal strut (refer to Figure 2.19) is limited to a permissible level. The magnitude of this compressive stress depends on the radius of the bend. Second, the length of the bend must be sufficient to allow the circumferential bond stress to be developed along the bend region of the bars. This bond stress is created by a difference in the forces of the two ties when the angle θ_c in Figure 2.19 is not equal to 45 degrees. In addition to these two criteria, the clear side cover measured to the bent bars should be at least $2d_b$ to avoid side splitting, where d_b is the diameter of the bars. If this cover is not

provided, the required radius should be multiplied by a factor of $2d_b$ divided by the specified side cover. The design of curved-bar nodes is presented in Sections 5.4.5 and 6.4.6. The design procedure recommended by Klein (2008) is used to design these nodes and is incorporated into the proposed STM specifications presented in Chapter 3 (see Articles 5.6.3.3.5 and 5.6.3.4.2 of the proposed specifications).

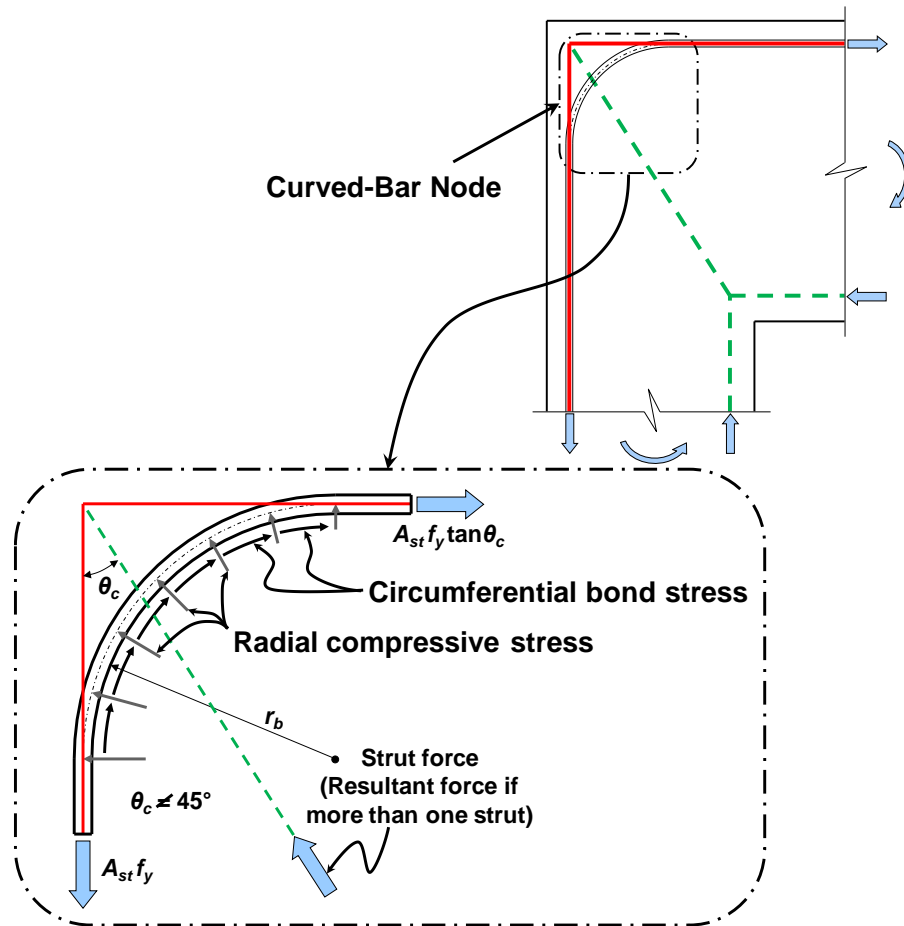


Figure 2.19: Curved-bar node at the outside of a frame corner (adapted from Klein, 2008)

2.9.7 Calculating Nodal Strengths

After the geometry of a node is defined, the design strength of each face is calculated and compared to the applied (factored) force. If the factored force is greater than the design strength, modifications must be made, such as increasing the compressive

strength of the concrete or the size of the bearing areas. The designer could also decide to change the geometry of the structural component to satisfy the nodal strength checks, requiring the STM to be updated to reflect the new state of equilibrium.

The nodal strength calculations are performed by following the three steps described below.

- Step 1 – Calculate the triaxial confinement factor, m (if applicable)

If a node abuts a bearing area with a width that is smaller than the width of the structural member, an increased concrete strength for all the faces of that node can be assumed due to triaxial confinement. The triaxial confinement factor, m , is determined from the following equation:

$$m = \sqrt{A_2/A_1} \leq 2.0 \quad (2.5)$$

where A_l is the loaded area and A_2 is measured on the plane (illustrated in Figure 2.20) defined by the location at which a line with a 2 to 1 slope extending from the loaded area meets the edge of the member. This modification factor is found in Article 5.7.5 of AASHTO LRFD (2010) and §10.14.1 of ACI 318-08.

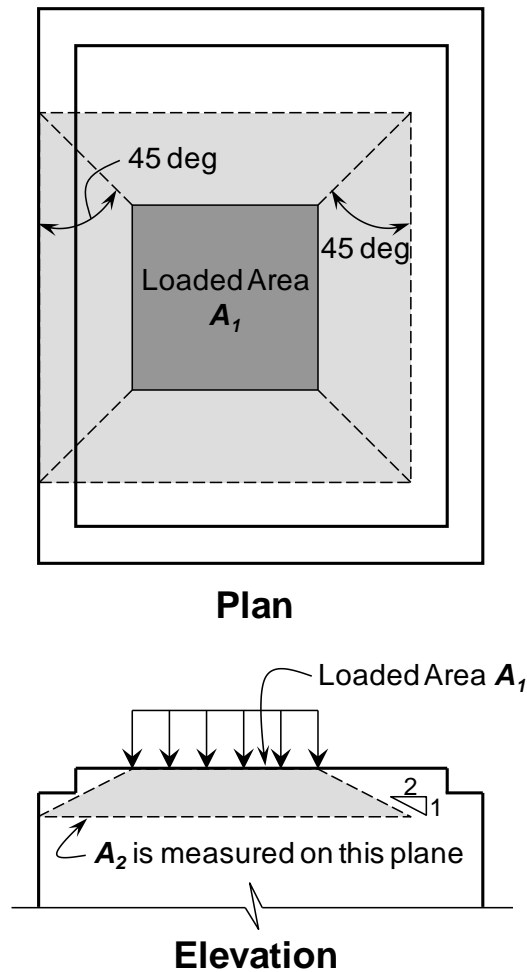


Figure 2.20: Determination of A_2 for stepped or sloped supports (from ACI 318-08)

- Step 2 – Determine the concrete efficiency factor, ν , for the nodal face

The value of the concrete efficiency factor, ν , depends on the type of node (CCC, CCT, or CTT) and the face (bearing face, back face, or strut-to-node interface) that is under consideration. These factors are given in Article 5.6.3.3.3 of the proposed STM specifications provided in Chapter 3 and are listed in Table 2.1 for convenience. The factors are also provided in Figure 2.21 along with illustrations of the three types of nodes. The efficiency factors for the strut-to-node interface given in Table 2.1 and Figure 2.21 should be used only if the crack control reinforcement requirement per Article 5.6.3.5 of the STM specifications in

Chapter 3 is satisfied (see Section 2.10). An efficiency factor of 0.45 should be used for the strut-to-node interface if this requirement is not met.

Table 2.1: Concrete efficiency factors, v

<i>Face</i>	<i>Node Type</i>		
	<i>CCC</i>	<i>CCT</i>	<i>CTT</i>
Bearing Face	0.85	0.70	$0.85 - f'_c/20 \text{ ksi}$ $0.45 \leq v \leq 0.65$
Back Face			
Strut-to-Node Interface*	$0.85 - f'_c/20 \text{ ksi}$ $0.45 \leq v \leq 0.65$	$0.85 - f'_c/20 \text{ ksi}$ $0.45 \leq v \leq 0.65$	

*Provided that crack control reinforcement requirement per Article 5.6.3.5 is satisfied

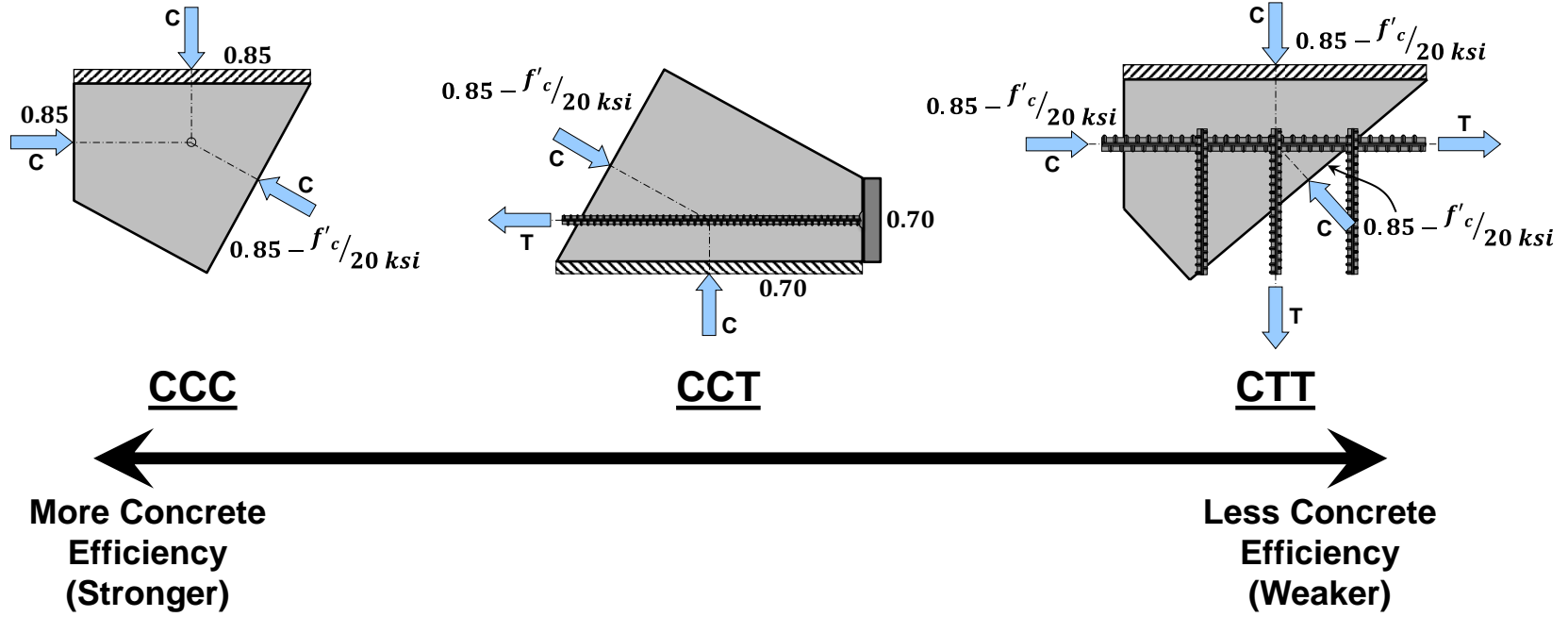


Figure 2.21: Concrete efficiency factors, ν (node illustrations)

- Step 3 – Calculate the design strength of the nodal face, ϕF_n

Next, the design strength of each nodal face is calculated and compared to the corresponding applied (factored) force. The value of the limiting compressive stress at the face of the node, f_{cu} , is calculated first using the following expression:

$$f_{cu} = m \cdot v \cdot f'_c \quad (2.6)$$

where m is the triaxial confinement factor, v is the concrete efficiency factor, and f'_c is the specified compressive strength of the concrete. The design strength of the nodal face, ϕF_n , is then calculated as follows:

$$\phi \cdot F_n = \phi \cdot f_{cu} \cdot A_{cn} \quad (2.7)$$

where ϕ is the resistance factor for compression in strut-in-tie models, F_n is the nominal resistance of the nodal face, and A_{cn} is the effective cross-sectional area of the face. According to Article 5.5.4.2.1 of AASHTO LRFD (2010), the value of ϕ is 0.7. The value of A_{cn} is obtained by multiplying the length of the face as described in Sections 2.9.3 through 2.9.5 by the width of the node perpendicular to the plane of the page when considering Figures 2.14 and 2.16. If the node abuts a bearing plate, the width of the node is taken as the width of the bearing plate. In some cases, the width of the node is the same as the width of the member, b_w (see the design examples of Chapters 6 and 7).

A back face acted upon by a direct compressive force can be strengthened by reinforcing bars. If compression reinforcement is provided parallel to the applied force (i.e. perpendicular to the back face) and is detailed to develop its yield stress in compression, the contribution of the reinforcement to the nodal strength can be considered. In this case, the design strength of the back face is evaluated as follows:

$$\phi \cdot F_n = \phi(f_{cu} \cdot A_{cn} + f_y A_{ss}) \quad (2.8)$$

where f_y is the yield strength of the compression steel and A_{ss} is the area of the steel entering the back face of the node.

The calculated design strength must be greater than or equal to the factored force acting on the nodal face, F_u , as the following expression indicates:

$$\phi F_n \geq F_u \quad (2.9)$$

Both the AASHTO LRFD (2010) and the ACI 318-08 STM specifications include a strut check that is separate from the nodal strength checks. When the proposed specifications are applied, the nodal strength checks ensure that the struts also have adequate strengths. The highest stresses within a strut occur at its ends because the areas over which the stresses act are limited at the nodes, as illustrated in Figure 2.22. For a bottle-shaped (diagonal) strut, the stresses are able to spread over a larger area at locations outside of the nodal regions. The design strengths of the strut-to-node interfaces, therefore, effectively limit the stresses within the diagonal strut. Similarly, back face checks are often equivalent to checking the stresses within prismatic struts.

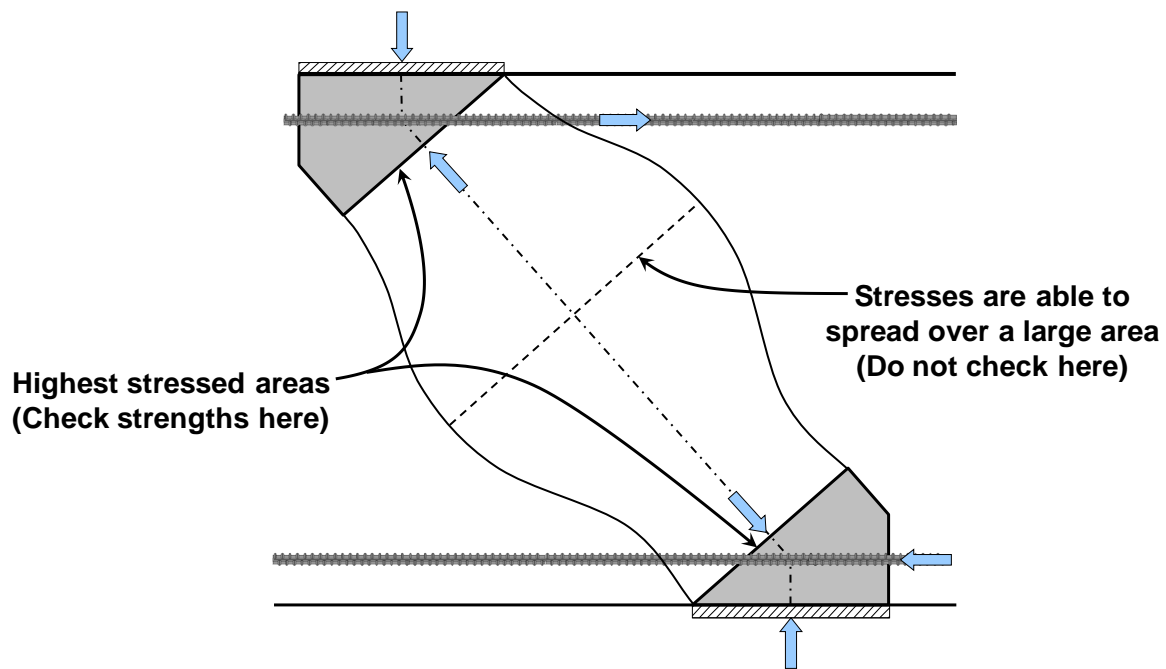


Figure 2.22: Stresses within a bottle-shaped strut

2.9.8 Special Consideration – Back Face of CCT/CTT Nodes

Based on the results of TxDOT Project 0-5253, the proposed STM specifications of Chapter 3 include an important comment regarding the back face of CCT and CTT nodes. The researchers concluded that the bond stresses from a tie that is adequately developed, as illustrated in Figure 2.23(a), do not need to be applied as a direct force to the back face when performing the nodal strength checks. This observation is also acknowledged by Thompson et al. (2003b) and fib (1999). If a condition other than the transfer of bond stresses exists and causes a force to be directly applied to the back face, the strength of the face must be sufficient to resist this force. This will occur, for example, when bars are anchored by a bearing plate or headed bar at a CCT node (see Figure 2.23(b)). In this case, the designer should assume that the bars are unbonded and are therefore fully developed at the anchor plate or bar head alone. A direct force also acts on the back face when diagonal struts join at a CCT node located over an interior support (see Figure 2.23(c)). The forces from the diagonal struts must be applied to the back face when performing the nodal strength checks.

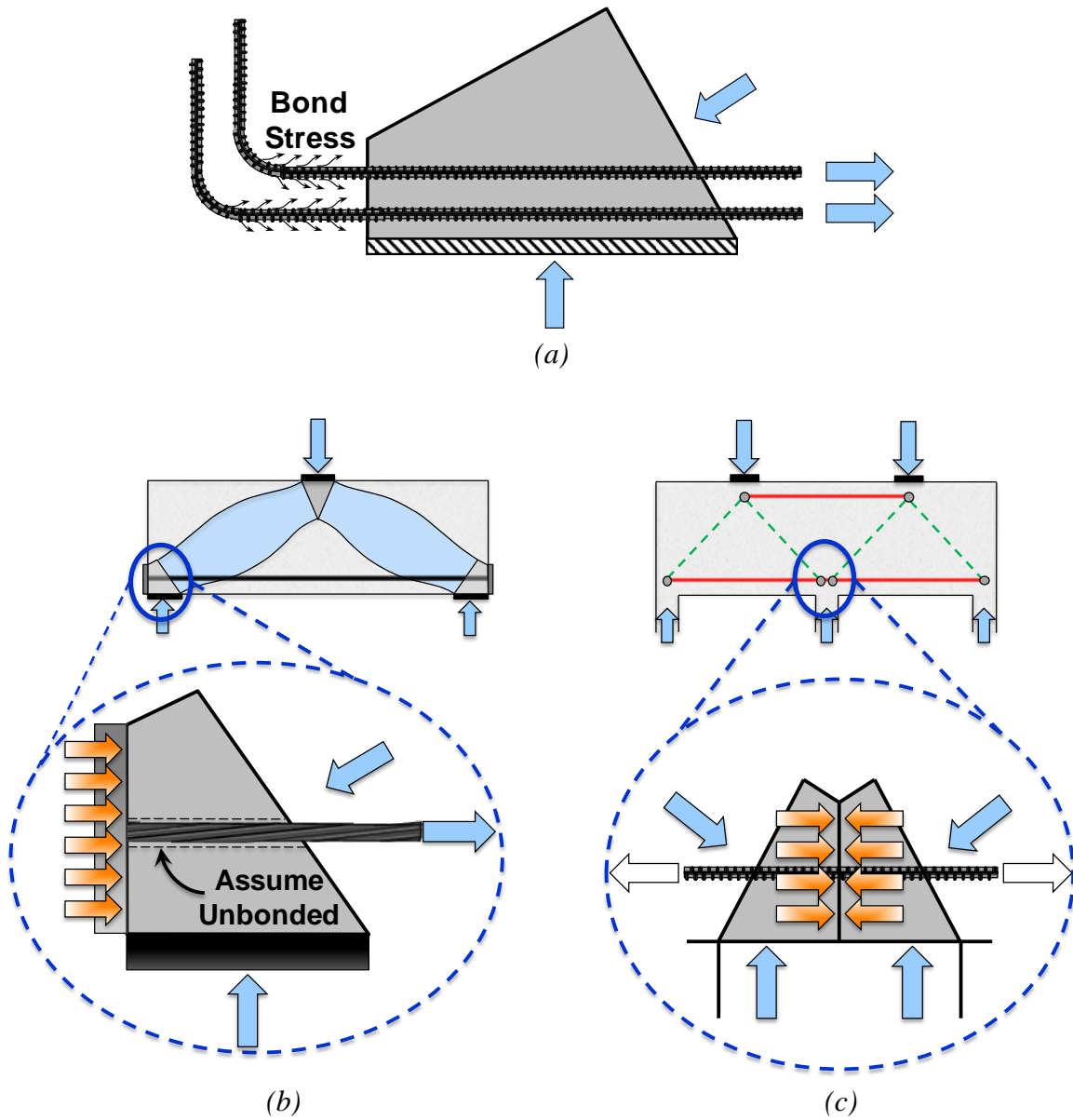


Figure 2.23: Stress condition at the back face of a CCT node – (a) bond stress resulting from the anchorage of a developed tie; (b) bearing stress applied from an anchor plate or headed bar; (c) interior node over a continuous support

2.10 PROPORTION CRACK CONTROL REINFORCEMENT

To restrain cracks in the concrete caused by the transverse tension that crosses diagonal bottle-shaped struts, crack control reinforcement should be provided throughout the structural component, except for slabs and footings (maintaining consistency with

other slab and footing provisions within AASHTO LRFD (2010)). To satisfy the crack control reinforcement requirement of the proposed STM specifications, 0.3% reinforcement must be provided in each orthogonal direction and should be evenly spaced within the effective strut area (refer to Figure 2.24). This is achieved by satisfying the following equations:

$$\frac{A_v}{b_w s_v} \geq 0.003 \quad (2.10)$$

$$\frac{A_h}{b_w s_h} \geq 0.003 \quad (2.11)$$

where:

- A_h = total area of horizontal crack control reinforcement within spacing s_h (in.²)
- A_v = total area of vertical crack control reinforcement within spacing s_v (in.²)
- b_w = width of member's web (in.)
- s_v, s_h = spacing of vertical and horizontal crack control reinforcement, respectively (in.)

These variables are illustrated in Figure 2.24. The spacing must not exceed $d/4$ or 12.0 in., where d is the effective depth of the member. The two equations above ensure that the bars are evenly spaced within the effective strut area indicated by the shaded region of Section A-A in Figure 2.24.

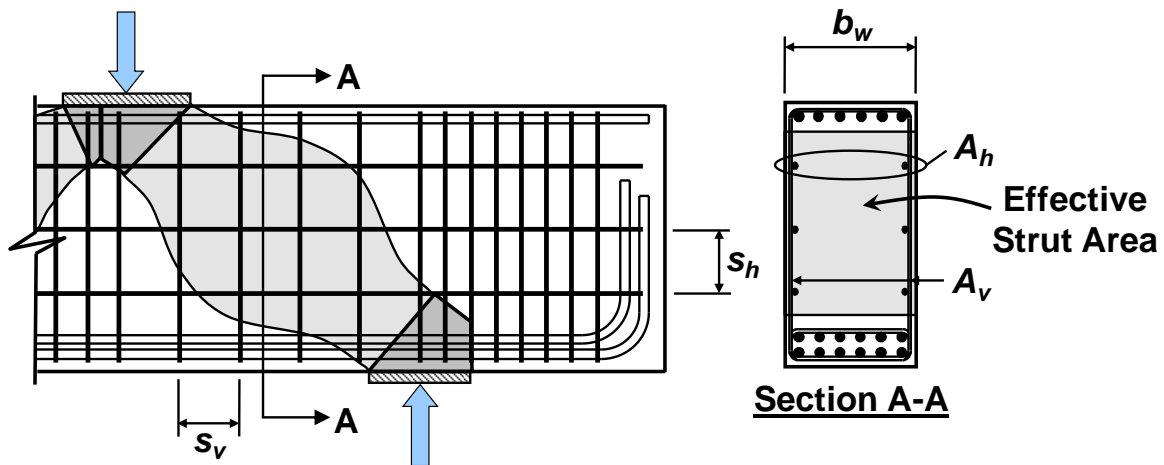


Figure 2.24: Web reinforcement within effective strut area (adapted from Birrcher et al., 2009)

The researchers of TxDOT Project 0-5253 concluded that providing 0.3% reinforcement in each direction is required for satisfactory serviceability performance. The amount of distributed web reinforcement is proportional to the widths of diagonal cracks that may form under service loads. Experimental tests revealed that 0.3% reinforcement is necessary “to adequately restrain maximum diagonal crack widths at first cracking and at estimated service loads” (Birrcher et al., 2009). The web reinforcement also prevents a premature strut-splitting failure and increases ductility by aiding in the redistribution of internal stresses. If crack control reinforcement is not provided, redistribution of stresses is virtually impossible. Not providing the required reinforcement may result in a reduction in the ultimate strength of the structural element. The possible strength degradation is reflected in the reduced concrete efficiency factor for the strut-to-node interfaces of the nodes within an element without 0.3% crack control reinforcement (refer to Section 2.9.7). Elements with little or no distributed web reinforcement were not of primary concern of TxDOT Project 0-5253. The concrete efficiency factor for the strut-to-node interface for such elements was therefore not subjected to the same level of scrutiny as the other efficiency factors. With this in mind, the importance of satisfying the minimum crack control reinforcement requirement cannot be overemphasized.

2.11 PROVIDE NECESSARY ANCHORAGE FOR TIES

The importance of careful detailing of the reinforcement within members designed using strut-and-tie modeling cannot be overemphasized. The ties must be properly anchored to ensure the structure can achieve the stress distribution assumed by the STM. For a tie to be properly anchored at a nodal region, the yield strength of the reinforcement should be developed at the point where the centroid of the bars exits the extended nodal zone (refer to Figure 2.25). In other words, the critical section for the development of the tie in Figure 2.25 is taken at the location where the centroid of the bars intersects the edge of the diagonal strut. This critical section is based on the provisions of ACI 318-08 §A.4.3. The experimental program of TxDOT Project 0-1855 revealed that “[s]hallow strut angles allowed a longer length of bar to be included within the bounds of the diagonal strut” and resulted in an increased anchorage (i.e. available) length (Thompson et al., 2003a). The development length that must be provided is determined from the provisions of Article 5.11.2 of AASHTO LRFD (2010) (development length \leq available length).

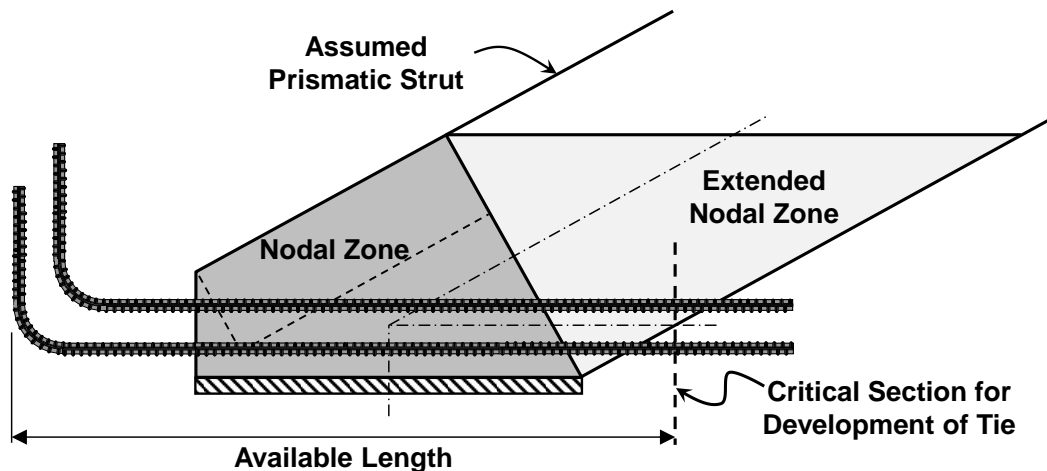


Figure 2.25: Available development length for ties (adapted from Birrcher et al., 2009)

At a curved-bar node, the bend radius of the bars must be sufficient to allow any difference in the forces of the two ties that extend from the node to be developed along

the bend region of the bars, as explained in Section 2.9.6 (Klein, 2008). This requirement can be satisfied by using the procedure presented in the commentary to Article 5.6.3.4.2 of the proposed STM specifications of Chapter 3.

Both the AASHTO LRFD (2010) and the ACI 318-08 specifications include a modification factor that can be used to reduce the development length when reinforcement is provided in excess of what is required. This modification factor is defined by the ratio $(A_s \text{ required})/(A_s \text{ provided})$. The use of this factor is acceptable when it is needed. Ignoring the factor, however, aids in the ability of the stresses to redistribute within the structural member and helps to increase the member's ductility. For these reasons, the factor is ignored in the design examples of the following chapters.

2.12 PERFORM SHEAR SERVICEABILITY CHECK

During the strut-and-tie modeling design process, a check of the expected shear serviceability behavior of the structural member should be performed, if applicable. This shear serviceability check is based on results from TxDOT Project 0-5253, and its purpose is to predict the likelihood of the formation of diagonal cracks within the D-regions of a beam. To perform the check, the shear forces in the D-regions of a beam due to unfactored service loads are calculated. The estimated load at which diagonal cracks begin to form, V_{cr} , is then determined for the D-regions using the following expression:

$$V_{cr} = \left[6.5 - 3 \left(\frac{a}{d} \right) \right] \sqrt{f'_c} b_w d \quad (2.12)$$

but not greater than $5\sqrt{f'_c} b_w d$ nor less than $2\sqrt{f'_c} b_w d$

where:

- a = shear span (in.)
- d = effective depth of the member (in.)
- f'_c = specified compressive strength of concrete (psi)
- b_w = width of member's web (in.)

Therefore, V_{cr} depends on the a/d ratio of the D-region under consideration as well as the compressive strength of the concrete, f'_c , and the effective shear area, $b_w d$.

After calculating the value of V_{cr} for a particular region, it is compared to the maximum service level shear force in that portion of the member. If the maximum service level shear force is less than V_{cr} , diagonal cracks are not expected to form under service loads. If the maximum service level shear force is larger than V_{cr} , the designer should expect diagonal cracking while the member is in service. The designer may choose to accept the risk of serviceability cracking if durability and aesthetic issues are not a concern. Otherwise, a few options are available to prevent the formation of serviceability cracks. First, the likelihood of diagonal cracks can be reduced by increasing the compressive strength of the concrete. Modifying the geometry of the member by increasing the effective shear area, $b_w d$, and/or by decreasing the a/d ratio can also reduce the risk of diagonal cracking. Alternatively, if these options are not feasible, additional distributed crack control reinforcement can be provided to better control the widths of the cracks that form. The experimental program of TxDOT Project 0-5253, however, revealed that providing web reinforcement in excess of 0.3% resulted in only a “moderate reduction in the maximum diagonal crack widths” at the expected service load (Birrcher et al, 2009).

Considering the modifications to the member’s geometry that the shear serviceability check may require, the designer is encouraged to size the structural component during the preliminary design phase using the diagonal cracking load equation to prevent the need for such modifications later.

A plot of the normalized cracking load versus the a/d ratio of specimens tested as part of TxDOT Project 0-5253 as well as other studies found in the literature is presented in Figure 2.26. The estimated diagonal cracking load equation is also included on the plot. The reader should note that the upper and lower limits of the equation occur at a/d ratios of 0.5 and 1.5, respectively. As shown by the plot, the equation is a reasonably conservative, lower-bound estimate.

The proposed serviceability check is performed for the structural components included in the design examples of the following chapters with the exception of the design of the drilled-shaft footing in Chapter 8 since the equation presented above is only applicable to beams.

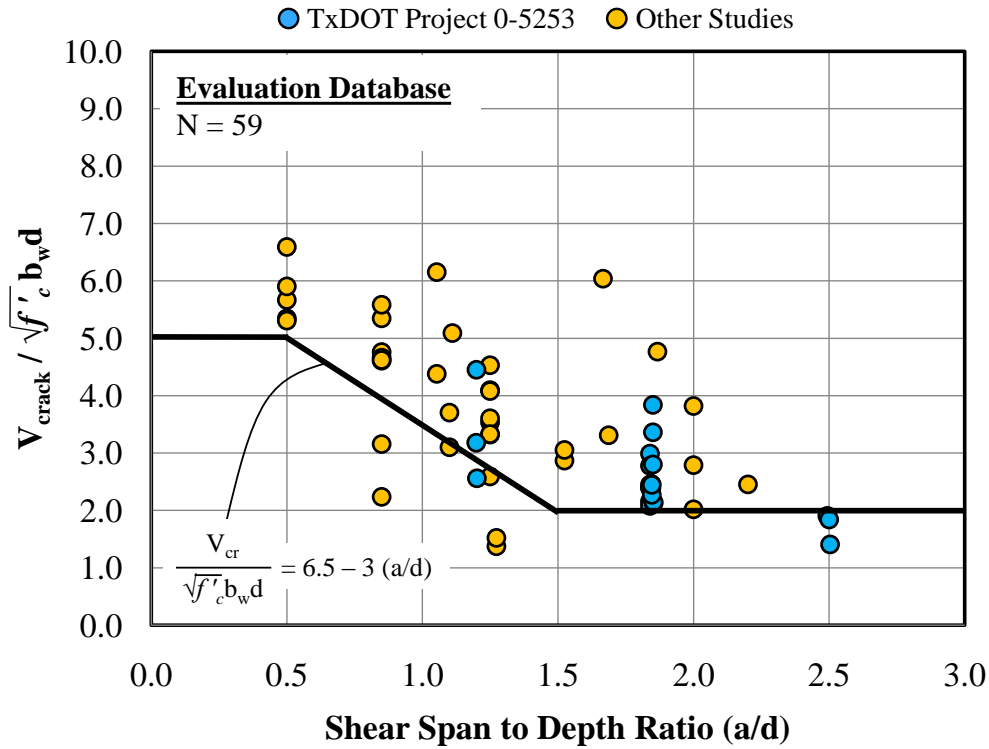


Figure 2.26: Diagonal cracking load equation with experimental data (from Birrcher et al., 2009)

2.12.1 Special Note – Shear Serviceability Check

The design examples presented within this guidebook serve to illustrate the application of the proposed STM specifications of Chapter 3. To enhance the value of the design examples for practicing bridge engineers, each example is based upon an existing field structure in Texas. Information provided by TxDOT (e.g. the geometry of the structural elements) serves as the starting point for each design example. The shear serviceability check is therefore performed as the last step of the design procedure in order to discuss the likelihood of diagonal crack formation under service loads. In

reality, the design engineer may wish to utilize the shear serviceability check during the preliminary design phase as a means of initially sizing the structural element.

2.13 SUMMARY

Strut-and-tie modeling is a lower-bound method used primarily to design D-regions of structural components. A nonlinear strain distribution exists within D-regions due to a load or geometric discontinuity. The assumptions inherent within the sectional design approach are therefore invalidated. The STM procedure is needed to design the regions of structures where the behavior is dominated by a nonlinear distribution of strains. Strut-and-tie modeling will always result in a conservative solution if the basic design principles are satisfied. During the design procedure, a truss model, or strut-and-tie model, is developed to represent the flow of forces within a structure. A strut-and-tie model consists of compression members referred to as struts, tension members called ties, and the regions where these two components intersect called nodes.

The beginning of the STM design procedure typically consists of separating the structural component into B- and D-regions, defining the load case(s), and performing an overall structural analysis of the component. Then, the strut-and-tie model is developed. Although several STMs may be valid for the particular geometry of a structural component and the applied loading, the designer should use the option that best represents the elastic flow of forces within the structure. Guidelines for making this decision have been provided. Once the chosen STM is analyzed, the amount of reinforcement needed to carry the tie forces is determined and the strengths of the nodes are ensured to be adequate to resist the applied forces. Crack control reinforcement must be provided to carry the tensile stresses that develop transverse to diagonal bottle-shaped struts within structures or regions designed using STM, with the exception of slabs and footings. The designer must also make certain that the tie reinforcement is properly anchored to ensure the state of stress assumed by the chosen strut-and-tie model can be achieved. The importance of the detailing of reinforcement cannot be overemphasized. During the design process, a shear serviceability check is performed to determine the

likelihood of the formation of diagonal cracks when the member is in service. If the existence of diagonal cracks is expected, the designer is given a set of options that can be incorporated into the structural design to prevent future serviceability cracking.

A brief overview of TxDOT Project 0-5253 is provided in Chapter 3 along with the proposed STM specifications.

Chapter 3. Proposed Strut-and-Tie Modeling Specifications

3.1 INTRODUCTION

The strut-and-tie modeling specifications developed as part of TxDOT Projects 0-5253 and 5-5253-01 are presented in this chapter. Revisions to the *AASHTO LRFD Bridge Design Specifications* (2008) were first recommended by the researchers of TxDOT Project 0-5253. Their recommendations were based on 35 large-scale experimental tests as well as a complementary deep beam database of 144 tests from the literature. A brief overview of the work completed during TxDOT Project 0-5253 precedes the presentation of the proposed strut-and-tie modeling specifications within this chapter. A few additions and minor changes to the recommendations of TxDOT Project 0-5253 were made within the context of the current implementation project (5-5253-01). The modifications are intended to facilitate practical application of strut-and-tie modeling to common bridge structures. The specifications proposed within this chapter serve as the basis for the structural designs presented in Chapters 4 through 8.

3.2 OVERVIEW OF TxDOT PROJECT 0-5253

TxDOT Project 0-5253, D-Region Strength and Serviceability Design, provided the experimental basis necessary for the development of safe, simple strut-and-tie modeling specifications. The proposed revisions to the *AASHTO LRFD Bridge Design Specifications* (2010) (presented in Section 3.3.3) are largely based upon the deep beam database and large-scale testing efforts of TxDOT Project 0-5253. The details of this project, as reported in Birrcher et al. (2009), are briefly summarized in the sections that follow.

3.2.1 Deep Beam Database

A database of deep beam shear tests was compiled to complement the experimental program and assist with the calibration of the proposed design specifications. Shear tests found within the literature were only included in the database if the shear span-to-depth ratio, a/d , of the specimen was 2.5 or less, characteristic of a

deep beam. The number of shear tests in the literature that met this criterion was 868. An additional 37 tests conducted as part of project 0-5253 resulted in a total of 905 shear tests within the *collection database*. The collection database was subsequently filtered to only include tests that were accompanied by the information necessary for an STM analysis to be performed. The resulting set of 607 tests was referred to as the *filtered database*. Lastly, tests on specimens that were not considered representative of field structures were removed; thereby establishing an *evaluation database* of 179 tests (35 tests from project 0-5253 plus 144 tests from the literature). The evaluation database was used to develop and evaluate the proposed STM specifications presented in Section 3.3.3. The database filtering process is summarized in Table 3.1; the variable ρ_{\perp} represents the distributed web reinforcement defined by Eq. A-4 in ACI 318-08 §A.3.3.1.

Table 3.1: Filtering of the deep beam database of TxDOT Project 0-5253 (from Birrcher et al., 2009)

<i>Collection Database</i>		<i>905 tests</i>
Stage 1 filtering	- incomplete plate size information	- 284 tests
	- subjected to uniform loads	- 7 tests
	- stub column failure	- 3 tests
	- $f'_c < 2,000$ psi	- 4 tests
<i>Filtered Database</i>		<i>607 tests</i>
Stage 2 filtering	- $b_w < 4.5$ in.	- 222 tests
	- $b_w d < 100$ in. ²	- 73 tests
	- $d < 12$ in.	- 13 tests
	- $\sum \rho_{\perp} < 0.001$	- 120 tests
<i>Evaluation Database</i>		<i>179 tests</i>

3.2.2 Experimental Program

The experimental program of TxDOT Project 0-5253 consisted of 37 tests of some of the largest deep beam specimens found in the literature. Figure 3.1 is provided to illustrate the scale of the project 0-5253 specimens relative to other database

specimens as well as bent caps currently in service within the state of Texas. The five cross-sections at the far right of the figure were tested as part of experimental programs that helped to provide the basis for much of the current deep beam design specifications.

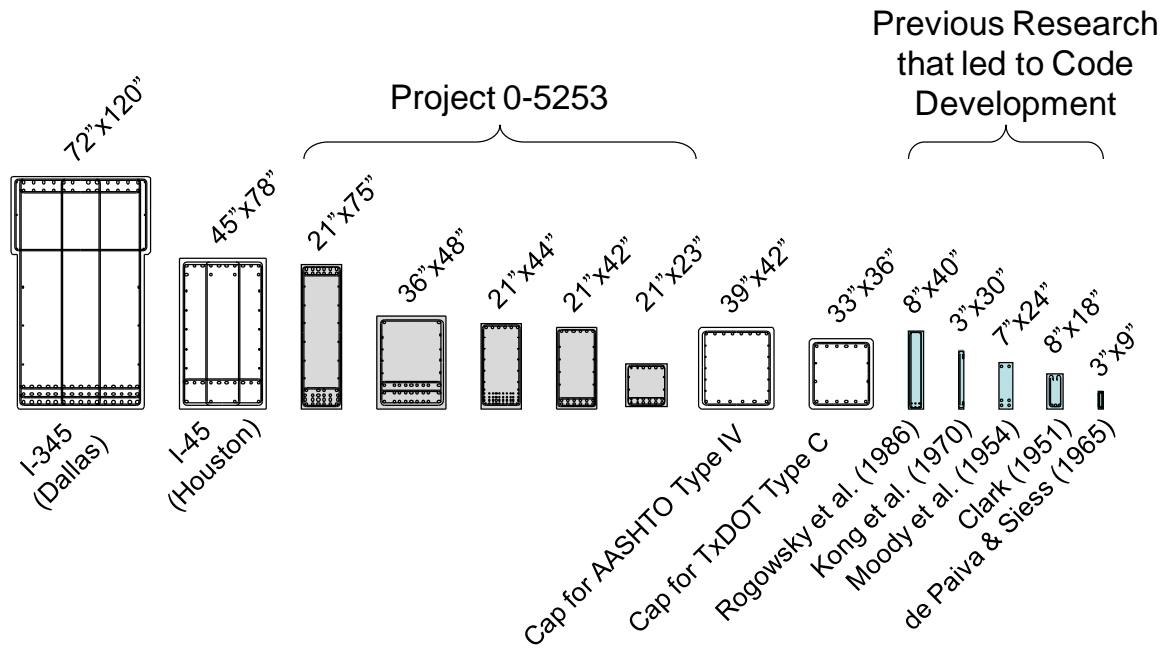


Figure 3.1: Scaled comparison of deep beams (from Birrcher et al., 2009)

The deep beams tested during project 0-5253 ranged in height from 23 in. to 75 in. Other variables of the testing program included beam width, bearing plate size, shear span-to-depth ratio, quantity of web reinforcement, and distribution of stirrups across the web of the member. The test setup built for the purposes of project 0-5253 is depicted in Figure 3.2.

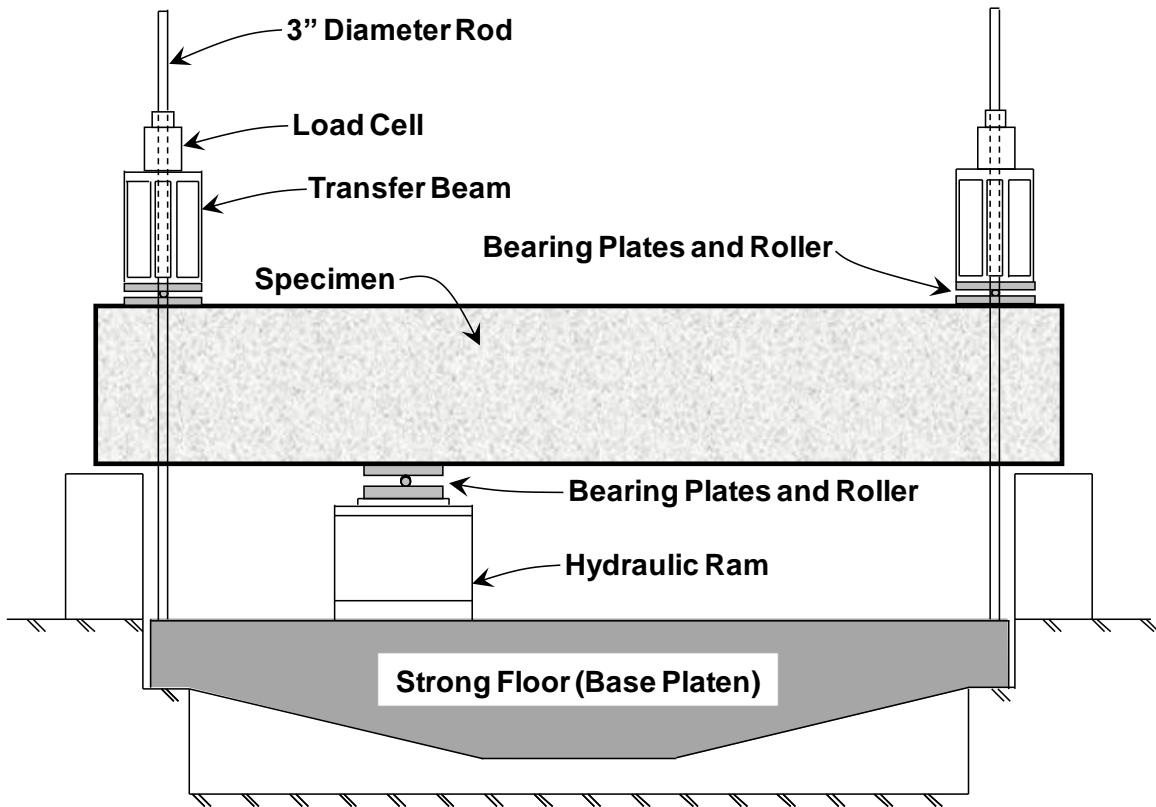


Figure 3.2: Elevation view of test setup for TxDOT Project 0-5253 (from Birrcher et al., 2009)

3.2.3 Objectives and Corresponding Conclusions

The researchers of TxDOT Project 0-5253 addressed eight objectives related to the design and performance of reinforced concrete deep beams. Each objective is listed below along with the corresponding conclusions most pertinent to the design implementation of strut-and-tie modeling. The complete details of the experimental work and findings of TxDOT Project 0-5253 can be found in Birrcher et al. (2009).

For the first four objectives of project 0-5253, the influence of four independent variables on the strength and serviceability of deep beams was examined. These variables were addressed with the experimental program of project 0-5253 (i.e. the 37 deep beam tests). Each of the variables is listed below and examined in the context of the final project recommendations:

1. The distribution of stirrups across the web of the beam (2 legs versus 4 legs) – The AASHTO LRFD (2008) STM specifications limit the assumed width of a strut framing into a CTT node within a D-region of a wide beam if stirrups are not distributed across the web of the beam (i.e. the width of the strut cannot be taken as the full width of the beam). The researchers concluded that the limitation is unnecessary primarily because the strength of CTT nodes is rarely critical within D-regions. Based on the results of the experimental program, the researchers also added the following statement to the commentary of the proposed STM specifications (Article C5.6.3.3.2 in Section 3.3.3): “Beams wider than 36 inches, or beams with a width to height aspect ratio greater than one may benefit from distributing stirrup legs across the width of the cross-section.”
2. Triaxial confinement (via concrete) of nodal regions – The researchers concluded that the triaxial confinement factor, m , presented in Section 2.9.7 can be applied to increase the strengths of nodal regions. The test results revealed that use of the m -factor results in greater STM accuracy and reduces the level of unwarranted conservatism. The confinement factor can be applied to all faces of a node that abuts a bearing area that has a width that is smaller than the width of the member (refer to Figure 2.20).
3. The amount of minimum web reinforcement (transverse and longitudinal) - The serviceability behavior of the test specimens revealed that 0.3% reinforcement spaced evenly in each direction within the effective strut area is needed to adequately restrain the maximum widths of diagonal cracks at both first cracking and at estimated service loads. Experimental evidence showed that providing 0.2% reinforcement in each direction (or less) results in unsatisfactory serviceability performance. Article 5.6.3.6 of the AASHTO LRFD (2010) STM specifications has been updated to comply with these findings.
4. The depth of the member – The researchers discovered that the strength of a deep beam region is not a direct function of the effective depth of the member but is instead governed by the size and stress conditions of the nodal regions (provided

that the force in the longitudinal tie does not control and the diagonal bottle-shaped strut is properly reinforced). In other words, strut-and-tie modeling should be used for the design of deep beam regions since the traditional sectional shear design approach unrealistically correlates member shear strength to effective depth.

Project recommendations concerning the last four objectives were based upon analysis of the evaluation database (i.e. project 0-5253 tests and results from the literature).

5. Improvement of strut-and-tie design method for deep beams – The final report of TxDOT Project 0-5253 includes STM design recommendations that are both simpler and more accurate than the STM specifications of AASHTO LRFD (2008) and ACI 318-08. While the STM methodology of *fib* (1999) served as the basis for the new recommendations, the design expressions were carefully calibrated against specimens within the project 0-5253 evaluation database that were more representative of actual field members. The researchers took care to further ensure that the recommendations would maintain a sense of consistency with the general design procedures of AASHTO LRFD (2008) and ACI 318-08.
6. Improvement of the discrepancy in shear design models at the transition from deep beam to sectional behavior at an a/d ratio of 2 – The shear behavior of a beam transitions from deep beam behavior to sectional shear behavior as the a/d ratio approaches and exceeds 2. This phenomenon is due to the variation of strains within the member as described in Section 2.2. The transition is gradual; within this transitional region, therefore, the discrepancy between the shear strengths calculated from the sectional design procedure and the STM procedure should be minimized. The AASHTO LRFD (2008) STM specifications, however, result in excessive conservatism at an a/d ratio of 2, causing an unnecessary discrepancy between the two design models. The proposed STM specifications largely eliminate this excessive conservatism, reducing the discrepancy between STM and sectional shear design for a/d ratios near 2. The researchers also

- recommend limiting the ratio of V_s/V_c of the sectional shear provisions to a value of 2 to further reduce the discrepancy (V_s and V_c are the shear resistance of the transverse steel and the concrete, respectively).
7. Recommendation for limiting diagonal cracking under service loads – An equation to predict the diagonal cracking load of a structure was developed using data from the tests within the evaluation database for which the load at first diagonal cracking was known. The proposed diagonal cracking load equation and all relevant details of the corresponding shear serviceability check that is performed as part of the STM design procedure were discussed in Section 2.12.
 8. Method to correlate maximum width of diagonal cracks to residual capacity of in-service bent caps – This task resulted in a means for engineers to estimate the residual capacity of an in-service bent cap by measuring the maximum diagonal crack width in the member. The researchers used data from 21 tests of the project 0-5253 experimental program to develop a chart that correlates the maximum crack width of a beam to the percent of its ultimate capacity that is expected to cause such cracking. The chart is a function of the amount of web reinforcement within the member, the primary variable found to affect the widths of cracks. The chart is applicable for deep beam regions with a/d ratios between 1 and 2 but should not be used for inverted-T bent caps.

The results of TxDOT Project 0-5253 also led to important insights that extend beyond the aforementioned conclusions, the most significant of which are described below:

- Emphasis should be placed on singular nodes since the stresses at smeared nodes are not critical and need not be checked (refer to Section 2.9.5). This conclusion is supported by *fib* (1999) and Schlaich et al. (1987) and is incorporated within Article 5.6.3.2 of the proposed STM specifications of Section 3.3.3. Unlike stresses acting on singular nodes, compressive stresses at smeared nodes are able to disperse over relatively large areas that do not have clearly defined boundaries.

- Bond stresses of an adequately developed bar do not need to be applied as a direct force to the back face of a CCT or CTT node (refer to Section 2.9.8). This principle is described in Article C5.6.3.3.3a of the proposed STM specifications of Section 3.3.3. The experimental tests revealed that the bond stresses do not concentrate at the back face. The crushing of concrete at a back face due to the bond stresses of adequately anchored bars is therefore very unlikely. None of the specimens of the project 0-5253 experimental program or those in the literature experienced failure at the back face of a CCT node where reinforcement was properly developed.
- The researchers recommend designing a deep beam region with an a/d ratio less than or equal to 2 with a single-panel STM. In contrast, they suggest using a sectional shear model to design regions with an a/d ratio greater than 2. These recommendations are consistent with the observed behavior of the test specimens. Evidence is given, however, that a single-panel STM can result in conservative designs for members with a/d ratios of up to 2.5.

If a member consists almost entirely of D-regions with only a small portion considered to be a B-region, a designer may wish to simplify the design process by using the STM procedure to design the entire member. In contrast to the sectional shear provisions, strut-and-tie modeling does not consider the contribution of the concrete to the shear strength of a structural component. Designing the entire member (i.e. the D-regions and the small B-region) using STM will therefore result in a conservative design. Using STM for the entire member may be a practical option despite the recommendation of the project 0-5253 researchers to design regions with an a/d ratio greater than 2 by using a sectional shear model (refer to the design of the inverted-T bent cap of Chapters 6 and 7).

3.3 PROPOSED STRUT-AND-TIE MODELING SPECIFICATIONS

3.3.1 Overview of Proposed Specifications

New STM specifications were developed as part of TxDOT Project 0-5253, and the researchers recommended that both the ACI 318 and AASHTO LRFD provisions be modified accordingly (Birrcher et al., 2009). Further updates have been applied to the proposed STM specifications as a result of the current implementation project. The specifications recommended for inclusion within future versions of the *AASHTO LRFD Bridge Design Specifications* are presented in Section 3.3.3. Two of the most significant revisions that are proposed for AASHTO LRFD are presented below:

- The proposed concrete efficiency factors, v , for the nodal faces have been revised based on the tests within the TxDOT Project 0-5253 deep beam evaluation database.
- The design of a strut is not explicitly performed but is accounted for in the design of the strut-to-node interface of the nodes, encouraging the engineer to focus on the most critically stressed regions of the structural member.

3.3.2 Updates to the TxDOT Project 0-5253 Specifications as a Result of the Current Implementation Project (5-5253-01)

As a result of the current implementation project, a few additions and fairly minor changes were incorporated into the STM specifications of TxDOT Project 0-5253. These additions and changes are intended to facilitate application of STM design to bridge components in practice. The major modifications are listed below alongside short explanations of why they have been incorporated into the proposed specifications:

- Provisions for the design of curved-bar nodes were added – The curved-bar node provisions included in the STM specifications are based on Klein (2008) and are incorporated into the design examples of Chapters 5 and 6. The provisions are considered extremely valuable for the proper design of nodes located at the outside of frame corners.

- The critical point at which the yield strength of tie bars must be developed was revised – Reinforcing bars should be fully developed at the point where their centroid exits the extended nodal zone as explained in Section 2.11 and illustrated in Figure 2.25. Research has shown (Thompson et al., 2003a, 2003b) that taking the critical development point at this location is more accurate than the AASHTO LRFD (2010) requirement that the tie be developed at the inner face of the nodal zone.
- The strength provided by compression reinforcement entering the back face of a node is now considered – The stress that can be carried by compression reinforcement at a back face can be significant, and considering the effect of this steel is often necessary for developing a practical design. A provision for considering the contribution of the compression reinforcement is included in the AASHTO LRFD (2010) STM specifications. Consistency was kept between this provision and the updated STM specifications in Section 3.3.3.
- Concrete efficiency factors, v , are now included for CTT nodes – The design examples reveal that CTT nodes are not always considered to be smeared. Nodal strength checks on CTT nodes, therefore, may be necessary. In addition, a curved-bar node at a frame corner is a CTT node, and a concrete efficiency factor is needed for their design (Klein, 2008). The proposed concrete efficiency factors, v , for CTT nodes are believed to be conservative. Further experimental tests, however, are recommended to develop more accurate factors for these nodes.
- The 65-degree limit for the angle between the axes of a strut and tie entering a single node was removed – The commentary of the STM specifications proposed in the TxDOT Project 0-5253 report (Article C5.6.3.1) states that “[t]he angle between the axes of a strut and tie should be limited between 25 to 65 degrees.” Limiting the angle to a value greater than 25 degrees is deemed sufficient considering the large angles between some of the struts and ties within the STM of Chapter 4. The orientation of these steep struts is necessary and should not

adversely affect the structural member. Therefore, the 65-degree limit has been removed.

- The proposed specifications were revised to correspond with the AASHTO LRFD (2010) STM specifications – The crack control reinforcement provisions recommended as a result of TxDOT Project 0-5253 were incorporated into the AASHTO LRFD (2010) STM specifications. The language and bold text (representing changes to the current AASHTO LRFD code) used within the specifications presented in Section 3.3.3 consider the updates included in AASHTO LRFD (2010).

3.3.3 Proposed Revisions to the AASHTO LRFD Bridge Design Specifications

The STM specifications presented below are proposed revisions to AASHTO LRFD (2010). The articles are therefore numbered to correspond with their placement within the AASHTO LRFD strut-and-tie modeling specifications. The proposed changes to the current provisions are denoted with bold text.

5.6.3—Strut-and-Tie Model

5.6.3.1—General

Strut-and-tie models may be used to determine internal force effects near supports and the points of application of concentrated loads at strength and extreme event limit states.

The strut-and-tie model should be considered for the design of deep footings and pile caps or other situations in which the distance between the centers of applied load and the supporting reactions is less than about twice the member **depth**.

The angle between the axes of any strut and any tie entering a single node shall not be taken as less than 25 degrees.

If the strut-and-tie model is selected for structural analysis, Articles 5.6.3.2 through 5.6.3.5 shall apply.

C5.6.3.1

Where the conventional methods of strength of materials are not applicable because of nonlinear strain distribution, strut-and-tie modeling may provide a convenient way of approximating load paths and force effects in the structure. The load paths may be visualized and the geometry of concrete and steel **reinforcement** selected to implement the load path.

The strut-and-tie model is new to these Specifications. More detailed information on this method is given by Schlaich et al. (1987) and Collins and Mitchell (1991).

Traditional section-by-section design is based on the assumption that the reinforcement required at a particular section depends only on the separated values of the factored section force effects V_u , M_u , and T_u and does not consider the mechanical interaction among these force effects as the strut-and-tie model does. The traditional method further assumes that shear distribution remains uniform and that the longitudinal strains will vary linearly over the depth of the beam.

For members such as the deep beam shown in Figure C5.6.3.2-1, these assumptions are not valid. The behavior of a component, such as a deep beam, can be predicted more accurately if the flow of forces through the complete structure is studied. Instead of determining V_u and M_u at different sections along the span, the flow of compressive stresses going from the loads, P , to the supports and the required tension force to be developed between the supports should be established.

The angle between the axes of a strut and tie should not be less than 25 degrees in order to mitigate wide crack openings and excessive strain in the reinforcement at failure.

For additional applications of the strut-and-tie model, see Articles 5.10.9.4, 5.13.2.3, and 5.13.2.4.1.

5.6.3.2—Structural Modeling

The structure and a component or region, thereof, may be modeled as an assembly of steel tension ties and concrete compressive struts interconnected at nodes to form a truss capable of carrying all applied loads to the supports. **The**

C5.6.3.2

Cracked reinforced concrete carries load principally by compressive stresses in the concrete and tensile stresses in the reinforcement. The principle compressive stress trajectories in the concrete can be approximated by compressive struts.

determination of a truss is dependent on the geometry of the singular nodal regions as defined in Figure 5.6.3.2-1. The geometry of CCC and CCT nodal regions shall be detailed as shown in Figures 5.6.3.2-1 and 5.6.3.2-2. Proportions of nodal regions are dependent on the bearing dimensions, reinforcement location, and depth of the compression zone as illustrated in Figure 5.6.3.2-2.

An interior node that is not bounded by a bearing plate and has no defined geometry is referred to as a smeared node. Since D-regions contain both smeared and singular nodes, the latter will be critical and a check of concrete stresses in smeared nodes is unnecessary.

The factored nominal resistance of each face of a nodal region and of a tie, ϕF_n , shall be proportioned to be greater than the factored force acting on the node face or in the tie, F_u :

$$\phi F_n \geq F_u \quad (5.6.3.2-1)$$

where:

F_n = nominal resistance of a node face or tie (kip)

Tension ties are used to model the principal reinforcement.

A strut-and-tie model is shown in Figure 5.6.3.2-1 for a simply supported deep beam. The zone of high unidirectional compressive stress in the concrete is represented by a compressive strut. The regions of the concrete subjected to multidirectional stresses, where the struts and ties meet the joints of the truss, are represented by nodal zones.

Research has shown that a direct strut is the primary mechanism for transferring shear within a D-region. Therefore, a single-panel truss model is illustrated in Figure 5.6.3.2-1 and may be used in common D-regions such as transfer girders, bents, pile caps, or corbels.

Stresses in a strut-and-tie model concentrate at the nodal zones. Failure of the structure may be attributed to the crushing of concrete in these critical nodal regions. For this reason, the capacity of a truss model may be directly related to the geometries of the nodal regions. Singular nodes have geometries that can be clearly defined and are more

F_u = **factored force acting on the face of a node or in a tie (kip)** **critical than smeared nodes (Schlaich et al., 1987). Conventional techniques to be used for proportioning singular nodes are illustrated in Figure 5.6.3.2-2.**

ϕ = resistance factor for tension or compression specified in Article 5.5.4.2, as appropriate

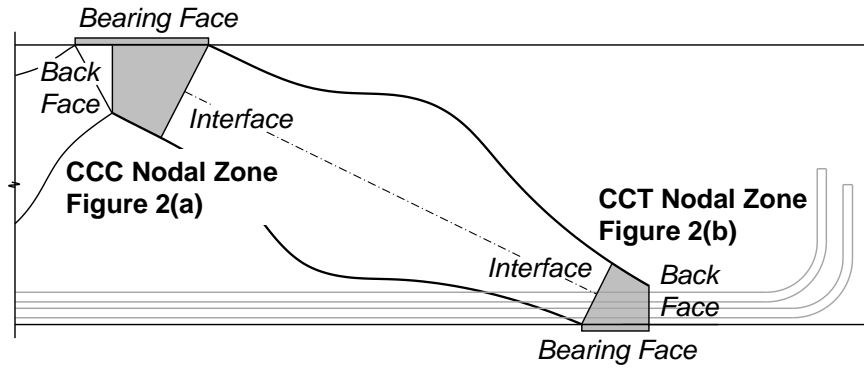
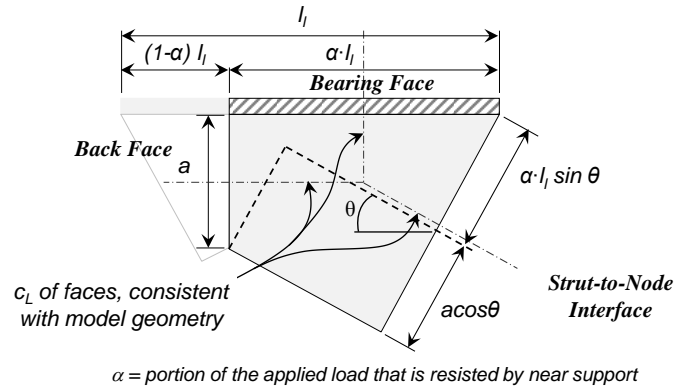
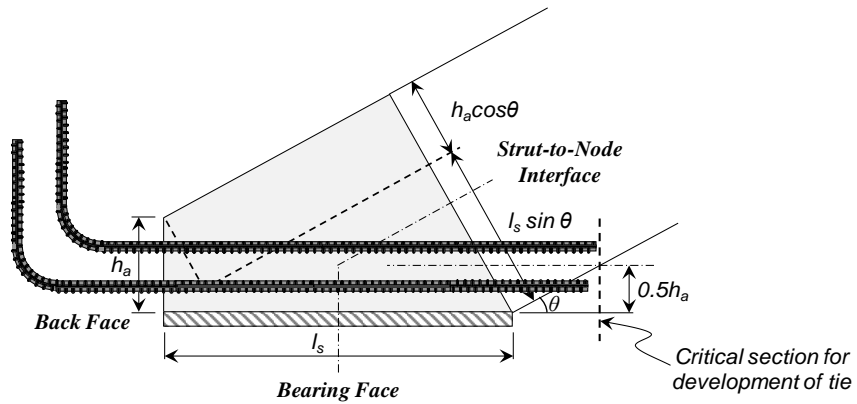


Figure 5.6.3.2-1—Strut-and-Tie Model for a Deep Beam



(a) CCC Node



(b) CCT Node

Figure 5.6.3.2-2—Nodal Geometries

5.6.3.3—Proportioning of Nodal Regions

5.6.3.3.1—Strength of the Face of a Node

The nominal resistance of **the face of a node** shall be taken as:

$$P_n = f_{cu}A_{cn} \quad (5.6.3.3.1-1)$$

where:

P_n = nominal resistance of **the face of a node** (kip)

f_{cu} = limiting compressive stress as specified in Article 5.6.3.3.3 (ksi)

A_{cn} = effective cross-sectional area of **the face of a node** as specified in Article 5.6.3.3.2 (in.²)

5.6.3.3.2—Effective Cross-Sectional Area of the Face of a Node

C5.6.3.3.2

The value of A_{cn} shall be determined by considering the **details of the nodal region as illustrated** in Figure 5.6.3.2-2.

When a strut is anchored by reinforcement, **the back face of the CCT node, h_a** , may be considered to extend **twice the distance from the exterior surface of the beam to the centroid of the longitudinal tension reinforcement**, as shown in Figure 5.6.3.2-2 (b).

Research has shown that the shear behavior of conventionally reinforced deep beams as wide as 36 in. are not significantly influenced by the distribution of stirrups across the section. Beams wider than 36 in. or beams with a width to height aspect ratio greater than one may benefit from distributing stirrup legs across the width of the cross-section.

The depth of the back face of a CCC node, h_s , as shown in Figure 5.6.3.2-2 (a), may be taken as the effective depth of the compression stress block determined from a conventional flexural analysis.

5.6.3.3.3—Limiting Compressive Stress at the Face of a Node

C5.6.3.3.3

Unless confining reinforcement is provided and its effect is supported by analysis or experimentation, the limiting compressive stress at the face of a node, f_{cu} , shall be taken as:

Concrete efficiency factors have been selected based on simplicity in application, compatibility with other sections of the Specifications, compatibility with tests of D-regions, and compatibility with other provisions.

$$f_{cu} = mvf'_c \quad (5.6.3.3.3-1)$$

where:

f'_c = specified compressive strength of concrete (ksi)

m = confinement modification factor, taken as $\sqrt{A_2/A_1}$ but not more than 2 as defined in Article 5.7.5

v = concrete efficiency factor:

0.85; bearing and back face of CCC node

0.70; bearing and back face of CCT node

The stress applied to the back face of CCT node may be reduced as permitted in Article 5.6.3.3.3a.

$0.85 - f'_c / 20 \text{ ksi}$; CCC and CCT
strut-to-node interface and all faces
of CTT node

*Not to exceed 0.65 nor less than
0.45*

**0.45; CCC, CCT, and CTT strut-to-
node interface:** *Structures that do not
contain crack control reinforcement
(Article 5.6.3.5)*

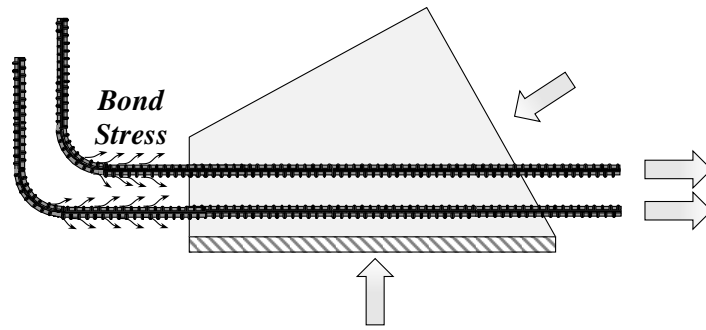
In addition to satisfying strength
criteria, the nodal regions shall be
designed to comply with the stress and
anchorage limits specified in Articles
5.6.3.4.1 and 5.6.3.4.2.

*5.6.3.3.3a—Back Face of CCT and
CTT Nodes*

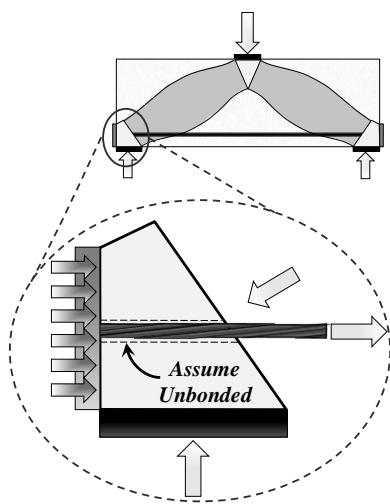
Bond stresses resulting from the
force in a developed tension tie need not
be applied to the back face of a CCT or
CTT node.

C5.6.3.3.3a

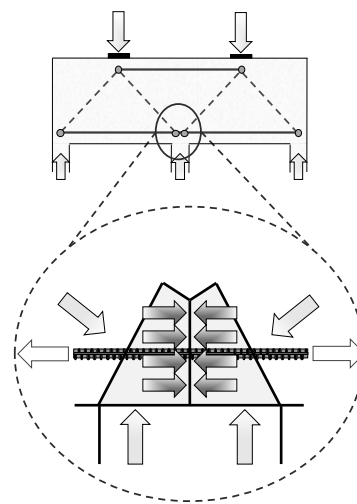
The stress that may act on the back
face of a CCT or CTT node can be
attributed to the anchorage of a tie,
bearing from an anchor plate or headed
bar, or a force introduced by a strut
such as that which acts on a node located
above a continuous support (Figure
C5.6.3.3.3a-1).



(a) Bond stress resulting from the anchorage of a developed tie



(b) Bearing stress applied from an anchor plate or headed bar



(c) Interior node over a continuous support

Figure C5.6.3.3.3a-1—Stress Condition at the Back Face of a CCT Node

If the tie is adequately developed, the bond stresses are not critical and need not be applied as a direct force to the back face of a CCT or CTT node when performing the nodal strength checks.

If the stress applied to the back face of a CCT or CTT node is from an

anchor plate or headed bar, a check of the back face strength should be made assuming that the bar is unbonded and all of the tie force is transferred to the anchor plate or bar head.

If the stress acting on the back face of a CCT or CTT node is the result of a combination of both anchorage and a discrete force from a strut, the node only needs to be proportioned to resist the direct compressive stresses. The bond stresses do not need to be applied to the back face, provided the tie is adequately anchored.

5.6.3.3.4—Back Face with Compression Reinforcement

If a compressive stress acts on the back face of a node and reinforcement is provided parallel to the applied stress and is detailed to develop its yield strength in compression, the nominal resistance of the back face of the node shall be taken as:

$$P_n = f_{cu}A_{cn} + f_y A_{sn} \quad (5.6.3.3.4-1)$$

where:

A_{sn} = area of reinforcement **entering the back face** (in.²)

5.6.3.3.5—Curved-Bar Nodes

Curved-bar nodes shall satisfy the provisions of Article 5.6.3.4.2, and the bend radius, r_b , of the tie bars at the node shall satisfy the following:

$$r_b \geq \frac{A_{st} f_y}{v b f'_c} \quad (5.6.3.3.5-1)$$

where:

r_b = bend radius of a curved-bar node, measured to the inside of a bar (in.)

A_{st} = total area of longitudinal mild steel reinforcement in the ties (in.²)

f_y = yield strength of mild steel longitudinal reinforcement (ksi)

v = back face concrete efficiency factor as specified in Article 5.6.3.3.3

b = width of the strut transverse to the plane of the strut-and-tie model (in.)

f'_c = specified compressive strength of concrete (ksi)

If the curved-bar node consists of two or more layers of reinforcement, the area, A_{st} , shall be taken as the total area of the tie reinforcement, and the radius,

C5.6.3.3.5

A curved-bar node consists of ties that represent a bend region of a continuous reinforcing bar (or bars) and a diagonal strut (or struts) that equilibrates the tie forces. The curved-bar node provisions are based on Klein (2008). Article 5.6.3.4.2 addresses proper development of the ties extending from a curved-bar node when they have unequal forces.

Eq. 5.6.3.3.5-1 ensures that the compressive stress acting on the node does not exceed the limiting compressive stress as calculated by Eq. 5.6.3.3.3-1. The equation is applicable whether the forces of the ties extending from the node are equal or not.

Generally, a curved-bar node is either considered a CTT node or a CCT node. CTT curved-bar nodes often occur at frame corners as illustrated in Figure C5.6.3.4.2-1. A curved-bar node formed by a 180-degree bend of a reinforcing bar (or bars) is considered a CCT node.

r_b , shall be measured to the inside layer of reinforcement.

The clear side cover measured to the bent bars should be at least $2d_b$ to avoid side splitting, where d_b is the diameter of the tie bars. If this cover is not provided, r_b calculated from Eq. 5.6.3.3.5-1 should be multiplied by a factor of $2d_b$ divided by the specified clear side cover.

5.6.3.4—Proportioning of Tension Ties

5.6.3.4.1—Strength of Tie

Tension tie reinforcement shall be anchored to the nodal zones by specified embedment lengths, hooks, or mechanical anchorages. The tension tie force shall be developed as specified in Article 5.6.3.4.2.

The nominal resistance of a tension tie in kips shall be taken as:

$$P_n = f_y A_{st} + A_{ps} [f_{pe} + f_y] \quad (5.6.3.4.1-1)$$

where:

A_{st} = total area of longitudinal mild steel reinforcement in the tie (in.²)

A_{ps} = area of prestressing steel (in.²)

C5.6.3.4.1

The second term of the equation for P_n is intended to ensure that the prestressing steel does not reach its yield point, thus a measure of control over unlimited cracking is maintained. It does, however, acknowledge that the stress in the prestressing elements will be increased due to the strain that will cause the concrete to crack. The increase in stress corresponding to this action is arbitrarily limited to the same increase in stress that the mild steel will undergo. If there is no mild steel, f_y may be taken as 60.0 ksi for the second term of the equation.

f_y = yield strength of mild steel
longitudinal reinforcement (ksi)

f_{pe} = stress in prestressing steel due to
prestress after losses (ksi)

5.6.3.4.2—Anchorage of Tie

The tension tie reinforcement shall be anchored to transfer the tension force therein to the **nodal** regions of the truss in accordance with the requirements for development of reinforcement as specified in Article 5.11. **At nodal zones where a tie is anchored, the tie force shall be developed at the point where the centroid of the reinforcement intersects the edge of the diagonal compression strut that is anchored by the tie. At a curved-bar node, the length of the bend shall be sufficient to allow any difference in force between the ties extending from the node to be developed.**

C5.6.3.4.2

The location at which the force of a tie should be developed is based on ACI 318-08, Section A.4.3, and is illustrated in Figure 5.6.3.2-2 (b). Experimental research has shown that full development of the tie force should be provided at this location (Thompson et al., 2003).

The curved-bar node provisions are based on Klein (2008). The design of curved-bar nodes must also satisfy the provisions of Article 5.6.3.3.5.

If the strut extending from the curved-bar node does not bisect the angle between the ties that represent the straight extensions of the reinforcing bar (or bars), the strut-and-tie model will indicate unequal forces in the ties. The length of the bend, l_b , must be sufficient to develop this difference in the tie forces. As shown in Figure C5.6.3.4.2-1, unequal tie forces cause the compressive normal stresses along the inside radius

of the bar to vary and circumferential bond stresses to develop along the bend. The value of l_b for a 90° bend may be determined as:

$$l_b \geq l_d(1 - \tan\theta_c) \quad (\text{C5.6.3.4.2-1})$$

where:

l_b = length of bend at a curved-bar node (in.)

l_d = tension development length as specified in Article 5.11.2.1 (in.)

θ_c = the smaller of the two angles between the axis of the strut (or the resultant of two or more struts) and the ties extending from a curved-bar node (degrees)

Using Eq. C5.6.3.4.2-1, the bend radius of a curved-bar node, r_b , formed by a 90° bend of the reinforcing bar (or bars) may be determined as:

$$r_b \geq \frac{2l_d(1-\tan\theta_c)}{\pi} - \frac{d_b}{2} \quad (\text{C5.6.3.4.2-2})$$

where:

r_b = bend radius of a curved-bar node, measured to the inside of a bar (in.)

d_b = diameter of bar (in.)

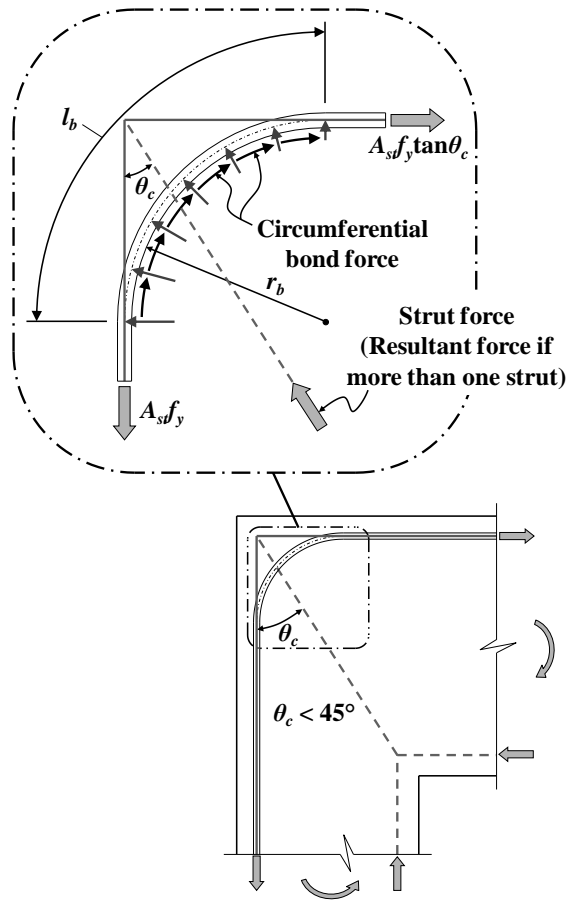


Figure C5.6.3.4.2-1—Curved-Bar Node with Unequal Tie Forces

5.6.3.5—Crack Control Reinforcement

Structures and components or regions thereof, except for slabs and footings, which have been designed in accordance with the provisions of Article 5.6.3, shall contain orthogonal grids of reinforcing bars. The spacing of the bars in these grids

C5.6.3.5

This reinforcement is intended to control the width of cracks and to ensure a minimum ductility for the member so that, if required, significant redistribution of internal stresses is possible.

The total horizontal reinforcement can be calculated as 0.003 times the effective

shall not exceed the smaller of $d/4$ and 12.0 in.

The reinforcement in the vertical and horizontal direction shall satisfy the following:

$$\frac{A_v}{b_w s_v} \geq 0.003 \quad (5.6.3.5-1)$$

$$\frac{A_h}{b_w s_h} \geq 0.003 \quad (5.6.3.5-2)$$

where:

A_h = total area of horizontal crack control reinforcement within spacing s_h (in.²)

A_v = total area of vertical crack control reinforcement within spacing s_v (in.²)

b_w = width of member's web (in.)

s_v, s_h = spacing of vertical and horizontal crack control reinforcement, respectively (in.)

Crack control reinforcement shall be distributed evenly within the strut area.

area of the strut denoted by the shaded portion of the cross-section in Figure C5.6.3.5-1. For thinner members, this crack control reinforcement will consist of two grids of reinforcing bars, one near each face. For thicker members, multiple grids of reinforcement through the thickness may be required in order to achieve a practical layout.

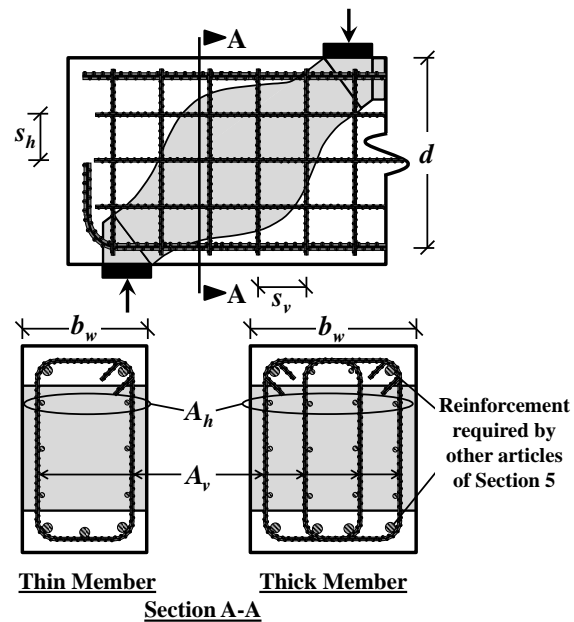


Figure C5.6.3.5-1—Distribution of Crack Control Reinforcement in Compression Strut

3.4 SUMMARY

TxDOT Project 0-5253 included the development of a comprehensive deep beam database as well as 37 tests on some of the largest deep beam specimens ever tested in the history of shear research (Birrcher et al., 2009). The project 0-5253 researchers focused primarily on eight objectives. Each objective and the corresponding conclusions most relevant to STM design were briefly discussed in this chapter. The conclusions drawn from the experimental program and deep beam database led to the development of new strut-and-tie modeling design specifications that are simpler and more accurate than the STM provisions of AASHTO LRFD (2010) and ACI 318-08. The proposed specifications recommended for inclusion within future versions of AASHTO LRFD were presented. A few additions and changes to the specifications based on the findings of the current implementation project were incorporated to facilitate their application to STM design in practice and minimize uncertainties experienced by designers. The designs of the bridge components that are demonstrated in the chapters that follow comply with the proposed specifications.

Chapter 4. Example 1: Five-Column Bent Cap of a Skewed Bridge

4.1 SYNOPSIS

The design of the five-column bent cap presented within this chapter is intended to familiarize engineers with implementation of the strut-and-tie modeling (STM) design procedure and specifications presented in Chapters 2 and 3. Multi-column bent caps are routinely encountered in design as they are a common feature of highway bridge construction. STM design of the five-column bent cap presented in this example is nonetheless challenging due to a skewed roadway and asymmetric span configurations. The complete design of the bent cap is presented for one of several load cases to be considered. The guidance provided for the development of the strut-and-tie model is general in nature and can be extended to other load cases and bent caps that may be encountered in practice. Furthermore, step-by-step instructions for defining fairly complicated nodal geometries are offered. These instructions are also applicable to other design examples within this guidebook. After the STM design is completed, it is compared to a design of the bent cap based on sectional methods.

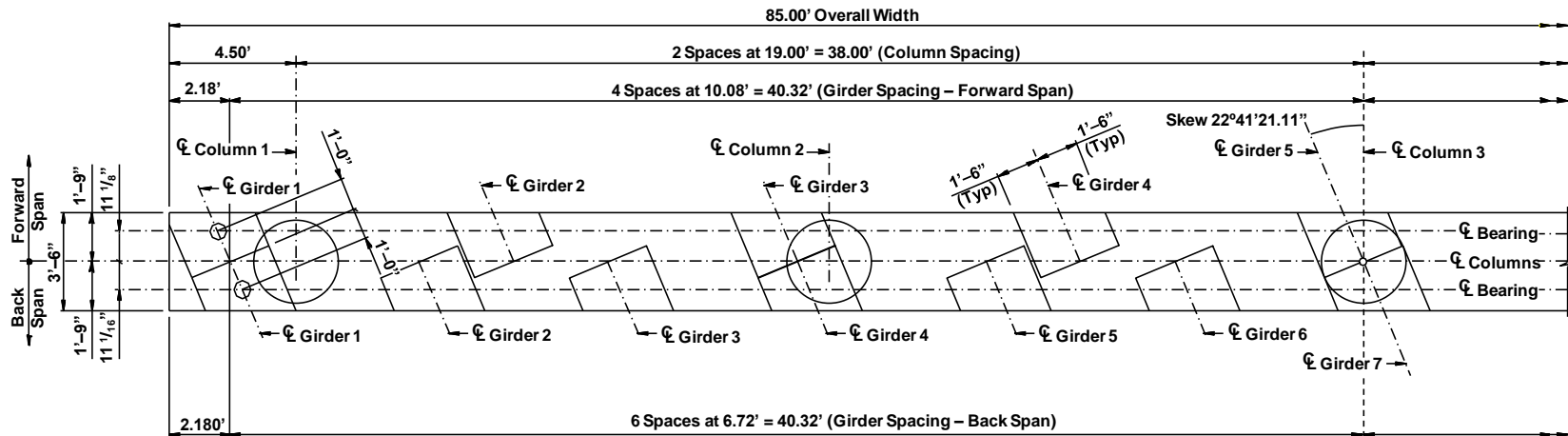
4.2 DESIGN TASK

The geometry of the multi-column bent cap and the load case that will be considered are presented in Sections 4.2.1 and 4.2.2. The details within these sections were provided by TxDOT. The bearing details described in Section 4.2.3 are consistent with standard TxDOT designs. The five-column bent cap is an existing field structure in Texas originally designed using sectional methods.

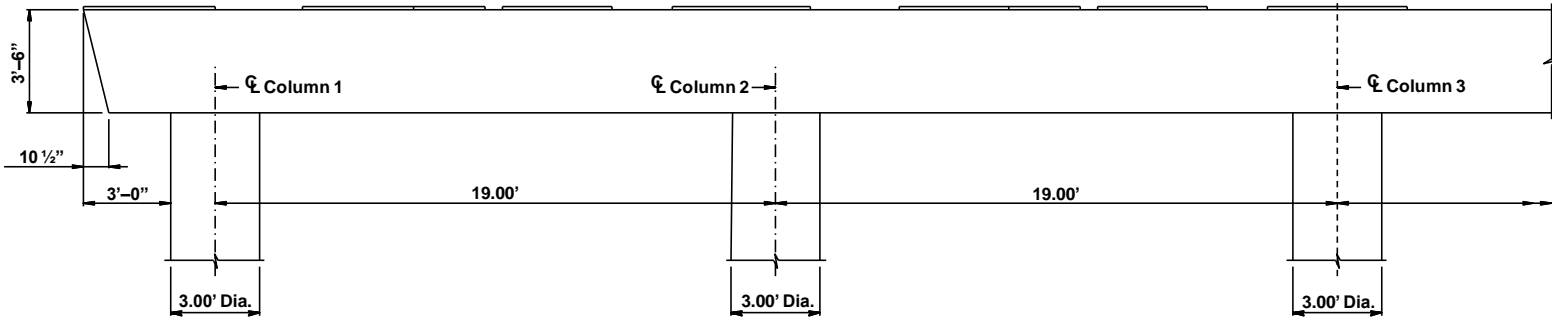
4.2.1 Bent Cap Geometry

The layout of the five-column bent cap is introduced in Figures 4.1 and 4.2. The bent cap supports 10 prestressed Tx46 girders from the forward span and 13 Tx46 girders from the back span and, in turn, is supported by five circular columns with 3-foot diameters. The columns are assumed to behave as pinned supports considering the manner in which the longitudinal column reinforcement is terminated within the bent cap

(i.e. straight bar anchorage). The transverse slab sections for both the forward and back spans are shown in Figure 4.3.



PLAN



ELEVATION

84

Figure 4.1: Plan and elevation views of five-column bent cap (left)

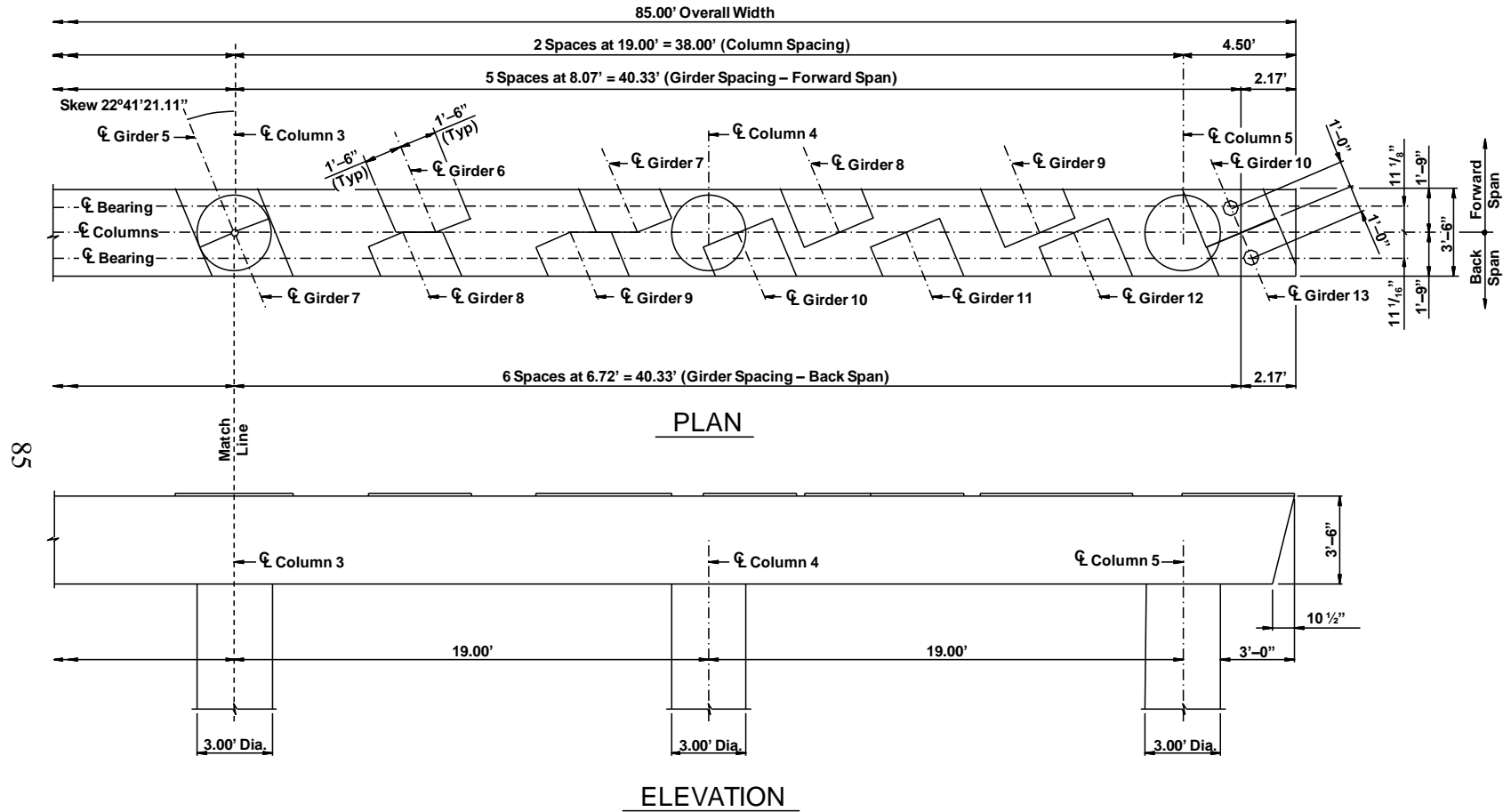


Figure 4.2: Plan and elevation views of five-column bent cap (right)

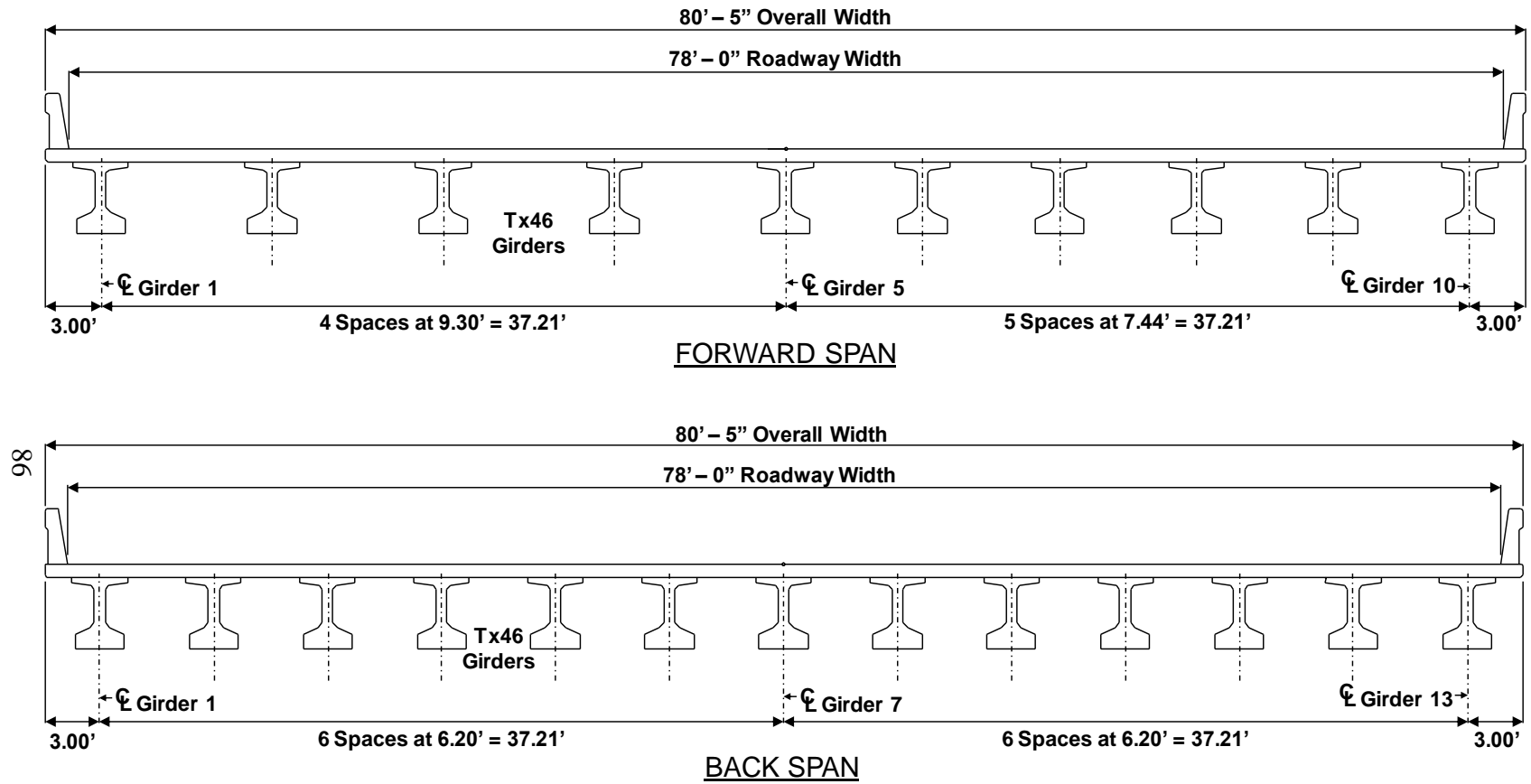


Figure 4.3: Transverse slab sections for forward and back spans

4.2.2 Determine the Loads

The factored loads acting on the bent cap from both the forward and back spans are depicted in Figure 4.4. The asymmetric span configurations cause such a loading pattern (i.e. 10 girders from the forward span and 13 girders from the back span). The live load is placed to maximize the shear force near Column 4; its position relative to the bent cap is shown in Figure 4.4. All loads are assumed to act at the longitudinal centerline of the top of the bent cap (illustrated in Figure 4.5), making the development of a two-dimensional STM possible. Only the particular load case of Figure 4.4 is considered in this design example. All other controlling load cases for the bent cap would need to be evaluated to develop the final design.

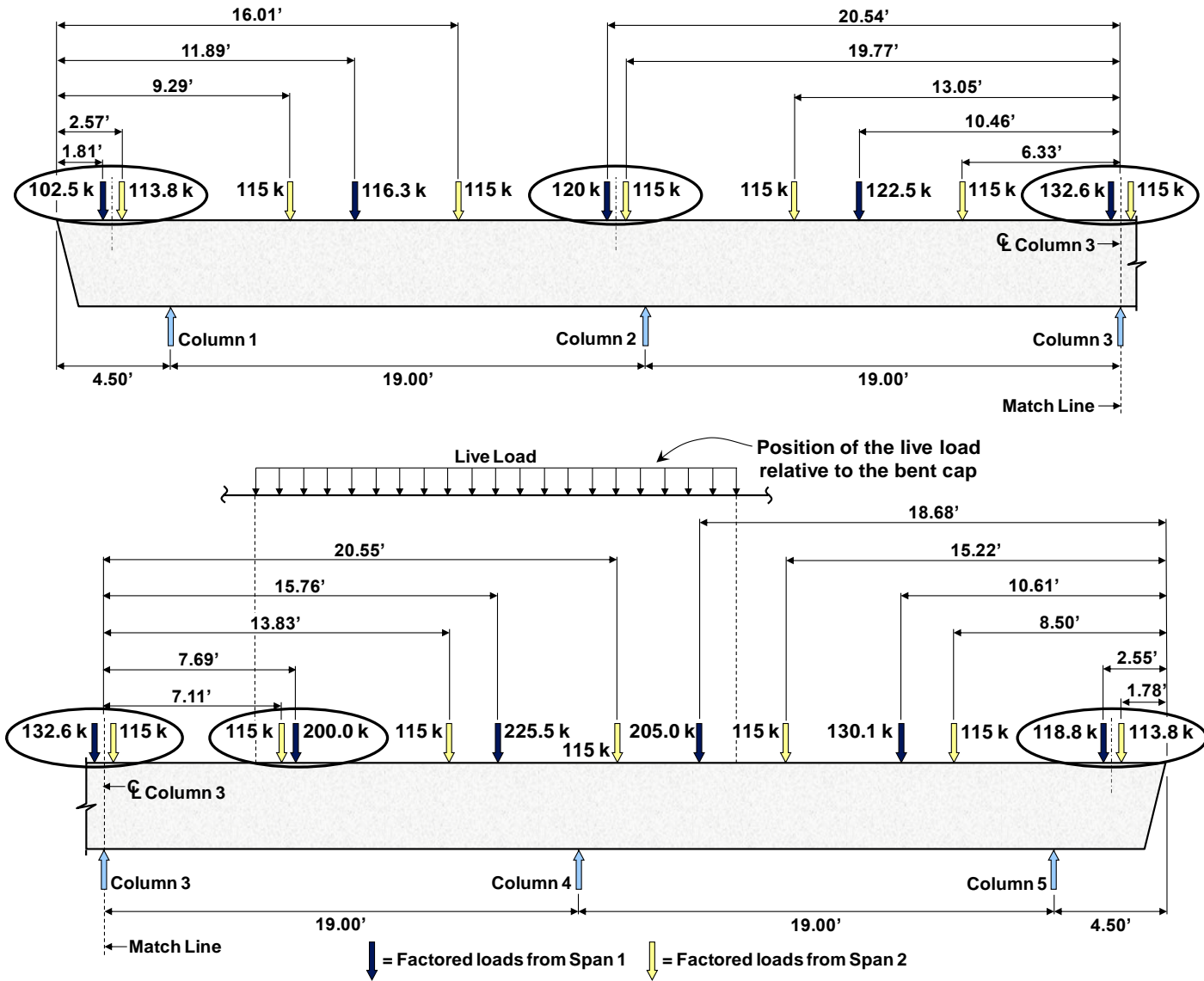


Figure 4.4: Factored loads acting on the bent cap (excluding self-weight)

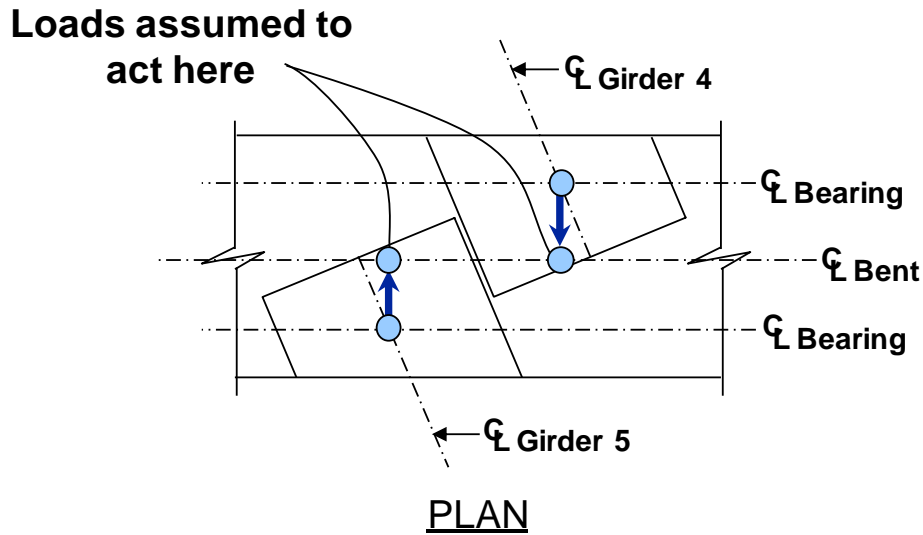


Figure 4.5: Assumed location of girder loads

In order to develop a simple, realistic strut-and-tie model, loads in close proximity to one another are resolved into a single load. The loads that are combined together are circled in Figure 4.4. The decision of whether to combine loads together is based on engineering judgment. A rule of thumb, however, is illustrated in Figure 4.6. If the STM will include a truss panel between two loads that act in close proximity to one another, the loads should be combined if the angles between the diagonal strut and vertical ties will be less than 25 degrees (Figure 4.6(a)). If the angles between the diagonal strut and the vertical ties will be greater than 25 degrees, the loads should remain independent (Figure 4.6(b)). Please recall that an angle between the axes of a strut and a tie entering a single node cannot be less than 25 degrees (refer to Section 2.7.2). When loads are combined, the location of the resulting force depends on the relative magnitudes of the independent point loads (refer to Figure 4.6(a)). Simplifying the load case by combining loads would likely be performed concurrently with the development of the STM.

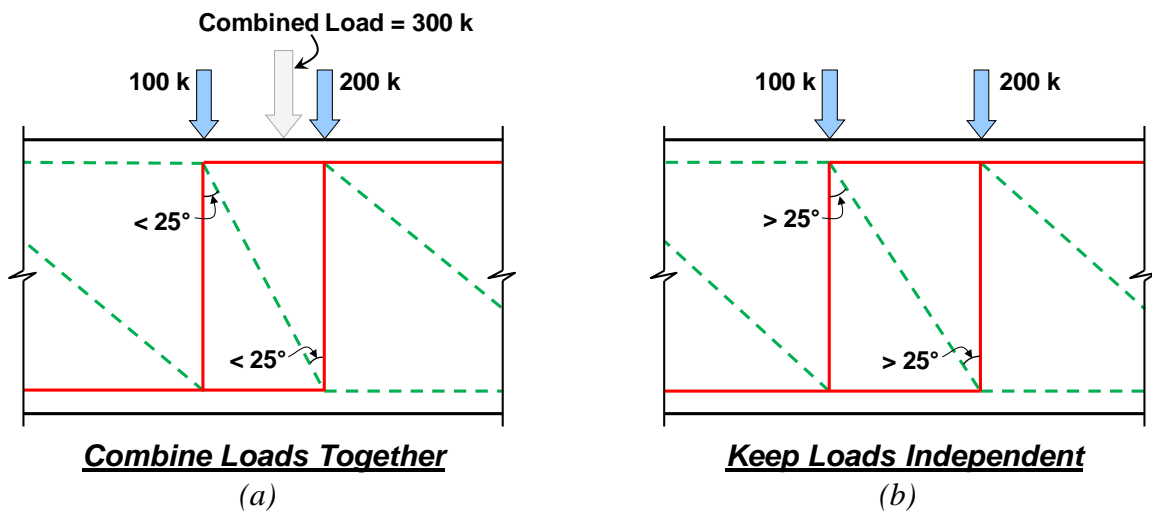


Figure 4.6: Determining when to combine loads – (a) Combine loads together; (b) keep loads independent

For this particular bent cap design, the force resulting from the combination of the two loads acting above Column 3 (refer to Figure 4.4) is assumed to act along the centerline of the column. The location of this resolved force is offset very slightly from the column centerline in reality. Assuming the force acts along the column centerline is an acceptable simplification given the potential for direct (practically vertical) load transfer between the bent cap and the column. The assumed location of the force will also help to simplify the geometry of the node located directly above the column (Node EE in Section 4.4.4).

As with any truss, the loads applied to a strut-and-tie model must act at the joints (i.e. nodes). The self-weight of the member, therefore, cannot be applied as a uniform distributed load but must be divided into point loads acting at the nodes. After the circled loads in Figure 4.4 are combined together and their locations are determined, the next step is to add to each load the factored self-weight of the bent cap based on tributary volumes. The unit weight of the reinforced concrete is assumed to be 150 lb/ft^3 , and a load factor of 1.25 is applied to the self-weight according to the AASHTO LRFD (2010) Strength I load combination. The final factored loads defined for the purposes of an STM analysis are shown in Figure 4.10.

4.2.3 Determine the Bearing Areas

Before the STM design can be performed, the bearing details must first be determined. The STM design of the bent cap requires that the bearing areas meet two criteria; otherwise, the geometries of the nodes cannot be determined. First, since the nodes of an STM always have rectangular faces, the bearing areas must be rectangular. Second, for a two-dimensional strut-and-tie model, as will be development for the bent cap, the bearing areas cannot be skewed relative to the longitudinal axis of the member. Satisfying these two conditions allows the nodal geometries to be defined as described in Section 4.4.4.

The bearing details of the columns will be determined first. The bent cap is supported by five circular columns. In order for the geometries of the nodes located directly above the columns to be defined, square bearings with areas equal to the areas of the 3-foot diameter columns are used. These square bearings (i.e. equivalent square columns) are 31.9 inches by 31.9 inches, as illustrated in Figure 4.7. This area defines the geometry of the bearing face of the node above each column. The dimension of the square bearing area is also used to determine the length of the strut-to-node interface and the width of the back face (transverse to the longitudinal axis of the bent cap), if applicable.

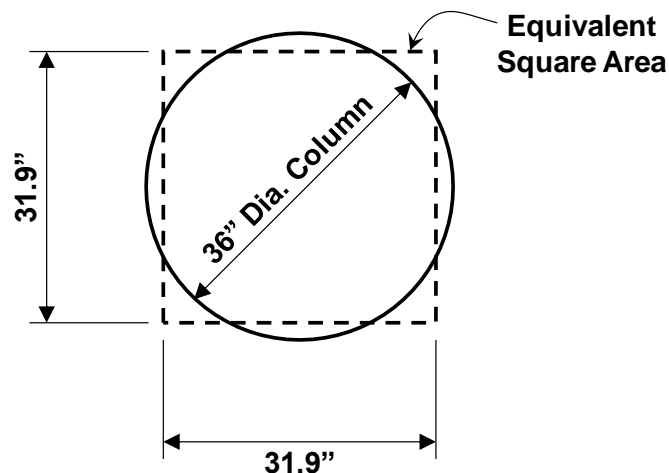


Figure 4.7: Assumed square area for the columns

Since the bearing pads supporting the girders are skewed relative to the longitudinal axis of the bent cap, simplifications are necessary to meet the criteria required for an STM design to be performed. Before the simplifications are made, the effective bearing area for each girder should be determined. The standard size of bearing pads supporting Tx46 girders with a skew between 18 and 30 degrees is 8 inches by 21 inches (*Bridge Standards*, 2007). For the five-column bent cap, the bearing pads are placed on bearing seats with a minimum height of 1.5 inches at the centerline of the bearings (see Figure 4.8). The applied forces will spread within the bearing seats, giving effective bearing areas at the top surface of the bent cap that are larger than the areas of the bearing pads themselves. These increased areas can be considered when defining the geometries of the nodes located directly below the applied girder loads. To account for the effect of the bearing seats, 1.5 inches is added to all sides of each bearing pad, increasing the effective bearing area to 11 inches by 24 inches (illustrated in Figure 4.8).

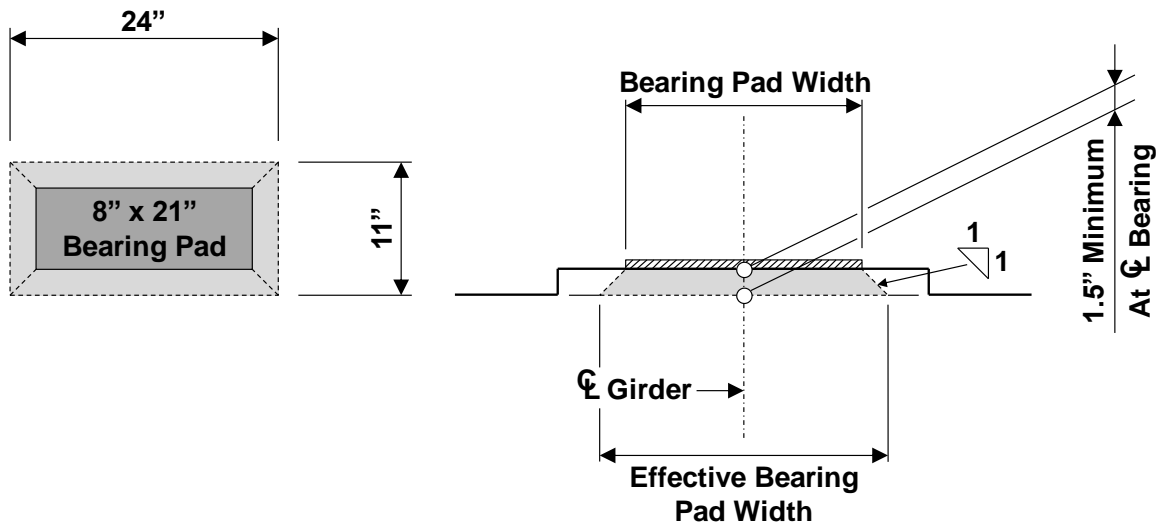


Figure 4.8: Effective bearing area considering effect of bearing seat

The effective bearing areas of the girders must now be modified so that they are oriented in the direction corresponding with the longitudinal axis of the bent cap (i.e. are not skewed). Each girder load is assumed to act at the longitudinal centerline of the top of the bent cap so that the development of a two-dimensional strut-and-tie model is

possible (refer to Figure 4.5). The bearing areas are therefore assumed to be located concentrically with the longitudinal axis of the bent cap, and they are also assumed to be square in shape. The designer may choose to keep the original rectangular shape of the effective bearing areas, but converting them to equivalent square areas is reasonable considering the change in position also being assumed. The determination of the assumed girder bearing areas is illustrated in Figure 4.9. For a single girder load, the 11-inch by 24-inch effective bearing area becomes a 16.2-inch by 16.2-inch square (Figure 4.9(a)). Similarly, the bearing area for two girder loads that have been combined together becomes a 23.0-inch by 23.0-inch square (Figure 4.9(b)). All loads are assumed to act at the center of the bearing areas.

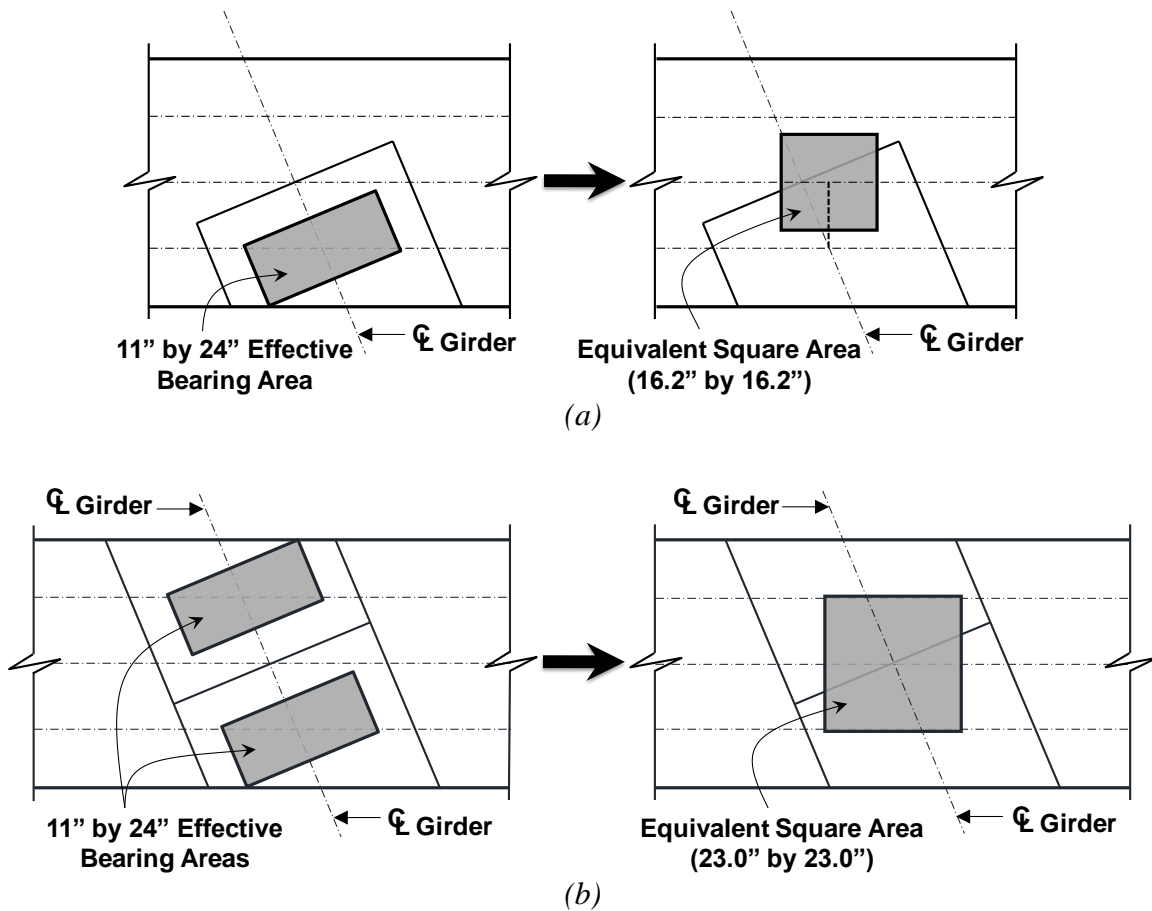


Figure 4.9: Assumed bearing areas for girder loads – (a) single girder load; (b) two girder loads that have been combined

4.2.4 Material Properties

- Concrete: $f'_c = 4 \text{ ksi}$
- Reinforcement: $f_y = 60 \text{ ksi}$

Recall that the five-column bent cap is an existing field structure in Texas. The specified concrete compressive strength, f'_c , of the existing structure is 3.6 ksi. The nodal strength checks of Section 4.4.4, however, will reveal that an increased concrete strength is required for the most critical node to resist the applied stresses.

4.3 DESIGN PROCEDURE

Due to the close spacing of the superstructure loads (i.e. load discontinuities), the full length of the bent cap is expected to exhibit deep beam behavior. Application of the STM procedure is therefore appropriate for design of the entire bent cap. The general design procedure introduced in Section 2.3.3 has been adapted to the current design scenario, resulting in the steps listed below:

- Step 1: Analyze structural component
- Step 2: Develop strut-and-tie model
- Step 3: Proportion longitudinal ties
- Step 4: Perform nodal strength checks
- Step 5: Proportion stirrups in high shear regions
- Step 6: Proportion crack control reinforcement
- Step 7: Provide necessary anchorage for ties
- Step 8: Perform shear serviceability check

The shear serviceability check is listed as the last step of the design procedure. In reality, the design engineer may wish to use the shear serviceability check as a means of initially sizing the structural element. The geometry of the five-column bent cap in this example, however, corresponds to that of an existing field structure. The shear serviceability check is therefore performed using the geometry of the existing bent cap (refer to Figures 4.1 and 4.2), followed by a discussion regarding the likelihood of diagonal cracking under service loads.

4.4 DESIGN CALCULATIONS

4.4.1 Step 1: Analyze Structural Component

Before the strut-and-tie model is developed, an overall analysis of the bent cap should be performed. The factored superstructure loads are applied to the bent cap (including the factored self-weight based on tributary volumes), and the bent cap is assumed to be pin-supported at the centerlines of the columns. The external column

reactions are then determined by performing a linear elastic analysis of the continuous beam. The reactions at Columns 1 through 5 are 440.2 kips, 620.0 kips, 680.5 kips, 918.5 kips, and 499.7 kips, respectively. These values are shown in Figure 4.10 being applied to the STM and will be used later to calculate the forces in the struts and ties.

4.4.2 Step 2: Develop Strut-and-Tie Model

The final strut-and-tie model with member forces is presented in Figure 4.10. The development and analysis of the STM is explained in detail within this section. The locations of the top and bottom chords of the STM are determined first. The diagonal struts and vertical ties are then added to model the flow of forces from the applied loads to the columns. Several guidelines are offered regarding the development of an efficient, realistic STM that closely matches the elastic distribution of stresses within the bent cap. Once the geometry of the STM is finalized, the forces in the struts and ties are calculated.

L6

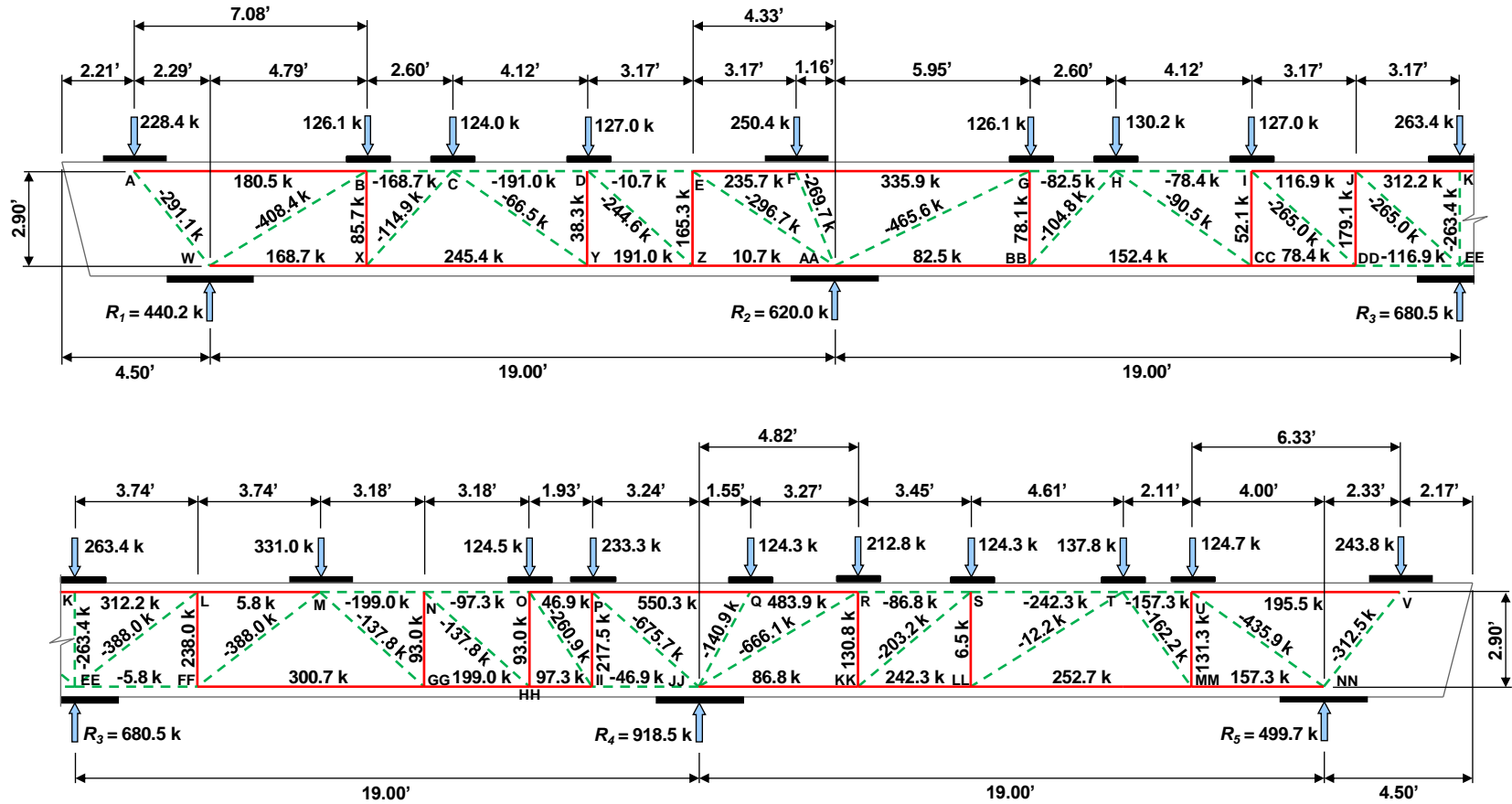


Figure 4.10: Strut-and-tie model for the five-column bent cap

The first step in the development of the STM is to determine the height of the truss by locating the top and bottom chords. A continuous beam analysis reveals that both positive and negative moment regions exist within the bent cap. Flexural tension reinforcement will be needed along both the top and bottom of the member, indicating that the truss model will include tension members (i.e. ties) in both the top and bottom chords. The position of both chords, therefore, should correspond with the centroids of the longitudinal reinforcement. To maintain consistency with the existing field structure, #5 stirrups and #11 longitudinal reinforcing bars will be used along the length of the member. To allow for 2.25-inch clear cover, #5 stirrups, and one layer of #11 bars, the top and bottom chords are positioned 3.58 inches from the top and bottom faces of the bent cap. The resulting height of the STM is 34.84 inches, or 2.90 feet (shown in Figure 4.11).

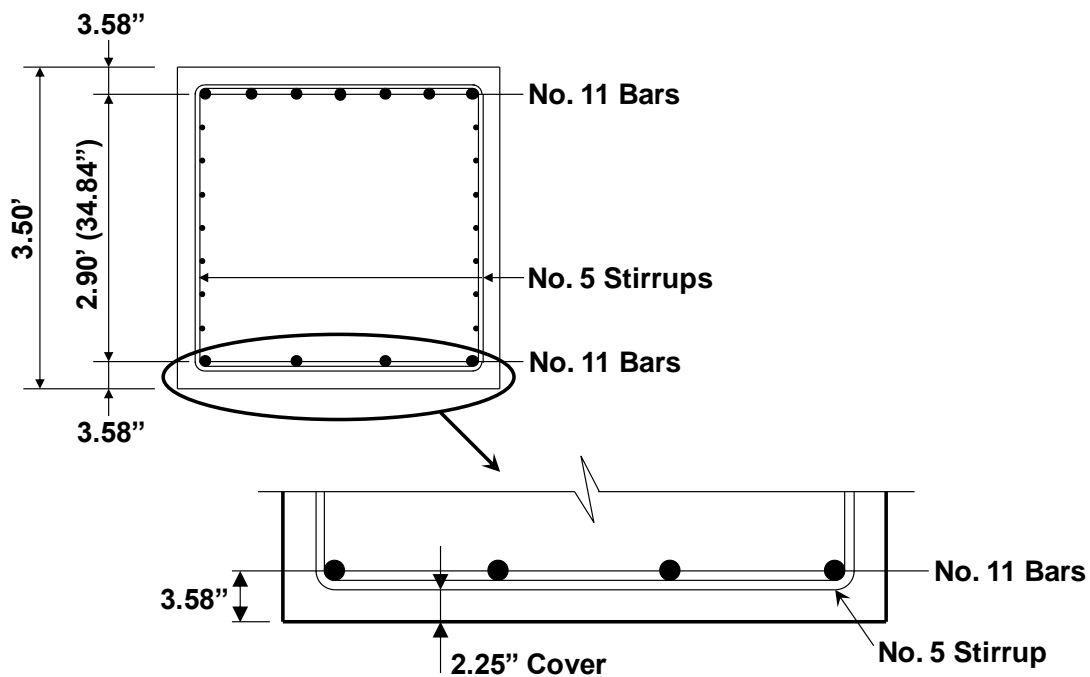


Figure 4.11: Determining the location of the top and bottom chords of the STM

The transfer of the superstructure loads (i.e. beam reactions) to each of the supports (i.e. columns) is accomplished by providing a combination of diagonal struts

and vertical ties within the strut-and-tie model. Guidance is provided below to assist designers with this task. With practice, the placement of these truss members will become more intuitive.

The first guideline to remember is that proper orientation of the diagonal members should result in compressive forces. If the diagonal members are oriented in the wrong direction, the forces will be tensile, and the orientation should be reversed as shown in Figure 4.12. A conventional shear force diagram can be used to determine the proper orientation of the diagonal struts: the point at which the sign of the shear force diagram changes is indicative of a reversal of the diagonal strut orientation (see Figure 4.12).

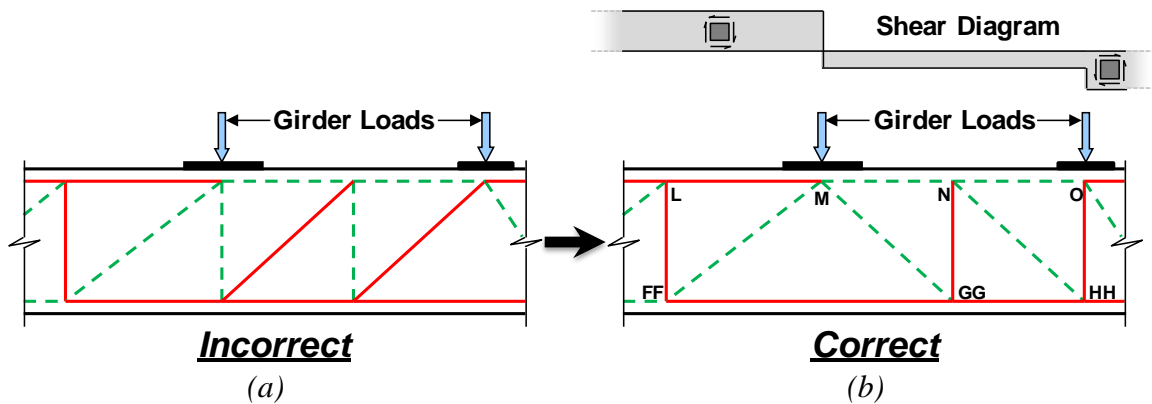


Figure 4.12: Orientation of diagonal members – (a) incorrect; (b) correct

The vertical members of the STM are expected to be in tension (compare two parts of Figure 4.12 above) and are generally referred to as vertical ties or stirrups. Considering equilibrium at the joints of the truss model can aid with determining where vertical ties are necessary. For example, Tie O/HH in Figure 4.12(b) is needed for equilibrium to be satisfied at Nodes O and HH. Under unique circumstances, such as the direct vertical transfer of load above Column 3, the vertical member may be in compression, as shown in Figure 4.10.

The number of truss panels within the STM should be minimized (i.e. minimize the number of vertical ties). Please recall that the angle between a strut and a tie entering the same node should not be less than 25 degrees (refer to Section 2.7.2). To satisfy this

requirement, providing two truss panels between adjacent loads or between a load and the nearest support that are an exceptionally long distance apart may be necessary. Only one panel should be used, however, between two adjacent loads or between a load and a support when the 25-degree rule can be satisfied with this one panel. Using more panels than necessary increases the number of vertical ties. This, in turn, results in an overly-conservative design and a large number of stirrups required to satisfy the STM. Figure 4.13 is provided to illustrate this concept. Only one truss panel is required between the applied load and Column 2 since the 25-degree rule can be satisfied with one panel (Figure 4.13(a)). Including an additional truss panel (Figure 4.13(b)) unnecessarily requires that stirrups be provided to carry an addition tie force of 204.3 kips, reducing the efficiency of the STM.

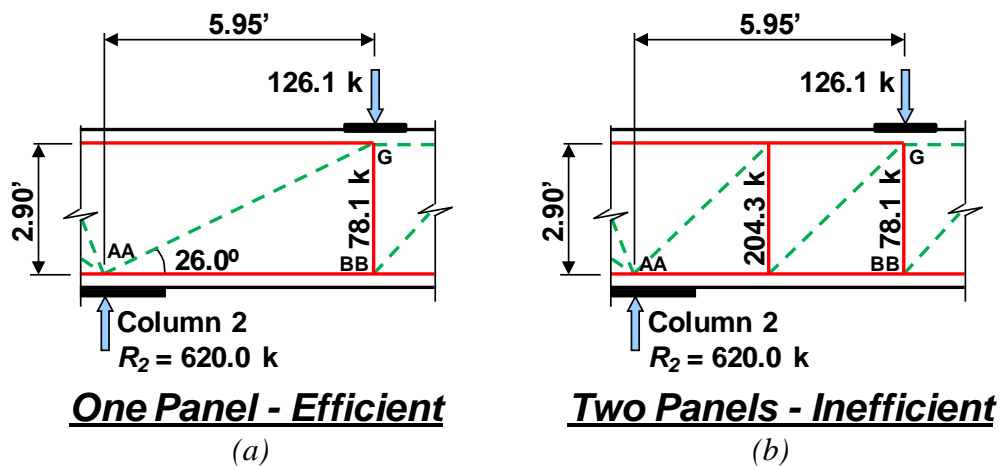


Figure 4.13: Minimizing number of truss panels – (a) efficient; (b) inefficient

Beyond the general strut-and-tie model development guidelines discussed above, the designer may wish to further refine the STM to more accurately represent the assumed (elastic) flow of forces. The STM could include a vertical tie under the load at Node Q as shown in Figure 4.14(b), representing an indirect load transfer between the applied load at Node R and Column 4. This additional vertical tie, however, is unnecessary because direct compression will exist between the load at Node R and the support. For this reason, no vertical tie representing shear forces is needed, resulting in a

more realistic and more efficient STM (Figure 4.14(a)). A similar scenario occurs near Column 2.

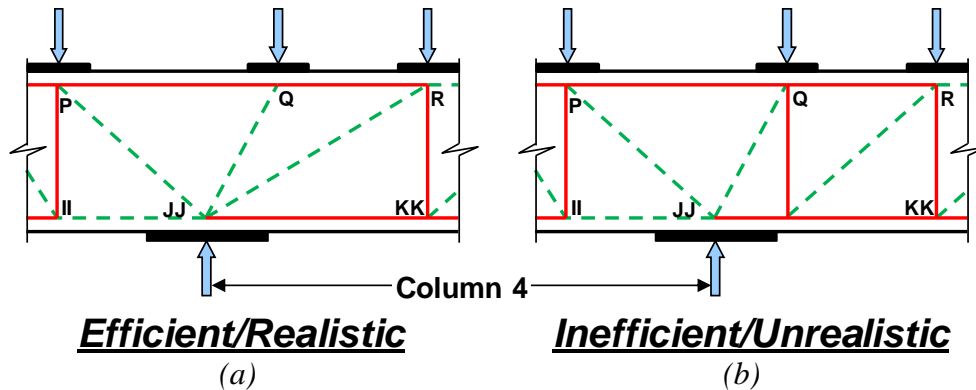


Figure 4.14: Modeling flow of forces near Column 2 – (a) efficient/realistic; (b) inefficient/unrealistic

After the geometry of the STM is determined, a truss analysis can be performed to find the member forces. The member forces shown in Figure 4.10 were determined by simultaneously imposing the factored superstructure loads and column reactions (from the continuous beam analysis) on the final STM. Structural analysis software was used to analyze the STM; alternatively, internally statically determinate truss models may be solved by using the traditional method of joints or method of sections (i.e. enforce equilibrium using statics). A general discussion on STM analysis is provided in Chapter 2 (Section 2.7.4).

4.4.3 Step 3: Proportion Longitudinal Ties

In accordance with standard TxDOT practice, a constant amount of longitudinal reinforcement will be maintained along the length of the bent cap. The location of the centroids of the top and bottom chord reinforcement was determined in Section 4.4.2 based upon the assumption that each chord consists of one layer of #11 reinforcing bars. If calculations reveal that additional layers of reinforcement are necessary to carry the tie forces, the geometry and analysis of the STM must be revisited to accurately model the internal flow of forces within the bent cap.

Top Chord

The force in Tie PQ (550.3 kips) controls the design of the top chord of the STM. The top chord reinforcement is therefore proportioned as follows:

$$\begin{aligned}\text{Factored Load:} & F_u = 550.3 \text{ kip} \\ \text{Tie Capacity:} & \varphi \cdot f_y \cdot A_{st} = F_u \\ & (0.9)(60 \text{ ksi})A_{st} = 550.3 \text{ kip} \\ & A_{st} = 10.19 \text{ in}^2\end{aligned}$$

$$\text{Number of \#11 bars required: } 10.19 \text{ in}^2 / 1.56 \text{ in}^2 = 6.5 \text{ bars}$$

Use 7 - #11 bars

Bottom Chord

The force in Tie FF/GG (300.7 kips) controls the design of the bottom chord of the STM. Using #11 bars, the bottom chord reinforcement is proportioned as follows:

$$\begin{aligned}\text{Factored Load:} & F_u = 300.7 \text{ kip} \\ \text{Tie Capacity:} & \varphi \cdot f_y \cdot A_{st} = F_u \\ & (0.9)(60 \text{ ksi})A_{st} = 300.7 \text{ kip} \\ & A_{st} = 5.57 \text{ in}^2\end{aligned}$$

$$\text{Number of \#11 bars required: } 5.57 \text{ in}^2 / 1.56 \text{ in}^2 = 3.6 \text{ bars}$$

Use 4 - #11 bars

More bars are likely to be required for the bottom chord when other governing load cases are considered.

4.4.4 Step 4: Perform Nodal Strength Checks

The strengths of the nodes are now checked to ensure the force acting on each nodal face can be resisted. The most heavily stressed nodes are first identified. After strength check calculations reveal that the critical nodes have adequate capacity, several of the remaining nodes can be deemed to have adequate strength by inspection. Strength check calculations, therefore, do not need to be performed for each node of the strut-and-tie model.

The critical bearing stresses on the bent cap will be checked prior to other nodal strength calculations. If the critical bearings have adequate strength, the bearing faces of all the nodes of the STM must also have sufficient strength to resist the applied forces.

Critical Bearings

Both the magnitude of the bearing stress and the type of node that abuts the bearing surface should be considered when identifying the critical bearings. Please recall from Chapter 2 that the presence of tensile forces at a node reduces the concrete efficiency. Considering the column reactions, the 918.5-kip force at Column 4 acting on Node JJ, a CCT node, is identified as being critical. The concrete efficiency factor for the bearing face of Node JJ is 0.70 (refer to Section 2.9.7). Given that the bent cap is wider than the columns on which it is supported, triaxial confinement of the nodal regions directly above the columns can be taken into account. The first step in evaluating the bearing strength is therefore to determine the triaxial confinement factor, m , as illustrated in Figure 4.15 and outlined in the calculation below. For this calculation as well as the strength calculation that follows, a 31.9-inch by 31.9-inch square bearing area is assumed for the column (refer to Section 4.2.3).

$$m = \sqrt{A_2/A_1} = \sqrt{(42 \text{ in})^2 / (31.9 \text{ in})^2} = 1.32 < 2 \quad \therefore \text{Use } m = 1.32$$

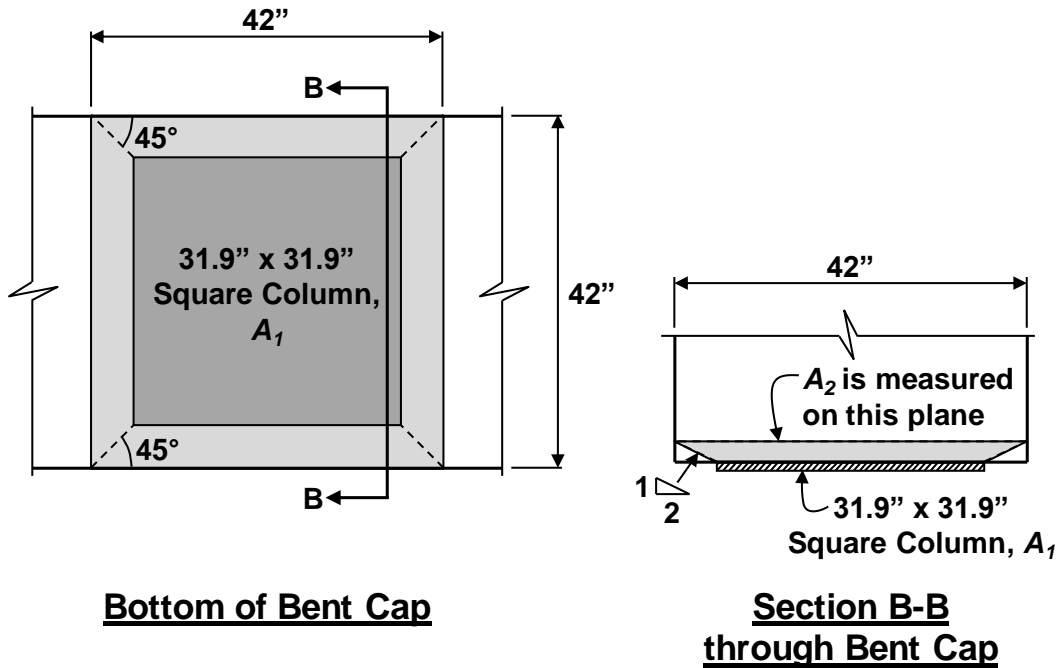


Figure 4.15: Determination of triaxial confinement factor, m , at Column 4

The bearing strength is calculated and compared to the column reaction as follows:

BEARING AT COLUMN 4 (NODE JJ – CCT)

Factored Load:	$F_u = 918.5 \text{ kip}$
Efficiency:	$\nu = 0.70$
Concrete Capacity:	$f_{cu} = m \cdot \nu \cdot f'_c = (1.32)(0.70)(4.0 \text{ ksi}) = 3.7 \text{ ksi}$
	$\phi \cdot F_n = (0.7)(3.7 \text{ ksi})(31.9 \text{ in})(31.9 \text{ in})$
	$= 2636 \text{ kip} > 918.5 \text{ kip} \text{ OK}$

Referring to the factored girder loads in Figure 4.4, the 225.5-kip force (acting near Column 4 at the location of Node P of the STM) is identified as the critical girder load. The strength of the actual bearing area of the girder load (i.e. the size for the bearing pad) should be checked for adequacy. If this bearing area can resist the applied load, the bearing face of Node P located at the top surface of the bent cap will also have adequate strength (refer to the effective bearing areas defined in Section 4.2.3). Since the node located below the girder load (Node P) is a CTT node, a concrete efficiency factor

of 0.65 is applied to the concrete capacity (see calculation below). The bearing strength calculations are performed as follows:

BEARING AT CRITICAL GIRDER LOAD

Bearing Area:	$A_{bearing} = (8 \text{ in})(21 \text{ in}) = 168 \text{ in}^2$
Factored Load:	$F_u = 225.5 \text{ kip}$
Efficiency:	$\nu = 0.85 - \frac{4.0 \text{ ksi}}{20 \text{ ksi}} = 0.65$
	$\therefore \text{Use } \nu = 0.65$
Concrete Capacity:	$f_{cu} = \nu \cdot f'_c = (0.65)(4.0 \text{ ksi}) = 2.6 \text{ ksi}$
	$\varphi \cdot F_n = (0.7)(2.6 \text{ ksi})(168 \text{ in}^2)$
	$= 306 \text{ kip} > 225.5 \text{ kip} \text{ OK}$

The triaxial confinement factor, m , could have been applied to the concrete capacity. As the strength check reveals, considering the effect of confinement is unnecessary. Since the critical bearings have adequate strength to resist the applied forces, all other bearings also have sufficient strength.

Node JJ (CCC/CCT)

Given the high bearing and strut forces entering Node JJ, it is identified as a critical node within the strut-and-tie model of Figure 4.10. The geometry of Node JJ depends on the bearing area of the column, the location of the bottom chord of the STM, and the angles of the struts entering the node. The final nodal geometry is presented in Figures 4.18 and 4.19. The total length of the bearing face of the node is taken as the dimension of the equivalent square column, 31.9 inches (refer to Section 4.2.3). The other dimensions of the node and the strut angles shown in Figures 4.18 and 4.19 are determined by following the procedure described within this section.

Node JJ is subject to forces from four struts, one tie, and a column reaction. Strength check calculations for Node JJ will be greatly simplified by (1) resolving struts entering the node from the same side and (2) subdividing the node into two parts. Node JJ is shown in Figure 4.16(a) as it appears in the context of the strut-and-tie model of Figure 4.10. The resolution of adjacent struts is performed first. Resolving adjacent struts is often necessary in order to reduce the number of forces acting on a node and to

allow the nodal geometry to be defined as described in Sections 2.9.3 through 2.9.5. Struts P/JJ and II/JJ are resolved into a single strut; similarly, Struts Q/JJ and R/JJ are also combined (resulting in Figure 4.16(b)). The designer should note that a strut and a tie should never be resolved into a single force.

Node JJ is then subdivided into two parts as shown in Figure 4.17. A node with struts entering from both sides (i.e. from the right and from the left) is generally subdivided in order to define the nodal geometry. The column reaction on the bent cap is subdivided into two forces acting on the two portions of the node. The 450.7-kip reaction acting on the left in Figure 4.17 equilibrates the vertical component of the 711.3-kip force of the resolved strut on the left. Similarly, the 467.8-kip reaction acting on the right equilibrates the vertical component of the 790.4-kip strut force. The line of action for each component of the column reaction is determined by maintaining uniform pressure over the column width. The line of action for each component is therefore calculated as follows:

$$\left[\frac{(711.3 \text{ kip}) \sin(39.32^\circ)}{918.5 \text{ kip}} \right] (31.9 \text{ in}) = 15.7 \text{ in} \quad 15.7 \text{ in} / 2 = 7.83 \text{ in}$$

$$\left[\frac{(790.4 \text{ kip}) \sin(36.29^\circ)}{918.5 \text{ kip}} \right] (31.9 \text{ in}) = 16.2 \text{ in} \quad 16.2 \text{ in} / 2 = 8.12 \text{ in}$$

where 31.9 in. is the dimension of the equivalent square column. All other values are labeled in Figure 4.16(b). The dimensions 15.7 in. and 16.2 in. in the calculations above will be used later as the length of the bearing face for each portion of the node (i.e. each nodal subdivision).

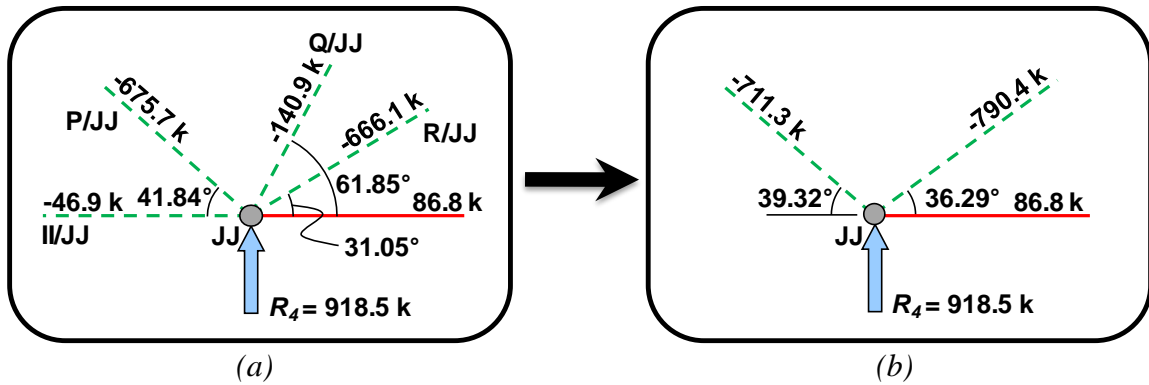


Figure 4.16: Node JJ – (a) from STM; (b) with resolved struts

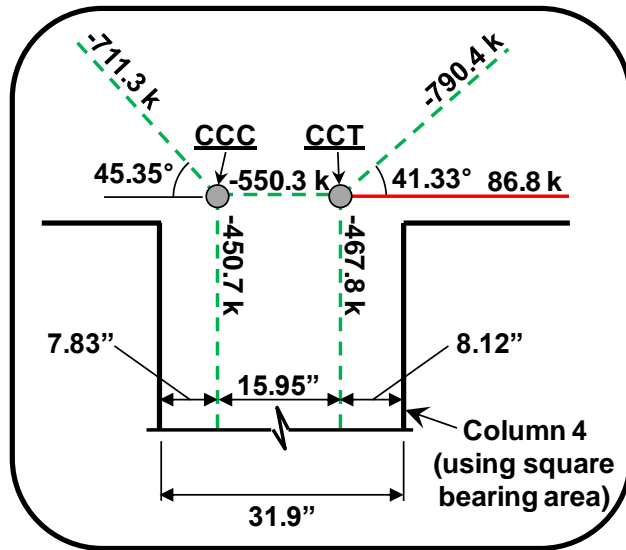


Figure 4.17: Node JJ subdivided into two parts

The division of the node into two parts causes a small change in the strut angles shown in Figure 4.16(b). The new angles of these resolved struts are labeled in Figure 4.17 and are determined by the calculations that follow. Neglecting these angle changes could lead to unconservative strength calculations.

For the resolved strut on the left (resulting from the combination of Struts P/JJ and II/JJ):

$$\tan(39.32^\circ) = \frac{34.84 \text{ in}}{x} \quad x = 42.54 \text{ in}$$

$$\theta = \tan^{-1} \left[\frac{34.84 \text{ in}}{42.54 \text{ in} - (31.9 \text{ in}/2 - 7.83 \text{ in})} \right] = 45.35^\circ$$

For the resolved strut on the right (resulting from the combination of Struts Q/JJ and R/JJ):

$$\tan(36.29^\circ) = \frac{34.84 \text{ in}}{x} \quad x = 47.45 \text{ in}$$

$$\theta = \tan^{-1} \left[\frac{34.84 \text{ in}}{47.45 \text{ in} - (31.9 \text{ in}/2 - 8.12 \text{ in})} \right] = 41.33^\circ$$

where 34.84 in. is the height of the STM, 39.32° and 36.29° are the original angles of the resolved struts, 31.9 in. is the dimension of the equivalent square column, and 7.83 in. and 8.12 in. define the line of action for each component of the column reaction (refer to Figure 4.17).

The change of the strut angles will also affect the magnitude of the strut forces acting at the node to some extent. The change in the forces can often be neglected, adding conservatism to the strength checks, as is done here. Alternatively, the forces can be adjusted to eliminate this added conservatism. This may be necessary when the strength of a node (i.e. the back face or strut-to-node interface) is determined to be inadequate by only a small margin.

Instead of resolving adjacent struts and then subdividing the node, the designer may wish to subdivide the node first (remembering to adjust the strut angles) and then resolve adjacent struts. The final result is the same regardless of the order in which the steps are performed.

The two portions of Node JJ are shown in Figures 4.18 and 4.19. The dimensions of the left portion of the node are presented in Figure 4.18, while the dimensions of the

right portion are shown in Figure 4.19. The length of the bearing face for each nodal subdivision was previously determined. The length of the back face is taken as twice the distance from the bottom surface of the bent cap to the centroid of the longitudinal reinforcement (i.e. bottom chord of the STM). Thus, the back face length is $2(3.58 \text{ in.}) = 7.2 \text{ in.}$ Calculation of the strut-to-node interface length, w_s , for each nodal subdivision is provided in the respective figures. The width of the node into the page is taken as the dimension of the equivalent square column, 31.9 inches (refer to the strength calculations below). The angles denoted “per global STM” in Figures 4.18 and 4.19 are the angles of the resolved struts before the node is subdivided. The force acting on the back face of each nodal subdivision (i.e. the compressive force that exists between the right and left portions of the node) was determined when the nodes were subdivided (the 550.3-kip force in Figure 4.17). This value was calculated by enforcing equilibrium for each portion of the node using the original strut angles. Since no tensile forces act on the left portion of the node, it is treated as a CCC node (i.e. the concrete efficiency factors for CCC nodes are applied). The right portion of the node is treated as a CCT node since one tie force is present.

Node JJ – Right (CCT)

$$\begin{aligned}
 w_s &= l_b \sin\theta + a \cos\theta \\
 &= (16.2 \text{ in}) \sin 41.33^\circ + (7.2 \text{ in}) \cos 41.33^\circ \\
 &= 10.70 \text{ in} + 5.41 \text{ in} = 16.1 \text{ in}
 \end{aligned}$$

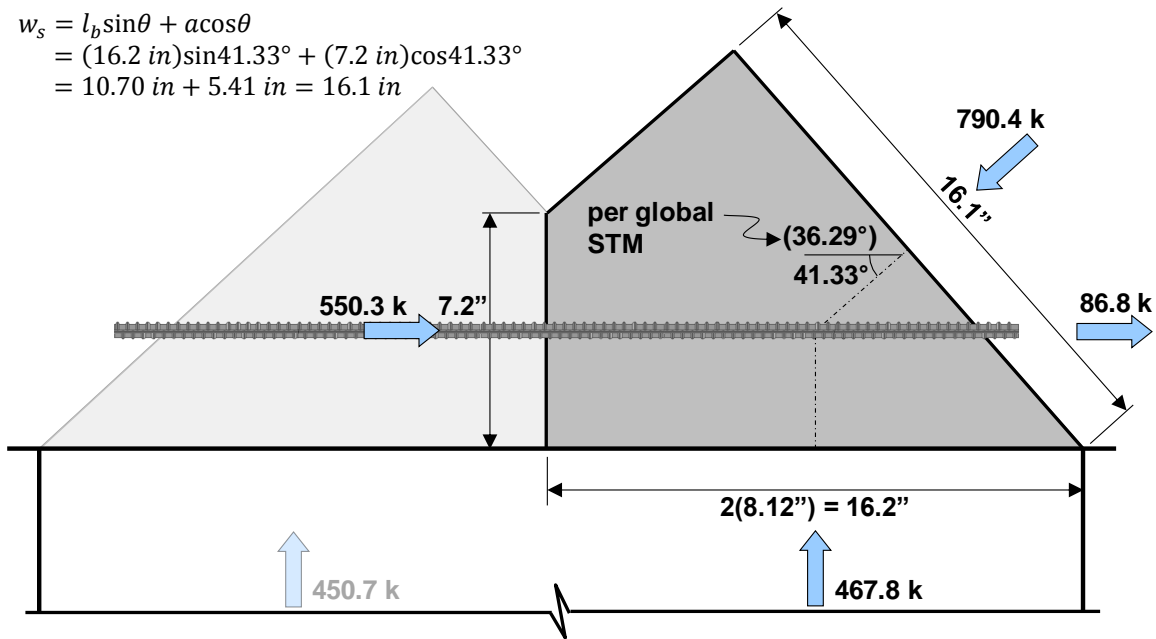


Figure 4.18: Node JJ – right nodal subdivision

Node JJ is triaxially confined since the width of Column 4 is smaller than the width of the bent cap. The triaxial confinement factor, m , was previously determined when the bearing strength check at Column 4 was performed, and its value was found to be 1.32. The m -factor can be applied to all faces of Node JJ. The bearing strength was already found to be sufficient; therefore, only the strengths of the back face and strut-to-node interfaces of Node JJ need to be checked. Strength checks for the back face and strut-to-node interface of the right nodal subdivision are presented below.

The 86.8-kip tensile force in the reinforcement (see Figure 4.18) does not need to be applied as a direct force to the back face. Recall that the bond stresses of an adequately developed tie do not concentrate at the back face of a node and are therefore not critical (refer to Section 2.9.8 in Chapter 2 and Article 5.6.3.3.3a of the proposed STM specifications in Chapter 3). Only the compressive force of 550.3 kips is directly applied to the back face of Node JJ.

Triaxial Confinement Factor: $m = 1.32$

BACK FACE

Factored Load: $F_u = 550.3 \text{ kip}$

Efficiency: $\nu = 0.70$

Concrete Capacity: $f_{cu} = m \cdot \nu \cdot f'_c = (1.32)(0.70)(4.0 \text{ ksi}) = 3.7 \text{ ksi}$
 $\varphi \cdot F_n = (0.7)(3.7 \text{ ksi})(7.2 \text{ in})(31.9 \text{ in})$
 $= 595 \text{ kip} > 550.3 \text{ kip} \text{ **OK**}$

This back face check is the most critical nodal strength check within the STM design of the bent cap. If the statement in Article 5.6.3.3.3a of the proposed STM specifications were ignored, the factored load would be 86.8 kips larger. The concrete would not have adequate strength to carry this load. The structural designer should always consider Article 5.6.3.3.3a to ensure the most economical design is achieved.

STRUT-TO-NODE INTERFACE

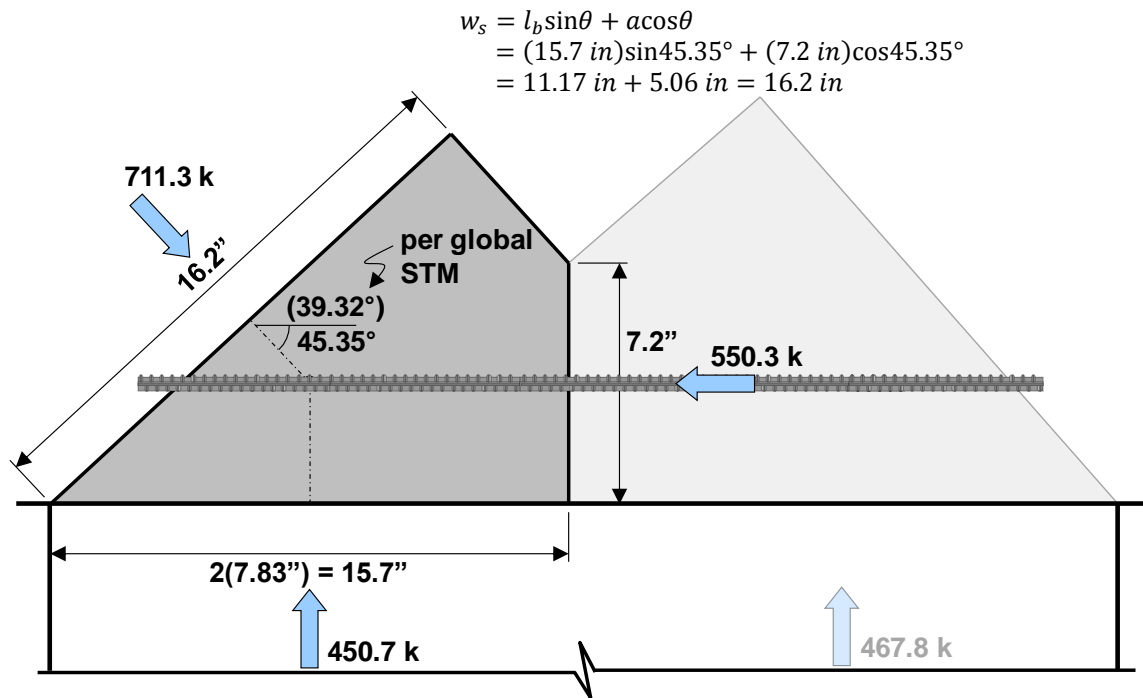
Factored Load: $F_u = 790.4 \text{ kip}$

Efficiency: $\nu = 0.85 - 4.0 \text{ ksi} / 20 \text{ ksi} = 0.65$

\therefore Use $\nu = 0.65$

Concrete Capacity: $f_{cu} = m \cdot \nu \cdot f'_c = (1.32)(0.65)(4.0 \text{ ksi}) = 3.4 \text{ ksi}$
 $\varphi \cdot F_n = (0.7)(3.4 \text{ ksi})(16.1 \text{ in})(31.9 \text{ in})$
 $= 1222 \text{ kip} > 790.4 \text{ kip} \text{ **OK**}$

Node JJ – Left (CCC)



$$\begin{aligned}
 w_s &= l_b \sin\theta + a \cos\theta \\
 &= (15.7 \text{ in}) \sin 45.35^\circ + (7.2 \text{ in}) \cos 45.35^\circ \\
 &= 11.17 \text{ in} + 5.06 \text{ in} = 16.2 \text{ in}
 \end{aligned}$$

Figure 4.19: Node JJ – left nodal subdivision

Comparing the back faces of both the left and right nodal subdivisions of Node JJ reveals that the strength checks are identical except for the concrete efficiency factors. The back face check of the right nodal subdivision governs the design since it has an efficiency factor of 0.7. The left nodal subdivision is treated as a CCC node, and its back face has a concrete efficiency factor of 0.85. The strut-to-node interface of the left nodal subdivision is therefore the only remaining face of Node JJ that needs to be checked.

Triaxial Confinement Factor: $m = 1.32$

STRUT-TO-NODE INTERFACE

Factored Load: $F_u = 711.3 \text{ kip}$

Efficiency: $v = 0.85 - 4.0 \text{ ksi} / 20 \text{ ksi} = 0.65$
 \therefore Use $v = 0.65$

Concrete Capacity: $f_{cu} = m \cdot v \cdot f'_c = (1.32)(0.65)(4.0 \text{ ksi}) = 3.4 \text{ ksi}$
 $\varphi \cdot F_n = (0.7)(3.4 \text{ ksi})(16.2 \text{ in})(31.9 \text{ in})$
 $= 1230 \text{ kip} > 711.3 \text{ kip} \text{ OK}$

Therefore, the strength of Node JJ is sufficient to resist the applied forces.

Node P (CTT)

Node P is presented along with Node JJ and Strut P/JJ in Figure 4.21. Since only one diagonal strut enters Node P, subdividing the node to simplify the strength checks is unnecessary. The lower end of Strut P/JJ was shifted to the left, however, as a result of the subdivision of Node JJ. The angle of Strut P/JJ, therefore, needs to be revised to reflect the geometry shown in Figure 4.20. (Note that the resulting angle is different from the angle that was previously calculated when Struts P/JJ and II/JJ were resolved into a single strut.) The calculation to determine the revised angle of Strut P/JJ (shown in Figure 4.20) is as follows:

$$\theta = \tan^{-1} \left[\frac{34.84 \text{ in}}{38.92 \text{ in} - (31.9 \text{ in}/2 - 7.83 \text{ in})} \right] = 48.52^\circ$$

where 34.84 in. is the height of the STM, 38.92 in. is the length of the truss panel between Node P and Column 4, 31.9 in. is the dimension of the equivalent square column, and 7.83 in. defines the line of action for the left component of the column reaction. All these values are shown in Figure 4.20.

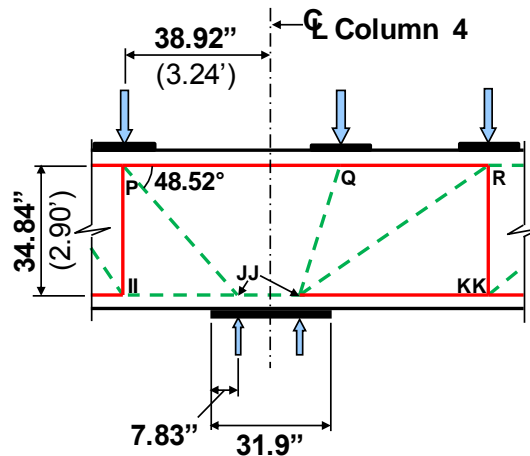


Figure 4.20: Adjusting the angle of Strut P/JJ due to the subdivision of Node JJ

The length of the back face of Node P is taken as twice the distance from the top surface of the bent cap to the centroid of the longitudinal reinforcement (i.e. top chord of the STM). The bearing area of Node P is assumed to be the square area defined in Section 4.2.3 and illustrated in Figure 4.9(a). The length of the bearing face and width of the node (into the page) is therefore taken as 16.2 inches. The length of the strut-to-node interface, w_s , is determined by the calculation in Figure 4.21.

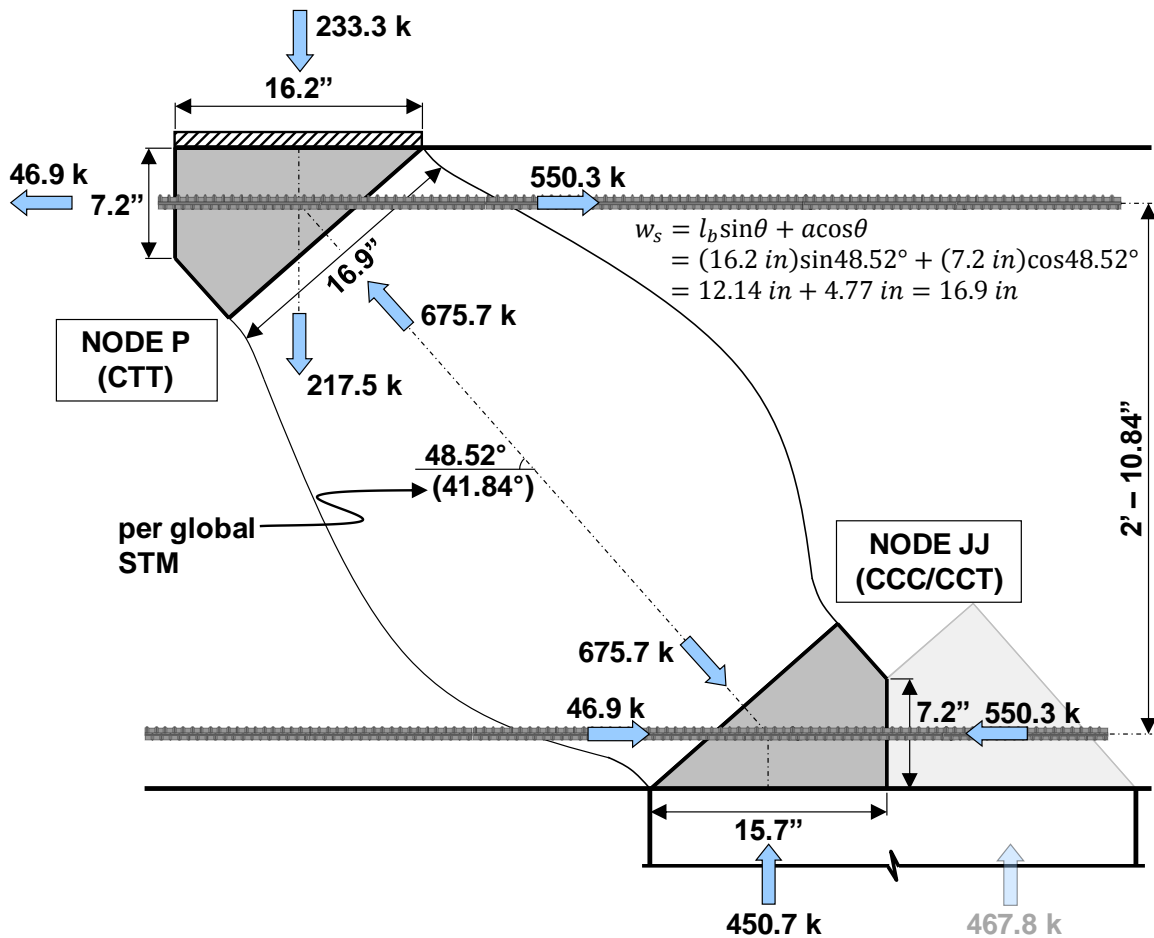


Figure 4.21: Node P shown with Node JJ and Strut P/JJ

The calculation for the triaxial confinement factor, m , for Node P is shown below. The factor can be applied to all the faces of Node P.

Triaxial Confinement Factor:

$$m = \sqrt{A_2/A_1} = \sqrt{(42 \text{ in})^2 / (16.2 \text{ in})^2} = 2.59 > 2 \quad \therefore \text{Use } m = 2$$

The bearing strength at Node P was previously checked. The tensile forces acting along the top chord of the STM at Node P (refer to Figure 4.21) are not critical if the tie reinforcement is adequately developed. Since no direct compressive forces act on the back face, it does not need to be checked. The strength of the strut-to-node interface is calculated and compared to the applied load as follows:

STRUT-TO-NODE INTERFACE

Factored Load:	$F_u = 675.7 \text{ kip}$
Efficiency:	$\nu = 0.65$ (See previous calculation for Node JJ)
Concrete Capacity:	$f_{cu} = m \cdot \nu \cdot f'_c = (2)(0.65)(4.0 \text{ ksi}) = 5.2 \text{ ksi}$
	$\varphi \cdot F_n = (0.7)(5.2 \text{ ksi})(16.9 \text{ in})(16.2 \text{ in})$
	$= 997 \text{ kip} > 675.7 \text{ kip} \quad \mathbf{OK}$

Therefore, the strength of Node P is sufficient to resist the applied forces.

Node R (CTT)

Node R is shown in Figure 4.22. The dimensions of the node and the revised angle of Strut R/JJ are determined in a manner similar to that of Node P and Strut P/JJ. The nodal strength calculations are provided below.

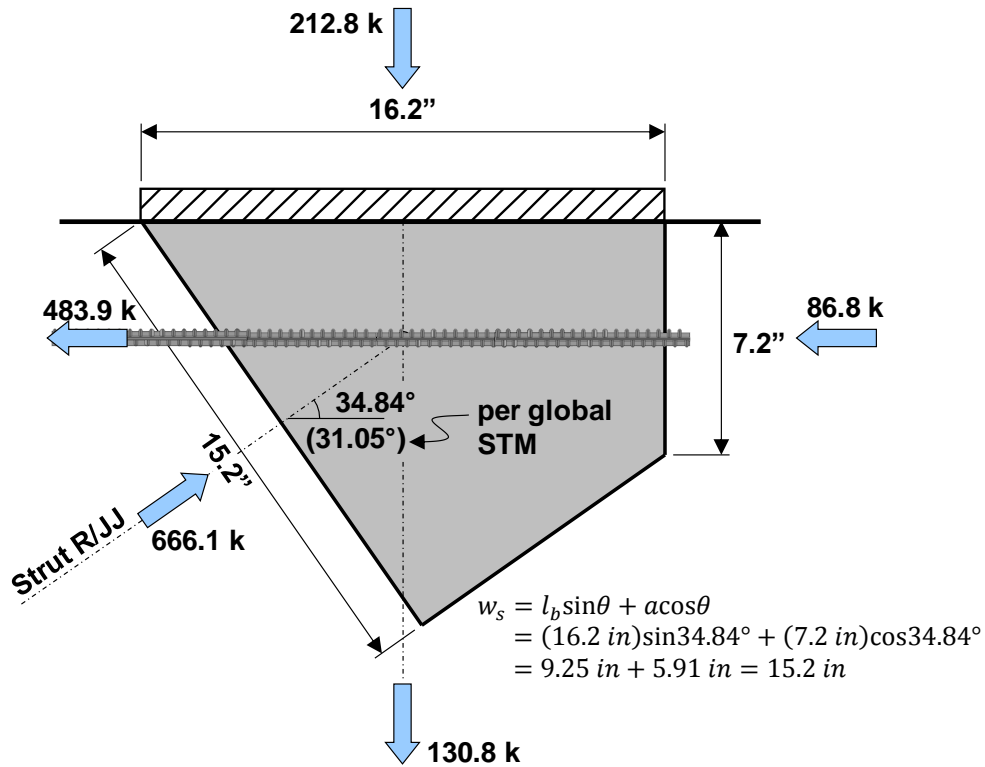


Figure 4.22: Node R

Triaxial Confinement Factor: $m = 2$

BEARING FACE

Factored Load: $F_u = 212.8 \text{ kip}$

The concrete capacity is the same as the bearing face of Node P, and the factored load is smaller. → **OK**

BACK FACE

Factored Load: $F_u = 86.8 \text{ kip}$

Efficiency: $\nu = 0.65$ (See previous calculation for Node JJ)

Concrete Capacity: $f_{cu} = m \cdot \nu \cdot f'_c = (2)(0.65)(4.0 \text{ ksi}) = 5.2 \text{ ksi}$

$\varphi \cdot F_n = (0.7)(5.2 \text{ ksi})(7.2 \text{ in})(16.2 \text{ in})$
 $= 425 \text{ kip} > 86.8 \text{ kip}$ **OK**

STRUT-TO-NODE INTERFACE

Factored Load: $F_u = 666.1 \text{ kip}$

Efficiency: $\nu = 0.65$ (See previous calculation for Node JJ)

Concrete Capacity: $f_{cu} = m \cdot v \cdot f'_c = (2)(0.65)(4.0 \text{ ksi}) = 5.2 \text{ ksi}$
 $\phi \cdot F_n = (0.7)(5.2 \text{ ksi})(15.2 \text{ in})(16.2 \text{ in})$
 $= 896 \text{ kip} > 666.1 \text{ kip} \text{ OK}$

Therefore, the strength of Node R is sufficient to resist the applied forces.

Node Q (CCT)

Node Q is presented in Figure 4.23. Strength calculations are not required to conclude that the node has adequate strength. Comparing Node Q with Nodes P and R reveals that Node Q has the strut-to-node interface with the largest area and the smallest applied force. Furthermore, the strength of the bearing face of Node Q does not need to be calculated since the critical bearing stresses on the bent cap were previously checked. Lastly, no direct compressive forces act on the back face provided the longitudinal reinforcement is adequately anchored. Node Q, therefore, has sufficient strength to resist the applied forces.

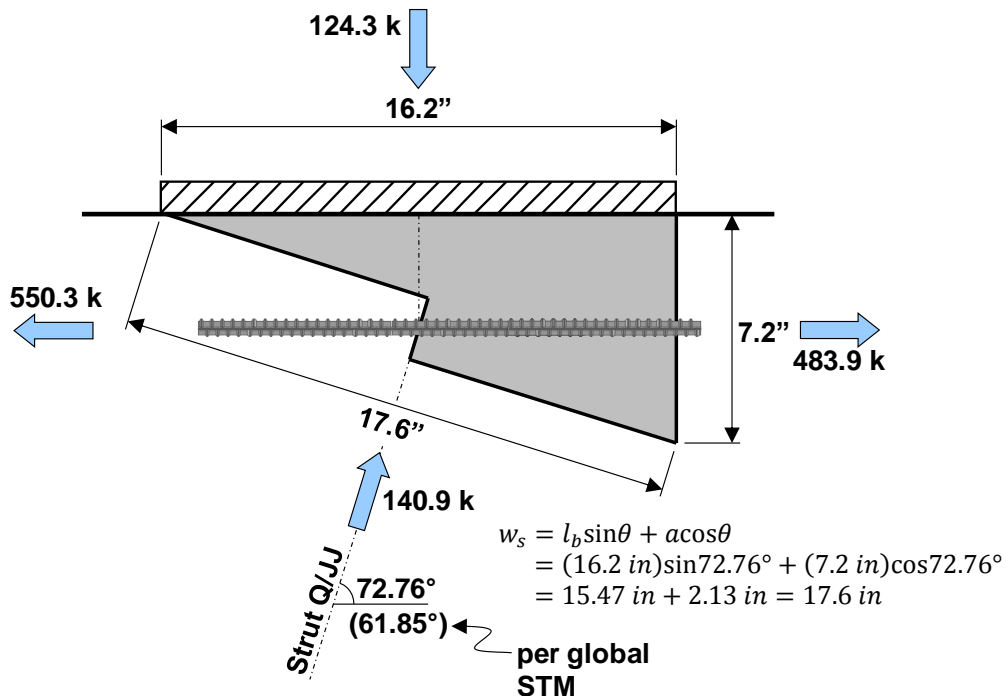


Figure 4.23: Node Q

Node EE (CCC)

Several struts enter Node EE from different directions. Resolution of adjacent struts and subdivision of the node will be necessary to define the nodal geometry. Node EE is depicted in Figure 4.24(a) as it appears in the strut-and-tie model of Figure 4.10. First, adjacent struts are resolved to reduce the number of forces acting at Node EE. Struts J/EE and DD/EE are resolved into a single strut; similarly, Struts L/EE and EE/FF are also combined. Struts separated by a large angle should not be resolved into a single strut. For this reason, Strut K/EE remains independent. For example, if Strut K/EE were combined together with Struts J/EE and DD/EE, the angle between two of the struts in the same grouping (i.e. the 90-degree angle between Struts K/EE and DD/EE) would be too large.

Following the resolution of adjacent struts, the node is subdivided into three parts as illustrated in Figure 4.24(b). The subdivision of the node is performed in a manner similar to that of Node JJ. The 179.1-kip reaction from the column equilibrates the vertical component of the 359.9-kip resolved strut on the left. Similarly, the 263.4-kip column reaction is equilibrated by the 263.4-kip vertical strut, and so forth. Please recall that the line of action for each component of the column reaction is determined by maintaining uniform pressure over the column width. The length of the bearing face of each nodal subdivision is again based on these lines of action of the reaction components. The angles of the two resolved struts are revised in the same manner as the strut angles at Node JJ. As an example, the revised angle of the resolved strut entering Node EE from the left (resulting from the combination of Struts J/EE and DD/EE) is calculated as follows:

$$\tan(29.84^\circ) = \frac{34.84 \text{ in}}{x} \quad x = 60.74 \text{ in}$$

$$\theta = \tan^{-1} \left[\frac{34.84 \text{ in}}{60.74 \text{ in} - (31.9 \text{ in}/2 - 4.20 \text{ in})} \right] = 35.42^\circ$$

where 29.84° is the original angle of the resolved strut on the left, 34.84 in. is the height of the STM, and all other values are shown in Figure 4.24(b).

As a result of the nodal subdivision, Strut K/EE is no longer vertical but is orientated at a slight angle. This angle, however, is considered negligible, and Strut K/EE is assumed to remain vertical and act along the same line as the 263.4-kip reaction from the column. This assumption simplifies the geometry of the node.

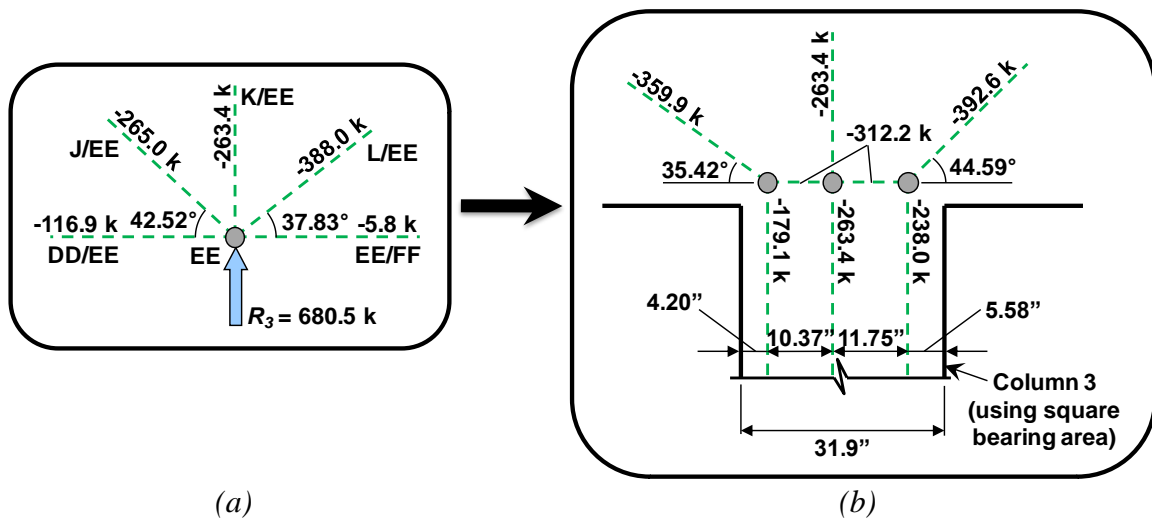


Figure 4.24: Node EE – (a) from STM and (b) with resolved struts and subdivided into three parts

The three subdivisions of Node EE are presented in Figure 4.25. The force acting on the back face of each nodal subdivision (i.e. the compressive force that exists between the three subdivisions) is determined by enforcing equilibrium for each portion of the node shown in Figure 4.24(b) using the original strut angles. This force is found to be 312.2 kips. Each part of the node can be treated as an independent CCC node.

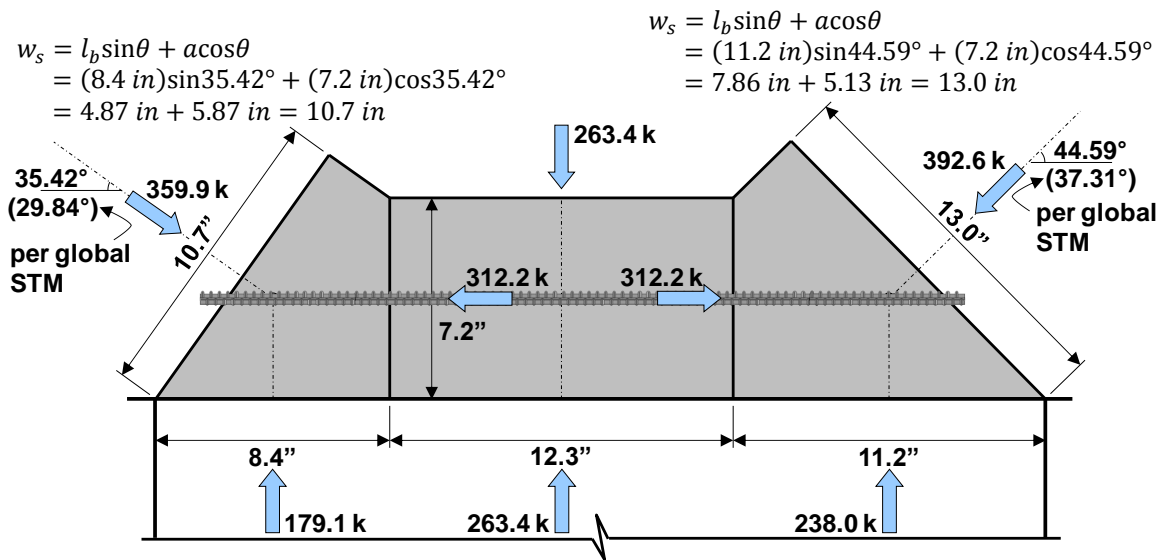


Figure 4.25: Node EE

Node EE – Left (CCC)

Triaxial Confinement Factor: $m = 1.32$

BEARING FACE

The critical bearings were previously checked.

BACK FACE

Factored Load: $F_u = 312.2 \text{ kip}$

Efficiency: $\nu = 0.85$

Concrete Capacity: $f_{cu} = m \cdot \nu \cdot f'_c = (1.32)(0.85)(4.0 \text{ ksi}) = 4.5 \text{ ksi}$
 $\phi \cdot F_n = (0.7)(4.5 \text{ ksi})(7.2 \text{ in})(31.9 \text{ in})$
 $= 723 \text{ kip} > 312.2 \text{ kip} \text{ OK}$

STRUT-TO-NODE INTERFACE

Factored Load: $F_u = 359.9 \text{ kip}$

Efficiency: $\nu = 0.85 - 4.0 \text{ ksi} / 20 \text{ ksi} = 0.65$

\therefore Use $\nu = 0.65$

Concrete Capacity: $f_{cu} = m \cdot \nu \cdot f'_c = (1.32)(0.65)(4.0 \text{ ksi}) = 3.4 \text{ ksi}$
 $\phi \cdot F_n = (0.7)(3.4 \text{ ksi})(10.7 \text{ in})(31.9 \text{ in})$
 $= 812 \text{ kip} > 359.9 \text{ kip} \text{ OK}$

Node EE – Right (CCC)

Triaxial Confinement Factor: $m = 1.32$

BEARING FACE

The critical bearings were previously checked.

BACK FACE

Factored Load: $F_u = 312.2 \text{ kip}$

This check is the same as the back face check for the left portion of Node EE. →

OK

STRUT-TO-NODE INTERFACE

Factored Load: $F_u = 392.6 \text{ kip}$

Efficiency: $v = 0.65$ (See previous calculation for Node JJ)

Concrete Capacity: $f_{cu} = m \cdot v \cdot f'_c = (1.32)(0.65)(4.0 \text{ ksi}) = 3.4 \text{ ksi}$
 $\phi \cdot F_n = (0.7)(3.4 \text{ ksi})(13.0 \text{ in})(31.9 \text{ in})$
 $= 987 \text{ kip} > 392.6 \text{ kip}$ **OK**

Node EE – Middle (CCC)

All strength checks are **OK** by inspection. The top face (treated as a strut-to-node interface) has a larger area and smaller applied force compared to the strut-to-node interface of the left portion of Node EE.

Therefore, the strength of Node EE is sufficient to resist the applied forces.

Nodes V (CCT) and NN (CCC/CCT)

Nodes V and NN along with Strut V/NN are shown in Figure 4.26. The geometry of the nodes and the revised angles of the struts are determined using the same procedures as before. The external load acting at Node V results from the combination of the loads from two girders, as described in Section 4.2.2. The bearing at this node is assumed to be square with an area equivalent to the sum of two effective rectangular bearing areas (refer to Section 4.2.3 and Figure 4.9). Therefore, the bearing area at Node V is 23.0 inches by 23.0 inches.

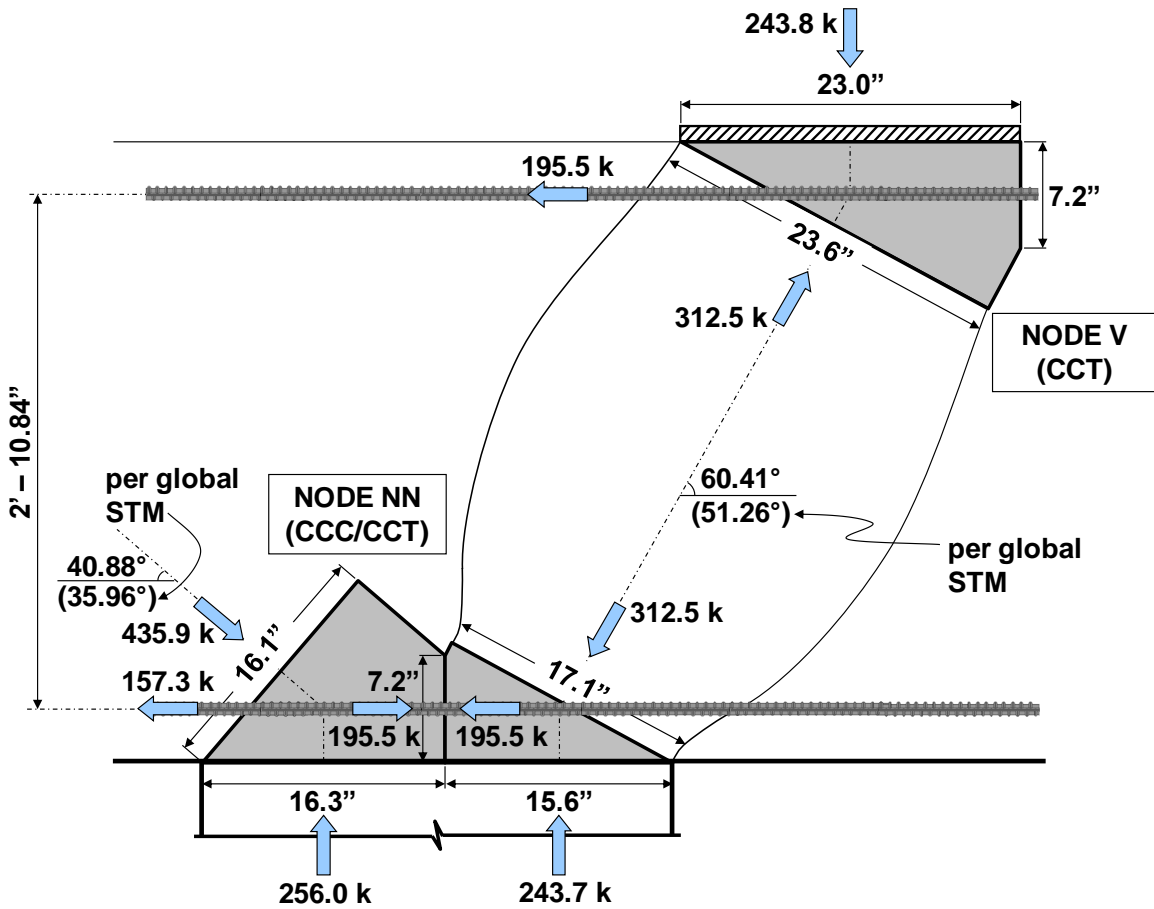


Figure 4.26: Nodes V and NN and Strut V/NN

Node NN – Left (CCT)

Triaxial Confinement Factor: $m = 1.32$

BEARING FACE

The critical bearings were previously checked.

BACK FACE

Factored Load: $F_u = 195.5 \text{ kip}$

The concrete capacity is the same as the back face of the right portion of Node JJ, and the factored load is smaller. $\rightarrow OK$

STRUT-TO-NODE INTERFACE

$$\begin{aligned}\text{Factored Load:} & F_u = 435.9 \text{ kip} \\ \text{Efficiency:} & \nu = 0.65 \text{ (See previous calculation for Node JJ)} \\ \text{Concrete Capacity:} & f_{cu} = m \cdot \nu \cdot f'_c = (1.32)(0.65)(4.0 \text{ ksi}) = 3.4 \text{ ksi} \\ & \varphi \cdot F_n = (0.7)(3.4 \text{ ksi})(16.1 \text{ in})(31.9 \text{ in}) \\ & = 1222 \text{ kip} > 435.9 \text{ kip } \mathbf{OK}\end{aligned}$$

Node NN – Right (CCC)

All strength checks are **OK** by inspection.

Node V (CCT)

All strength checks are **OK** by inspection.

Therefore, the strengths of Nodes V and NN are sufficient to resist the applied forces.

Other Nodes

The other nodes of the STM can be checked using the same procedure. Several nodes for which explicit calculations are not provided herein can be deemed to have adequate strength by inspection. In this design example, all nodes have sufficient strength to resist the applied factored forces. To expedite the calculations, the designer may wish to conduct nodal strength checks in a spreadsheet or other automated format, especially if multiple STM iterations are needed (i.e. if modifications to the strut-and-tie model are required).

4.4.5 Step 5: Proportion Stirrups in High Shear Regions

The reinforcement required to carry the forces in the vertical ties of the strut-and-tie model is determined next. Ties L/FF, J/DD, P/II, and U/MM are identified as the critical vertical ties within the STM (Figure 4.10). Identification of the critical ties must take into account two factors: (1) the magnitude of the force in the tie and (2) the length over which the reinforcement comprising the tie can be distributed (i.e. the tie width). For each of the critical ties, the stirrup spacing and corresponding reinforcement area that is required to carry the tie force will be compared to the minimum crack control reinforcement required by the proposed STM specifications in Chapter 3. The calculations will reveal that the stirrups that must be provided along the length of the bent

cap to satisfy the minimum crack control reinforcement provisions will be sufficient to carry the forces in most of the vertical ties of the STM. The required crack control reinforcement is determined in Section 4.4.6.

Tie L/FF

Nodes L and FF are interior nodes that are not bounded by bearing plates or any other boundary condition that clearly define their geometries. Such nodes are referred to as *smear nodes*. To determine the amount of stirrup reinforcement required to carry the force in Tie L/FF, the tie width must first be defined. In other words, the available length over which the reinforcement comprising Tie L/FF can be distributed must be determined. To estimate the available length, l_a , a proportioning technique recommended by Wight and Parra-Montesinos (2003) is used (refer to Section 2.9.5). Assuming that Struts L/EE and M/FF fan out over a large area at either end of Tie L/FF, the stirrups that are engaged by the struts as indicated in Figure 4.27 can be considered as a part of the vertical tie.

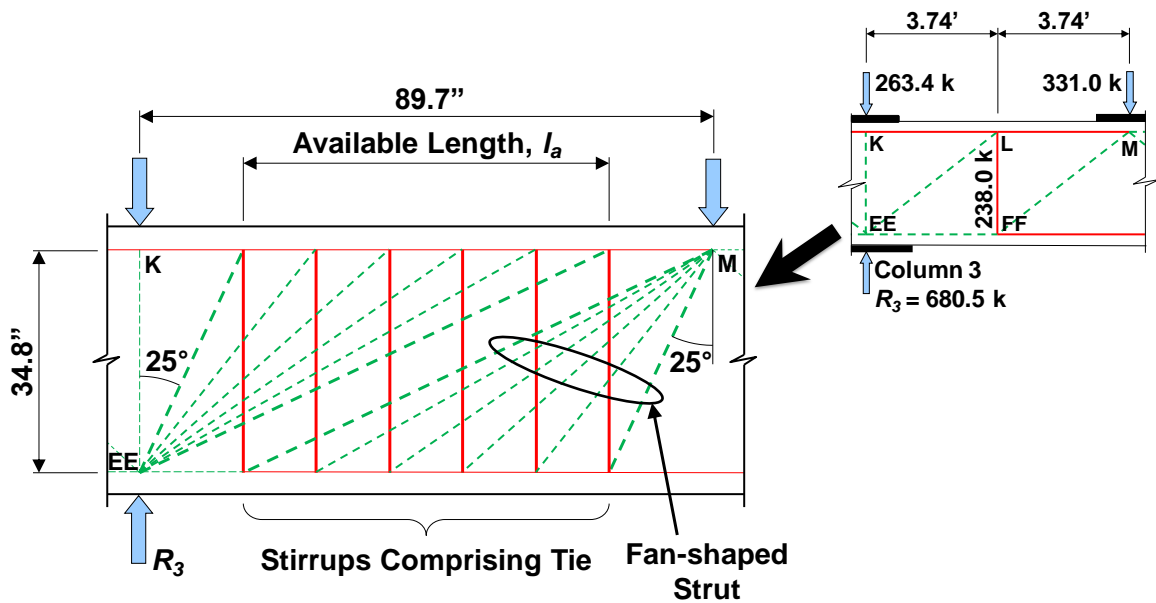


Figure 4.27: Determination of the available length for Tie L/FF (adapted from Wight and Parra-Montesinos, 2003)

Using this method, the length l_a can be calculated as follows:

$$l_a = 89.7 \text{ in} - 2(34.8 \text{ in})(\tan 25^\circ) = 57.2 \text{ in}$$

where 89.7 in. is the total length of the two panels of the STM between Nodes K and M and 34.8 in. is the height of the STM (refer to Figure 4.27).

Two-legged stirrups may be spaced over the available length, l_a , to carry the force in Tie L/FF. Using #5 stirrups, the required stirrup spacing for Tie L/FF is calculated as follows:

$$\begin{aligned} \text{Factored Load:} & \quad F_u = 238.0 \text{ kip} \\ \text{Tie Capacity:} & \quad \phi \cdot f_y \cdot A_{st} = F_u \\ & \quad (0.9)(60 \text{ ksi})A_{st} = 238.0 \text{ kip} \\ & \quad A_{st} = 4.41 \text{ in}^2 \end{aligned}$$

$$\text{Number of \#5 stirrups (2 legs) required: } 4.41 \text{ in}^2 / (2)(0.31 \text{ in}^2) = 7.11 \text{ stirrups}$$

$$l_a = 57.2 \text{ in} \quad s = 57.2 \text{ in} / 7.11 = 8.0 \text{ in}$$

Use 2 legs of #5 stirrups with spacing no greater than 8.0 in.

The spacing of two-legged stirrups required by the crack control reinforcement provisions (refer to Section 4.4.6) is smaller than the spacing required to carry the force in Tie L/FF. The crack control reinforcement requirement, therefore, governs within this region of the bent cap.

Tie J/DD

The reinforcement required for Tie J/DD is determined in the same manner as that of Tie L/FF. The required crack control reinforcement specified in Section 4.4.6 will satisfy the stirrup spacing that is required to carry the force in Tie J/DD.

The designer should ensure that the assumed length over which the reinforcement comprising Tie I/CC can be distributed does not overlap the stirrups assumed to carry the force in Tie J/DD, as illustrated in Figure 4.28. This is a general rule that should be satisfied when specifying the required stirrup spacing for any member. For the five-

column bent cap, the crack control reinforcement governs the stirrup spacing for both Ties I/CC and J/DD.

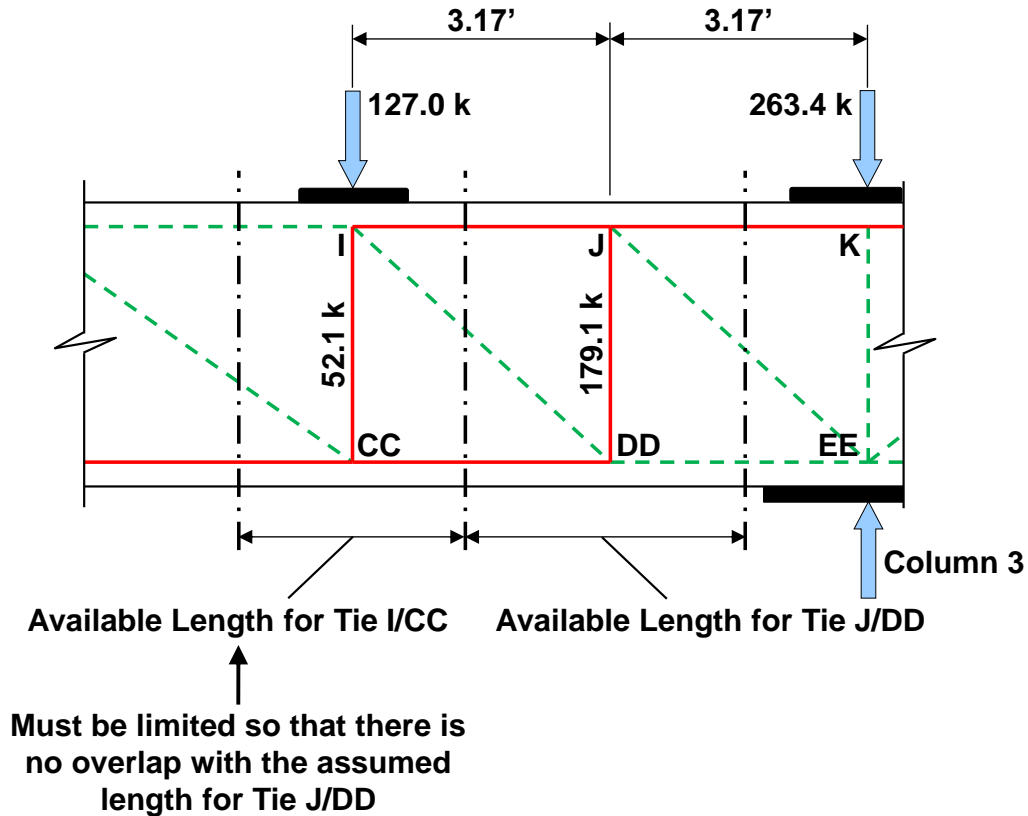


Figure 4.28: Limiting the assumed available lengths for ties to prevent overlap

Tie P/II

Since Node P is bounded by a bearing plate, its geometry can be defined (i.e. it is a singular node, not a smeared node). The recommendation of Wight and Parra-Montesinos (2003) pertains to a tie connecting two smeared nodes and, therefore, cannot be used to determine the available length over which the reinforcement comprising Tie P/II can be distributed. For cases when a vertical tie joins at a singular node, the available length is limited to the smaller length of the two adjacent truss panels. The available length for Tie P/II is therefore equivalent to the distance between Nodes O and P, 1.93 feet, and is centered on Tie P/II (refer to Figure 4.29(a)). In other words, the

stirrups comprising Tie P/II can be spread over a distance of 1.93 ft ÷ 2 on either side of the tie.

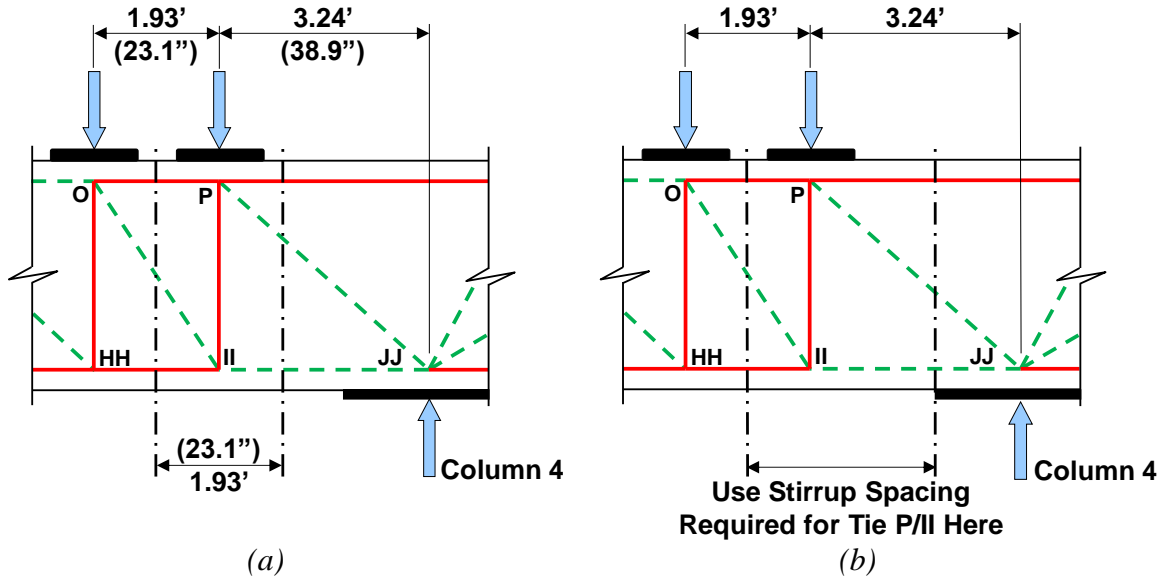


Figure 4.29: (a) Available length for Tie P/II; (b) required spacing for Tie P/II extended to the column

Four-legged stirrups will be required to carry the force in Tie P/II to comply with the 4-inch minimum stirrup spacing specified in TxDOT's *Bridge Design Manual - LRFD* (2009). The stirrups are proportioned as follows:

$$\begin{aligned}
 \text{Factored Load:} & & F_u &= 217.5 \text{ kip} \\
 \text{Tie Capacity:} & & \phi \cdot f_y \cdot A_{st} &= F_u \\
 & & (0.9)(60 \text{ ksi})A_{st} &= 217.5 \text{ kip} \\
 & & A_{st} &= 4.03 \text{ in}^2
 \end{aligned}$$

$$\text{Number of \#5 stirrups (4 legs) required: } 4.03 \text{ in}^2 / (4)(0.31 \text{ in}^2) = 3.25 \text{ stirrups}$$

$$l_a = 23.1 \text{ in} \quad s = 23.1 \text{ in} / 3.25 = 7.1 \text{ in}$$

Use 4 legs of #5 stirrups with spacing less than 7.1 in.

The region of the bent cap between the load at Node P and the column reaction at Node JJ is a high shear region. For this reason, reinforcement required for Tie P/II should be extended to the face of the column, at a minimum (refer to Figure 2.29(b)). Providing only minimum crack control reinforcement within the high shear region to the left of the column is inadvisable.

Tie U/MM

Tie U/MM is identified as a critical vertical tie because of the small available length over which the stirrups can be distributed. The available length is determined in the same manner as that of Tie P/II (using the length of the smaller adjacent truss panel). The required crack control reinforcement specified in Section 4.4.6 below will be sufficient to carry the force in Tie U/MM.

4.4.6 Step 6: Proportion Crack Control Reinforcement

To satisfy the crack control reinforcement requirement of the proposed STM specifications, 0.3% reinforcement must be provided in each orthogonal direction along the length of the bent cap. The reinforcement in the vertical and horizontal directions must therefore satisfy the following expressions (refer to Section 2.10):

$$\rho_v = \frac{A_v}{b_w s_v} \geq 0.003 \tag{4.1}$$

$$\rho_h = \frac{A_h}{b_w s_h} \geq 0.003 \tag{4.2}$$

Using two-legged #5 stirrups and #5 bars as horizontal skin reinforcement, the required spacing of the crack control reinforcement is calculated as follows:

$$A_v = 0.003 b_w s_v \quad \rightarrow \quad \begin{aligned} 2(0.31 \text{ in}^2) &= 0.003(42 \text{ in})s_1 \\ s_v &= 4.9 \text{ in} \end{aligned}$$

$$A_h = 0.003 b_w s_h \quad \rightarrow \quad \begin{aligned} 2(0.31 \text{ in}^2) &= 0.003(42 \text{ in})s_2 \\ s_h &= 4.9 \text{ in} \end{aligned}$$

The crack control reinforcement is adequate to carry the forces in all the vertical ties except for Tie P/II. For this tie, the required stirrups calculated in Section 4.4.5 must be used.

Summary

- Use 2 legs of #5 stirrups with spacing less than 4.9 in. along the length of the bent cap except for Tie P/II
- Use 4 legs of #5 stirrups with spacing less than 7.1 in. for Tie P/II
- Use #5 bars with spacing less than 4.9 in. as horizontal skin reinforcement
(Final reinforcement details are provided in Figures 4.33 and 4.34)

4.4.7 Step 7: Provide Necessary Anchorage for Ties

Per Article 5.6.3.4.2 of the proposed STM specifications in Chapter 3, the top and bottom chord (i.e. longitudinal) reinforcement must be properly anchored at either end of the five-column bent cap (i.e. the bars should be developed at Nodes A, V, W, and NN). Continuity of the reinforcement over the bent cap length will be provided via longitudinal splices. The available length for development of the tie bars is measured from the point where the centroid of the longitudinal reinforcement exits the extended nodal zone, as shown at Node NN in Figure 4.30 (refer to Section 2.11).

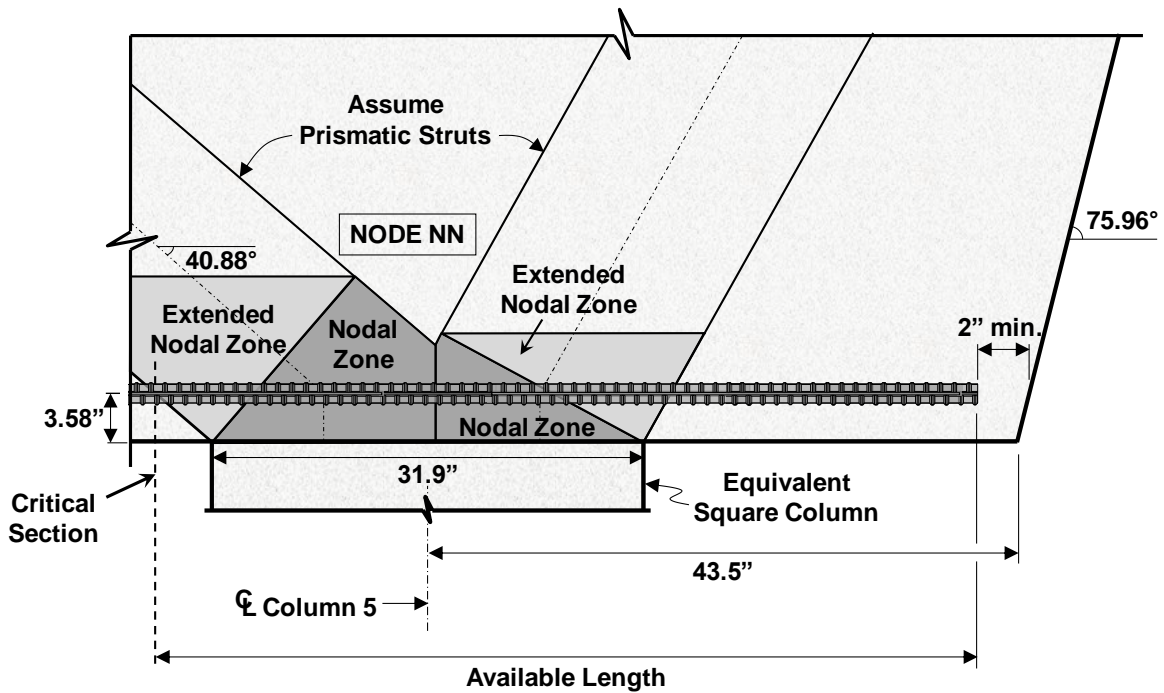


Figure 4.30: Anchorage of bottom chord reinforcement at Node NN

The development length available for the bottom chord reinforcement at Node NN assuming 2-inch clear cover is:

$$\begin{aligned} \text{Available length} &= \\ &= 43.5 \text{ in} + 31.9 \text{ in}/2 + 3.58 \text{ in}/\tan 40.88^\circ + 3.58 \text{ in}/\tan 75.96^\circ - 2 \text{ in} \\ &= 62.5 \text{ in} \end{aligned}$$

All the dimensional values within this calculation are shown in Figure 4.30. The available length at Node W is determined in a similar manner using the appropriate strut angle. If straight bars are used, the required development length is calculated as follows (per Article 5.11.2.1 of AASHTO LRFD (2010)):

$$l_d = \frac{1.25A_b f_y}{\sqrt{f'_c}} = \frac{1.25(1.56 \text{ in}^2)(60 \text{ ksi})}{\sqrt{4.0 \text{ ksi}}} = 58.5 \text{ in} < 62.5 \text{ in} \text{ OK}$$

Enough length is available for straight-bar anchorage at both Nodes NN and W.

For the top chord reinforcement, the available length is not sufficient for straight bar anchorage; therefore, hooks will be used. The available length at Node V is illustrated in Figure 4.31 and calculated as follows:

$$\begin{aligned} \text{Available length} &= 26.1 \text{ in} + 23.0 \text{ in}/2 + 3.58 \text{ in}/\tan 60.41^\circ - 10 \text{ in}/\tan 75.96^\circ - 2 \text{ in} \\ &= 35.1 \text{ in} \end{aligned}$$

All the dimensional values within this calculation are shown in Figure 4.31. The available length at Node A is determined in a similar manner using the appropriate strut angle and replacing 26.1 in. with 26.5 in., the distance from the center of the bearing area of Node A to the upper corner of the bent cap. The required development length for 90-degree hooks is calculated as follows (per Article 5.11.2.4 of AASHTO LRFD (2010)):

$$l_{dh} = \frac{38.0d_b}{\sqrt{f'_c}} \cdot 0.7 = \frac{38.0(1.41 \text{ in})}{\sqrt{4.0 \text{ ksi}}} \cdot 0.7 = 18.8 \text{ in} < 35.1 \text{ in} \text{ **OK**}$$

Hooked bars are used at both Nodes A and V. The final reinforcement details are presented in Figures 4.33 and 4.34.

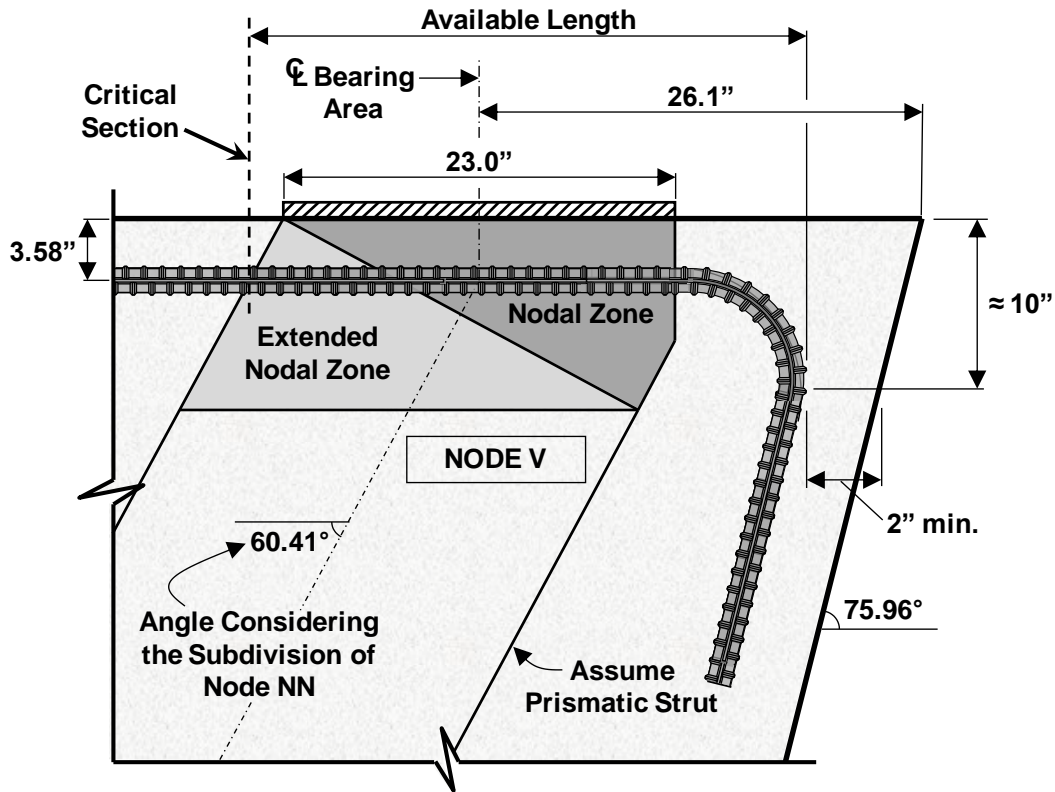


Figure 4.31: Anchorage of top chord reinforcement at Node V

4.4.8 Step 8: Perform Shear Serviceability Check

The estimated diagonal cracking strength of the concrete can be compared to the unfactored service level shear to determine the likelihood of the formation of service cracks. Identifying the critical region for the serviceability check depends on the service shear, effective depth, web width, and shear span at a given point. The serviceability check allows designers to estimate the likelihood of diagonal cracking due to highly stressed diagonal struts. The diagonal cracking strength, V_{cr} , can be estimated by the following expression (refer to Section 2.12):

$$V_{cr} = \left[6.5 - 3 \left(\frac{a}{d} \right) \right] \sqrt{f'_c} b_w d \quad (4.3)$$

but not greater than $5\sqrt{f'_c} b_w d$ nor less than $2\sqrt{f'_c} b_w d$

where:

- a = shear span (in.)
- d = effective depth of the member (in.)
- f'_c = specified compressive strength of concrete (psi)
- b_w = width of member's web (in.)

Applying the AASHTO LRFD (2010) Service I load case to the bent cap and analyzing it as a continuous beam reveals that the region near Column 4 is critical (recall that the load case maximizes shear near Column 4). The highest service shear occurs between the support reaction at Column 4 and the load at Node Q. A portion of the loaded bearing area, however, is directly above the column reaction. Therefore, the shear span between the load at Node Q and Column 4 is not critical. Loads will flow directly from the location of the applied load to the support.

Although the serviceability behavior of the short shear span between Node Q and the column does not need to be checked, the possibility of diagonal crack formation within the shear span between Column 4 and the load at Node R should be considered. Within this region, the magnitude of the service shear is 255.7 kips (the shear between Nodes Q and R). The shear span, or the distance between the load at Node R and the reaction of Column 4, is 57.9 inches. The shear span-to-depth ratio, a/d , is calculated to be 1.51 ($a/d = 57.9 \text{ in.}/38.4 \text{ in.}$). Please recall from Section 2.12 that the upper and lower limits of the diagonal cracking load equation occur at a/d ratios of 0.5 and 1.5, respectively. Therefore, the magnitude of V_{cr} for the region right of Column 4 (i.e. between Node R and Column 4) is:

$$\begin{aligned} V_{cr} &= 2\sqrt{f'_c} b_w d = 2\sqrt{4000 \text{ psi}}(42 \text{ in})(38.4 \text{ in}) \\ &= 204 \text{ kip} < 255.7 \text{ kip } \mathbf{NG} - \text{Expect diagonal cracks} \end{aligned}$$

The data point of the normalized service shear for this region is plotted in Figure 4.32 (labeled "Right of Column 4"). Further discussion regarding this plot can be found in Section 2.12.

The shear serviceability check reveals the risk of the formation of diagonal cracks in the region right of the column when the full service loads act on the bent cap. The required crack control reinforcement should help to minimize the widths of the cracks that may form and alleviates the cause for concern regarding significant diagonal crack formation in this region. Moreover, the shear force measured at first diagonal cracking exhibits significant scatter (refer to the experimental data of Figure 4.32 relative to the data point for the region under consideration). Lastly, the expression for V_{cr} presented above estimates the diagonal cracking load with a reasonable amount of conservatism. For these reasons, significant serviceability problems are not expected within the region right of Column 4 given the current service load case.

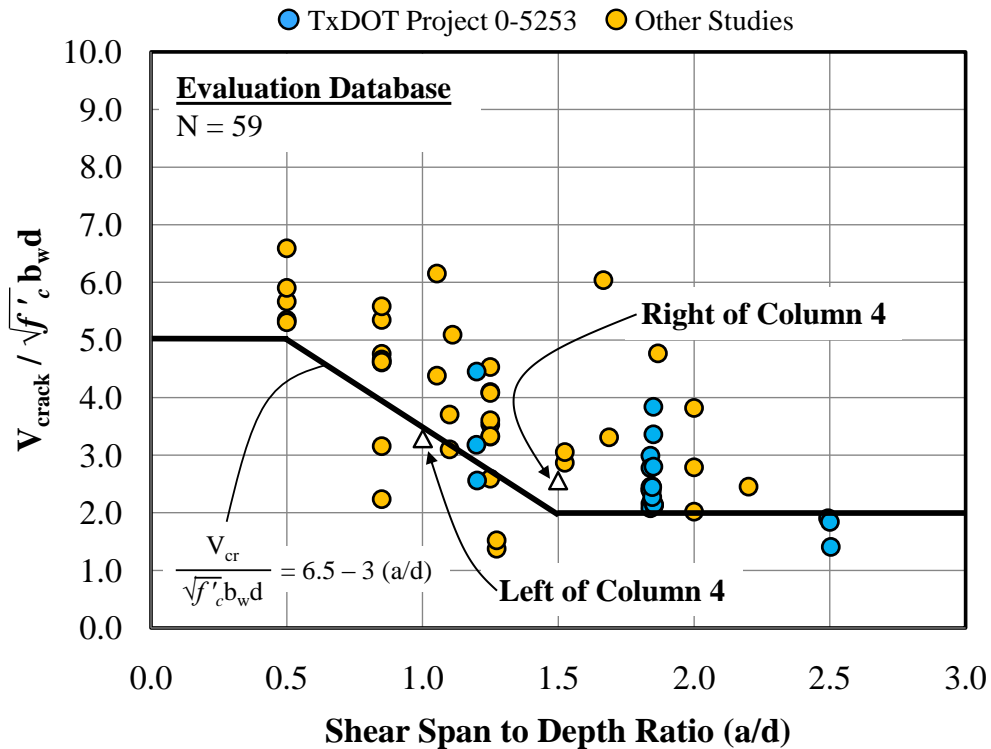


Figure 4.32: Diagonal cracking load equation with experimental data and the normalized service shear for two regions of the bent cap (adapted from Birrcher et al., 2009)

The region between the load at Node P and Column 4 is checked next. Here, the shear force due to service loads is 330.3 kips. Although the magnitude of this shear force is greater than the magnitude of the shear force in the region right of Column 4 (255.7 kips), it is less critical due to the shorter shear span. For the region left of Column 4, the estimated diagonal cracking strength is:

$$V_{cr} = \left[6.5 - 3 \left(\frac{38.9 \text{ in}}{42 \text{ in} - 3.58 \text{ in}} \right) \right] (\sqrt{4000 \text{ psi}})(42 \text{ in})(42 \text{ in} - 3.58 \text{ in})$$

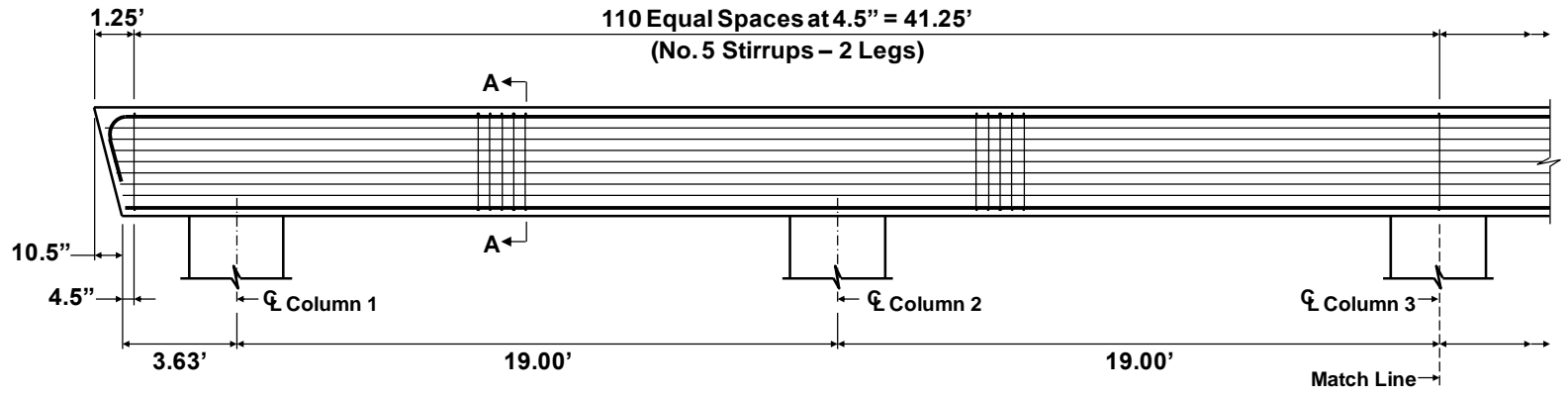
$$= 353 \text{ kip} > 330.3 \text{ kip} \text{ **OK** - Diagonal cracking is not expected}$$

This value is within the $5\sqrt{f'_c}b_wd$ and $2\sqrt{f'_c}b_wd$ limits. Since the estimated diagonal cracking load, 353 kips, is greater than the service shear, 330.3 kips, diagonal cracks are not expected to form in this region for the particular service load case being considered (refer to corresponding data point in Figure 4.32).

Please recall that the bent cap that exists in the field has the same geometry as the bent cap of this design example but has a specified concrete compressive strength of 3.6 ksi. Using this value in the calculations above would slightly lower the magnitudes of the estimated diagonal cracking strengths.

4.5 REINFORCEMENT LAYOUT

The reinforcement details for the load case considered in this design example are presented in Figures 4.33 and 4.34.



136

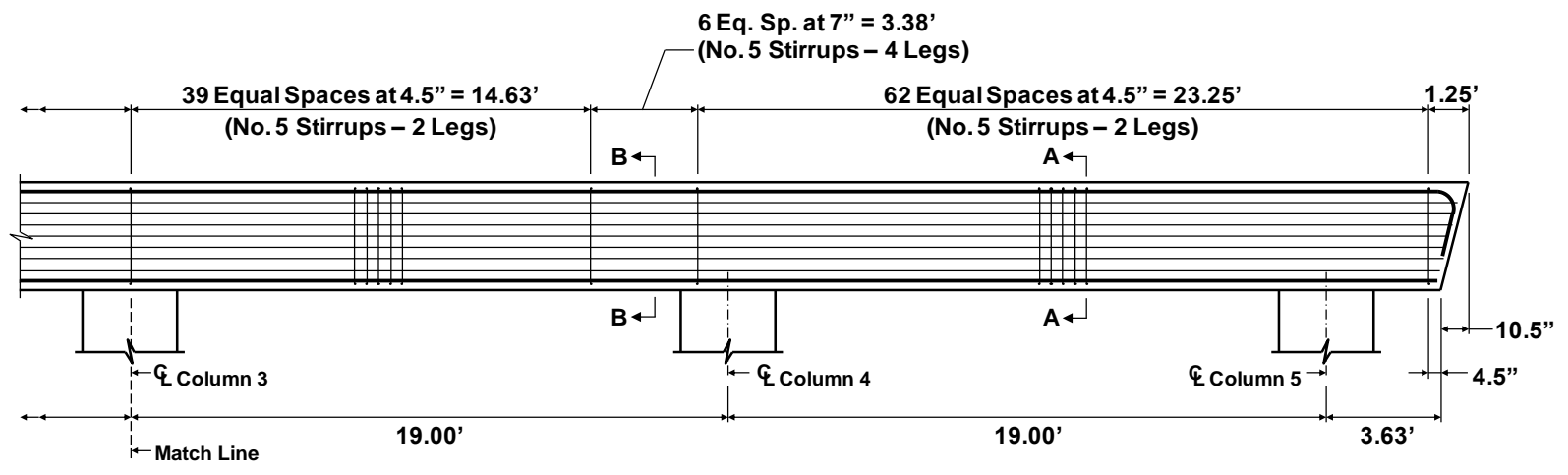
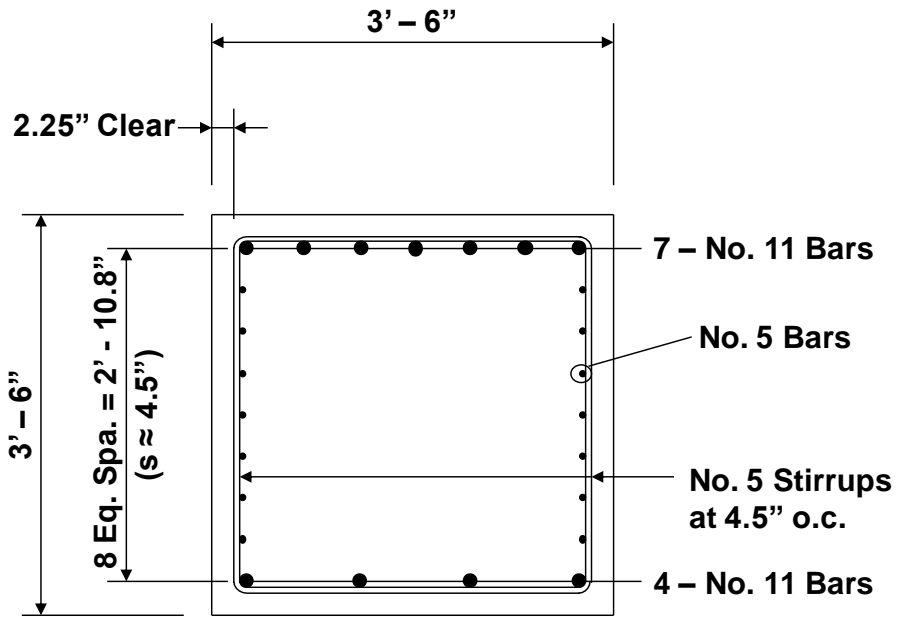
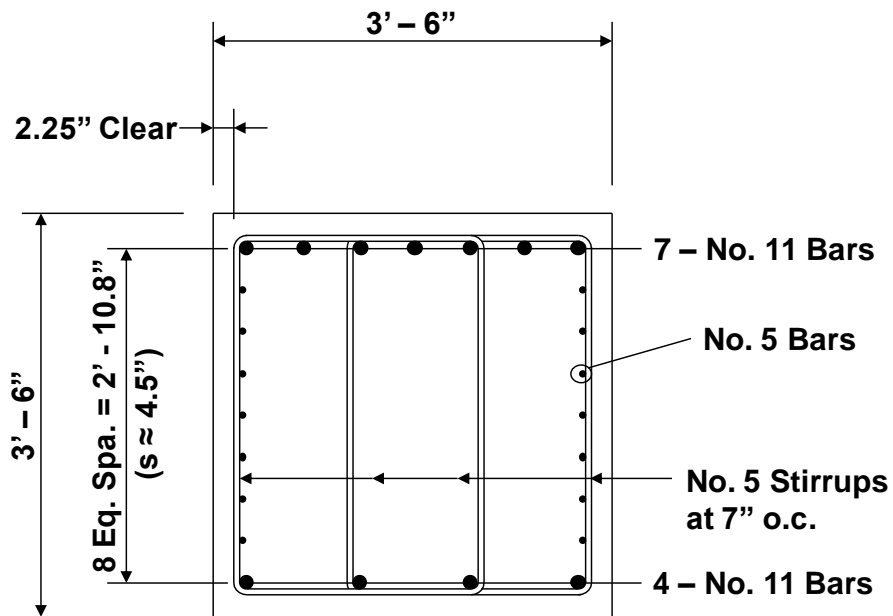


Figure 4.33: Reinforcement details – elevation (design per proposed STM specifications)



Section A-A



Section B-B

Figure 4.34: Reinforcement details – cross-sections (design per proposed STM specifications)

4.6 COMPARISON OF STM DESIGN TO SECTIONAL DESIGN

The five-column bent cap is an existing field structure that was originally designed using sectional methods. The load case considered in this design example maximizes the shear near Column 4. The reinforcement details of the region near Column 4 are therefore presented in Figure 4.35 for both the STM design and the existing structure.

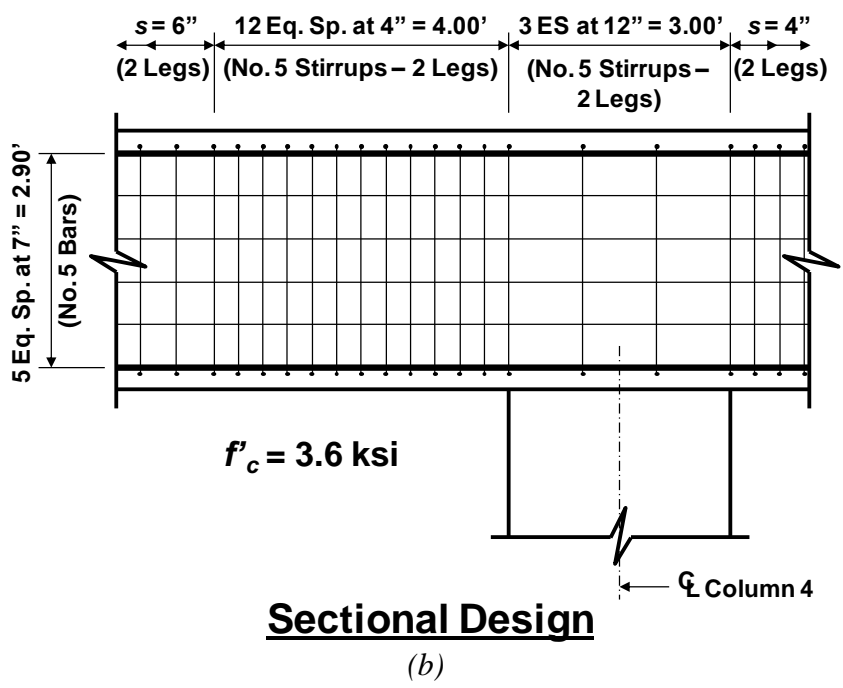
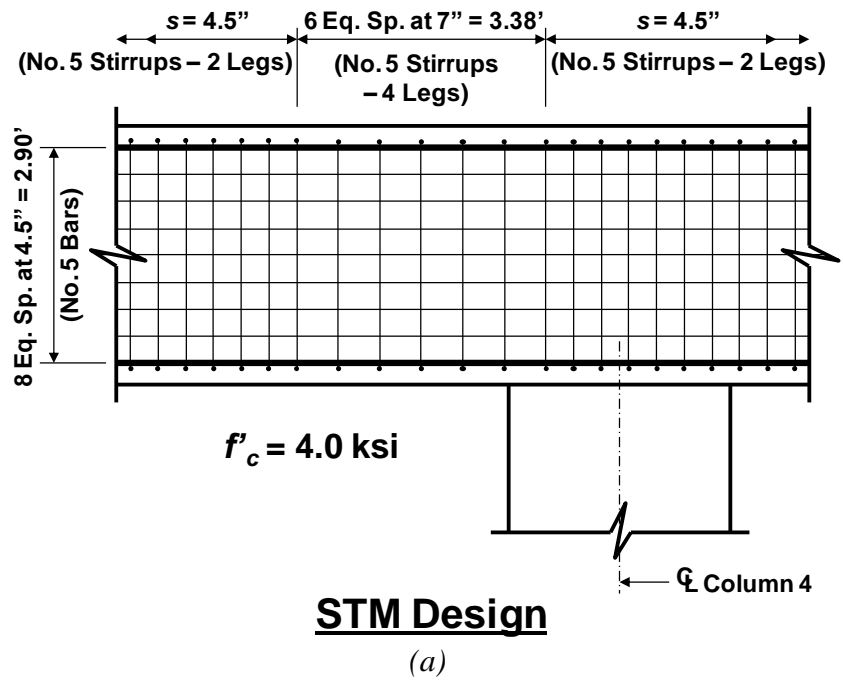


Figure 4.35: Reinforcement details near Column 4 – (a) STM design; (b) sectional design

A few points of comparison are identified between the two designs in Figure 4.35. First, the amount of stirrup reinforcement provided within the high shear region left of Column 4 is slightly greater for the STM design compared to the sectional design (four legs at approximately 7 inches versus two legs at 4 inches). Moreover, the specified compressive strength of the concrete for the existing bent cap is 3.6 ksi but was increased to 4.0 ksi to satisfy the nodal strength checks of the STM design (see the critical back face of Node JJ in Section 4.4.4). The strut-and-tie model identifies the large compressive forces that concentrate over Column 4. Lastly, 0.3% crack control reinforcement is provided in both the vertical and horizontal directions along the length of the bent cap designed per the STM specifications. This reinforcement should adequately restrain the widths of the diagonal cracks that may form (refer to Section 4.4.8). Experimental research has shown that 0.3% reinforcement in each direction is needed in order for the member to exhibit satisfactory serviceability performance at first cracking and at service loads (Birrcher et al., 2009).

4.7 SUMMARY

The STM design of a five-column bent cap of a skewed bridge was performed for one of several load cases to be considered. The strut-and-tie modeling and reinforcement detailing were completed according to the STM specifications proposed in Chapter 3 and all relevant provisions in the *AASHTO LRFD Bridge Design Specifications* (2010) (e.g. development length provisions). The defining features and challenges of this design example are listed below:

- Resolving girder loads in close proximity to each other in order to develop a simple, realistic strut-and-tie model
- Simplifying bearing areas of skewed girders so that the nodal geometries can be defined
- Developing an efficient strut-and-tie model for a beam with varying shear-span lengths

- Realistically modeling the flow of forces within a region near a column above which several girders are supported
- Defining relatively complicated nodal geometries above columns where several truss members join

Chapter 5. Example 2: Cantilever Bent Cap

5.1 SYNOPSIS

The design of a cantilever bent cap is presented within this chapter as a means of introducing new challenges that are likely to be encountered in practice when implementing the strut-and-tie modeling (STM) design procedure. Unique challenges of this example include (1) developing a strut-and-tie model that accurately represents the flow of forces around a frame corner subjected to closing loads, (2) designing a curved-bar node, and (3) strut-and-tie modeling of a sloped structure (applied loads are not perpendicular to the primary longitudinal chord of the STM). The cantilever bent cap is sloped to accommodate the banked grade of the direct connector lanes supported by the bent. Step-by-step guidance is offered for overcoming each challenge. The complete STM design of the bent cap is demonstrated for one of several load cases to be considered.

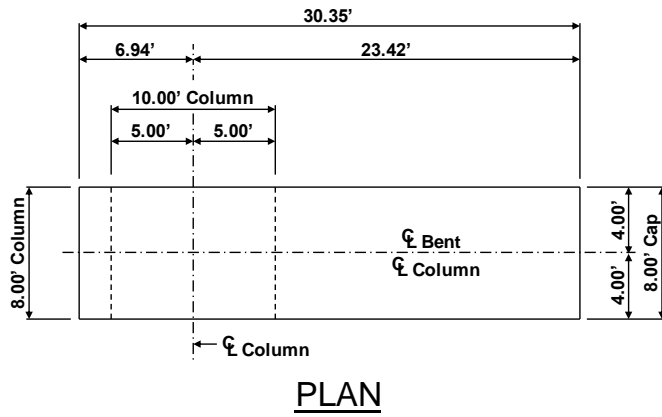
5.2 DESIGN TASK

The geometry of the cantilever bent cap and the load case that will be considered are presented in Sections 5.2.1 and 5.2.2. The bent cap geometry is based on that of an existing field structure in Texas. The geometry of the existing bent cap has been simplified for this design example (e.g. architectural details have been removed). In addition, the width of the cap has been increased in order to satisfy the proposed STM specifications of Chapter 3. The load case presented in Section 5.2.2 was provided by TxDOT.

5.2.1 Bent Cap Geometry

Elevation and plan views of the cantilever bent cap are provided in Figures 5.1 and 5.2. For clarity, only the basic geometry of the bent cap, excluding the bearing pads and bearing seats, is shown in Figure 5.1. A more detailed geometry of the cap is presented in Figure 5.2. The bent cap has a width of 8 feet and a height of 8.50 feet (measured perpendicular to the longitudinal axis of the cap). The column is 10 feet by 8

feet (i.e. the column has the same width as the bent cap). The cross slope of the bent cap relative to the horizontal is approximately 3.0 degrees. The cantilever cap supports two prestressed concrete U-beams from one direction and two steel girders from the opposite direction. Each of the U-beams rests on two neoprene bearing pads, while each of the steel girders is supported by a single pot bearing. The bearing conditions of each girder are shown in Figure 5.2 and will be further discussed in Section 5.2.3. The plan views of the bent cap in Figures 5.1 and 5.2 and elsewhere in this chapter are horizontal projections of the topside of the cap.



144

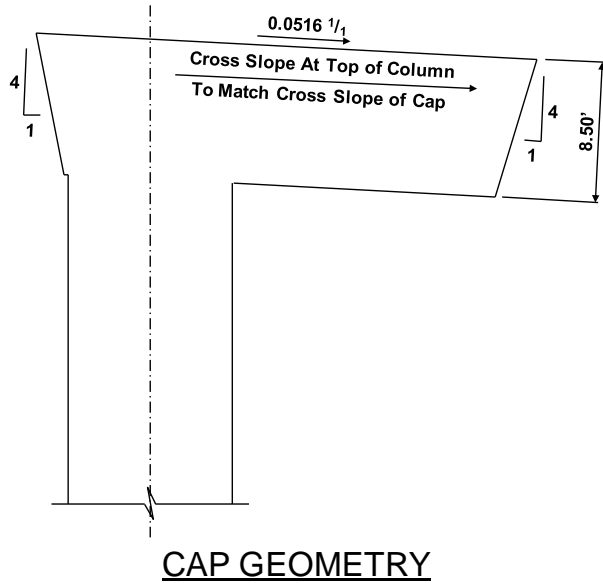


Figure 5.1: Plan and elevation views of cantilever bent cap (simplified geometry)

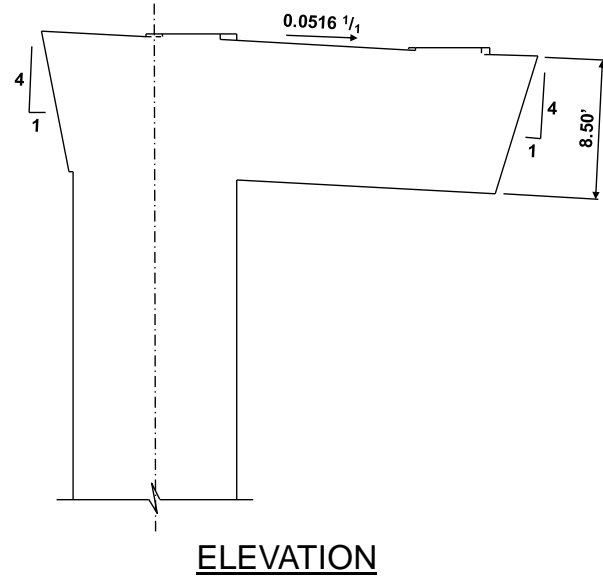
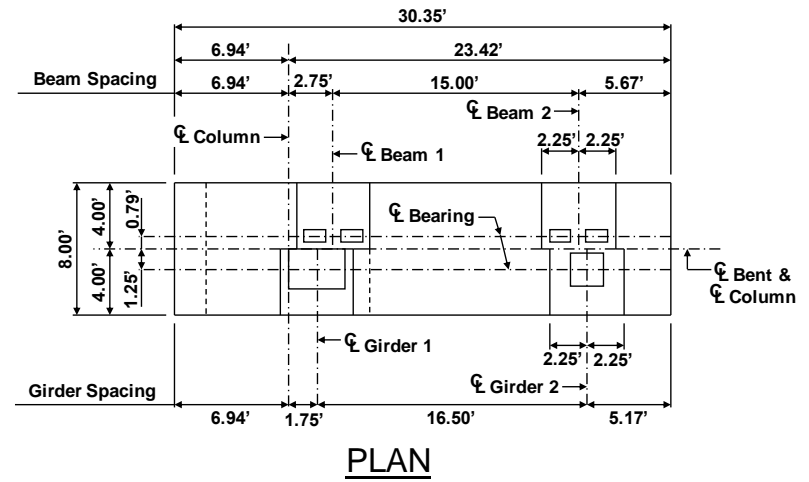


Figure 5.2: Plan and elevation views of cantilever bent cap (detailed geometry)

5.2.2 Determine the Loads

The factored loads from the two steel girders and two concrete U-beams are shown in Figure 5.3(a). These loads correspond to one particular load case of many considered by TxDOT during the original design process. The final design of the bent cap would be contingent on the consideration of all governing load cases. Each of the loads in Figure 5.3(a) is assumed to act at the point where the longitudinal centerline of a beam/girder coincides with the transverse centerline of the respective bearing pad(s).

In the same manner as with the load case of Example 1, the point loads in close proximity to one another are resolved together to simplify the load case and facilitate development of a practical strut-and-tie model. The 1396.4-kip and 403.7-kip factored loads on the left are resolved into a single load; similarly, the 403.7-kip and 366.8-kip loads on the right are combined together. The resulting loads are shown in Figure 5.3(b). The locations of the resolved loads are determined by the calculations below. In these calculations, x_1 is the horizontal distance from the centerline of the column to the 1800.1-kip resolved load, P_1 . Similarly, x_2 is the horizontal distance from the centerline of the column to the 770.5-kip resolved load, P_2 (refer to the plan view of Figure 5.3(b)).

$$x_1 = \frac{(403.7 \text{ kip})(2.75 \text{ ft}) + (1396.4 \text{ kip})(1.75 \text{ ft})}{403.7 \text{ kip} + 1396.4 \text{ kip}} = 1.97 \text{ ft}$$

$$x_2 = \frac{(403.7 \text{ kip})(2.75 \text{ ft} + 15.00 \text{ ft}) + (366.8 \text{ kip})(1.75 \text{ ft} + 16.50 \text{ ft})}{403.7 \text{ kip} + 366.8 \text{ kip}} = 17.99 \text{ ft}$$

All dimensions in the calculations can be found in Figure 5.3(a). The resolved loads are assumed to act at the longitudinal centerline of the top of the bent cap (see Figure 5.3(b)).

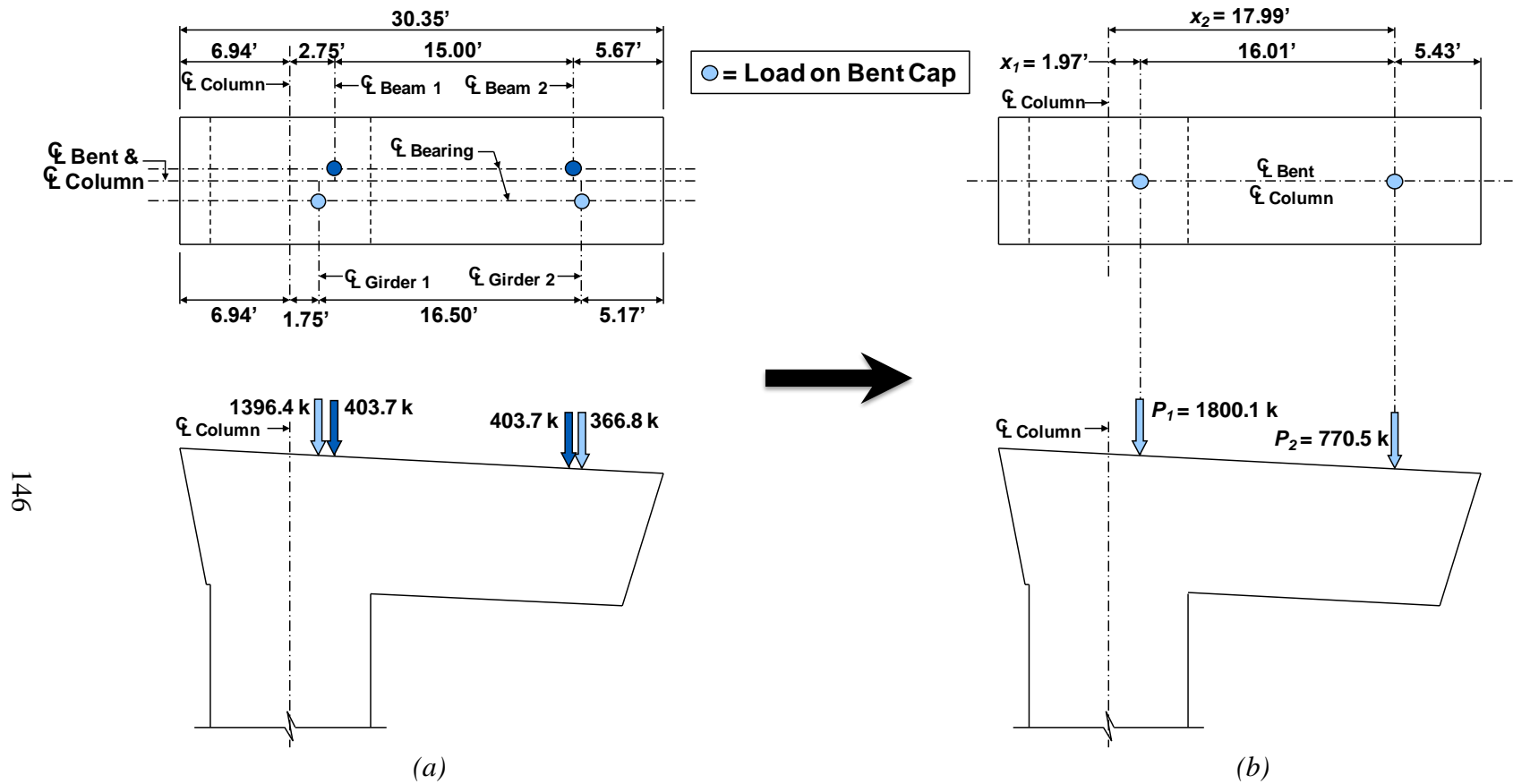


Figure 5.3: Factored loads acting on the bent cap (excluding self-weight) – (a) from each beam/girder; (b) resolved loads

Once the loads acting on the bent cap in Figure 5.3(b) are determined, the factored self-weight of the cap based on tributary volumes is added to each load (refer to Figure 5.4). The unit weight of the reinforced concrete is assumed to be 150 lb/ft³. The magnitude of each load acting on the strut-and-tie model, including the self-weight of the bent cap, is:

$$P_1 = 1800.1 \text{ kip} + 1.25(164.20 \text{ kip}) = 2005.3 \text{ kip}$$

$$P_2 = 770.5 \text{ kip} + 1.25(124.15 \text{ kip}) = 925.6 \text{ kip}$$

The first value in each calculation is the factored superstructure load. The second value is the tributary self-weight of the bent cap factored by 1.25 (in accordance with the AASHTO LFRD (2010) Strength I load combination). The calculations result in the final loads acting on the bent cap in Figure 5.4.

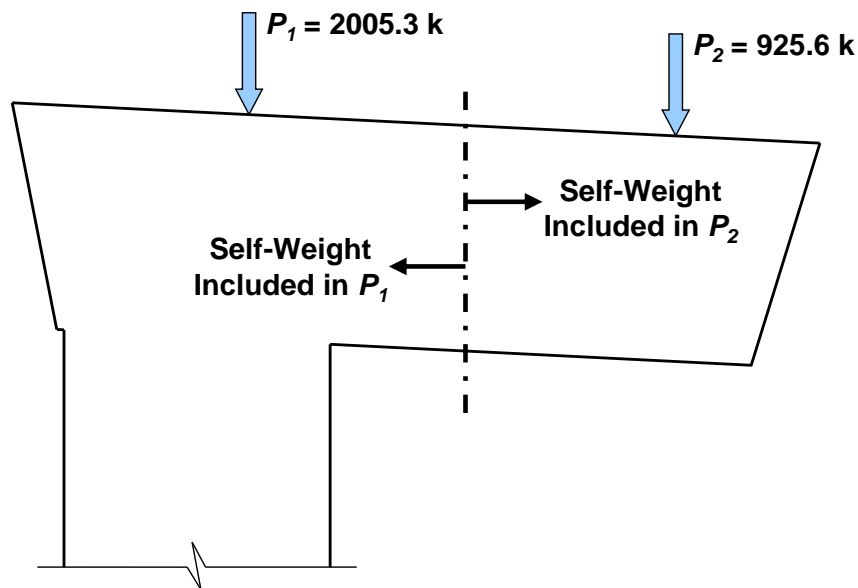


Figure 5.4: Adding factored self-weight to the superstructure loads

5.2.3 Determine the Bearing Areas

According to TxDOT's Bridge Standards (2006), each of the bearing pads supporting the prestressed concrete U-Beams are 16 inches by 9 inches. The steel girders are supported by pot bearings with masonry plates that rest on the bearing seats. The

sizes of the masonry plates for Girder 1 and Girder 2 are 42 by 29.5 inches and 24 by 24 inches, respectively. Each bearing pad/plate is placed on a bearing seat that allows the applied force to spread over an area of the cap surface that is larger than the pad/plate itself. Accounting for the beneficial effect of the bearing seats is similar to that of Example 1 (refer to Figure 4.8) with one exception. In the current example, the top surface of the bent cap is not parallel to the bearing seats. Each of the effective bearing areas at the top surface of the cap is therefore trapezoidal in shape. Considering the elevation views of each bearing seat in Figure 5.5, an applied force is able to spread more at the right portion of a bearing seat as compared to the left portion (a function of the bearing seat thickness). The longitudinal dimensions (i.e. effective lengths) of the effective areas are measured at the top surface of the bent cap and labeled in Figure 5.5. A plan view of the bearings is presented in Figure 5.6. The transverse dimensions (i.e. effective widths) shown in the figure are measured at the centerline of each bearing pad/plate. The effective width of the bearing area of Girder 1 has been limited to prevent overlap with the effective bearing area of Beam 1. The dimensions of the bearing areas are summarized in Table 5.1 along with the size of the effective bearing area for each beam/girder. The use of a computer-aided design program facilitates determination of these values.

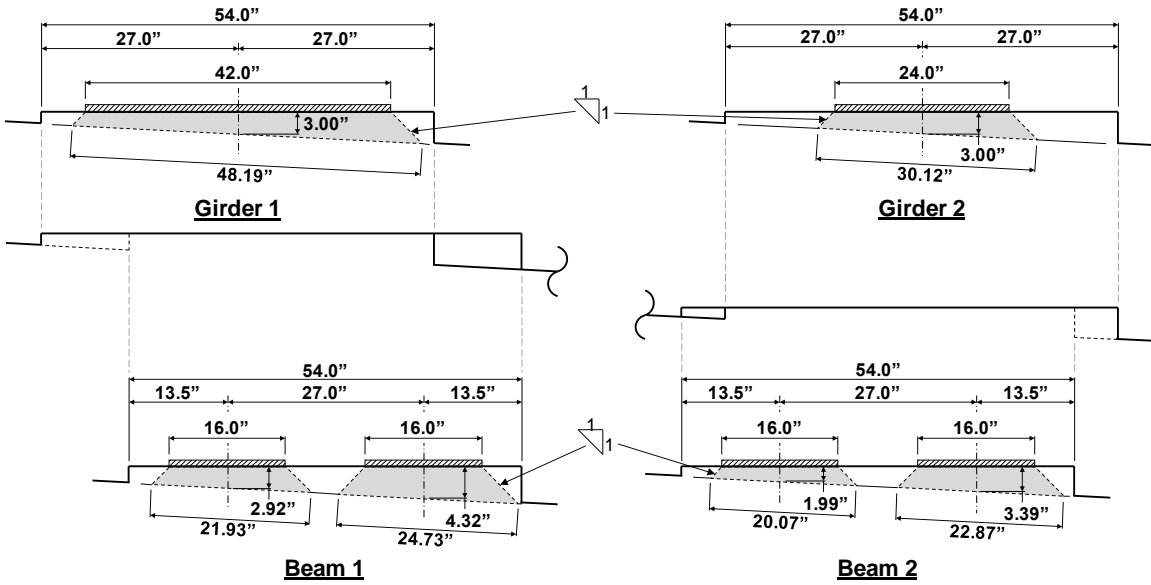


Figure 5.5: Effective bearing areas considering effect of bearing seats (elevation)

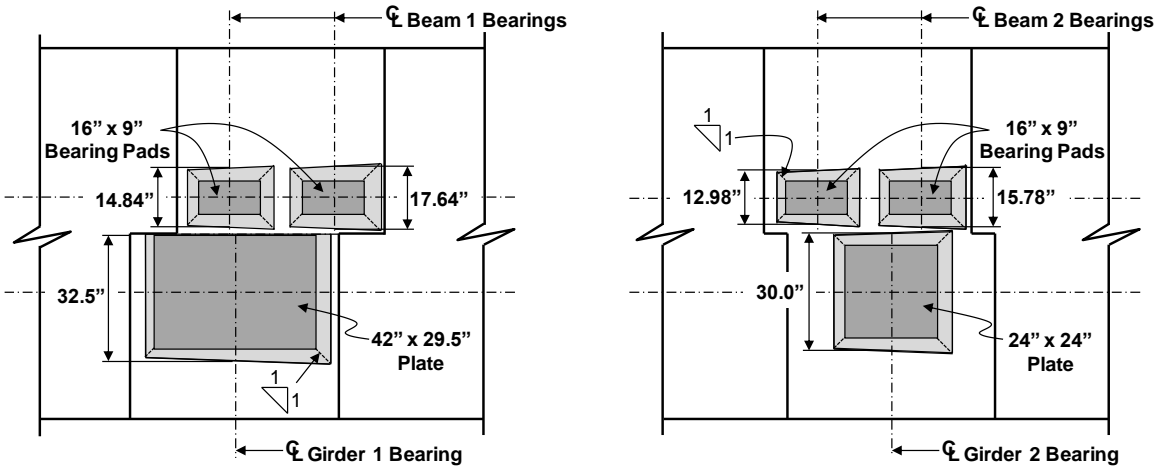


Figure 5.6: Effective bearing areas considering effect of bearing seats (plan)

Table 5.1: Bearing sizes and effective bearing areas for each beam/girder

	Girder 1	Girder 2	Beam 1		Beam 2	
			Pad 1	Pad 2	Pad 1	Pad 2
Bearing Size	42" x 29.5"	24" x 24"	16" x 9"	16" x 9"	16" x 9"	16" x 9"
Effective Length	48.19"	30.12"	21.93"	24.73"	20.07"	22.87"
Effective Width	32.5"	30.0"	14.84"	17.64"	12.98"	15.78"
Effective Area	1566.2 in. ²	903.6 in. ²	761.7 in. ²		621.4 in. ²	

To be able to easily define the geometry of the nodes that are located directly below the applied superstructure loads, the bearing areas are assumed to be square and located concentrically with the longitudinal axis of the bent cap. The same simplification was assumed in Example 1 (refer to Section 4.2.3). The effective bearing area for the load P_1 acting on the bent cap in Figure 5.4 is the combination of the effective bearing areas for Beam 1 and Girder 1, or 2327.9 in.², and is assumed to be a 48.2-inch by 48.2-inch square (i.e. $\sqrt{2327.9 \text{ in}^2} = 48.2 \text{ in}$). Similarly, the effective bearing area for the load P_2 acting on the cap is assumed to be a 39.1-inch by 39.1-inch square. Both loads are assumed to act at the center of these effective bearing areas.

5.2.4 Material Properties

- Concrete: $f'_c = 6.0 \text{ ksi}$
- Reinforcement: $f_y = 60 \text{ ksi}$

Recall that the cantilever bent cap is an existing field structure. The specified concrete compressive strength, f'_c , shown here is greater than that of the existing structure (3.6 ksi). The increased concrete strength is required to satisfy the nodal strength checks performed in accordance with the proposed STM specifications. Design iterations were necessary to determine both the concrete strength and bent cap width that are necessary to provide adequate strength to the critical node. Since the geometry of the strut-and-tie

model is dependent on the value of f'_c and the cap width (refer to Section 5.4.2), the geometry of the STM must be updated for every iteration that is performed.

5.3 DESIGN PROCEDURE

The entire cantilever bent cap is a D-region due to the applied superstructure loads (i.e. load discontinuities) and the geometric discontinuity of the frame corner. The behavior of the bent cap is therefore dominated by a nonlinear distribution of strains, and the STM procedure should be followed for its design. The general STM procedure introduced in Section 2.3.3 has been adapted to the current design scenario, resulting in the steps listed below. Two strut-and-tie models will be developed for the load case under consideration. The decision to use two models is discussed in Section 5.4.2.

- Step 1: Analyze structural component
- Step 2: Develop strut-and-tie models
- Step 3: Proportion vertical tie and crack control reinforcement
- Step 4: Proportion longitudinal ties
- Step 5: Perform nodal strength checks
- Step 6: Provide necessary anchorage for ties
- Step 7: Perform shear serviceability check

5.4 DESIGN CALCULATIONS

5.4.1 Step 1: Analyze Structural Component

During this step of the design process, the boundary forces that act on the D-region under consideration are determined. The transition from a D-region to a B-region occurs approximately one member depth away from a load or geometric discontinuity (refer to Section 2.2). Considering the bent, the D-region/B-region interface is assumed to be located at a distance of one column depth (i.e. 10 feet) from the bottom of the bent cap. According to St. Venant's principle, a linear distribution of stress can be assumed at

this interface. This linear stress distribution is shown in Figure 5.7. Determination of the extreme fiber stress for the right side of the column is illustrated below:

$$f_{Right} = \frac{P_1 + P_2}{A_{Column}} + \frac{M(60 \text{ in})}{I_{Column}}$$

$$M = P_1 x_1 + P_2 x_2$$

$$f_{Right} = \frac{2005.3 \text{ kip} + 925.6 \text{ kip}}{(96 \text{ in})(120 \text{ in})} + \frac{(247,313 \text{ kip-in})(60 \text{ in})}{1.38 \times 10^7 \text{ in}^4} = 1328 \text{ psi}$$

where A_{Column} is the cross-sectional area of the column, I_{Column} is its moment of inertia, and M is the moment at the centerline of the column due to P_1 and P_2 . The distances x_1 and x_2 were defined in Section 5.2.2. Similar calculations can be completed for the extreme fiber stress at the left side of the column.

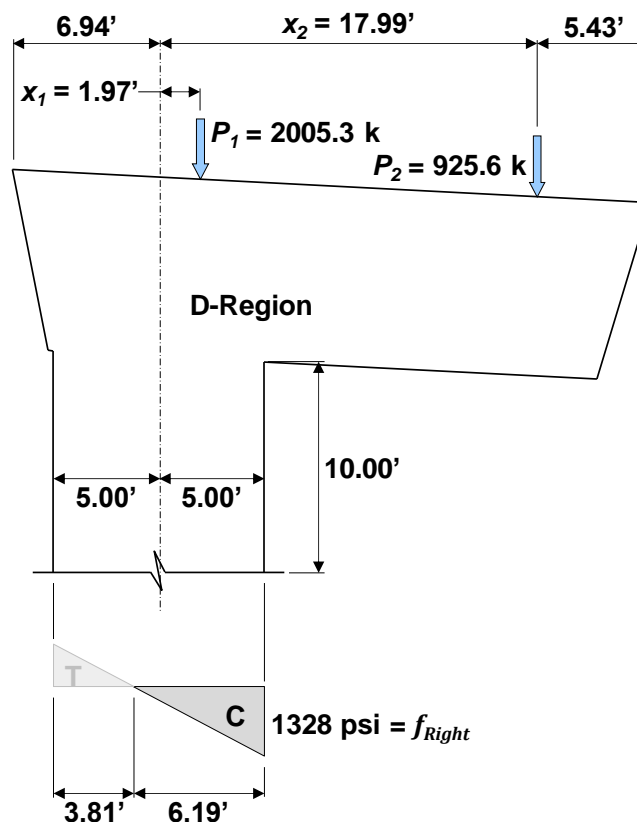


Figure 5.7: Linear stress distribution at the boundary of the D-region

5.4.2 Step 2: Develop Strut-and-Tie Models

The final strut-and-tie models for the cantilever bent cap are shown in Figures 5.8 and 5.9. The development of the STMs is described in detail within this section. First, the placement of the two vertical struts carrying the compressive forces within the column is decided. The reasoning behind using two struts versus a single strut is discussed. Struts and ties are then placed within the cap to accurately model the transfer of forces from the superstructure loads to the column. Two STMs are used to model the flow of forces within the cantilevered portion of the bent. Option 1 shown in Figure 5.8 features one truss panel in the cantilevered portion and models a direct flow of forces to the column. Option 2 shown in Figure 5.9 was developed to investigate the need for supplementary shear reinforcement within the cantilever; it features two truss panels with an intermediate vertical tie. The other aspects of the STM geometry are the same for both models. The following explanation of the STM development will therefore focus on Option 1 unless otherwise noted.

The width of the bent cap and the specified concrete compressive strength were modified from that of the existing field structure in order to satisfy the STM specifications proposed in Chapter 3. Finding the optimal combination of the bent cap width and concrete strength required several iterations of the design procedure to be performed. Since the geometries of the STMs depend on both the bent cap width and the concrete strength, the STMs were updated for each iteration. The details that follow explain the development of the final STMs for the last iteration that was performed.

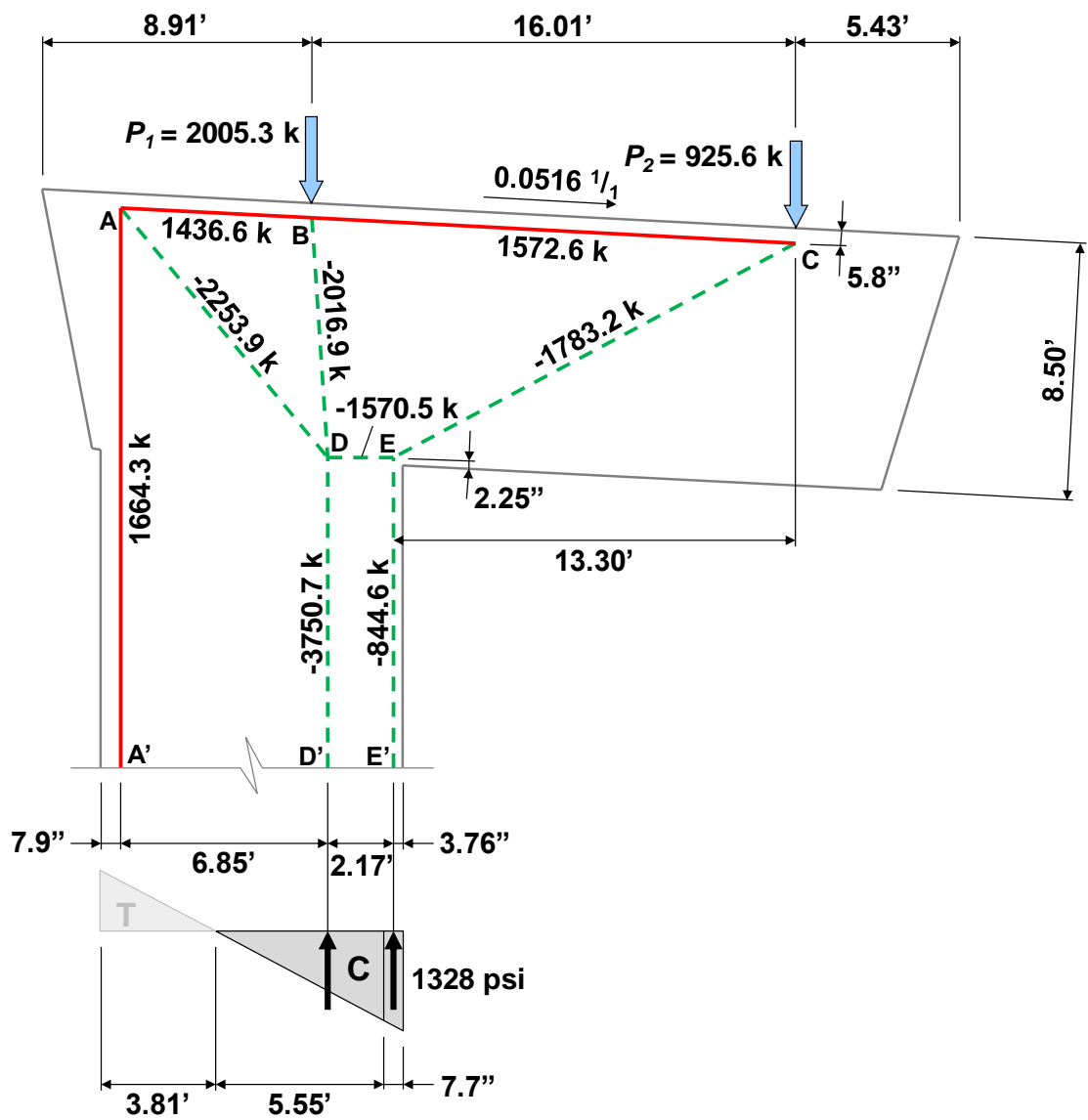


Figure 5.8: Strut-and-tie model for the cantilever bent cap – Option 1

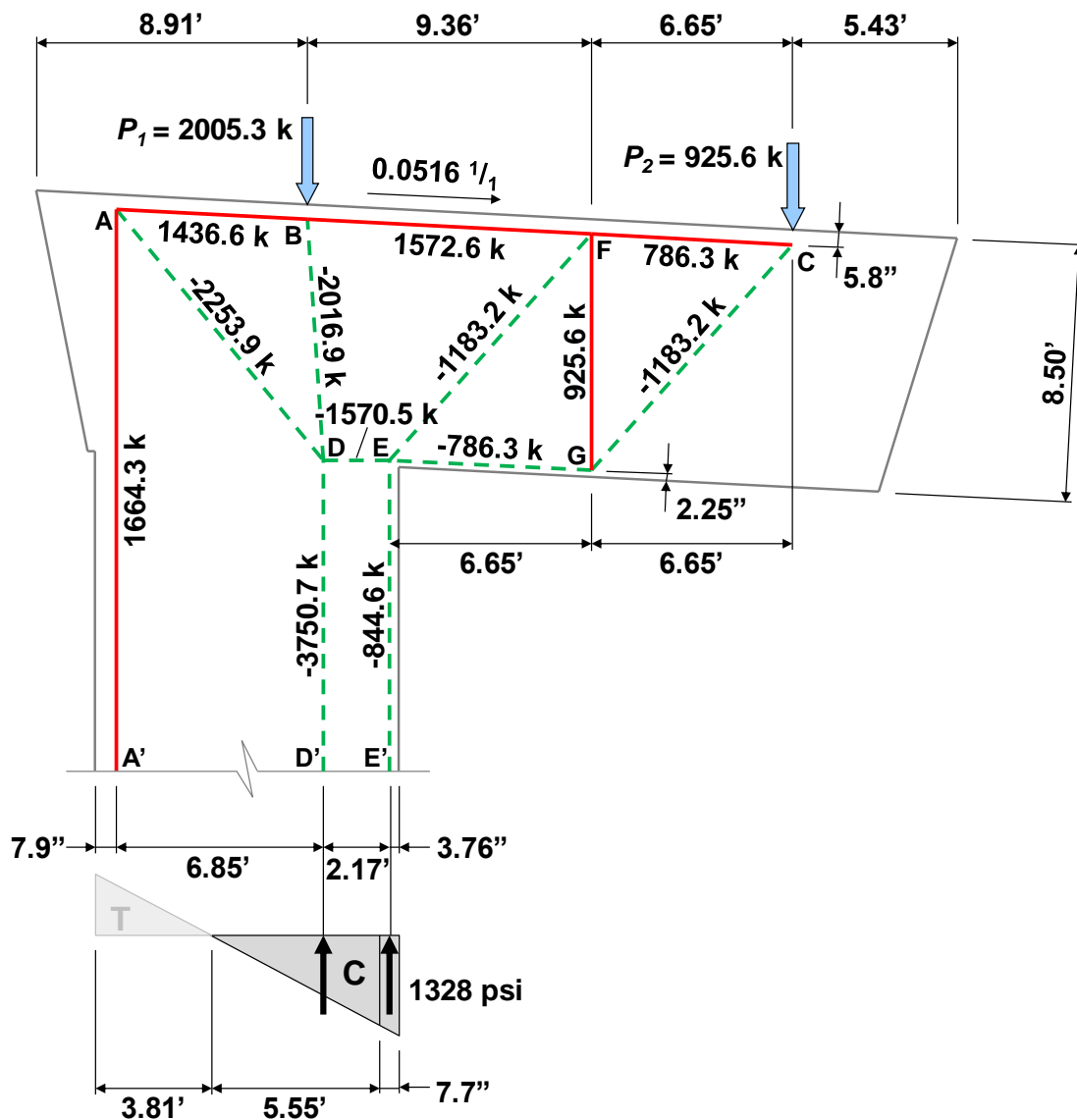


Figure 5.9: Strut-and-tie model for the cantilever bent cap – Option 2

The locations of the vertical struts within the column, Struts DD' and EE' in Figure 5.8, are determined first. The struts should be placed to correspond with the resultants of the compressive portion of the linear stress diagram at the boundary of the D-region. Some designers, however, may wish to use a single vertical strut near the compression face of the column with a position corresponding to the centroid of the rectangular compression stress block from a traditional flexural analysis (i.e. $a/2$ from the

column face). Positioning a strut at this location greatly limits the fraction of the 10-foot column width that is assumed to carry compressive forces. As a result, the node at the inside of the frame corner (i.e. Node E) will not have adequate strength to resist the large stresses that are assumed to concentrate within the small nodal region. The location of the vertical struts within the column should instead be based on the linear distribution of stress that is assumed at the D-region/B-region interface. Positioning the struts in this manner allows more of the column's 10-foot width to be utilized, resulting in a model that more closely corresponds to the actual elastic flow of forces within the bent (refer to Figure 2.8).

A single strut positioned to correspond with the resultant of the compressive portion of the linear stress diagram could be used to model the forces within the column, as shown in Figure 5.10(a). When the nodal strength checks are performed, the CCC node at the inside of the frame corner will need to be subdivided into two parts in order for its geometry to be defined (refer to the subdivision of Node JJ in Section 4.4.4 of Example 1). The nodal subdivision essentially results in the STM shown in Figure 5.10(b) with two vertical struts within the column. The development of an STM with two vertical struts, therefore, results in a more realistic model that better represents the elastic flow of forces within the bent. From a different perspective, a second vertical strut is needed to model the direct transfer of load P_1 into the column. If only P_2 acted on the bent cap, one vertical strut within the column would be sufficient.

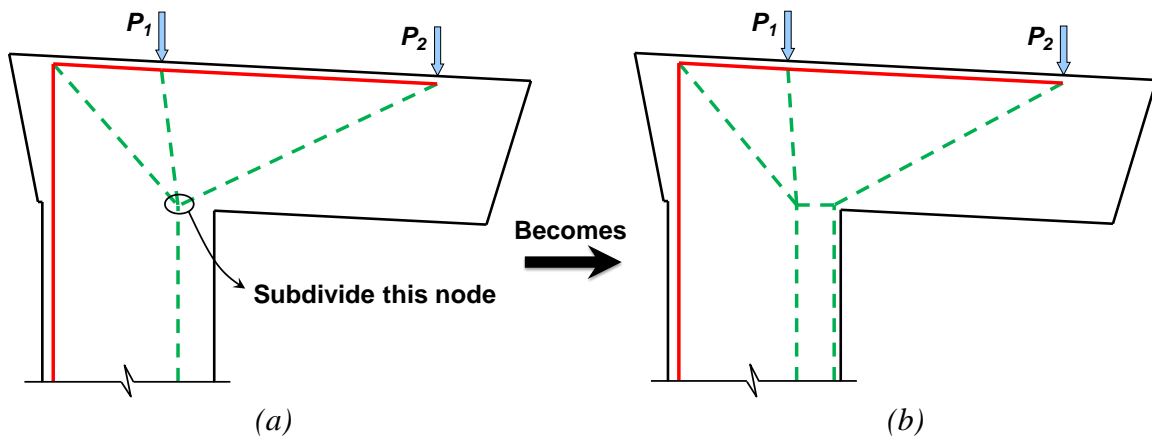


Figure 5.10: Modeling compressive forces within the column – (a) single strut; (b) two struts

In order to position the two vertical struts within the column, the compressive portion of the stress diagram is subdivided into two parts (a trapezoidal shape and a triangular shape) as shown in Figures 5.8 and 5.9. The geometry of each subdivision is determined by setting its resultant force equal to the corresponding force within the structure. The resultant of the trapezoidal shape at the right is equal to the magnitude of P_2 , 925.6 kips. The resultant of the triangular shape is equal to P_1 plus the resultant of the tensile portion of the stress diagram. The location of each vertical strut within the column, Struts DD' and EE' in Figure 5.8, corresponds to the position of each respective stress diagram resultant (i.e. the centroid of each subdivision).

The placement of Ties AB, BC, and AA' in Figure 5.8 is determined next. The locations of the ties must correspond with the centroids of the longitudinal tension steel that will be provided within the structure. Two layers of main tension reinforcement are likely to be necessary for each tie given the loads acting on the bent cap. The centroid of the reinforcement along the top of the bent cap is assumed to be located 5.8 inches from the top surface of the member. The centroid of the main tension steel within the column is assumed to be located 7.9 inches from the left face of the column. Considering the final reinforcement layout presented in Figures 5.19 and 5.20 following the STM design, the locations of Ties AB and BC described above correspond precisely with the centroids

of the main longitudinal reinforcement within the bent cap. Design iterations were needed to achieve this level of accuracy. When using the STM procedure, the designer should compare the final reinforcement details (i.e. the centroids of the longitudinal reinforcement) with the locations of the longitudinal ties of the strut-and-tie model to decide whether another iteration would affect the final design.

Before the remaining members of the STM are positioned, the location of Node E should be determined. The horizontal position of Node E is defined by the location of the vertical strut near the right face of the column (Strut EE'). Only the vertical position of the node, therefore, needs to be decided. In contrast to the placement of the column struts, a linear distribution of stress cannot be used to position the node since no D-region/B-region interface exists within the cap (i.e. the entire cap is a D-region). The vertical position of Node E is therefore defined by optimizing the height of the STM (i.e. the moment arm jd of the bent cap) to achieve efficient use of the bent cap depth (refer to Section 2.9.4 and Figure 2.17). Node E is placed so that the factored force acting on the back face will be about equal to its design strength. In other words, the moment arm jd is as large as possible while still ensuring that the back face of Node E has adequate strength. The calculation necessary to determine the vertical location of Node E is shown below (refer to Figure 5.11). The moment at the right face of the column due to load P_2 (neglecting the slight angle of the bent cap) is set equal to the factored nominal resistance (i.e. design strength) of the back face of Node E times the moment arm, jd .

$$\begin{aligned}
 & \text{Back face} \\
 & \text{design} \\
 & \text{strength} \quad \quad \quad \overbrace{jd} \\
 P_2(12.98 \text{ ft}) &= \underbrace{\varphi \nu f'_c b_w a}_{\text{Back face design strength}} \left(d - \frac{a}{2} \right) \\
 925.6 \text{ kip}(12.98 \text{ ft}) &= (0.7)(0.85)(6.0 \text{ ksi})(96 \text{ in})a \left(96.2 \text{ in} - \frac{a}{2} \right) \\
 a &= 4.48 \text{ in}
 \end{aligned}$$

The resistance factor, φ , in the calculation is the AASHTO LRFD (2010) factor of 0.7 for compression in strut-and-tie models. The concrete efficiency factor, ν , is taken as the factor for the back face of Node E (0.85 for a CCC node). The term left of the equal sign

is the moment at the right face of the column. The vertical location of Node E is taken as 2.25 inches from the bottom face of the bent, a distance slightly larger than $a/2$. As shown in Figures 5.8 and 5.9, this distance is perpendicular to the bottom face of the bent cap. The exact location of Node E is clearly shown in Figure 5.12.

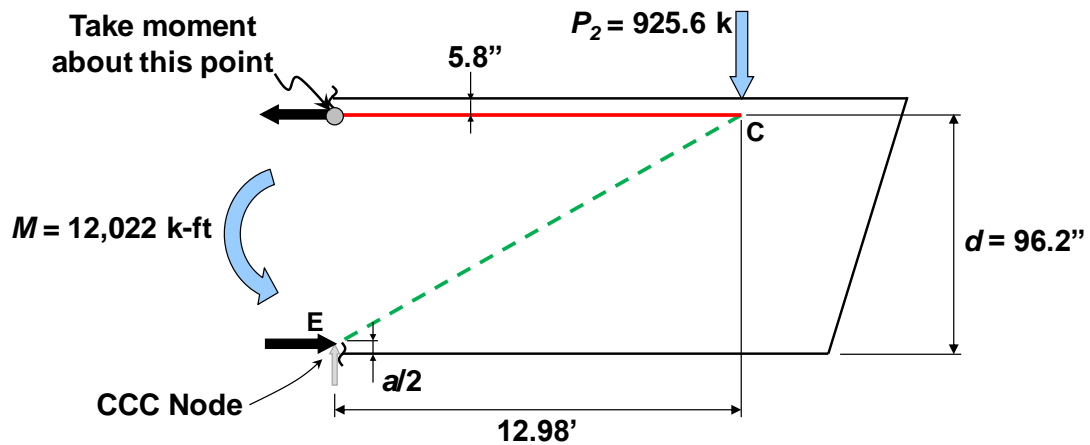


Figure 5.11: Determining the vertical position of Node E

The remaining nodes within STM Option 1 shown in Figure 5.8 can now be positioned. Node D is located horizontally from Node E at the end of Strut DD'. Strut DE connects the two nodes. Nodes B and C are located vertically below the applied superstructure loads. Struts AD, BD, and CE are then added to model the elastic flow of forces within the bent cap. These struts connect the nodes that have already been positioned.

For STM Option 2, the vertical Tie FG is located midway between Strut EE' and Node C (refer to Figure 5.9). Strut EG is parallel to the bottom face of the bent cap at a distance of 2.25 inches from the face.

Once the geometry of the STMs has been determined, the member forces of the struts and ties are found by enforcing equilibrium. Since both models are statically determinate systems, all member forces can be calculated by satisfying equilibrium at the joints of the truss (i.e. by using the method of joints). Given the small number of joints, the forces can easily be determined using hand calculations. The resulting forces in the

vertical struts within the column (Struts DD' and EE') do not equal the resultants of the stress diagram subdivisions that were previously determined. This discrepancy is to be expected since Tie AA' within the column does not coincide with the resultant of the tensile portion of the stress diagram (the tie must instead coincide with the column reinforcement). The slight angle of Ties AB and BC also contribute to the difference in forces. The combined effect of the forces in Strut DD', Strut EE', and Tie AA', however, is equivalent to the axial force and moment within the column at the D-region/B-region interface. The strut-and-tie models, therefore, satisfy the requirements for a lower-bound (i.e. conservative) design (refer to Section 2.3.1).

5.4.3 Step 3: Proportion Vertical Tie and Crack Control Reinforcement

The only significant difference between the two STM options is the additional vertical Tie FG of Option 2. Since a vertical tie is not provided within the cantilevered portion of the bent cap in STM Option 1, Option 2 was developed to determine if additional stirrups are needed in the cantilever in excess of that required to satisfy the crack control reinforcement provisions. Prior to detailing both models, therefore, the spacing of stirrups necessary to carry the force in Tie FG should be determined and then compared to the stirrup spacing required by the minimum crack control reinforcement provisions. If the crack control reinforcement requirement controls the design, only STM Option 1 needs to be considered for the remainder of the design example.

Both Nodes F and G are smeared nodes. The available length over which the reinforcement comprising Tie FG can be distributed is therefore determined using the technique recommended by Wight and Parra-Montesinos (2003) (refer to Section 2.9.5 or 4.4.5 for details). The available length is:

$$l_a = 2(79.8 \text{ in}) - 2(94.1 \text{ in})(\tan 25^\circ) = 71.8 \text{ in}$$

where 2(79.8 in.) is the horizontal distance between Nodes E and C in Figure 5.9 and 94.1 in. is the vertical distance between Nodes F and G, or the length of Tie FG. The

value of l_a is slightly conservative because the cross slope of the bent cap is ignored in its calculation.

Distributing four-legged #6 stirrups over the available length, the required spacing necessary to carry the force in Tie FG is determined as follows:

$$\begin{aligned} \text{Factored Load:} & \quad F_u = 925.6 \text{ kip} \\ \text{Tie Capacity:} & \quad \varphi \cdot f_y \cdot A_{st} = F_u \\ & \quad (0.9)(60 \text{ ksi})A_{st} = 925.6 \text{ kip} \\ & \quad A_{st} = 17.14 \text{ in}^2 \end{aligned}$$

$$\text{Number of \#6 stirrups (4 legs) required: } 17.14 \text{ in}^2 / (4)(0.44 \text{ in}^2) = 9.74 \text{ stirrups}$$

$$l_a = 71.8 \text{ in} \quad s = 71.8 \text{ in} / 9.74 = 7.4 \text{ in}$$

Therefore, the spacing of four-legged #6 stirrups should be no greater than 7.4 inches to satisfy the requirements for Tie FG of STM Option 2.

The minimum crack control reinforcement requirement will now be compared to the stirrups necessary to satisfy STM Option 2. Using four-legged #6 stirrups, the required spacing of the vertical crack control reinforcement is:

$$\begin{aligned} A_{v1} = 0.003b_w s_{v1} & \quad \rightarrow \quad 4(0.44 \text{ in}^2) = 0.003(96 \text{ in})s_{v1} \\ & \quad s_{v1} = 6.1 \text{ in} \end{aligned}$$

Since this spacing is less than the stirrup spacing necessary for Tie FG of STM Option 2, the crack control reinforcement is sufficient to carry the shear forces within the cantilevered portion of the bent cap. Therefore, only STM Option 1 of Figure 5.8 will be evaluated for the remainder of the design example.

The vertical crack control reinforcement detailed above (i.e. four-legged #6 stirrups) will be used throughout the bent cap with one exception: the region directly above the column will instead feature two-legged #8 stirrups to alleviate congestion and enhance constructability. The required spacing of the vertical crack control reinforcement at the frame corner is:

$$A_{v2} = 0.003b_w s_{v2} \quad \rightarrow \quad \begin{aligned} 2(0.79 \text{ in}^2) &= 0.003(96 \text{ in})s_{v2} \\ s_{v2} &= 5.5 \text{ in} \end{aligned}$$

Lastly, the required spacing of #8 bars provided as skin reinforcement parallel to the longitudinal axis of the bent cap is:

$$A_h = 0.003b_w s_h \quad \rightarrow \quad \begin{aligned} 2(0.79 \text{ in}^2) &= 0.003(96 \text{ in})s_h \\ s_h &= 5.5 \text{ in} \end{aligned}$$

The required crack control reinforcement is used along the length of the bent cap.

Summary

- Use 4 legs of #6 stirrups with spacing less than 6.1 in. within the cantilevered portion of the bent cap
- Use 2 legs of #8 stirrups with spacing less than 5.5 in. above the column
- Use #8 bars with spacing less than 5.5 in. as horizontal skin reinforcement
(Final reinforcement details are provided in Figures 5.18, 5.19, and 5.20)

5.4.4 Step 4: Proportion Longitudinal Ties

Since the forces in Ties AA', AB, and BC are all similar, a constant amount of reinforcement will be provided along the top of the bent cap and then down the tension face of the column.

Ties AB and BC

For the longitudinal reinforcement along the top of the bent cap, the force in Tie BC controls. Two layers of #11 bars will be provided. The reinforcement is proportioned as follows:

Factored Load:	$F_u = 1572.6 \text{ kip}$
Tie Capacity:	$\varphi \cdot f_y \cdot A_{st} = F_u$
	$(0.9)(60 \text{ ksi})A_{st} = 1572.6 \text{ kip}$
	$A_{st} = 29.12 \text{ in}^2$

$$\text{Number of \#11 bars required: } 29.12 \text{ in}^2 / 1.56 \text{ in}^2 = 18.7 \text{ bars}$$

Use 20 - #11 bars in two layers

Tie AA'

For the reinforcement in the column comprising Tie AA', two layers of #11 bars will be provided as the main tension steel. The reinforcement is proportioned as follows:

$$\begin{aligned} \text{Factored Load:} & \quad F_u = 1664.3 \text{ kip} \\ \text{Tie Capacity:} & \quad \varphi \cdot f_y \cdot A_{st} = F_u \\ & \quad (0.9)(60 \text{ ksi})A_{st} = 1664.3 \text{ kip} \\ & \quad A_{st} = 30.82 \text{ in}^2 \end{aligned}$$

$$\text{Number of \#11 bars required: } 30.82 \text{ in}^2 / 1.56 \text{ in}^2 = 19.8 \text{ bars}$$

Use 20 - #11 bars in two layers

The calculated amount of main column tension reinforcement is only satisfactory for the load case under consideration and the STM analysis that was performed. The final reinforcement details for the column are dependent on the complete design that considers all governing load cases and applicable articles in AASHTO LRFD (2010).

5.4.5 Step 5: Perform Nodal Strength Checks

The strengths of each node of the strut-and-tie model are now ensured to be sufficient to resist the applied forces.

Node E (CCC)

Due to the limited geometry of and high forces resisted by Node E, it is identified as the most critical node of the STM. The geometry of Node E is detailed in Figure 5.12. Referring back to Figure 5.8, the lateral spread of Strut EE' at Node E will be limited by the right face of the column. The bottom bearing face of Node E (and the width of Strut EE') is therefore taken as double the distance from the centroid of Strut EE' to the right face of the column, or $2(3.76 \text{ in.}) = 7.5 \text{ in.}$ The length of the back face, or vertical face, of Node E is double the vertical distance from the center of Node E (i.e. the point where

the centroids of the struts meet) to its bottom bearing face. This length can be calculated as follows:

$$a = 2 \left[\frac{2.25 \text{ in}}{\cos 2.95^\circ} + (3.76 \text{ in}) \tan 2.95^\circ \right] = 4.9 \text{ in}$$

where 2.95° is the angle between the longitudinal axis of the cap and the horizontal (i.e. the cross slope of the cap). The other dimensions can be found in Figures 5.8 and 5.12. The length of the strut-to-node interface, w_s , where Strut CE enters Node E is determined by the calculation in Figure 5.12. The use of a computer-aided design program can facilitate determination of the geometry of such a node.

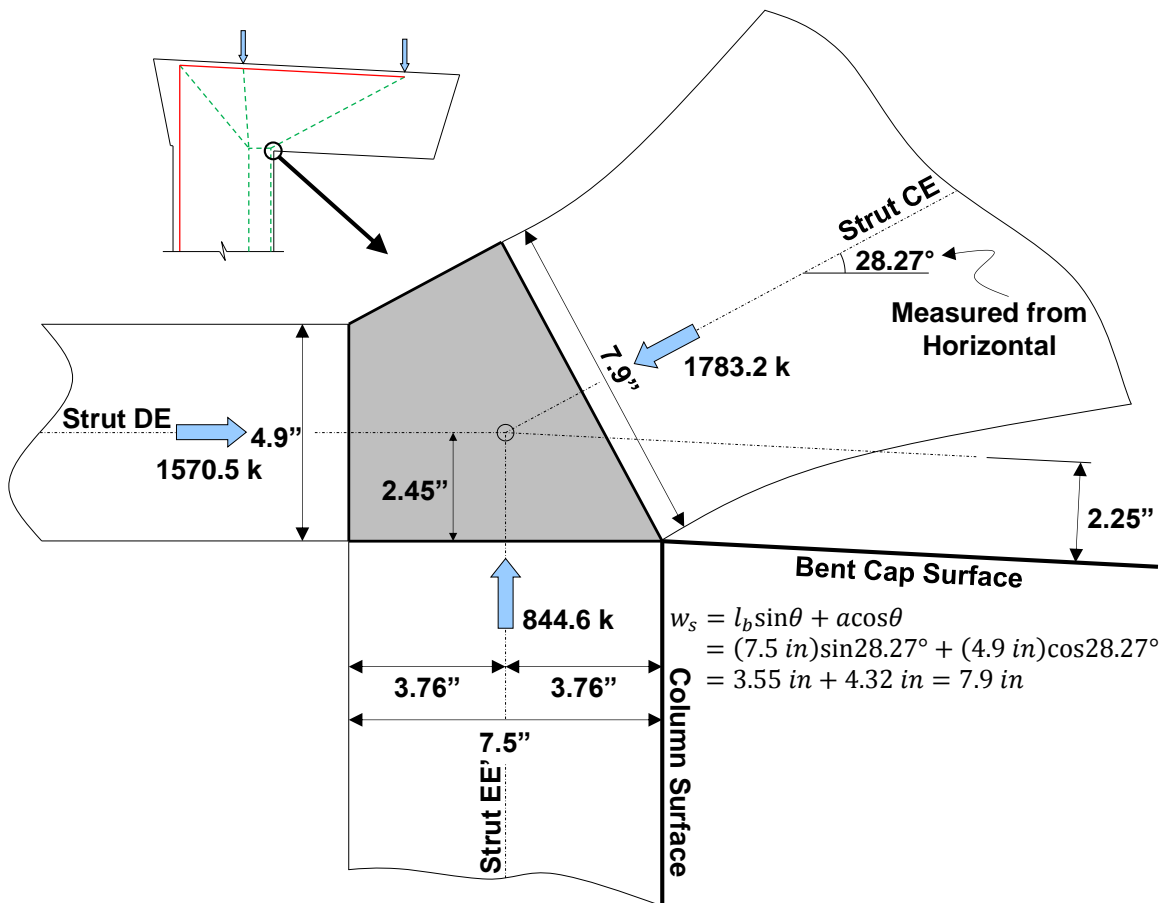


Figure 5.12: Node E

Node E is a CCC node with concrete efficiency factors of 0.85 for the bearing and back faces and 0.55 for the strut-to-node interface (see calculation below). The triaxial confinement factor, m , is 1 since the column and the bent cap have the same width. The faces of Node E are checked as follows:

Triaxial Confinement Factor: $m = 1$

BEARING FACE

$$\begin{aligned}
 \text{Factored Load:} & \quad F_u = 844.6 \text{ kip} \\
 \text{Efficiency:} & \quad \nu = 0.85 \\
 \text{Concrete Capacity:} & \quad f_{cu} = m \cdot \nu \cdot f'_c = (1)(0.85)(6.0 \text{ ksi}) = 5.1 \text{ ksi} \\
 & \quad \varphi \cdot F_n = (0.7)(5.1 \text{ ksi})(7.5 \text{ in})(96 \text{ in}) \\
 & \quad \quad \quad = 2570 \text{ kip} > 844.6 \text{ kip} \quad \mathbf{OK}
 \end{aligned}$$

BACK FACE

$$\begin{aligned}
 \text{Factored Load:} & \quad F_u = 1570.5 \text{ kip} \\
 \text{Efficiency:} & \quad \nu = 0.85 \\
 \text{Concrete Capacity:} & \quad f_{cu} = m \cdot \nu \cdot f'_c = (1)(0.85)(6.0 \text{ ksi}) = 5.1 \text{ ksi} \\
 & \quad \varphi \cdot F_n = (0.7)(5.1 \text{ ksi})(4.9 \text{ in})(96 \text{ in}) \\
 & \quad \quad \quad = 1679 \text{ kip} > 1570.5 \text{ kip} \quad \mathbf{OK}
 \end{aligned}$$

STRUT-TO-NODE INTERFACE

$$\begin{aligned}
 \text{Factored Load:} & \quad F_u = 1783.2 \text{ kip} \\
 \text{Efficiency:} & \quad \nu = 0.85 - 6.0 \text{ ksi} / 20 \text{ ksi} = 0.55 \\
 & \quad \therefore \text{Use } \nu = 0.55 \\
 \text{Concrete Capacity:} & \quad f_{cu} = m \cdot \nu \cdot f'_c = (1)(0.55)(6.0 \text{ ksi}) = 3.3 \text{ ksi} \\
 & \quad \varphi \cdot F_n = (0.7)(3.3 \text{ ksi})(7.9 \text{ in})(96 \text{ in}) \\
 & \quad \quad \quad = 1751.9 \text{ kip} < 1783.2 \text{ kip} \quad \mathbf{OK}
 \end{aligned}$$

Although the strut-to-node interface does not have enough capacity to resist the applied stress according to the calculation above, the percent difference between the demand and the capacity is less than 2 percent:

$$\% \text{ Difference} = \left(\frac{1783.2 \text{ kip} - 1751.9 \text{ kip}}{1783.2 \text{ kip}} \right) (100) = 1.76\%$$

This difference is insignificant, and the strut-to-node interface is considered to have adequate strength. Therefore, the strengths of all the faces of Node E are sufficient to resist the applied forces.

Node B (CCT)

Node B is shown in Figure 5.13. Its geometry is defined by the effective square bearing area calculated in Section 5.2.3, the location of the tie along the top of the bent cap, and the angle of Strut BD. The length of the bearing face of the node is equal to the dimension of the effective square bearing area, or 48.2 inches. The length of the back face is taken as double the distance from the centroid of the longitudinal reinforcement, or Tie AB, to the top face of the bent cap (measured perpendicularly to the top face). The length of the strut-to-node interface is determined by the calculation shown in Figure 5.13, where 83.18° is the angle of Strut BD relative to the top surface of the cap.

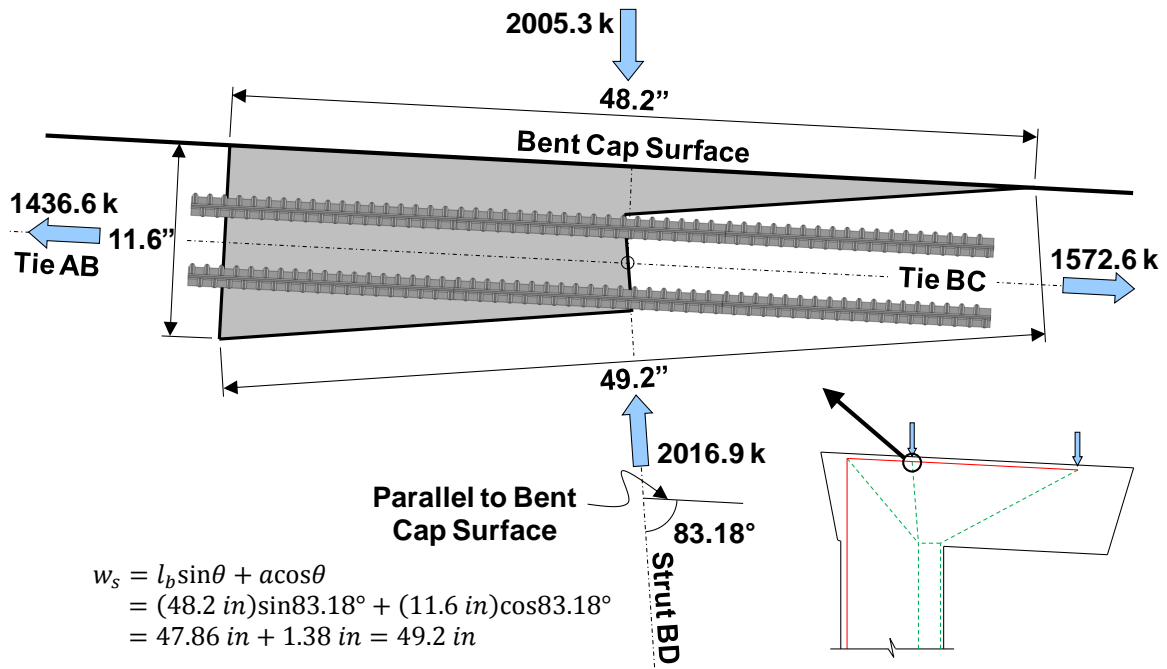


Figure 5.13: Node B

The strengths of the individual bearing areas at Node B (i.e. those supporting Beam 1 and Girder 1) should be checked for adequacy. If the individual bearing areas

are sufficient to resist the applied loads, the bearing face of Node E located at the top surface of the bent cap will also have adequate strength.

The bearings for Beam 1 and Girder 1 are checked as follows. The size of each bearing pad/plate is summarized in Table 5.1, and the factored load corresponding to each beam/girder is shown in Figure 5.3(a). Since Node E is a CCT node (i.e. ties intersect the node in only one direction), a concrete efficiency factor, ν , of 0.70 is applied to the strengths of the bearings.

BEARING FOR BEAM 1

Bearing Area:	$A_{bearing} = 2(16 \text{ in})(9 \text{ in}) = 288 \text{ in}^2$
Factored Load:	$F_u = 403.7 \text{ kip}$
Efficiency:	$\nu = 0.70$
Concrete Capacity:	$f_{cu} = \nu \cdot f'_c = (0.70)(6.0 \text{ ksi}) = 4.2 \text{ ksi}$ $\varphi \cdot F_n = (0.7)(4.2 \text{ ksi})(288 \text{ in}^2)$ $= 847 \text{ kip} > 403.7 \text{ kip} \text{ OK}$

BEARING FOR GIRDER 1

Bearing Area:	$A_{bearing} = (42 \text{ in})(29.5 \text{ in}) = 1239 \text{ in}^2$
Factored Load:	$F_u = 1396.4 \text{ kip}$
Efficiency:	$\nu = 0.70$
Concrete Capacity:	$f_{cu} = \nu \cdot f'_c = (0.70)(6.0 \text{ ksi}) = 4.2 \text{ ksi}$ $\varphi \cdot F_n = (0.7)(4.2 \text{ ksi})(1239 \text{ in}^2)$ $= 3643 \text{ kip} > 1396.4 \text{ kip} \text{ OK}$

The triaxial confinement factor, m , could have been applied to the concrete capacity. Considering the effect of confinement is unnecessary, however, since the calculations reveal that the concrete capacity is much greater than the demand.

The tie forces at Node B result from the anchorage of the reinforcing bars and do not concentrate at the back face. In cases where the back face does not resist a direct force, no back face check is necessary (refer to Section 2.9.8). The strength of the strut-to-node interface of Node B is checked below. The triaxial confinement factor is first calculated using the area of the bearing face and the width of the bent cap. The width of the node (into the page) is taken as the dimension of the effective square bearing area, 48.2 inches.

Triaxial Confinement Factor:

$$m = \sqrt{A_2/A_1} = \sqrt{(96 \text{ in})^2 / (48.2 \text{ in})^2} = 1.99 < 2 \quad \therefore \text{Use } m = 1.99$$

STRUT-TO-NODE INTERFACE

Factored Load: $F_u = 2016.9 \text{ kip}$
Efficiency: $v = 0.85 - 6.0 \text{ ksi} / 20 \text{ ksi} = 0.55$
 $\therefore \text{Use } v = 0.55$
Concrete Capacity: $f_{cu} = m \cdot v \cdot f'_c = (1.99)(0.55)(6.0 \text{ ksi}) = 6.6 \text{ ksi}$
 $\varphi \cdot F_n = (0.7)(6.6 \text{ ksi})(49.2 \text{ in})(48.2 \text{ in})$
 $= 10956 \text{ kip} > 2016.9 \text{ kip} \quad \mathbf{OK}$

Therefore, the strength of Node B is sufficient to resist the applied forces.

Node C (CCT)

Node C is shown in Figure 5.14. The geometry of the node is determined in a manner similar to that of Node B. The length of the bearing face of the node, 39.1 inches, was calculated in Section 5.2.3. The following set of checks is analogous to that performed for Node B (both nodes are CCT nodes).

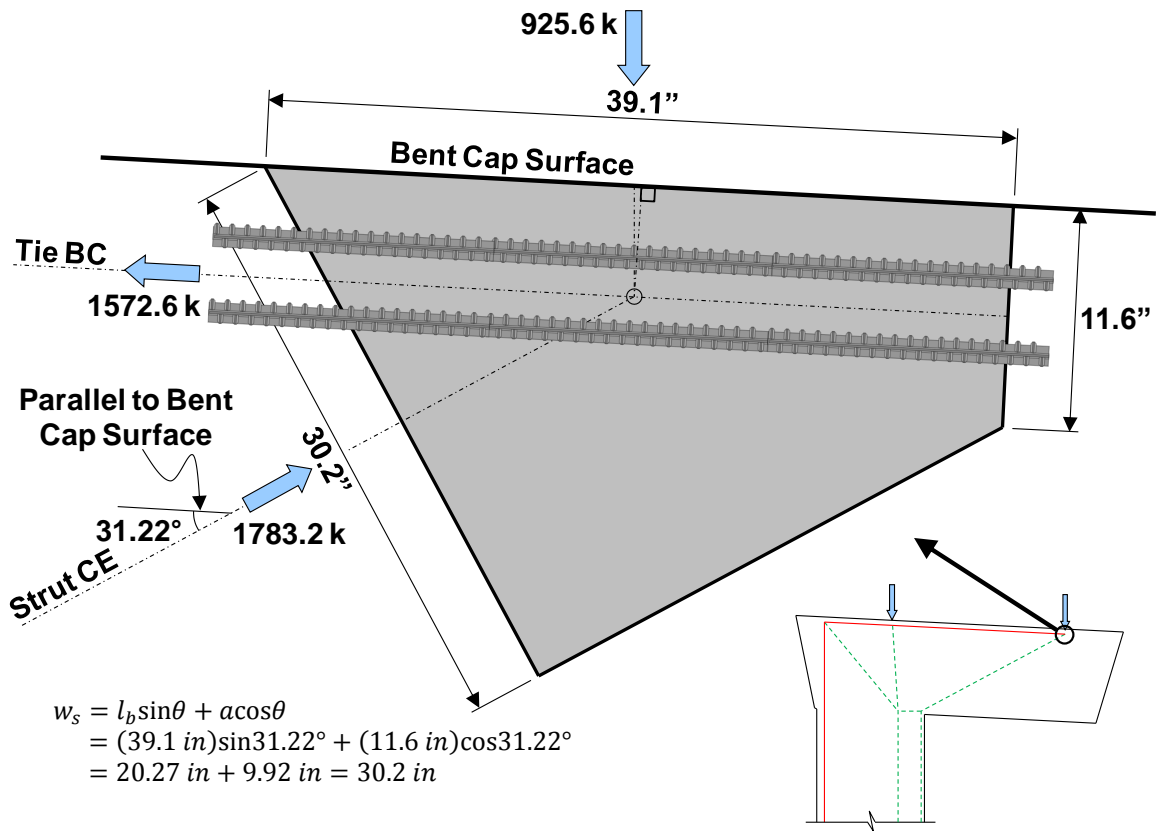


Figure 5.14: Node C

BEARING FOR BEAM 2

Bearing Area: $A_{bearing} = 2(16 \text{ in})(9 \text{ in}) = 288 \text{ in}^2$
 Factored Load: $F_u = 403.7 \text{ kip}$

The bearing check is the same as that of Beam 1. → **OK**

BEARING FOR GIRDER 2

Bearing Area: $A_{bearing} = (24 \text{ in})(24 \text{ in}) = 576 \text{ in}^2$
 Factored Load: $F_u = 366.8 \text{ kip}$
 Efficiency: $v = 0.70$
 Concrete Capacity: $f_{cu} = v \cdot f'_c = (0.70)(6.0 \text{ ksi}) = 4.2 \text{ ksi}$
 $\varphi \cdot F_n = (0.7)(4.2 \text{ ksi})(576 \text{ in}^2)$
 $= 1693 \text{ kip} > 366.8 \text{ kip}$ **OK**

Triaxial Confinement Factor:

$$m = \sqrt{A_2/A_1} = \sqrt{(96 \text{ in})^2 / (39.1 \text{ in})^2} = 2.46 > 2 \quad \therefore \text{Use } m = 2$$

STRUT-TO-NODE INTERFACE

Factored Load:	$F_u = 1783.2 \text{ kip}$
Efficiency:	$v = 0.85 - 6.0 \text{ ksi} / 20 \text{ ksi} = 0.55$ $\therefore \text{Use } v = 0.55$
Concrete Capacity:	$f_{cu} = m \cdot v \cdot f'_c = (2)(0.55)(6.0 \text{ ksi}) = 6.6 \text{ ksi}$ $\varphi \cdot F_n = (0.7)(6.6 \text{ ksi})(30.2 \text{ in})(39.1 \text{ in})$ $= 5455 \text{ kip} > 1783.2 \text{ kip} \text{ OK}$

Therefore, the strength of Node C is sufficient to resist the applied forces.

Node A (CTT – Curved-Bar Node)

In order to resist the large tensile stresses at the outside of the frame corner subjected to closing loads, the longitudinal reinforcement from the cantilevered portion of the cap is continued around the corner and spliced with the column reinforcement. Klein (2008) comprehensively studied the stress conditions of nodes located at the bend regions of reinforcing bars under tension. Such nodes are referred to as curved-bar nodes. According to Klein (2008), a curved-bar node is defined as “the bend region of a continuous reinforcing bar (or bars) where two tension ties are in equilibrium with a compression strut in an STM.” Node A in Figure 5.8 is therefore an example of a curved-bar node. Curved-bar node design recommendations were developed by Klein (2008) and form the basis of the reinforcement detailing at Node A (refer to Section 2.9.6).

To design a curved-bar node, the bend region of the reinforcing bars must satisfy two criteria: (1) the inside radius, r_b , of the bar bend must be large enough to limit the compressive stresses acting at the node to a permissible level, and (2) the length of the bend, l_b , must be sufficient to allow any differences in the tie forces to be developed along the bend region of the bars.

First, the bars are detailed to ensure the stresses acting at Node A do not exceed the nodal stress limit. The bend radius directly affects the magnitude of the compressive stresses that act at the curved region of the reinforcement (Klein, 2008). To ensure that the capacity of the nodal region is adequate, the following equation must be satisfied (refer to Article 5.6.3.3.5 of the proposed STM specifications of Chapter 3). The equation from Klein (2008) has been modified to include the concrete efficiency factors, ν , of the proposed STM specifications of Chapter 3.

$$r_b \geq \frac{A_{st}f_y}{\nu b f'_c} \quad (5.1)$$

Here, A_{st} is the area of the tie reinforcement specified at the frame corner, ν is the concrete efficiency factor for the back face of the node under consideration, and b is the width of the strut transverse to the plane of the STM. For the cantilever bent cap, the value of A_{st} is $20(1.56 \text{ in.}^2) = 31.2 \text{ in.}^2$, and the value of b is the full width of the bent cap, or 96 in. The value of ν is taken as 0.55 for the back face of Node A, a CTT node, as calculated below:

$$\nu = 0.85 - 6.0 \text{ ksi} / 20 \text{ ksi} = 0.55$$

As the following calculation reveals, the bend radius must be at least 5.91 inches for the reinforcement to develop its full capacity.

$$r_b \geq \frac{A_{st}f_y}{\nu b f'_c} = \frac{(31.2 \text{ in}^2)(60 \text{ ksi})}{(0.55)(96 \text{ in})(6.0 \text{ ksi})} = 5.91 \text{ in}$$

According to Article 5.10.2.3 of *AASHTO LRFD Bridge Design Specifications* (2010), the minimum inside bend diameter of a #11 bar is $8.0d_b$. The corresponding minimum inside radius is therefore $4.0d_b$, or 5.64 inches. In order to satisfy the permissible stress limit, however, the inside bend radius must be equal to or greater than 5.91 inches.

Since the force in Tie AA' is different than the force in Tie AB, circumferential bond stress develops along the curved bars to equilibrate the unbalanced force. To satisfy the second design criteria for curved-bar nodes, the radius of the bend must be large enough to allow the unbalanced force to be developed along the bend length, l_b (see Figure 5.15). The bend length required to develop the unbalanced force around a 90-degree corner will be provided when the following minimum bend radius expression recommended by Klein (2008) is satisfied (refer to Article C5.6.3.4.2 of the proposed STM specifications of Chapter 3):

$$r_b \geq \frac{2l_d(1 - \tan\theta_c)}{\pi} - \frac{d_b}{2} \quad (5.2)$$

where l_d is the development length for straight bars, θ_c is the smaller of the two angles between the strut and the ties that extend from the node, and d_b is the diameter of a longitudinal bar. From Figure 5.16, the value of θ_c for Node A is determined to be 39.53°. Considering that the frame corner of the bent is slightly less than 90 degrees, the above expression becomes somewhat more conservative when applied to Node A.

To determine the required radius, the development length, l_d , for the top bars should be considered and is calculated as follows (per Article 5.11.2.1 of AASHTO LRFD (2010)):

$$l_d = \frac{1.25A_b f_y}{\sqrt{f'_c}} \cdot 1.4 = \frac{1.25(1.56 \text{ in}^2)(60 \text{ ksi})}{\sqrt{6.0 \text{ ksi}}} \cdot 1.4 = 66.9 \text{ in}$$

Therefore, the minimum radius necessary to allow the unbalanced bond stresses to be developed along the circumference of the bend is:

$$r_b \geq \frac{2l_d(1 - \tan\theta_c)}{\pi} - \frac{d_b}{2} = \frac{2(66.9 \text{ in})(1 - \tan 39.53^\circ)}{\pi} - \frac{1.41 \text{ in}}{2} = 6.74 \text{ in}$$

Comparing this value with the minimum radius required to satisfy the nodal stress limit reveals that r_b must be at least 6.74 inches. When multiple layers of reinforcement are

provided, the expressions developed by Klein (2008) should be used to determine the inside bend radius for the innermost layer of reinforcement.

Note that the required bend radius is larger than the standard bend radius of a #11 bar. Standard mandrels for larger bars are therefore considered to determine the practicality of specifying a bend radius larger than 6.74 inches. The standard mandrel for #14 bars has a radius of approximately 8.5 inches. Therefore, an inside bend radius, r_b , of 8.5 inches will be used for the innermost layer of reinforcement (see Figure 5.16).

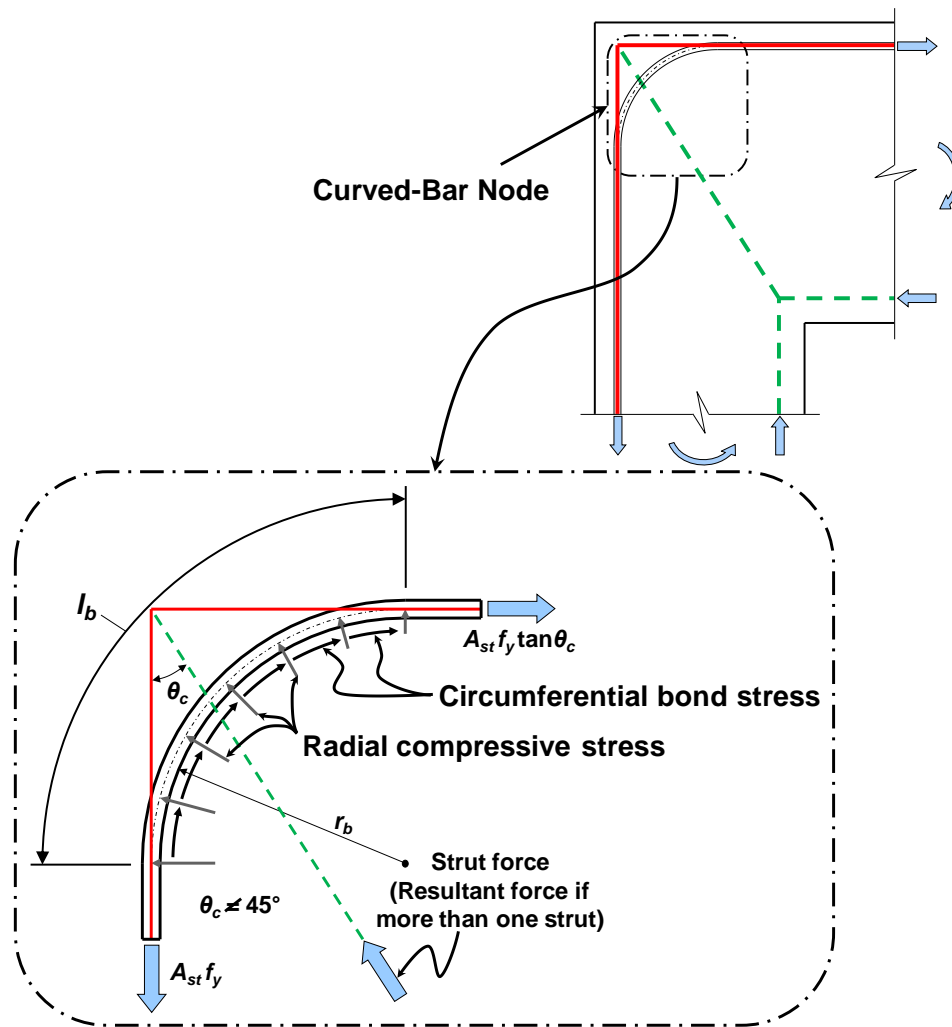


Figure 5.15: Stresses acting at a curved bar (adapted from Klein, 2008)

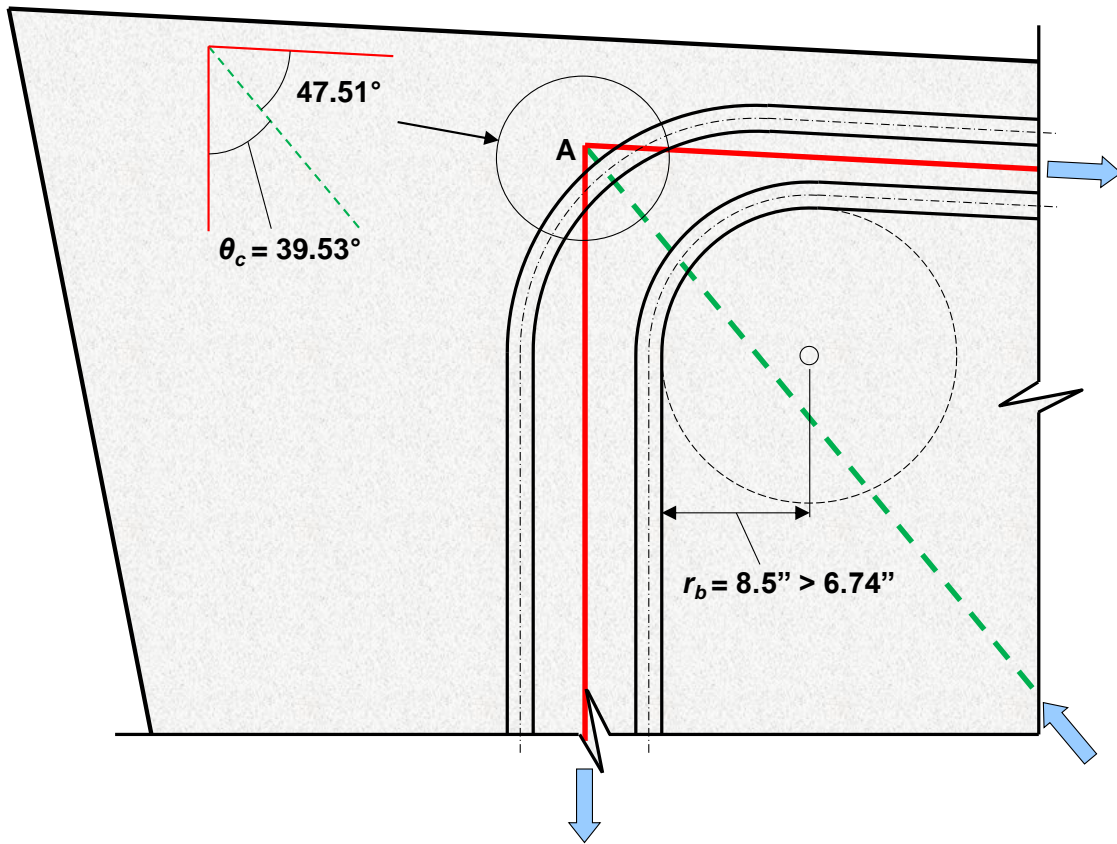


Figure 5.16: Bend radius, r_b , at Node A

Lastly, the clear side cover measured to the bent bars should be at least $2d_b$ to avoid side splitting (Klein, 2008). The cover to the bent bars at Node A, therefore, must be at least $2(1.41 \text{ in.}) = 2.82 \text{ in.}$ Considering that the #11 longitudinal bars will be enclosed within #8 stirrups above the column, providing a clear cover of at least 2 inches to the stirrups will satisfy the cover requirement for the bent bars (i.e. $2 \text{ in.} + 1 \text{ in.} = 3 \text{ in.} > 2.82 \text{ in.}$).

Node D (CCC)

Node D is an interior node with no bearing plate or geometrical boundaries to clearly define its geometry. It is therefore a smeared node and will not be critical. Checking the concrete strength at Node D is unnecessary.

5.4.6 Step 6: Provide Necessary Anchorage for Ties

The primary longitudinal reinforcement of the cantilever must be properly developed at Node C in accordance with Article 5.6.3.4.2 of the proposed STM specifications in Chapter 3 and Article 5.11.2 of *AASHTO LRFD Bridge Design Specifications* (2010). The available length for the development of the tie bars is measured from the point where the centroid of the reinforcement enters the extended nodal zone (assuming the diagonal strut is prismatic) to the tip of the cantilever, leaving the required clear cover (Figure 5.17).

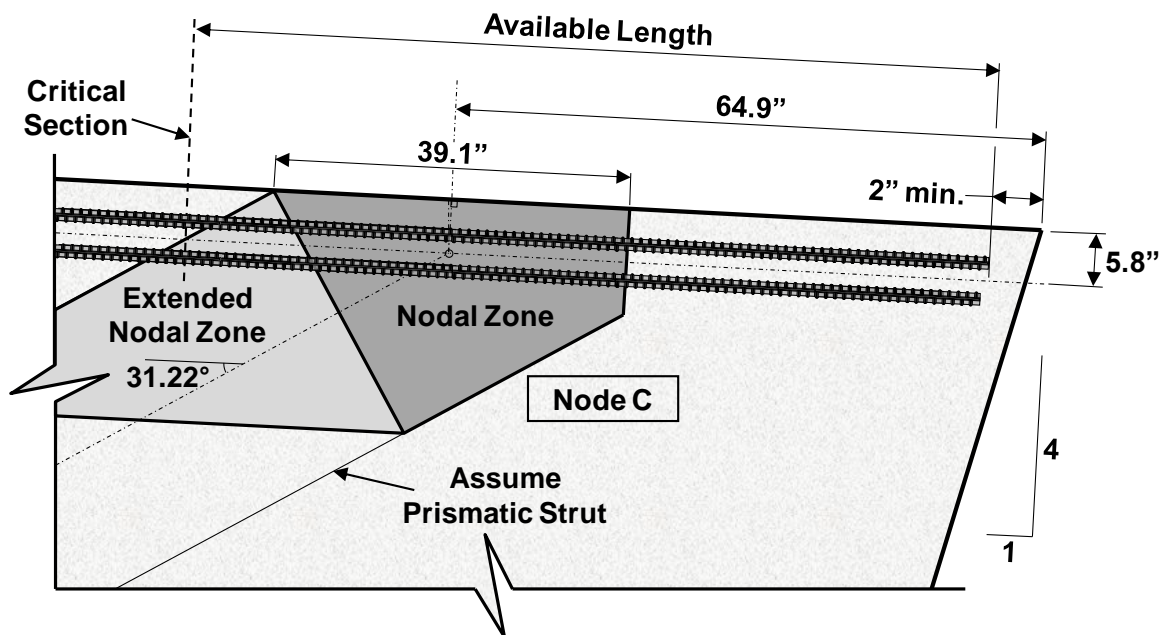


Figure 5.17: Anchorage of longitudinal bars at Node C

Providing 2-inches of clear cover, the available length for the primary longitudinal reinforcement of the cantilever (measured at the centroid of the bars) is:

$$\begin{aligned} \text{Available length} &= 64.9 \text{ in} + 39.1 \text{ in}/2 + 5.8 \text{ in}/\tan 31.22^\circ - 5.8 \text{ in}/4 - 2 \text{ in} \\ &= 90.6 \text{ in} \end{aligned}$$

All the dimensional values within this calculation are shown in Figure 5.17. The straight development length was determined in Section 5.4.5 and is repeated below for convenience:

$$l_d = \frac{1.25A_b f_y}{\sqrt{f'_c}} \cdot 1.4 = \frac{1.25(1.56 \text{ in}^2)(60 \text{ ksi})}{\sqrt{6.0 \text{ ksi}}} \cdot 1.4 = 66.9 \text{ in} < 90.6 \text{ in } \mathbf{OK}$$

Therefore, enough length is available for straight-bar anchorage at Node C.

In addition to ensuring adequate anchorage of the tie bars, a splice is designed between the primary longitudinal reinforcement of the cantilever and the main column tension reinforcement. A contact lap splice is specified in accordance with Articles 5.11.5.2 and 5.11.5.3 of AASHTO LRFD (2010). All 20 longitudinal reinforcing bars will be spliced, and the ratio of the area of the steel provided to the area required is less than 2. The splice is therefore a Class C splice with a required length of $1.7l_d$, calculated as follows:

$$1.7l_d = 1.7 \cdot \frac{1.25A_b f_y}{\sqrt{f'_c}} = 1.7 \cdot \frac{1.25(1.56 \text{ in}^2)(60 \text{ ksi})}{\sqrt{6.0 \text{ ksi}}} = 81.2 \text{ in}$$

The required splice length is available within the depth of the cap. The splice is shown within the final reinforcement details in Figure 5.20.

5.4.7 Step 7: Perform Shear Serviceability Check

To limit diagonal cracking, the unfactored service level shear force should be less than the estimated diagonal cracking strength of the member. The TxDOT Project 0-5253 expression for the diagonal cracking strength was presented in Section 2.12 and is repeated here for convenience:

$$V_{cr} = \left[6.5 - 3 \left(\frac{a}{d} \right) \right] \sqrt{f'_c} b_w d \quad (5.3)$$

but not greater than $5\sqrt{f'_c} b_w d$ nor less than $2\sqrt{f'_c} b_w d$

where:

- a = shear span (in.)
- d = effective depth of the member (in.)
- f'_c = specified compressive strength of concrete (psi)
- b_w = width of member's web (in.)

The likelihood of the formation of diagonal cracks in the cantilevered portion of the bent cap should be considered. Using the AASHTO LRFD (2010) Service I load case, the service level shear force at the face of the column is 688.7 kips. To estimate the diagonal cracking strength, the shear span, a , is taken as the horizontal distance between Node E and the applied load at Node C, or 159.6 inches. The resulting shear span-to-depth ratio, a/d , is 1.66 ($a/d = 159.6 \text{ in.}/96.2 \text{ in.}$). The diagonal cracking load equation is only valid for a/d ratios from 0.5 to 1.5 (refer to Section 2.12). Therefore, the value of V_{cr} for the cantilevered portion of the bent cap is:

$$\begin{aligned} V_{cr} &= 2\sqrt{f'_c} b_w d = 2\sqrt{6000 \text{ psi}}(96 \text{ in})(96.2 \text{ in}) \\ &= 1431 \text{ kip} > 688.7 \text{ kip } \mathbf{OK} - \text{Diagonal cracking is not expected} \end{aligned}$$

The estimated diagonal cracking strength is much greater than the service level shear force. Diagonal cracks are therefore not expected to form under the service loads considered in this example.

5.5 REINFORCEMENT LAYOUT

The reinforcement details for the load case considered in this design example are presented in Figures 5.18, 5.19, and 5.20. Any reinforcement details not previously described within the example are consistent with standard TxDOT practice.

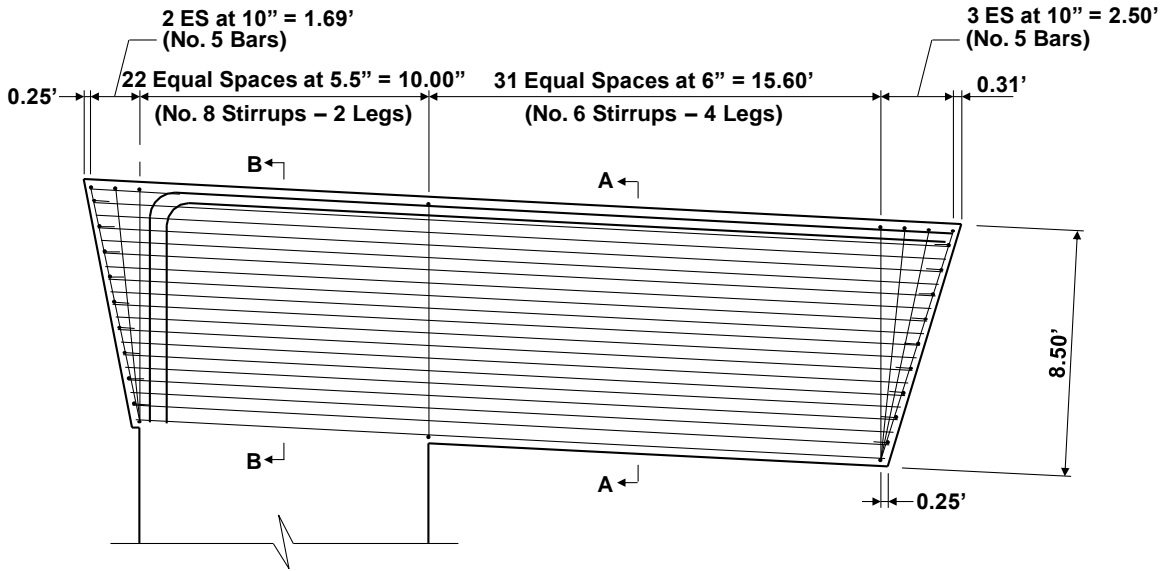
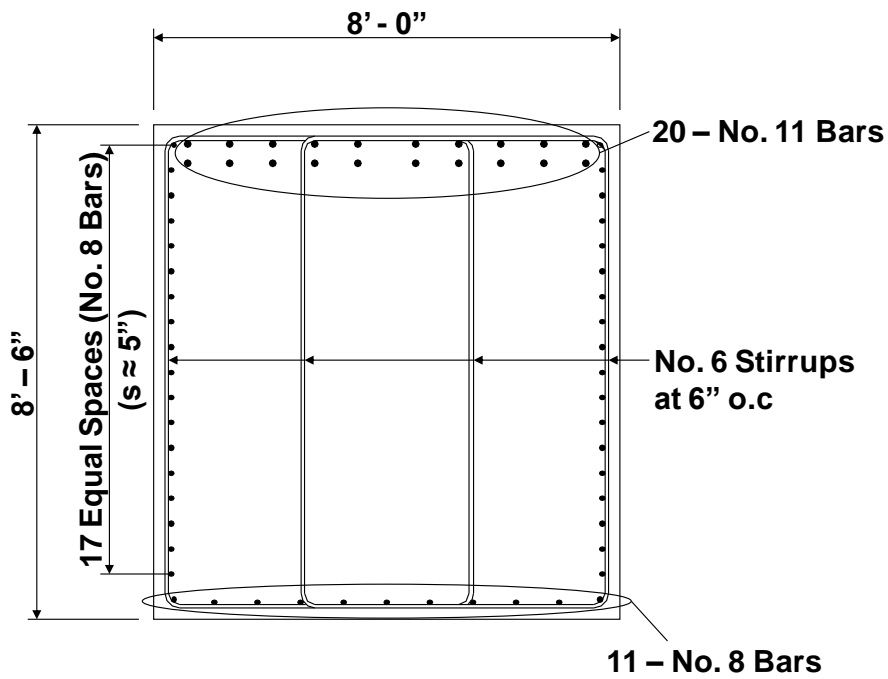
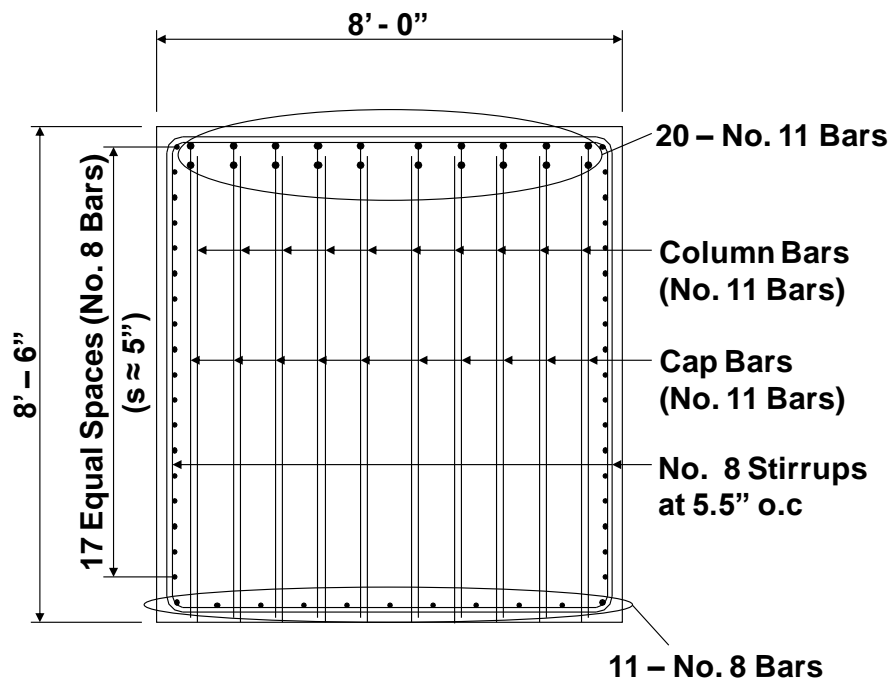


Figure 5.18: Reinforcement details – elevation (design per proposed STM specifications)



Section A-A

Figure 5.19: Reinforcement details – Section A-A (design per proposed STM specifications)



Section B-B

Figure 5.20: Reinforcement details – Section B-B (design per proposed STM specifications)

5.6 SUMMARY

The STM design of a cantilever bent cap supporting a direct connector was presented for a particular load case. The design was based on the STM procedure introduced in Chapter 2 and satisfies the specifications proposed in Chapter 3. The defining features and challenges of this design example are listed below:

- Simplifying the load case and the bearing areas so that reasonable strut-and-tie models can be developed and nodal geometries can be defined
- Modeling the flow of forces at a frame corner subjected to closing loads
- Positioning vertical struts within a column based on the assumed linear distribution of stresses at a D-region/B-region interface
- Developing STMs and defining the nodal geometries for a sloped structure

- Considering an alternative STM to investigate the need for supplementary shear reinforcement within the cantilever
- Designing a curved-bar node at the outside of a frame corner (i.e. determining the required bend radius of the longitudinal bars)

Chapter 6. Example 3a: Inverted-T Straddle Bent Cap (Moment Frame)

6.1 SYNOPSIS

The strut-and-tie modeling (STM) specifications of Chapter 3 are applied to the design of an inverted-T straddle bent cap within this example. The design of an inverted-T is significantly different from the design of a rectangular beam (such as the multi-column bent cap of Example 1). Application of the girder loads at the ledge (1) necessitates the use of supplementary vertical ties (stirrups) to transfer the loads upward through the inverted-T stem toward the compression face of the member and (2) results in tension across the beam width that must be resisted (and modeled) by transverse ledge reinforcement. In order to account for the flow of forces through the beam cross section and along the beam length, a three-dimensional STM must be developed for the design of an inverted-T.

The inverted-T bent cap is designed in two ways based on the assumed behavior of the bridge substructure. In the current example (Example 3a), the substructure is designed to behave as a moment frame. The bent must therefore be modeled to allow forces to “turn” around the frame corners. In Example 3b, the bent cap is designed as a member that is simply supported at the columns.

6.2 DESIGN TASK

The geometry of the inverted-T straddle bent cap and the load case that will be considered are presented in Sections 6.2.1 and 6.2.2. The bent is an existing field structure in Texas originally designed using sectional methods. The geometry, load case, and bearing details described within the following sections were all provided by TxDOT.

6.2.1 Bent Cap Geometry

Elevation and plan views of the inverted-T straddle bent cap are presented in Figure 6.1. The bent cap is 47.50 feet long and 5.00 feet tall. The stem of the cap is 3.34 feet wide, and the ledges protrude 1.33 feet from either side of the stem. The bottom

width of the cap at the ledge is therefore 6.00 feet. The columns supporting the cap are 5.00 feet by 3.00 feet. A 44-inch tall trapezoidal box beam is supported at each of the six bearing locations. The bent cap has a slight cross slope to accommodate the banked grade of the roadway supported by the bent. The slope is deemed insignificant and a simplified, orthogonal layout serves as the basis for design. Please recall that the strut-and-tie model for the cantilever bent cap of Chapter 5 accounted for the sloped orientation of the cap. Either approach can be valid (depending on the significance of the slope); the engineer should use discretion when deciding which approach is appropriate.

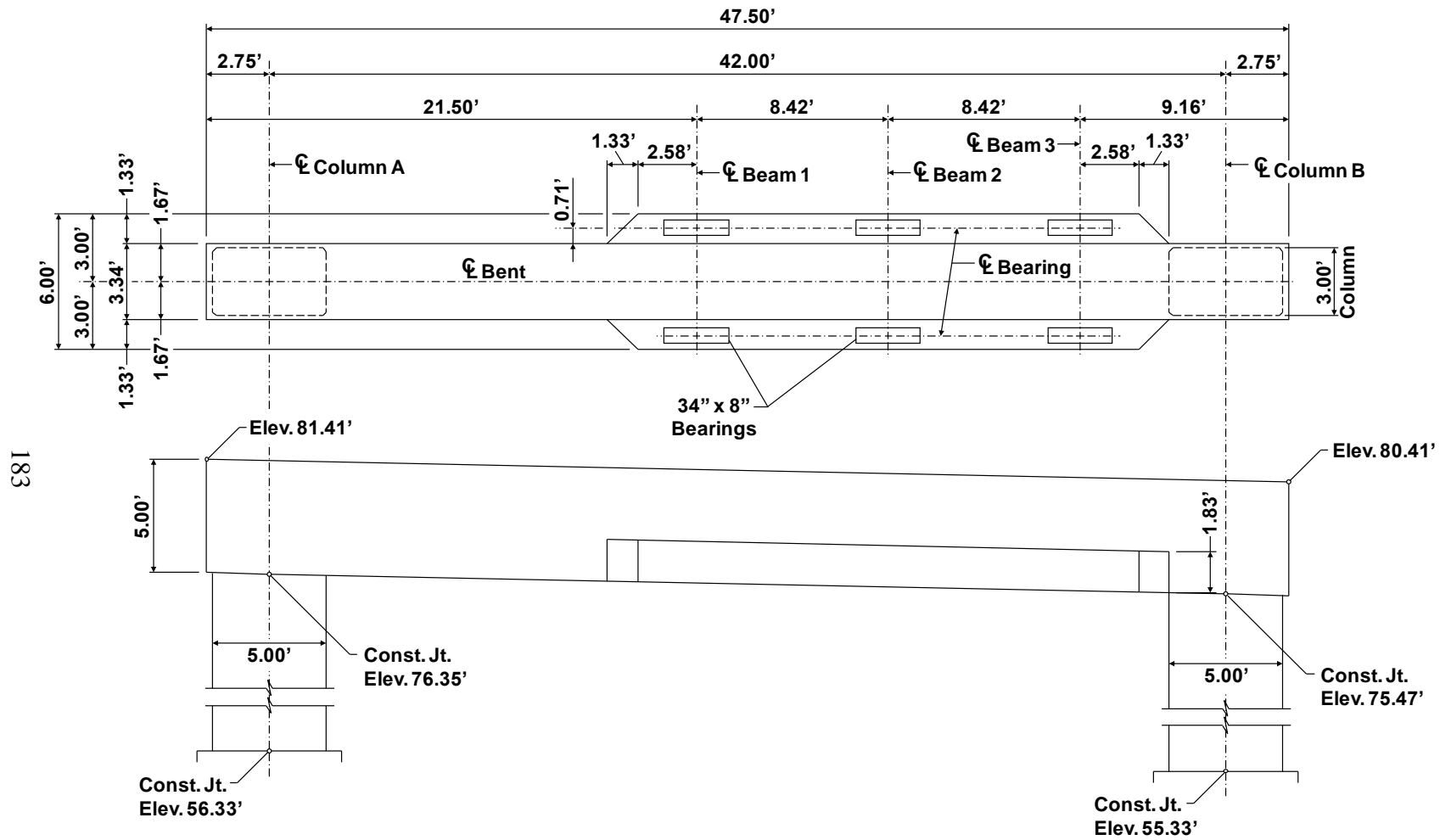


Figure 6.1: Plan and elevation views of inverted-T bent cap

6.2.2 Determine the Loads

The factored beam load acting on each bearing pad is shown in Figure 6.2. Loading of the bent cap is symmetrical about its centerline. The total factored load for each beam line is also provided in Figure 6.2. This particular load case maximizes the shear force in the bent cap within the shear span between the left column (Column A) and Beam Line 1. The load case is one of many considered by TxDOT during the original design process. All other governing load cases for the bent cap would need to be evaluated to develop the final design.

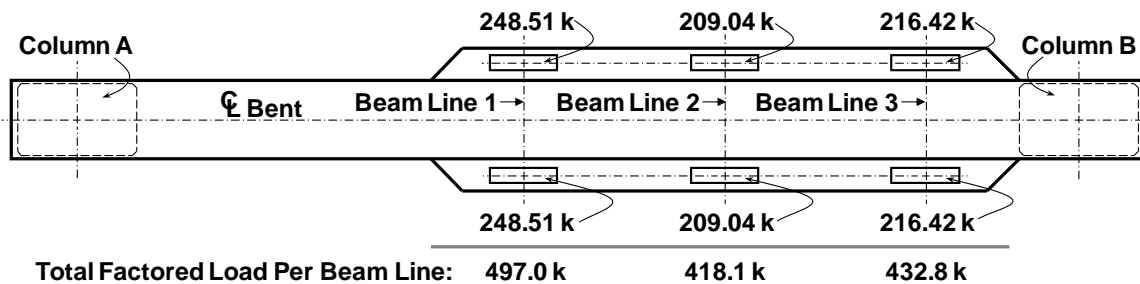


Figure 6.2: Factored superstructure loads acting on the bent cap

The load for each beam line is shown acting on the bottom chord of the global STM in Figure 6.3. The factored self-weight of the bent cap should also be applied to the model. Distributed loads, however, cannot be applied on the STM, as with any truss. The self-weight must therefore act at the model's joints, or nodes. The factored tributary self-weight of the bent cap, assuming a unit weight of 150 lb/ft³, is distributed among all the nodes of the STM except Nodes A and F (refer to Figure 6.3). The self-weight is not applied at Nodes A and F since they are located at the top corners of the bent cap and assuming any significant self-weight accumulates within these regions seems unreasonable. A load factor of 1.25 is applied to the self-weight in accordance with the AASHTO LRFD (2010) Strength I load combination. The factored tributary self-weight has been added to the three superstructure loads acting on the STM in Figure 6.3.

Since the self-weight of the cap is distributed among the nodes of the strut-and-tie model, the magnitude of each self-weight load depends on the STM geometry. The self-

weight is therefore applied during the development of the truss model. This process is described in detail within Section 6.4.1.

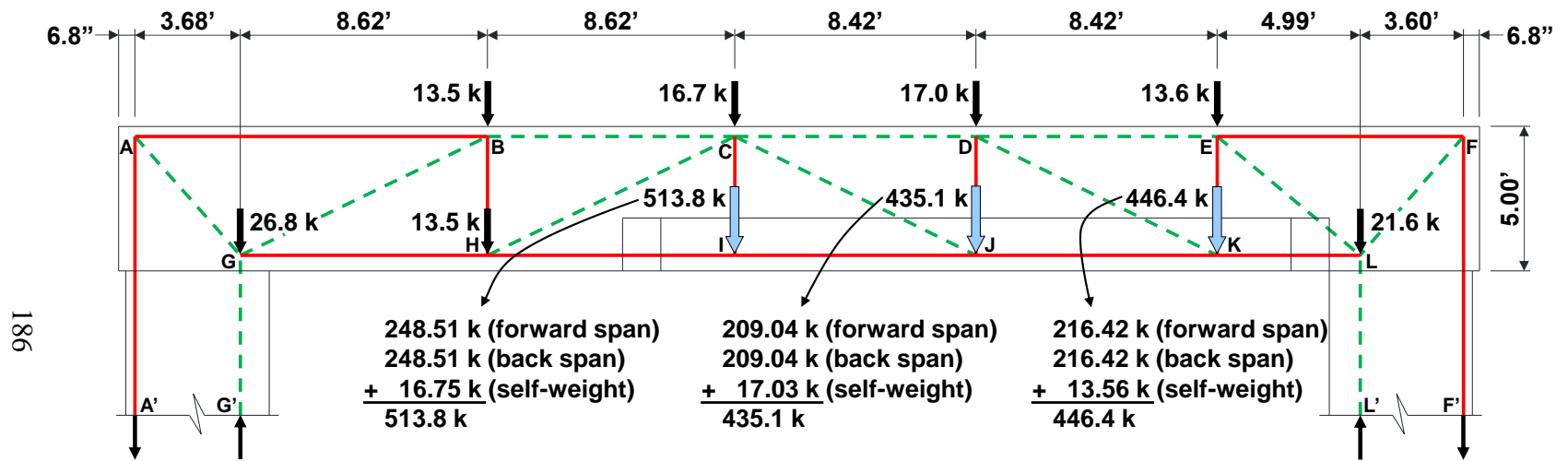


Figure 6.3: Factored loads acting on the global strut-and-tie model for the inverted-T bent cap (moment frame case)

6.2.3 Determine the Bearing Areas

The size of the bearing pads for the 44-inch trapezoidal box beams is 34 inches by 8 inches (refer to Figure 6.1). Each of the pads rests on a concrete bearing seat, and the bearing stresses can be assumed to spread laterally through the seat. The effective bearing area at the cap surface is likely larger than that of the bearing pad itself. For simplicity, however, the effect of the bearing seats will be ignored in this design example. The size of the bearing pads does not control the design of the bent cap.

6.2.4 Material Properties

- Concrete: $f'_c = 5.0 \text{ ksi}$
- Reinforcement: $f_y = 60 \text{ ksi}$

Recall that the inverted-T straddle bent cap is an existing field structure. The specified concrete compressive strength, f'_c , of the existing structure is 3.6 ksi. The nodal strength checks of Section 6.4.6, however, reveal that an increased concrete strength is necessary for all the nodes to be able to resist the applied forces.

6.2.5 Inverted-T Terminology

Throughout Examples 3a and 3b in Chapters 6 and 7, special terminology is used to describe the reinforcement within inverted-T members (refer to Figure 6.4). Hanger reinforcement (or hanger ties) refers to the vertical reinforcement of the stem that is located within a specified distance from an applied ledge load. The hanger reinforcement transfers the ledge load upward toward the compression face of the member. Ledge reinforcement refers to the horizontal reinforcement that carries tensile forces (imposed by the ledge loads) across the ledge.

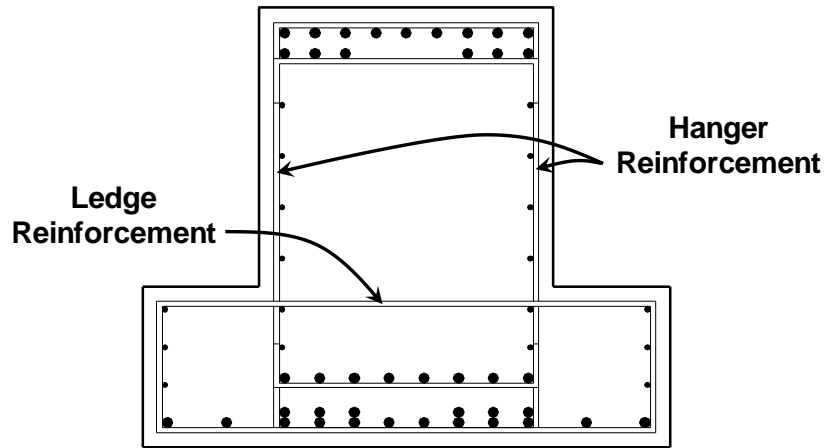


Figure 6.4: Defining hanger and ledge reinforcement

6.3 DESIGN PROCEDURE

Behavior of the inverted-T bent cap will be influenced by a number of disturbances (e.g. superstructure loads, ledges, and frame corners). Although a small portion of the bent cap is a B-region (see Figure 6.5), the entire member is conservatively designed using the STM procedure (refer to the discussion near the end of Section 3.2.3).

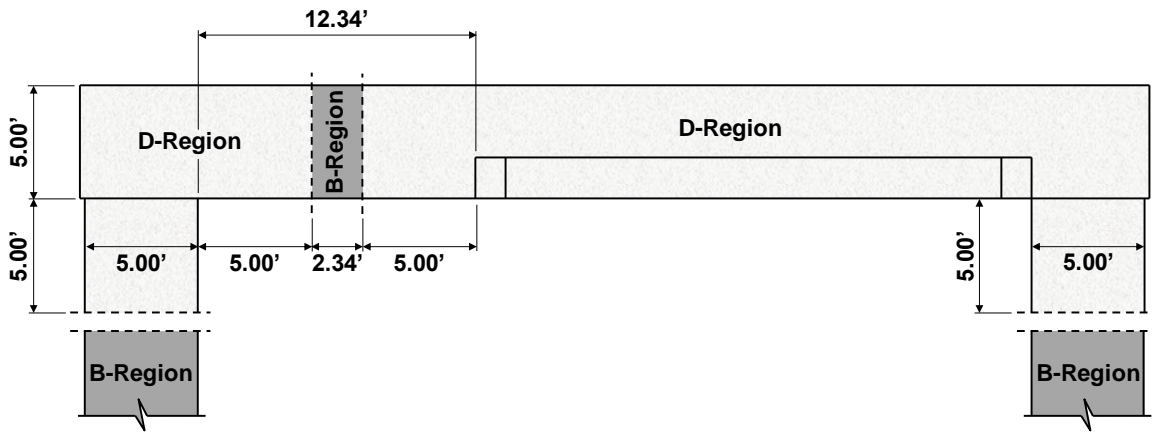


Figure 6.5: Bent divided into D-regions and B-regions

A global STM as well as local STMs will be developed for design of the bent cap. The global STM models the flow of forces through the bent cap from the applied loads to the columns (refer to Figure 6.3). The local STMs model the flow of forces through the

bent cap's cross section and are used to design the ledge. Together, the global STM and the local STMs form a three-dimensional STM for the inverted-T.

The general STM design procedure introduced in Section 2.3.3 has been adapted to the current design scenario, resulting in the steps listed below:

- Step 1: Analyze structural component and develop global strut-and-tie model
- Step 2: Develop local strut-and-tie models
- Step 3: Proportion longitudinal ties
- Step 4: Proportion hanger reinforcement/vertical ties
- Step 5: Proportion ledge reinforcement
- Step 6: Perform nodal strength checks
- Step 7: Proportion crack control reinforcement
- Step 8: Provide necessary anchorage for ties
- Step 9: Perform other necessary checks
- Step 10: Perform shear serviceability check

6.4 DESIGN CALCULATIONS

6.4.1 Step 1: Analyze Structural Component and Develop Global Strut-and-Tie Model

The STM for the inverted-T straddle bent cap (with full moment connections) is shown in Figure 6.6. To proportion the ties and perform the nodal strength checks, this STM is assumed to be located within a plane along the longitudinal axis of the bent cap and is referred to as the global strut-and-tie model. The development of the global STM and the analysis of the overall structural component are grouped within the same step of the design procedure since application of the tributary self-weight loads is dependent on the STM geometry (refer to Section 6.2.2).

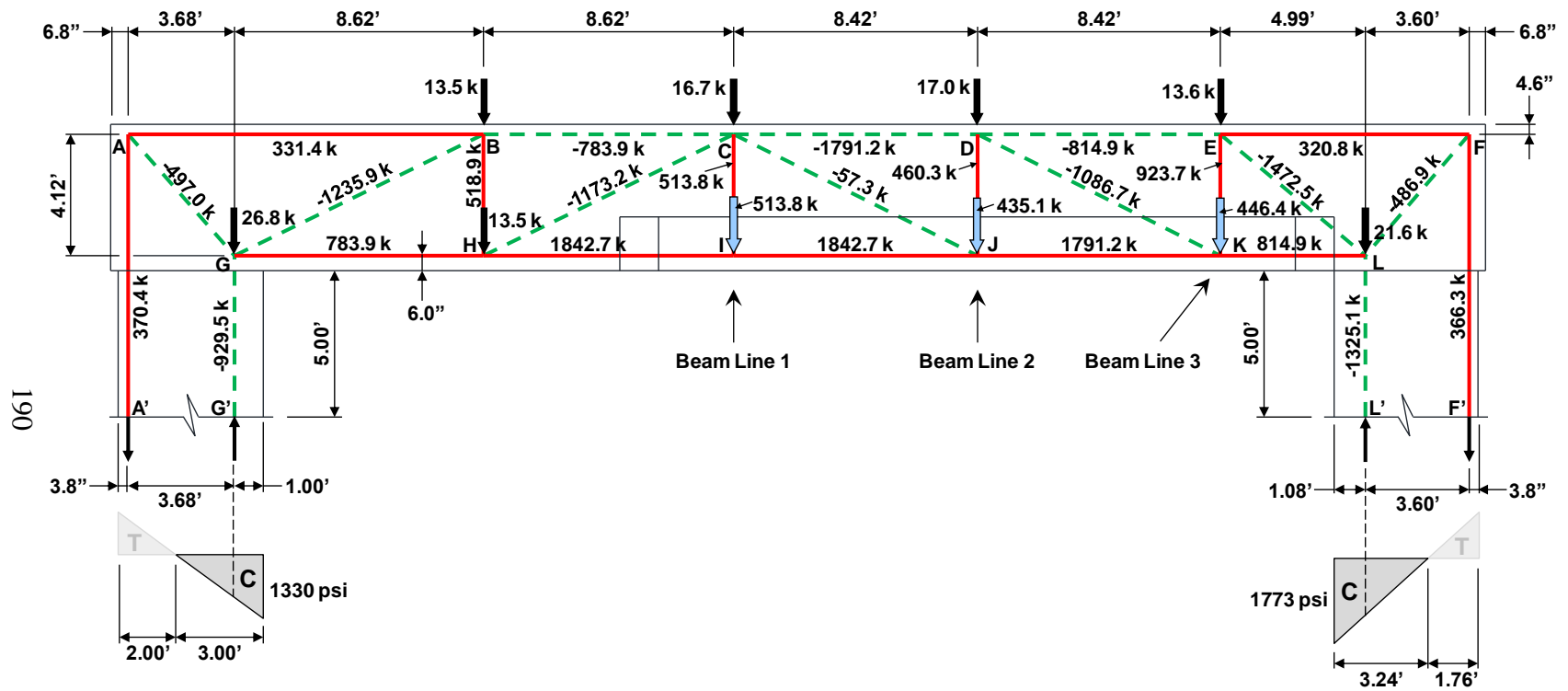


Figure 6.6: Global strut-and-tie model for the inverted-T bent cap (moment frame case)

To determine the geometry of the global STM, an analysis of the moment frame substructure subjected to the factored superstructure loads must first be performed (Figure 6.7). A constant flexural stiffness is assumed for the entire length of the bent cap based on the stem geometry (i.e. the 5.00-foot by 3.34-foot rectangular section), and the columns are modeled as 5-foot by 3-foot rectangular sections. Each frame member is located at the centroid of its respective cross section (i.e. centroid of the column or the beam stem). As stated earlier, the slope of the structure is ignored to simplify the design process. The self-weight of the bent cap is not applied at this point of the structural analysis since the locations where the tributary self-weight loads act are not yet known. Furthermore, applying the self-weight to the frame as a distributed load would create discrepancies between the frame analysis and the subsequent analysis of the STM. The reactions at the base of each column due to application of the three superstructure loads are shown in Figure 6.7.

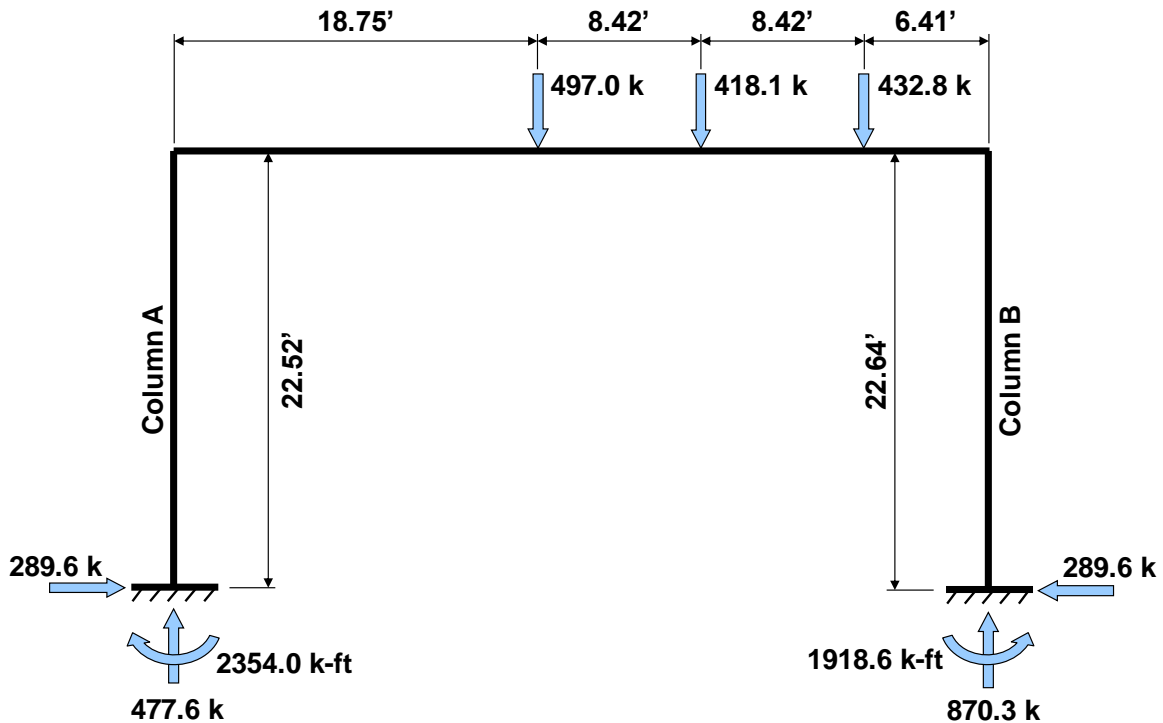


Figure 6.7: Analysis of moment frame – factored superstructure loads

The locations of the vertical struts within the columns, Struts GG' and LL' (Figure 6.6), are based on the results of the moment frame analysis. A linear distribution of stress can be assumed to exist within each column at a distance of one member depth (here, the width of the column) from the bottom face of the bent cap (i.e. at the D-region/B-region interface). The bending moment at this location is 1995.8 kip-ft for the left column (Column A) and 2465.9 kip-ft for the right column (Column B). The resulting stress distributions are shown in Figure 6.6. The position of the vertical strut in each column corresponds to the location of the compressive stress resultant. The struts are placed 1.00 feet and 1.08 feet from the compression faces of the left and right columns, respectively. Please recall that two vertical struts were used to carry the large compressive force within the column supporting the cantilever bent cap of Example 2. The width of each column supporting the inverted-T bent cap as well as the compressive forces carried by the columns is significantly smaller than that of the cantilever cap. A single strut can therefore be used within each column of the current example. The designer should note that positioning two vertical struts within each column in a manner similar to that of Example 2 is also acceptable. Using a single strut within each column, however, simplifies the development of the STM.

Each vertical column tie (Ties AA' and FF') is then positioned at the centroid of the exterior layer of column reinforcement. As shown in Figure 6.6, this location is estimated to be 3.8 inches from the tension face of each column.

Next, the locations of the top and bottom chords of the STM are determined. Positive and negative moment regions exist within the bent cap, indicating that the STM will include ties in both the top and bottom chords. The chords of the STM are therefore placed at the centroids of the longitudinal reinforcement along the top and bottom of the bent cap. In the final STM of Figure 6.6, the bottom chord is located 6.0 inches from the bottom face of the bent cap, while the top chord is located 4.6 inches from the top face. A review of the final reinforcement details of Section A-A shown in Figure 6.27 reveals that the top and bottom chords of the STM are precisely located at the centroids of the main longitudinal reinforcement. A few iterations of the design procedure were

necessary to achieve this level of accuracy. After the layout of the required number of longitudinal reinforcing bars is decided, the designer should compare the centroids of the bars with the placement of the top and bottom chords of the STM. If the locations differ, the designer should then determine if another iteration (i.e. modifying the STM) would affect the final design of the structural member.

The vertical Ties CI, DJ, and EK are placed at the locations of the applied superstructure loads and represent the required hanger reinforcement. These ties “hang up” the loads applied to the ledge of the inverted-T, or transfer stresses from the ledge to the top chord and diagonal struts of the STM. Please recall that the angle between a tie and a diagonal strut entering the same node must not be less than 25 degrees (refer to Section 2.7.2). Another vertical tie (Tie BH) is placed halfway between Nodes G and I to satisfy this requirement. Lastly, each of the diagonal members is oriented in a manner that causes its force to be compressive (i.e. all diagonal members are struts). The resulting STM geometry is shown in Figure 6.6.

The total loads for each beam line are applied to the bottom chord at Nodes I, J, and K. The self-weight based on tributary volumes is then distributed among the nodes of the top and bottom chords of the STM. Now that the magnitudes and locations of the tributary self-weight loads acting on the STM are known, the frame is re-analyzed (with the tributary self-weight loads applied) to eliminate discrepancies between the internal forces of the frame and the member forces of the STM. The tributary self-weight, superstructure loads, and column reactions are shown acting on the frame in Figure 6.8.

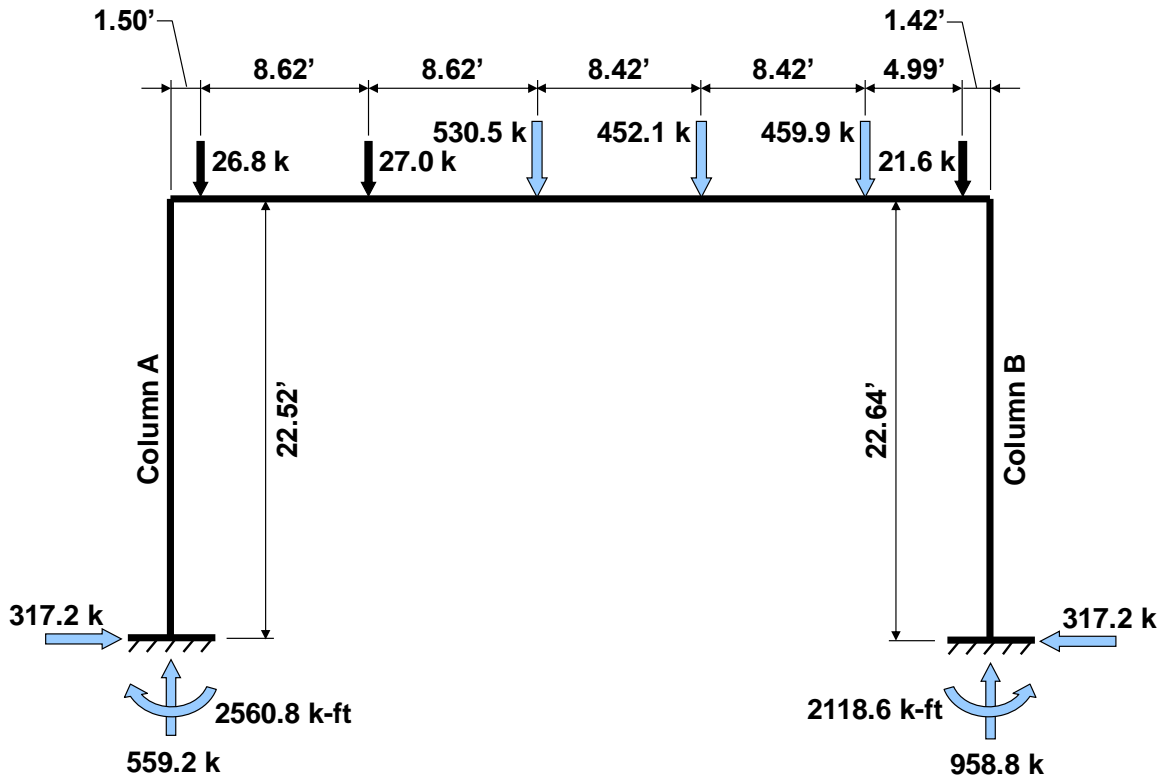


Figure 6.8: Analysis of moment frame – factored superstructure loads and tributary self-weight

The forces applied to the STM at the D-region/B-region interfaces are determined from the frame analysis of Figure 6.8. In other words, the forces of the struts and ties within the columns, Struts GG' and LL' and Ties AA' and FF', are calculated based on the frame analysis results so that the STM forces are in equilibrium with the internal forces within the columns. The bending moment at the section 5 feet down each column (from the bottom surface of the cap) is found once again. These moments are determined to be 2203.4 kip-ft and 2683.6 kip-ft for the left and right columns, respectively. The effect of the forces in the strut and tie within each column must be equivalent to the axial force and bending moment at the respective D-region/B-region interface. The strut and tie forces are determined by solving two simultaneous equations for each column.

For the strut and tie forces within the left column (Column A):

$$\begin{cases} -F_{Tie} + F_{Strut} = 559.2 \text{ kip} \\ F_{Tie}(2.18 \text{ ft}) + F_{Strut}(1.50 \text{ ft}) = 2203.4 \text{ k-ft} \end{cases}$$

Solving: $F_{Tie} = 370.4 \text{ kip}$ $F_{Strut} = 929.5 \text{ kip}$

For the strut and tie forces within the right column (Column B):

$$\begin{cases} -F_{Tie} + F_{Strut} = 958.8 \text{ kip} \\ F_{Tie}(2.18 \text{ ft}) + F_{Strut}(1.42 \text{ ft}) = 2683.6 \text{ k-ft} \end{cases}$$

Solving: $F_{Tie} = 366.3 \text{ kip}$ $F_{Strut} = 1325.1 \text{ kip}$

In the first equation of each pair, the strut-and-tie model is made certain to satisfy equilibrium with respect to the axial force within each column. In the second equation, the moment about the centerline of the column due to the strut and tie forces is set equal to the bending moment at the D-region/B-region interface.

To summarize, the geometry of the global STM is based on the moment frame analysis of Figure 6.7, while the boundary forces acting on the STM at the D-region/B-region interfaces must be determined from the frame analysis of Figure 6.8.

With the member forces of the struts and ties within the columns known, the remaining member forces are found by satisfying equilibrium at each joint of the truss model (i.e. by using statics). This results in the STM forces of Figure 6.6. If structural analysis software is used to analyze the STM, the predetermined forces of the strut and tie within each column should be imposed on these members.

6.4.2 Step 2: Develop Local Strut-and-Tie Models

Due to the complex flow of forces within the inverted-T cross section, a separate local STM should be developed at each section where a beam load is supported by the ledge. The STM for the section at Beam Line 1 (refer to Figure 6.6) is shown in Figure 6.9. Ties A_sG_s and B_sH_s are placed to coincide with the vertical stirrup legs (i.e. hanger

reinforcement) that will serve as transverse reinforcement in the stem of the bent cap. Similarly, Tie C_sF_s coincides with the top horizontal portion of the stirrups provided within the ledge. The position of Strut G_sH_s corresponds to the location of the bottom chord of the global STM (refer back to Figure 6.6). Throughout the design of an inverted-T, the engineer should keep in mind that the flow of forces within the bent cap can be visualized as one three-dimensional STM. Placement of Strut G_sH_s to coincide with the bottom longitudinal chord of the global STM is therefore reasonable.

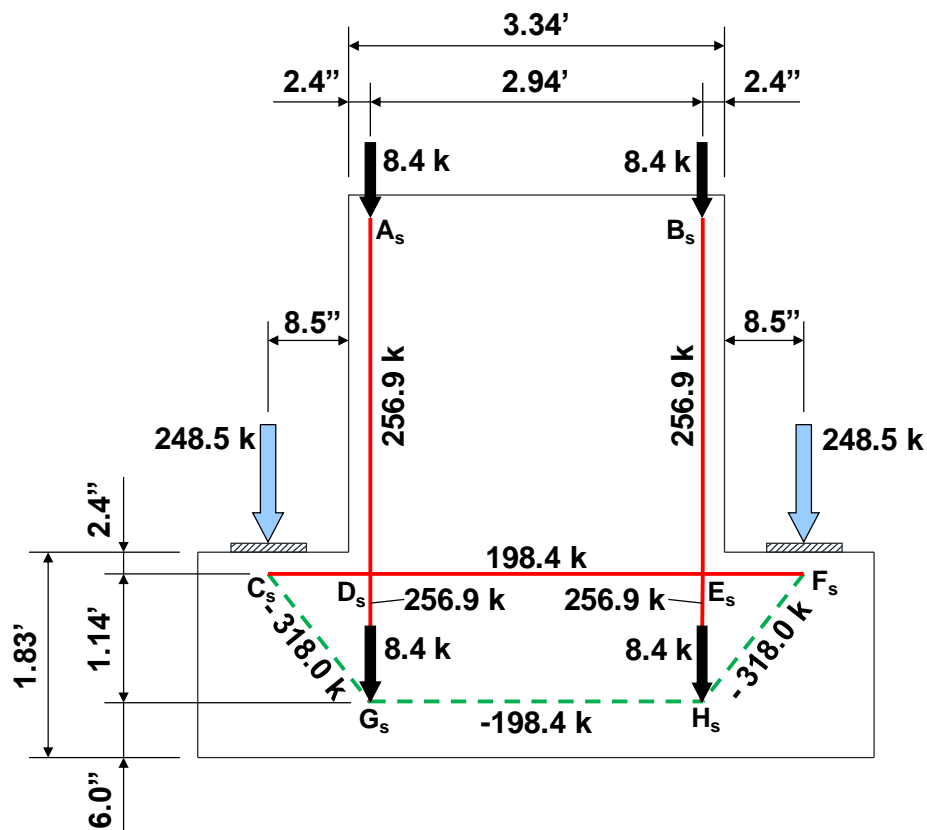


Figure 6.9: Local strut-and-tie model at Beam Line 1 (moment frame case)

The 248.5-kip beam loads acting on the local STM (Figure 6.9) were presented in Figure 6.2. The self-weight based on tributary volumes is divided evenly between Nodes A_s , B_s , G_s , and H_s . The remaining member forces are calculated by satisfying equilibrium at the nodes. Visualizing the three-dimensional STM, Struts CH and CJ of the global

STM are located in the plane perpendicular to the plane of the local STM (Figure 6.9). These struts connect at Nodes A_s and B_s , requiring the 256.9-kip forces in the vertical ties of the local STM for equilibrium to be satisfied. Please note that these 256.9-kip forces are each half of the force in Tie CI of the global STM.

Local strut-and-tie models are also developed at the locations of Beam Lines 2 and 3. The local STMs for all three beam lines (summarized in Figure 6.10) are geometrically identical but are each subjected to a different set of external forces. Comparing the three local STMs, design of the horizontal ledge reinforcement (Tie C_sF_s) and the nodal strength checks are governed by the STM at Beam Line 1. To simplify design and construction, the spacing of ledge reinforcement required by the STM at Beam Line 1 will be satisfied along the entire length of the ledge. All other reinforcement details (namely the vertical ties) will be based on the global STM.

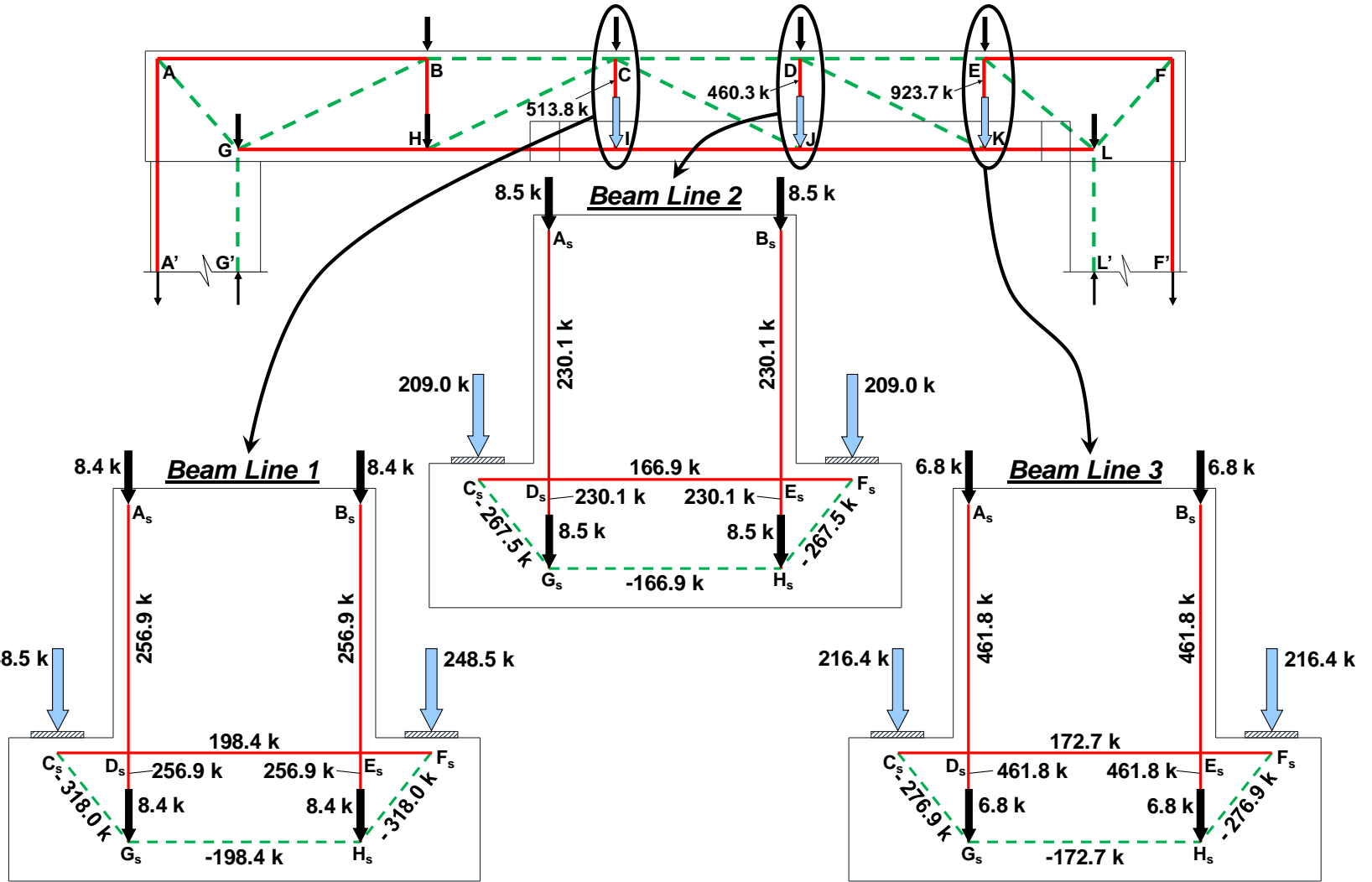


Figure 6.10: Comparing the local strut-and-tie models (moment frame case)

6.4.3 Step 3: Proportion Longitudinal Ties

The tie forces of the global STM are used to proportion the longitudinal reinforcement along the top and bottom chords of the beam as well as the exterior face of each column. A constant amount of longitudinal steel will be provided along the length of the inverted-T for ease of construction.

Bottom Chord

The force in Ties HI and IJ controls the design of the bottom chord of the STM. Using #11 bars, the longitudinal reinforcement required for the bottom chord is:

$$\begin{aligned}\text{Factored Load:} & F_u = 1842.7 \text{ kip} \\ \text{Tie Capacity:} & \varphi \cdot f_y \cdot A_{st} = F_u \\ & (0.9)(60 \text{ ksi})A_{st} = 1842.7 \text{ kip} \\ & A_{st} = 34.12 \text{ in}^2\end{aligned}$$

$$\text{Number of \#11 bars required: } 34.12 \text{ in}^2 / 1.56 \text{ in}^2 = 21.9 \text{ bars}$$

Use 22 - #11 bars

Top Chord

The longitudinal reinforcement along the top chord of the STM is governed by the force in Tie AB, and the required number of bars is:

$$\begin{aligned}\text{Factored Load:} & F_u = 331.4 \text{ kip} \\ \text{Tie Capacity:} & \varphi \cdot f_y \cdot A_{st} = F_u \\ & (0.9)(60 \text{ ksi})A_{st} = 331.4 \text{ kip} \\ & A_{st} = 6.14 \text{ in}^2\end{aligned}$$

$$\text{Number of \#11 bars required: } 6.14 \text{ in}^2 / 1.56 \text{ in}^2 = 3.9 \text{ bars}$$

Use 4 - #11 bars

As discussed in Section 6.4.6, additional top chord reinforcement will be necessary to strengthen the back face of Node C. The designer should note that consideration of compression reinforcement in nodal strength calculations is only acceptable if the reinforcement is sufficiently anchored.

Column Longitudinal Tie

The longitudinal tension reinforcement within the two columns will be identical. The amount of steel in the columns is controlled by Tie AA'.

$$\begin{aligned} \text{Factored Load:} & \quad F_u = 370.4 \text{ kip} \\ \text{Tie Capacity:} & \quad \varphi \cdot f_y \cdot A_{st} = F_u \\ & \quad (0.9)(60 \text{ ksi})A_{st} = 370.4 \text{ kip} \\ & \quad A_{st} = 6.86 \text{ in}^2 \end{aligned}$$

$$\text{Number of \#11 bars required: } 6.86 \text{ in}^2 / 1.56 \text{ in}^2 = 4.4 \text{ bars}$$

Use 5 - #11 bars

The final reinforcement details for the columns are dependent on the complete design that considers all governing load cases and applicable articles in AASHTO LRFD (2010).

6.4.4 Step 4: Proportion Hanger Reinforcement/Vertical Ties

The geometry of the node above each beam line (Nodes C, D, and E in Figure 6.6) will be defined by the distribution of the corresponding hanger reinforcement. For that reason, the reinforcement for Ties CI, DJ, and EK of the global STM is proportioned here. Design of the reinforcement for Tie BH is also covered within this section.

Unlike a rectangular bent cap with an STM loaded on its top chord, a bottom-chord loaded STM requires hanger reinforcement to transfer the applied superstructure loads upward toward the top chord. According to Article 5.13.2.5.5 of *AASHTO LRFD Bridge Design Specifications* (2010), the length over which the hanger reinforcement can be distributed (i.e. the width of a hanger tie) is $W + 2d_f$. Referring to Figure 6.11, W is defined as the dimension of the bearing pad measured along the length of the ledge, and d_f is defined as the distance from the top of the ledge to the bottom horizontal portion of the stirrups. Article 5.13.2.5.5 effectively defines the length over which the compressive stresses may spread between the top surface of the ledge and the point at which the vertical (hanger) reinforcement is engaged (here, the bottom horizontal portion of the stirrups). The AASHTO LRFD (2010) provision also states the following: “The edge

distance between the exterior bearing pad and the end of the inverted T-beam shall not be less than d_f .” The geometry of the inverted-T does not meet this AASHTO LRFD (2010) requirement. Keeping the geometry consistent with that of the existing field structure, the effective tie widths at the outside beam lines is limited to $2c$, where c is the distance from the centerline of the bearing pad to the end of the ledge (see Figure 6.11). The effect of the tapered ends of the ledge is conservatively neglected. As illustrated in Figure 6.11, the available length for Ties CI and EK is $2c$, or 5.17 feet, while the available length for Tie DJ is $W + 2d_f$, or 6.10 feet.

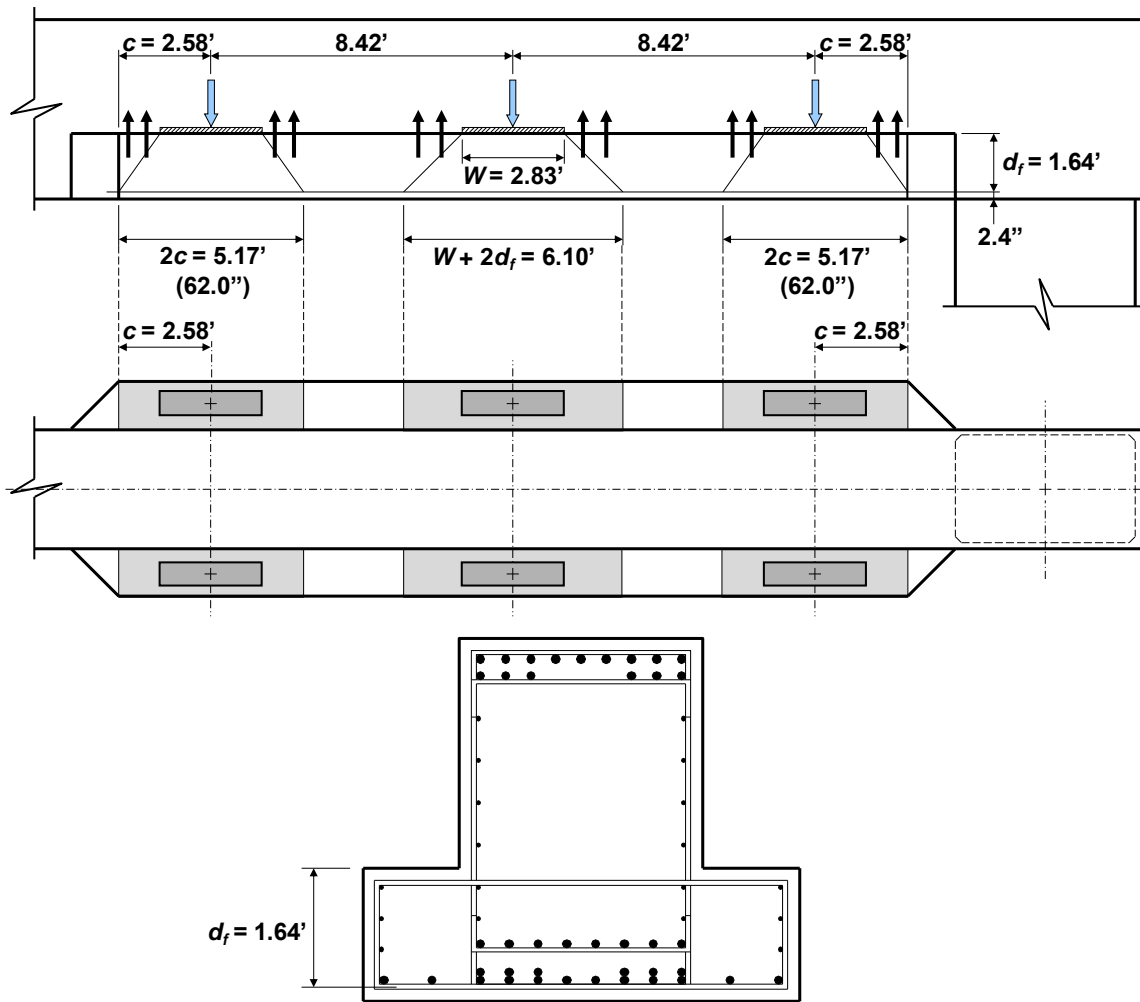


Figure 6.11: Available lengths for hanger reinforcement – plan and elevation views

The hanger reinforcement along the ledge will be proportioned first. Then, the required stirrup spacing for Tie BH within the shear span left of Beam Line 1 will be determined.

Tie EK

Tie EK is the most critical hanger tie; it is subjected to a large tensile force that must be resisted by a narrow band of reinforcement. To maintain consistency with the original design, two-legged #6 stirrups will be bundled together and spaced as necessary to resist the tie force. Alternatively, the designer may wish to utilize #6 stirrups with four legs. The required spacing of the paired #6 stirrups is:

Factored Load:	$F_u = 923.7 \text{ kip}$
Tie Capacity:	$\phi \cdot f_y \cdot A_{st} = F_u$
	$(0.9)(60 \text{ ksi})A_{st} = 923.7 \text{ kip}$
	$A_{st} = 17.11 \text{ in}^2$

Number of double #6 stirrups required: $17.11 \text{ in}^2 / (4)(0.44 \text{ in}^2) = 9.72$ stirrups

$$l_a = 2c = 62.0 \text{ in} \quad s = 62.0 \text{ in} / 9.72 = 6.4 \text{ in}$$

Use 2 legs of double #6 stirrups with spacing less than 6.4 in.

Tie CI

Tie CI is the second most critical vertical tie within the bent cap. The reinforcement detailing for Tie CI will be conservatively used along the entire length of the ledge with the exception of the region that comprises Tie EK. The required spacing of two-legged #6 stirrups is:

Factored Load:	$F_u = 513.8 \text{ kip}$
Tie Capacity:	$\phi \cdot f_y \cdot A_{st} = F_u$
	$(0.9)(60 \text{ ksi})A_{st} = 513.8 \text{ kip}$
	$A_{st} = 9.51 \text{ in}^2$

Number of #6 stirrups (2 legs) required: $9.51 \text{ in}^2 / (2)(0.44 \text{ in}^2) = 10.81$ stirrups

$$l_a = 2c = 62.0 \text{ in} \quad s = 62.0 \text{ in} / 10.81 = 5.7 \text{ in}$$

Use 2 legs of #6 stirrups with spacing less than 5.7 in.

Tie BH

In contrast to Nodes C, D, and E, Nodes B and H are smeared (interior) nodes with undefined geometries. Use of the proportioning technique recommended by Wight and Parra-Montesinos (2003) (refer to Section 2.9.5) would indicate that the reinforcement for Tie BH could be distributed over a length, l_a , of 160.9 inches, or 13.41 feet. In reality, this available length, l_a , is partially occupied by the reinforcement of Tie CI. The reinforcement for Tie BH will therefore be distributed over a shorter length equal to the distance between Nodes G and H. The length of the truss panel between Nodes G and H is 103.5 inches, or 8.62 feet. The required reinforcement will be centered on Tie BH and should be spaced over the available length as follows:

Factored Load:	$F_u = 518.9 \text{ kip}$
Tie Capacity:	$\phi \cdot f_y \cdot A_{st} = F_u$
	$(0.9)(60 \text{ ksi})A_{st} = 518.9 \text{ kip}$
	$A_{st} = 9.61 \text{ in}^2$

Number of #6 stirrups (2 legs) required: $9.61 \text{ in}^2 / (2)(0.44 \text{ in}^2) = 10.92$ stirrups

$$l_a = 103.5 \text{ in} \quad s = 103.5 \text{ in} / 10.92 = 9.5 \text{ in}$$

Use 2 legs of #6 stirrups with spacing less than 9.5 in.

The minimum required crack control reinforcement, proportioned in Section 6.4.7, ultimately controls the reinforcement detailing within this region of the bent cap.

6.4.5 Step 5: Proportion Ledge Reinforcement

Next, the ledge reinforcement required to carry the force in Tie C_sF_s of Figure 6.9 is determined. According to Article 5.13.2.5.3 of AASHTO LRFD (2010), the reinforcement comprising this tie should be uniformly spaced within a length of $W + 5a_f$

or $2c$, whichever is less (refer to Figure 6.12). The dimension a_f is the distance between the ledge load and the reinforcement parallel to the load as shown in Figure 6.13. Moreover, the available length for each ledge load should not overlap that of adjacent ledge loads. Considering a three-dimensional flow of forces within the inverted-T, the ledge reinforcement and the hanger stirrups work together to carry forces through the member's cross section. Therefore, instead of applying the provisions of Article 5.13.2.5.3, the length over which the ledge reinforcement can be distributed is conservatively limited to the width of the corresponding hanger tie. In the current example, the available length of the ledge reinforcement (i.e. Tie C_sF_s of Figure 6.9) is taken as the width of Tie CI of the global STM (Figure 6.6), or 5.17 feet. For this case, the available length happens to match the requirements of Article 5.13.2.5.3.

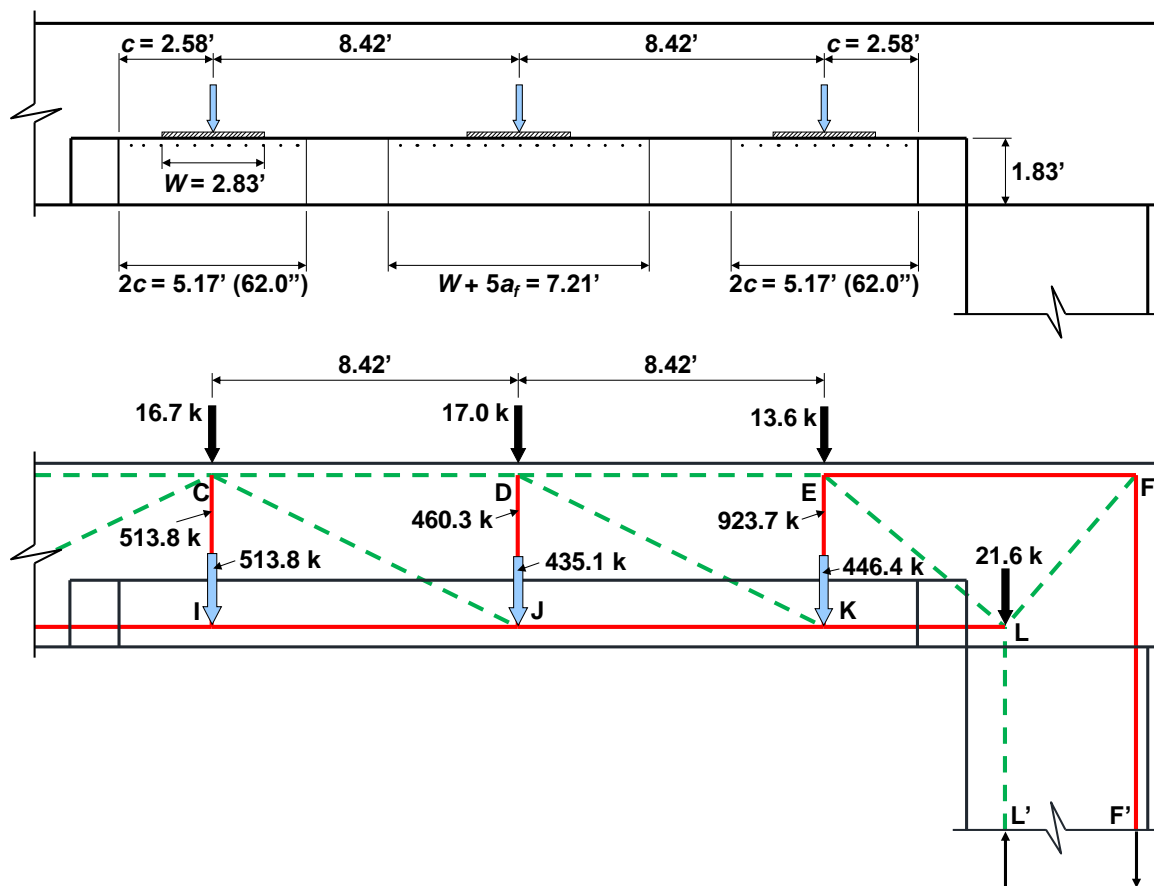


Figure 6.12: Available lengths for ledge reinforcement

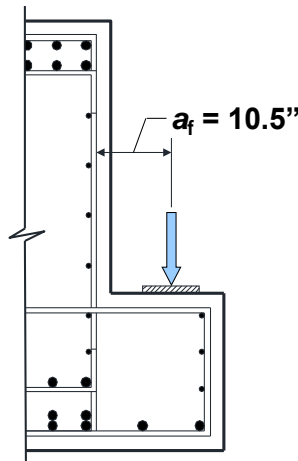


Figure 6.13: Dimension a_f

The force in Tie $C_s F_s$ of the local STM at Beam Line 1 is greater than that of the corresponding tie within each of the other local STMs. The length over which the ledge reinforcement can be distributed is also shorter for the two exterior beam lines (compared to the available length at Beam Line 2). The spacing of #6 bars required to carry the force in Tie $C_s F_s$ of the STM at Beam Line 1 is:

$$\begin{aligned}
 \text{Factored Load:} & \quad F_u = 198.4 \text{ kip} \\
 \text{Tie Capacity:} & \quad \phi \cdot f_y \cdot A_{st} = F_u \\
 & \quad (0.9)(60 \text{ ksi})A_{st} = 198.4 \text{ kip} \\
 & \quad A_{st} = 3.67 \text{ in}^2
 \end{aligned}$$

$$\text{Number of \#6 bars required: } 3.67 \text{ in}^2 / 0.44 \text{ in}^2 = 8.35 \text{ bars}$$

$$l_a = 2c = 62.0 \text{ in} \quad s = 62.0 \text{ in} / 8.35 = 7.4 \text{ in}$$

Use #6 bars with spacing less than 7.4 in.

The top portion of the #6 stirrups provided within the ledge will satisfy the former requirement (see Figure 6.14). Each of the stirrups within the ledge will be paired with the stirrups of the stem to simplify construction. Since the required spacing of the stirrups within the stem is smaller than the required spacing for the ledge reinforcement

(i.e. less than 7.4 inches), pairing the stirrups in this manner along the entire length of the ledge ensures sufficient ledge reinforcement is provided.

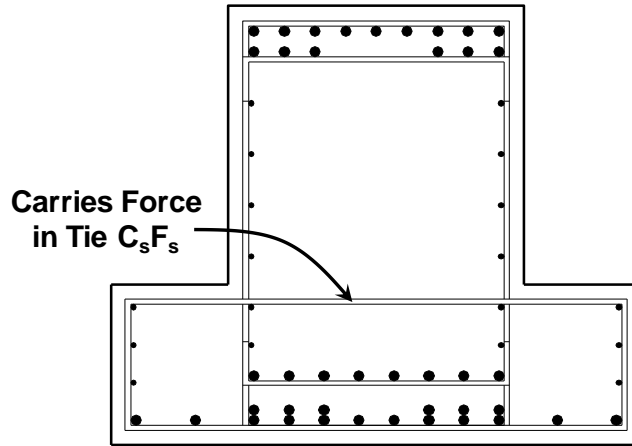


Figure 6.14: Top portion of ledge reinforcement carries force in Tie $C_s F_s$

6.4.6 Step 6: Perform Nodal Strength Checks

Figure 6.15 is a visualization of how the struts and nodes fit within the inverted-T bent cap. An arbitrary size was chosen for the smeared nodes, and they were only drawn for illustrative purposes. Some of the struts intersecting at the nodes along the top chord of the STM can be resolved to simplify the nodal geometries.

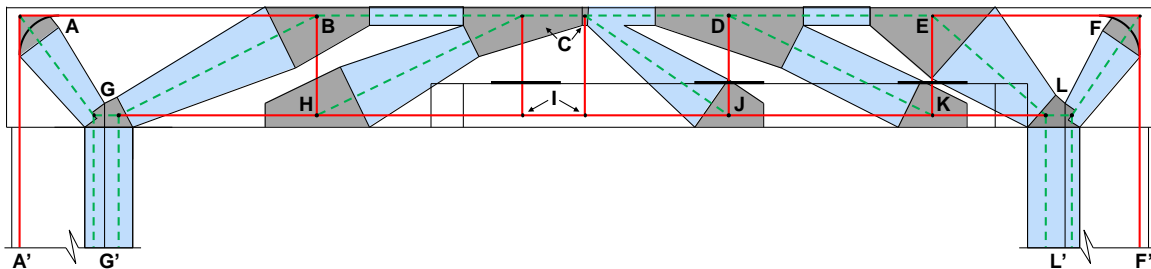


Figure 6.15: Illustration of struts and nodes within the inverted-T bent cap

Within this section, the nodes of the global STM will be considered first. The most critical nodes will be identified, and the corresponding strength calculations are provided herein. Some of the remaining nodes can be deemed to have adequate strength by inspection. Nodes A and F are curved-bar nodes and will be detailed to resist the

applied stresses and develop the unbalanced tie forces. The singular nodes of the local STM at Beam Line 1 will then be evaluated.

Node G (CCC/CCT)

Nodes G and L are located near the inside faces of the left and right frame corners, respectively. Due to tight geometric constraints and large forces (reactions), these nodes are among the most highly stressed regions in the model. Node G is shown in Figure 6.16. The total width of the bearing face is double the distance from the inside column face to Strut GG' (shown in Figure 6.6). The height of the back face is taken as double the distance from the bottom surface of the bent cap to the centroid of the bottom chord reinforcement. Diagonal struts enter the node from both its left and right sides. The node is therefore subdivided into two parts in a manner similar to that of Nodes JJ and NN of Example 1 (see Section 4.4.4). The force acting on the bearing face of the left portion of the node equilibrates the vertical component of the diagonal strut acting on the left (Strut AG) and a portion of the applied self-weight (11.0 kips). Equilibrium is satisfied for the right nodal subdivision using the same approach. In addition, the inclinations of the diagonal struts are revised to account for the subdivision of the node.

$$\begin{aligned}
 w_s &= l_b \sin\theta + a \cos\theta \\
 &= (9.8 \text{ in}) \sin 53.07^\circ + (12.0 \text{ in}) \cos 53.07^\circ \\
 &= 7.83 \text{ in} + 7.21 \text{ in} = 15.0 \text{ in}
 \end{aligned}$$

$$\begin{aligned}
 w_s &= l_b \sin\theta + a \cos\theta \\
 &= (14.1 \text{ in}) \sin 26.62^\circ + (12.0 \text{ in}) \cos 26.62^\circ \\
 &= 6.32 \text{ in} + 10.73 \text{ in} = 17.0 \text{ in}
 \end{aligned}$$

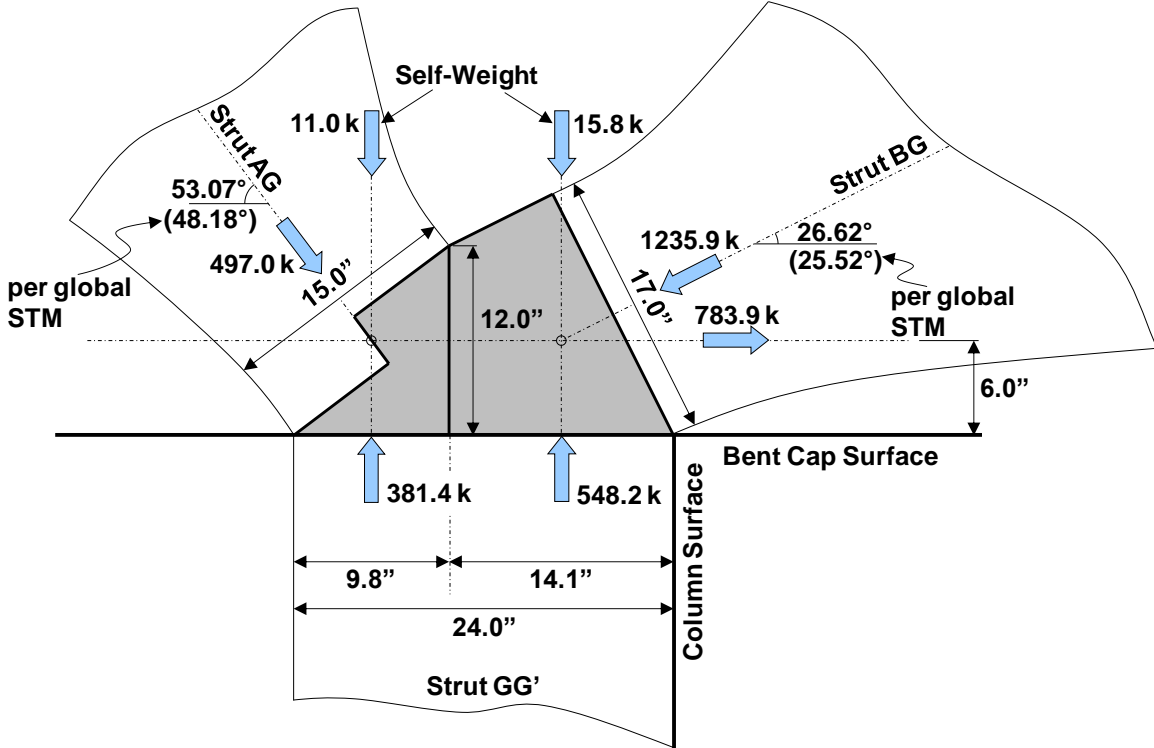


Figure 6.16: Node G (moment frame case)

The dimension of the bearing face of each nodal subdivision is based upon the magnitude of the vertical component of each diagonal strut in relation to the net vertical force from Strut GG' (929.5 kips) and the applied self-weight (26.8 kips). Uniform pressure is maintained over the total 24.0-inch width of Strut GG'. The length of each bearing face is:

$$\left[\frac{(497.0 \text{ kip}) \sin(48.18^\circ)}{929.5 \text{ kip} - 26.8 \text{ kip}} \right] (24.0 \text{ in}) = 9.8 \text{ in}$$

$$\left[\frac{(1235.9 \text{ kip}) \sin(25.52^\circ)}{929.5 \text{ kip} - 26.8 \text{ kip}} \right] (24.0 \text{ in}) = 14.1 \text{ in}$$

where 929.5 kips is the force in Strut GG' within the column, 26.8 kips is the total self-weight load applied at Node G, and the other values are shown in Figure 6.16. The revised inclination of each diagonal strut resulting from the nodal subdivision is:

$$\theta = \tan^{-1} \left[\frac{49.40 \text{ in}}{44.21 \text{ in} - (24.0 \text{ in}/2 - 9.8 \text{ in}/2)} \right] = 53.07^\circ$$

$$\theta = \tan^{-1} \left[\frac{49.40 \text{ in}}{103.50 \text{ in} - (24.0 \text{ in}/2 - 14.1 \text{ in}/2)} \right] = 26.62^\circ$$

where 49.40 in. is the height of the STM (from the top chord to the bottom chord), 44.21 in. is the horizontal distance from Node G to Tie AA' (considering the global STM of Figure 6.6), 103.50 in. is the distance from Node G to Node H, and the other dimensions are labeled in Figure 6.16. Only compressive forces act on the left portion of the node, while one tensile force acts on the right portion. Therefore, the left portion is treated as a CCC node, and the right portion is treated as a CCT node.

Node G – Right (CCT)

Given that the bent cap is wider than the column, the triaxial confinement factor, m , can be applied to the strength of Node G (see Section 2.9.7). Referring to Figure 6.17 and the corresponding calculation below, the value of A_1 is taken as the total area of the bearing face for Node G. Determination of A_2 is illustrated in Figure 6.17.

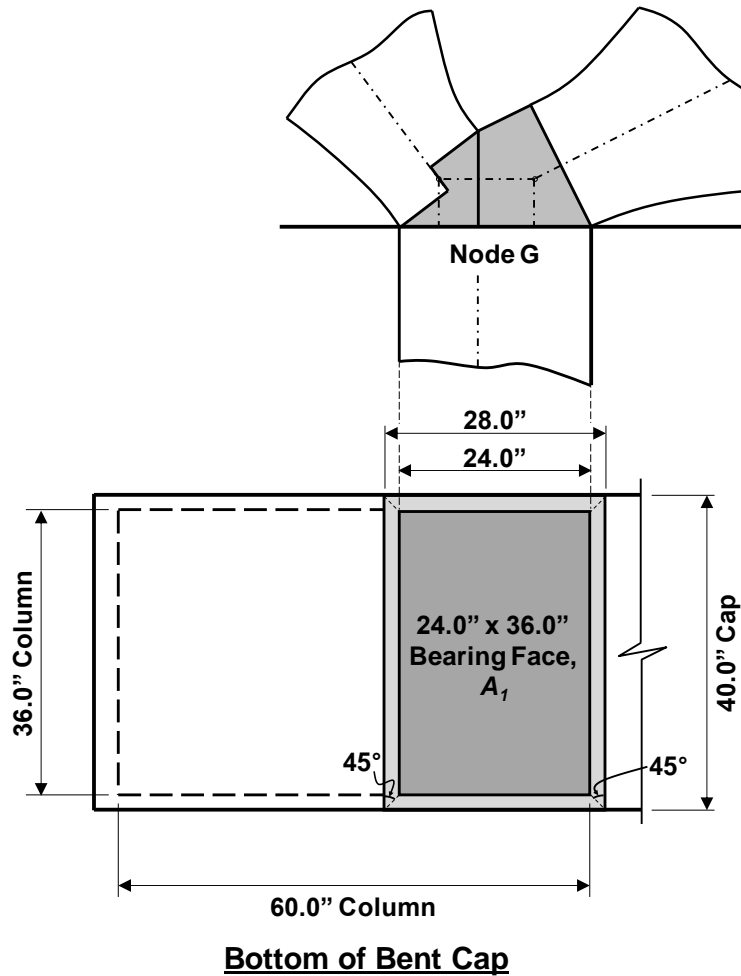


Figure 6.17: Determination of triaxial confinement factor, m , for Node G

Triaxial Confinement Factor:

$$m = \sqrt{\frac{A_2}{A_1}} = \sqrt{\frac{(40.0 \text{ in})(28.0 \text{ in})}{(24.0 \text{ in})(36.0 \text{ in})}} = 1.14 < 2 \quad \therefore \text{Use } m = 1.14$$

The faces of the right nodal subdivision are checked as follows:

BEARING FACE

Factored Load: $F_u = 548.2 \text{ kip}$
 Efficiency: $\nu = 0.7$

Concrete Capacity: $f_{cu} = m \cdot v \cdot f'_c = (1.14)(0.7)(5.0 \text{ ksi}) = 4.0 \text{ ksi}$
 $\varphi \cdot F_n = (0.7)(4.0 \text{ ksi})(14.1 \text{ in})(36 \text{ in})$
 $= 1421 \text{ kip} > 548.2 \text{ kip } \mathbf{OK}$

BACK FACE

Factored Load: $F_u = (497.0 \text{ kip})\cos 48.18^\circ = 331.4 \text{ kip}$
Efficiency: $v = 0.7$
Concrete Capacity: $f_{cu} = m \cdot v \cdot f'_c = (1.14)(0.7)(5.0 \text{ ksi}) = 4.0 \text{ ksi}$
 $\varphi \cdot F_n = (0.7)(4.0 \text{ ksi})(12.0 \text{ in})(36 \text{ in})$
 $= 1210 \text{ kip} > 331.4 \text{ kip } \mathbf{OK}$

STRUT-TO-NODE INTERFACE

Factored Load: $F_u = 1235.9 \text{ kip}$
Efficiency: $v = 0.85 - \frac{5.0 \text{ ksi}}{20 \text{ ksi}} = 0.6$
 \therefore Use $v = 0.6$
Concrete Capacity: $f_{cu} = m \cdot v \cdot f'_c = (1.14)(0.6)(5.0 \text{ ksi}) = 3.4 \text{ ksi}$
 $\varphi \cdot F_n = (0.7)(3.4 \text{ ksi})(17.0 \text{ in})(36 \text{ in})$
 $= 1457 \text{ kip} > 1235.9 \text{ kip } \mathbf{OK}$

Node G – Left (CCC)

The pressures acting over the bearing faces and the back faces of both the left and right portions of Node G are the same. Since the right portion of the node is treated as a CCT node, the strengths of the bearing and back face of the right portion control. Only the strut-to-node interface check needs to be performed for the left nodal subdivision.

Triaxial Confinement Factor: $m = 1.14$

STRUT-TO-NODE INTERFACE

Factored Load: $F_u = 497.0 \text{ kip}$
Efficiency: $v = 0.85 - \frac{5.0 \text{ ksi}}{20 \text{ ksi}} = 0.6$
 \therefore Use $v = 0.6$
Concrete Capacity: $f_{cu} = m \cdot v \cdot f'_c = (1.14)(0.6)(5.0 \text{ ksi}) = 3.4 \text{ ksi}$
 $\varphi \cdot F_n = (0.7)(3.4 \text{ ksi})(15.0 \text{ in})(36 \text{ in})$
 $= 1285 \text{ kip} > 497.0 \text{ kip } \mathbf{OK}$

Therefore, the strength of Node G is sufficient to resist the applied forces.

Node L (CCC/CCT)

For Node L, the geometry is determined and the nodal strength checks are performed using the same methods as presented for Node G. The checks reveal that all faces of Node L have adequate strength to resist the applied forces.

Node C (CCT)

The nodal strength checks for Node C, located directly above Beam Line 1, are performed next. The diagonal Strut CH entering the node is highly stressed, and large compressive forces act over a relatively small area at the back face of Node C. The node is therefore identified as critical. Since diagonal struts enter the node from both its left and right sides, the node is subdivided into two parts (shown in Figure 6.18). The total length of the top nodal face is assumed to be the same as the width of the corresponding hanger tie (Tie CI). The width of the top face is therefore 5.17 feet, or 62.0 inches (refer to Figure 6.11). The height of the back face is double the distance from the top of the bent cap to the centroid of the top chord reinforcement.

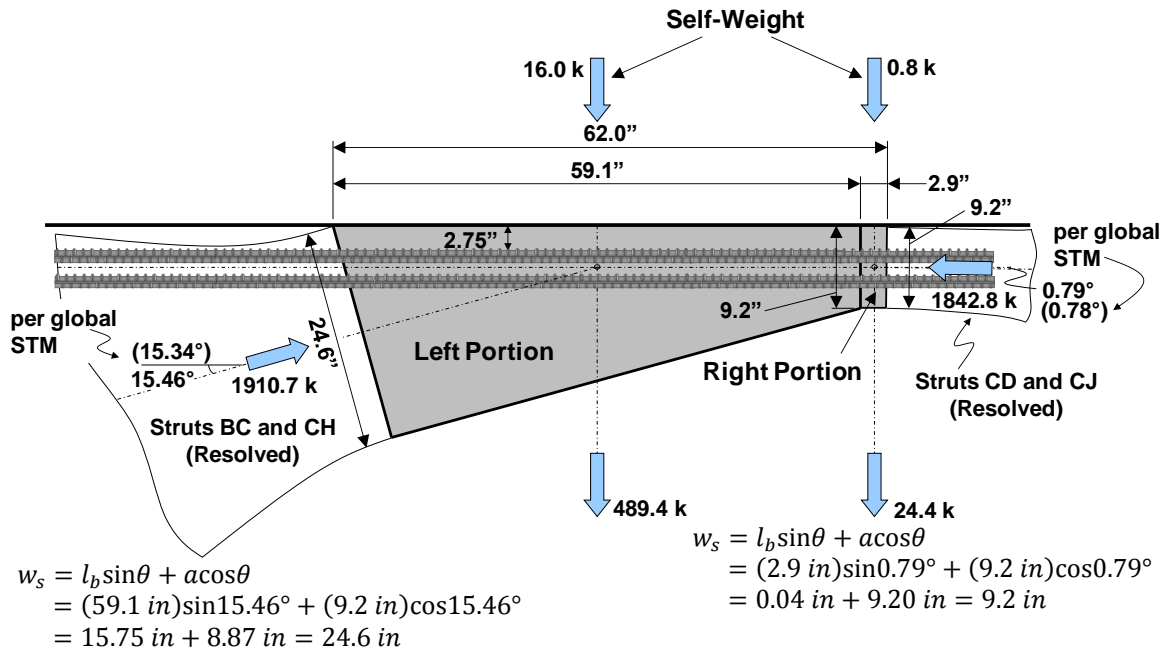


Figure 6.18: Node C (moment frame case)

Here, the length of the top face for each nodal subdivision is based upon the magnitude of the vertical component of each diagonal strut in relation to the net vertical force from Tie CI and the applied self-weight (analogous to the corresponding calculations for Node G). The length of each top face is:

$$\left[\frac{(1173.2 \text{ kip}) \sin(25.52^\circ)}{513.8 \text{ kip} + 16.7 \text{ kip}} \right] (62.0 \text{ in}) = 59.1 \text{ in}$$

$$\left[\frac{(57.3 \text{ kip}) \sin(26.05^\circ)}{513.8 \text{ kip} + 16.7 \text{ kip}} \right] (62.0 \text{ in}) = 2.9 \text{ in}$$

where 25.52° and 26.05° are the inclinations of Strut CH and Strut CJ with respect to the horizontal, 513.8 kips is the force in Tie CI, and 16.7 kips is the total self-weight load applied at Node C. The 1173.2-kip and 57.3-kip strut forces are shown in Figure 6.6. Please note that the right portion of the node is very small relative to the left portion.

Prior to revising the diagonal strut angles, adjacent struts are resolved to reduce the number of forces acting on the node. Struts BC and CH as well as Struts CD and CJ are resolved into two separate forces acting on the left and right portions of Node C, respectively. The force and angle (per global STM) of each resolved diagonal strut are shown in Figure 6.18. Revision of the resolved strut angles, per the subdivided nodal geometry, is outlined below. (Please refer to Node JJ of Example 1 in Section 4.4.4 for the determination of a similar nodal geometry.)

For the resolved strut on the left (resulting from the combination of Struts BC and CH):

$$\tan(15.34^\circ) = \frac{49.40 \text{ in}}{x} \quad x = 180.13 \text{ in}$$

$$\theta = \tan^{-1} \left[\frac{49.40 \text{ in}}{180.13 \text{ in} - \left(62.0 \text{ in}/2 - 59.1 \text{ in}/2 \right)} \right] = 15.46^\circ$$

For the resolved strut on the right (resulting from the combination of Struts CD and CJ):

$$\tan(0.78^\circ) = \frac{49.40 \text{ in}}{x} \quad x = 3616.96 \text{ in}$$

$$\theta = \tan^{-1} \left[\frac{49.40 \text{ in}}{3616.96 \text{ in} - (62.0 \text{ in}/2 - 2.9 \text{ in}/2)} \right] = 0.79^\circ$$

Node C – Left (CCT)

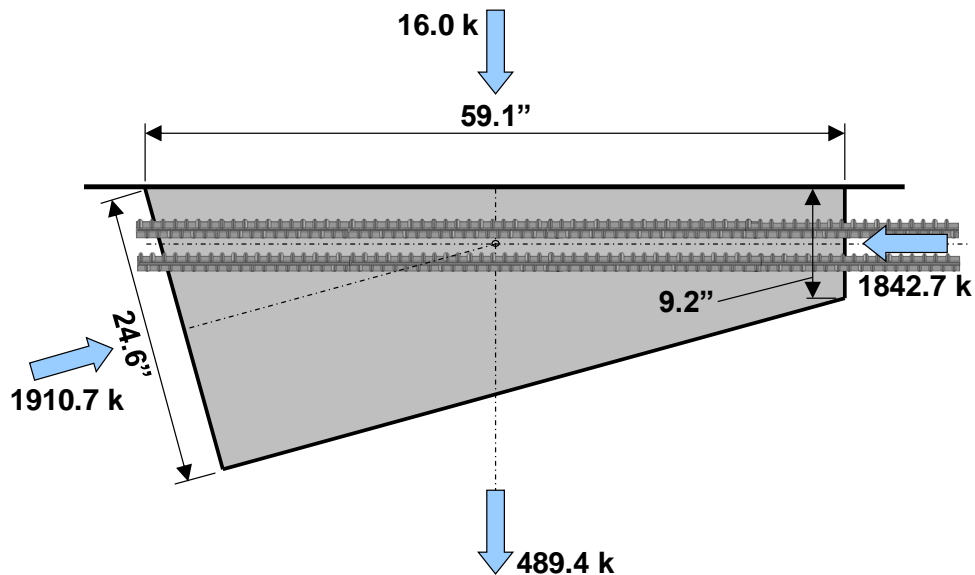


Figure 6.19: Node C – left nodal subdivision (moment frame case)

Node C has no bearing surface; therefore, no bearing check is necessary. Longitudinal reinforcement is provided along the top chord of the STM. If the reinforcement is detailed to develop its yield stress in compression, the longitudinal bars will contribute to the strength of the back face of Node C (refer to Section 2.9.7). Given the top chord reinforcement specified in Section 6.4.3 (4-#11 bars), the back face of Node C is checked and found to be understrength. Additional longitudinal bars are required to strengthen the node. A total of 15 bars must be provided to satisfy the back face check at Node C ($A_{st} = 15 * 1.56 \text{ in.}^2 = 23.4 \text{ in.}^2$).

Triaxial Confinement Factor: $m = 1$

BACK FACE

Factored Load: $F_u = 1842.7 \text{ kip}$

Efficiency: $\nu = 0.7$

Concrete Capacity: $f_{cu} = m \cdot \nu \cdot f'_c = (1)(0.7)(5.0 \text{ ksi}) = 3.5 \text{ ksi}$

$$\begin{aligned} \phi \cdot F_n &= (0.7)[(3.5 \text{ ksi})(9.2 \text{ in})(40 \text{ in}) + (23.4 \text{ in}^2)(60 \text{ ksi})] \\ &= 1884 \text{ kip} > 1842.7 \text{ kip} \quad \mathbf{OK} \end{aligned}$$

STRUT-TO-NODE INTERFACE

Factored Load: $F_u = 1910.7 \text{ kip}$

Efficiency: $\nu = 0.85 - 5.0 \text{ ksi} / 20 \text{ ksi} = 0.6$

\therefore Use $\nu = 0.6$

Concrete Capacity: $f_{cu} = m \cdot \nu \cdot f'_c = (1)(0.6)(5.0 \text{ ksi}) = 3.0 \text{ ksi}$

$$\begin{aligned} \phi \cdot F_n &= (0.7)(3.0 \text{ ksi})(24.6 \text{ in})(40 \text{ in}) \\ &= 2066 \text{ kip} > 1910.7 \text{ kip} \quad \mathbf{OK} \end{aligned}$$

Considering the number of bars required to adequately strengthen the back face, increasing the depth of the bent cap may be a feasible alternative solution. In the current design example, the geometry is kept consistent with that of the existing field structure.

Node C – Right (CCT)

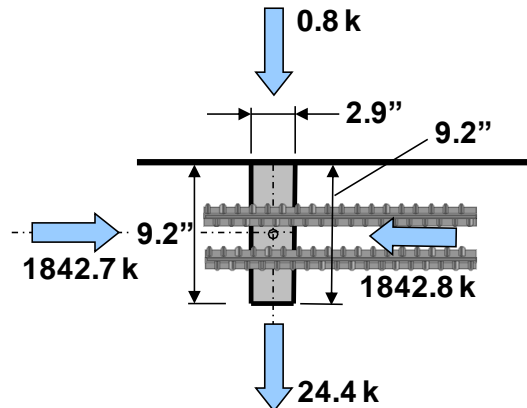


Figure 6.20: Node C – right nodal subdivision (moment frame case)

Triaxial Confinement Factor: $m = 1.0$

BACK FACE

Factored Load: $F_u = 1842.7 \text{ kip}$

This check is the same as the back face check for the left portion of Node C. →
OK

STRUT-TO-NODE INTERFACE

Factored Load: $F_u = 1842.8 \text{ kip}$

Efficiency: $\nu = 0.85 - 5.0 \text{ ksi} / 20 \text{ ksi} = 0.6$

∴ Use $\nu = 0.6$

Concrete Capacity: $f_{cu} = m \cdot \nu \cdot f'_c = (1)(0.6)(5.0 \text{ ksi}) = 3.0 \text{ ksi}$
 $\phi \cdot F_n = (0.7)(3.0 \text{ ksi})(9.2 \text{ in})(40 \text{ in})$
 $= 773 \text{ kip} < 1842.8 \text{ kip}$

The strut-to-node interface calculations indicate that the node does not have adequate strength to resist the resolved strut force. However, the inclination of the resolved strut is negligible (nearly horizontal), and the strut-to-node interface check is virtually equivalent to the back face check of Node C. The node, therefore, has adequate strength to resist the applied forces.

Node I

Node I is located directly below Beam Line 1. Referring to the global STM in Figure 6.6, only ties intersect at Node I. Nodal checks are therefore unnecessary since no compressive forces act on the node. The strength of the bearings along Beam Line 1 must nonetheless be checked. Bearing calculations are performed as part of the local STM evaluation.

Node K (CTT)

Node K, located below Beam Line 3, is shown in Figure 6.21. The length of the bottom face of the node is conservatively assumed to be the dimension, W, of the bearing pad. Alternatively, the designer may wish to reduce the nodal stresses by accounting for the lateral spread of the applied beam load through the ledge depth (refer back to Figure

6.11). Considering the spread of the force would increase the assumed length of the bottom face. Such an approach was not necessary to satisfy the nodal strength checks in this example. The forces and strut angle displayed in Figure 6.21 are defined in relation to the global STM.

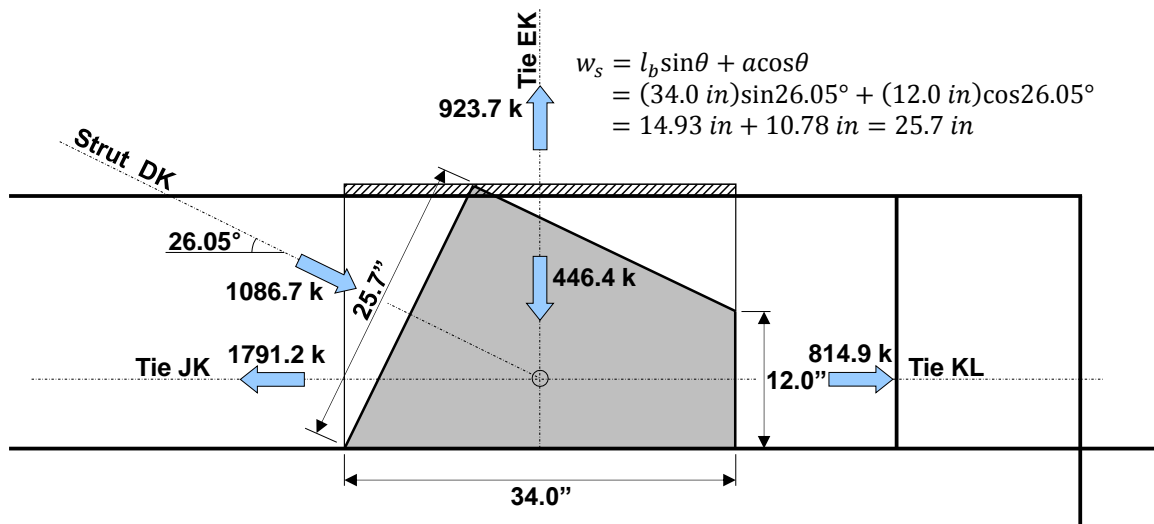


Figure 6.21: Node K (moment frame case)

Despite the presence of a bearing pad on the ledge, a bearing force does not act directly on the node, and the triaxial confinement factor cannot be applied to Node K. Moreover, the node illustrated in Figure 6.21 is assumed to be confined within the stem of the inverted-T and not the ledges. Please note the use of b_w , or 40 inches, for the width of the strut-to-node interface in the calculations below.

The back face of Node K does not need to be checked because the bonding stresses from the longitudinal reinforcement do not need to be applied as a direct force (refer to Section 2.9.8).

Triaxial Confinement Factor: $m = 1.0$

STRUT-TO-NODE INTERFACE

Factored Load: $F_u = 1086.7 \text{ kip}$

Efficiency: $\nu = 0.85 - 5.0 \text{ ksi} / 20 \text{ ksi} = 0.6$

\therefore Use $\nu = 0.6$

$$\begin{aligned}
\text{Concrete Capacity: } f_{cu} &= m \cdot v \cdot f'_c = (1)(0.6)(5.0 \text{ ksi}) = 3.0 \text{ ksi} \\
\varphi \cdot F_n &= (0.7)(3.0 \text{ ksi})(25.7 \text{ in})(40 \text{ in}) \\
&= 2159 \text{ kip} > 1086.7 \text{ kip } \mathbf{OK}
\end{aligned}$$

Therefore, the strength of Node K is sufficient to resist the applied forces.

Nodes A and F (CTT – Curved-Bar Nodes)

Nodes A and F of the global STM in Figure 6.6 are curved-bar nodes. A curved-bar node occurs at a frame corner where a diagonal strut is equilibrated by two ties that represent curved, continuous reinforcing bars (Klein, 2008, 2011). The method recommended by Klein (2008), also used in Section 5.4.5 of Example 2, will be implemented in the design of Nodes A and F.

To ease construction, the specified reinforcement details will be the same for Nodes A and F. The orientation (θ_c) of the diagonal strut at each node (Struts AG and FL) is compared to that of the companion node to determine which node controls the design. The angle θ_c is defined as the smaller of the two angles between the diagonal strut and the ties extending from a curved-bar node. The value of θ_c for Node F is smaller than the value of θ_c for Node A. Node F, therefore, controls the design of the curved-bar nodes. A steeper strut leads to a greater imbalance in the tie forces, necessitating a larger bend radius, r_b , to develop the unbalanced force along the bend region of the bars. The value of θ_c for Node F, or the angle between Strut FL and Tie FF', is found to be 34.50° and is shown in Figure 6.22. The revised orientation of Strut FL due to the subdivision of Node G is considered when determining the value of θ_c .

The design of a curved-bar node requires two criteria to be satisfied. First, the nodal region must have sufficient capacity to resist the applied compressive stresses. Satisfying the following expression ensures the node has adequate strength:

$$r_b \geq \frac{A_{st} f_y}{v b f'_c} \quad (6.1)$$

The concrete efficiency factor, v , within the expression corresponds to the back face of a CTT node. For a CTT node with a concrete strength, f'_c , of 5.0 ksi, the value of v is 0.6.

For the given load case, 5-#11 bars should be bent around the frame corner (a continuous segment of reinforcement) to carry the forces within the top chord and exterior column ties ($A_{st} = 5 * 1.56 \text{ in.}^2 = 7.8 \text{ in.}^2$). The corresponding bend radius must be at least 3.90 inches to ensure that the stresses acting at the node are within the permissible limits.

$$r_b \geq \frac{A_{st} f_y}{\nu b f'_c} = \frac{(7.8 \text{ in}^2)(60 \text{ ksi})}{(0.6)(40 \text{ in})(5.0 \text{ ksi})} = 3.90 \text{ in}$$

This value must be compared to the minimum bend radius for a #11 bar according to Article 5.10.2.3 of AASHTO LRFD (2010):

$$r_b \geq \frac{1}{2}(8d_b) = 4(1.41 \text{ in}) = 5.64 \text{ in} > 3.90 \text{ in}$$

This minimum bend radius is greater than the radius required to resist the applied compressive stresses.

To satisfy the second design criterion, the bend radius of the bars must be large enough to allow the difference in the tie forces to be developed along the bend region. The following expression ensures that the length of the bend is sufficient for development of the unbalanced force (Klein, 2008):

$$r_b \geq \frac{2l_d(1 - \tan\theta_c)}{\pi} - \frac{d_b}{2} \tag{6.2}$$

The development length, l_d , of straight #11 bars located along the top of the bent cap should be considered and is calculated as follows:

$$l_d = \frac{1.25A_b f_y}{\sqrt{f'_c}} \cdot 1.4 = \frac{1.25(1.56 \text{ in}^2)(60 \text{ ksi})}{\sqrt{5.0 \text{ ksi}}} \cdot 1.4 = 73.25 \text{ in}$$

Therefore, the minimum radius necessary to allow the bond stresses to be developed along the circumference of the bend is:

$$r_b \geq \frac{2l_d(1 - \tan\theta_c)}{\pi} - \frac{d_b}{2} = \frac{2(73.25 \text{ in}^2)(1 - \tan 34.50^\circ)}{\pi} - \frac{1.41 \text{ in}}{2} = 13.88 \text{ in}$$

This minimum bend radius required to develop the bond stresses supersedes the minimum bend radius necessary to satisfy the nodal stress limit.

Klein (2008) also recommends that a clear side cover of at least $2d_b$ be provided to the bent bars of the curved-bar node in order to avoid side splitting. Therefore, a clear cover of $2(1.41 \text{ in.}) = 2.82 \text{ in.}$ is needed. If the specified clear side cover is less than this value, Klein (2008) states the calculated bend radius should be multiplied “by a factor of 2 bar diameters divided by the specified clear cover.” Since the clear cover to the bent bars is only 2.75 inches (refer to the final reinforcement details in Figure 6.27), the bend radius, r_b , should be at least:

$$r_b \geq (13.88 \text{ in}) \left(\frac{2.82 \text{ in}}{2.75 \text{ in}} \right) = 14.23 \text{ in}$$

A bend radius greater than 14.23 inches will be used at both Nodes A and F. The bend radius is measured as shown in Figure 6.22. The bars along the inside of the frame corner in this figure are necessary to satisfy the back face strength checks of the nodes along the top chord of the STM and are also needed to limit the reinforcement stress to 22 ksi (see Section 6.4.9). As shown in Figure 6.22, these bars are terminated before entering the column and are not considered as part of the curved-bar node. If the inner layer of bars was part of the curved-bar node design, the bend radius would be measured from that layer of reinforcement.

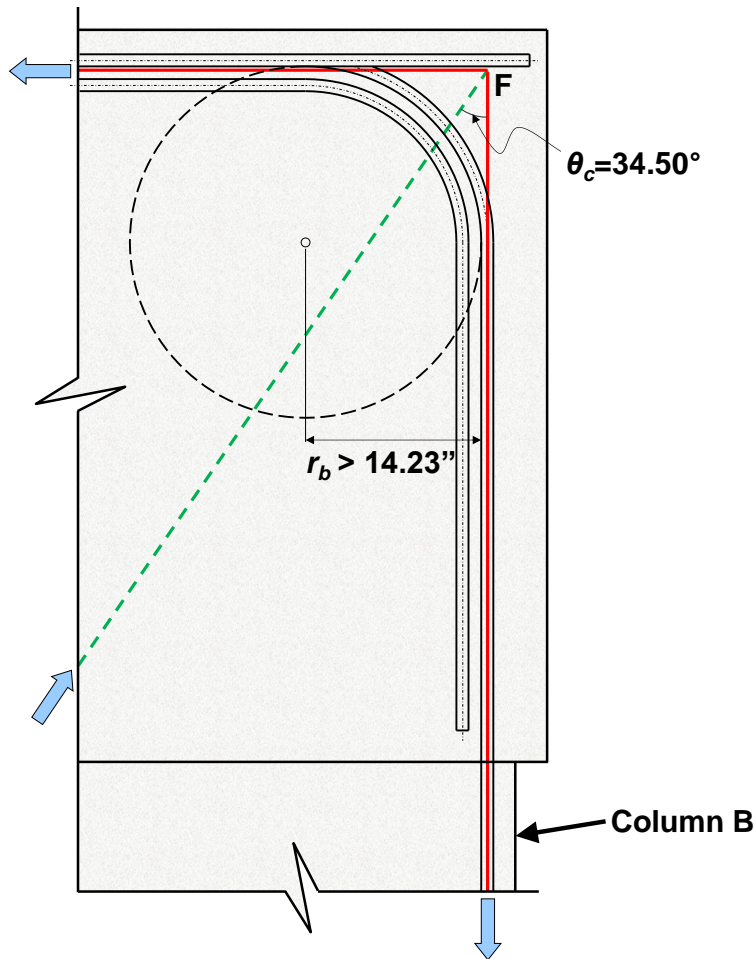


Figure 6.22: Bend radius, r_b , at Node F (moment frame case)

The required radius is larger than that of standard mandrels. Specifying such a bend radius may therefore result in fabrication issues. Proper detailing of the curved-bar nodes is required, however, if moment connections between the bent cap and the columns are desired.

Nodes C_s and F_s of the Local STM (CCT)

Nodes C_s and F_s at Beam Line 1 are the most critical nodes of the three local STMs developed in Section 6.4.2 (refer to Figure 6.10). Since Nodes C_s and F_s are mirror images of each other, only one needs to be checked. An illustration of Node C_s is given in Figure 6.23. The length of the bearing face is taken as the dimension of the

bearing pad, or 8.0 inches, and the height of the back face is double the distance from the top surface of the ledge to the top horizontal portion of the ledge stirrup. The width of the node into the page (refer to Figure 6.23) is assumed to be the length of the bearing pad, W , or 34.0 inches.

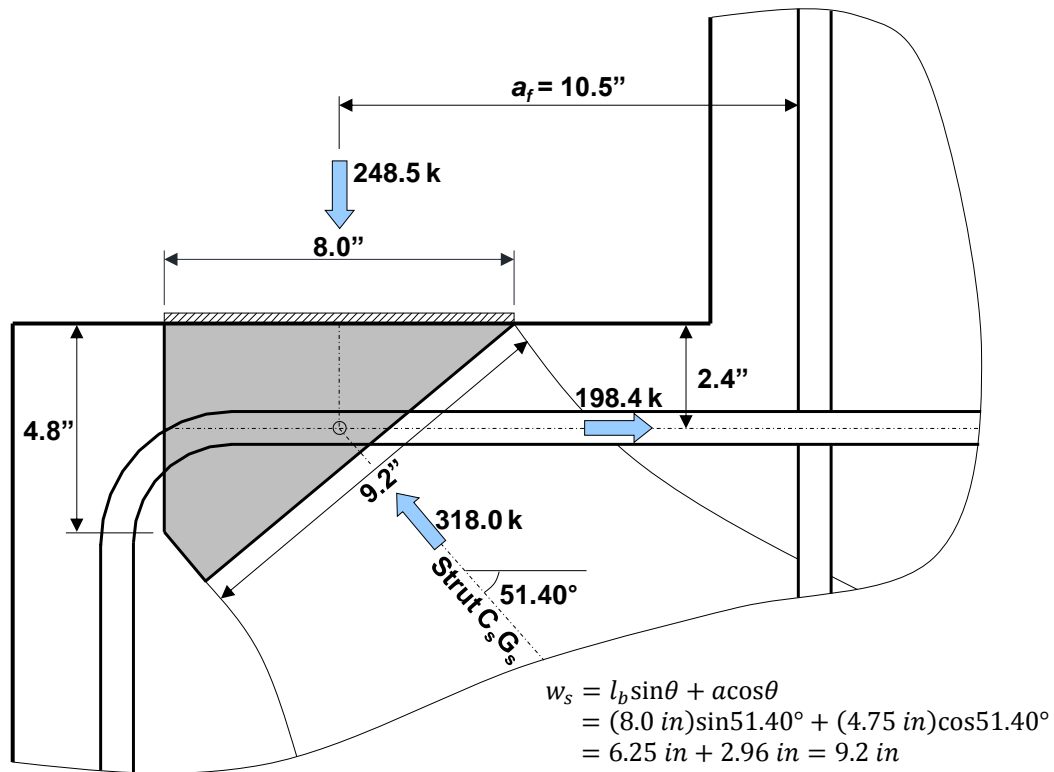


Figure 6.23: Node C_s of local STM at Beam Line 1 (moment frame case)

To simplify the calculations, the triaxial confinement factor, m , is conservatively taken as 1.0. All faces of Node C_s have sufficient strength without consideration given to the effects of triaxial confinement. The bearing demand is equivalent to the factored load applied by one trapezoidal box beam (refer to Figure 6.2). The largest bearing stresses on the bent cap occur at Beam Line 1.

Triaxial Confinement Factor: $m = 1$

BEARING FACE

$$\begin{aligned}\text{Factored Load:} & F_u = 248.5 \text{ kip} \\ \text{Efficiency:} & \nu = 0.7 \\ \text{Concrete Capacity:} & f_{cu} = m \cdot \nu \cdot f'_c = (1)(0.7)(5.0 \text{ ksi}) = 3.5 \text{ ksi} \\ & \varphi \cdot F_n = (0.7)(3.5 \text{ ksi})(8 \text{ in})(34 \text{ in}) \\ & = 666 \text{ kip} > 248.5 \text{ kip} \text{ OK}\end{aligned}$$

No direct compressive force acts on the back face; therefore, no strength check is necessary.

STRUT-TO-NODE INTERFACE

$$\begin{aligned}\text{Factored Load:} & F_u = 318.0 \text{ kip} \\ \text{Efficiency:} & \nu = 0.85 - \frac{5.0 \text{ ksi}}{20 \text{ ksi}} = 0.6 \\ & \therefore \text{Use } \nu = 0.6 \\ \text{Concrete Capacity:} & f_{cu} = m \cdot \nu \cdot f'_c = (1)(0.6)(5.0 \text{ ksi}) = 3.0 \text{ ksi} \\ & \varphi \cdot F_n = (0.7)(3.0 \text{ ksi})(9.2 \text{ in})(34 \text{ in}) \\ & = 657 \text{ kip} > 318.0 \text{ kip} \text{ OK}\end{aligned}$$

Therefore, the strengths of Nodes C_s and F_s are sufficient to resist the applied forces.

Other Nodes

Nodes D, E and J of the global STM shown in Figure 6.6 can be checked using the methods previously presented. All of the nodes have adequate strength to resist the forces imposed by the given load case. Nodes B and H in Figure 6.6 are smeared nodes; therefore, no strength checks are necessary. Referring to the local STM of Figure 6.9, Nodes G_s and H_s are also smeared nodes since they are interior nodes that have no defined geometry. By observation, the struts entering these nodal regions have adequate space over which to spread and are not critical.

6.4.7 Step 7: Proportion Crack Control Reinforcement

Requirements for minimum crack control reinforcement are now compared to the vertical ties detailed in Section 6.4.4. Using two-legged #6 stirrups, the required spacing

of the vertical reinforcement is calculated as follows, where b_w is the width of the stem of the inverted-T bent cap:

$$A_v = 0.003b_w s_v \quad \rightarrow \quad \begin{aligned} 2(0.44 \text{ in}^2) &= 0.003(40 \text{ in})s_v \\ s_v &= 7.3 \text{ in} \end{aligned}$$

Please recall that the stirrup spacing specified for Tie CI (at Beam Line 1) will be used along the entire length of the ledge with the exception of the region where a closer spacing is required for Tie EK (at Beam Line 3). The stirrups provided along the ledge will therefore satisfy the minimum crack control reinforcement provisions. The required crack control reinforcement, however, governs the stirrup spacing over the width of Tie BH and must also be provided over the remaining length of the bent cap (e.g. above the columns).

The required spacing of #6 bars provided as skin reinforcement parallel to the longitudinal axis of the bent cap is:

$$A_h = 0.003b_w s_h \quad \rightarrow \quad \begin{aligned} 2(0.44 \text{ in}^2) &= 0.003(40 \text{ in})s_h \\ s_h &= 7.3 \text{ in} \end{aligned}$$

The required skin reinforcement is used along the length of the bent cap.

Summary

- Use 2 legs of #6 stirrups with spacing less than 5.7 in. along the length of the ledge except for Tie EK
- Use 2 legs of double #6 stirrups with spacing less than 6.4 in. for Tie EK
- Pair the ledge stirrups with the stirrups in the stem along the entire length of the ledge
- Use 2 legs of #6 stirrups with spacing less than 7.3 in. along the remainder of the bent cap
- Use #6 bars with spacing less than 7.3 in. as horizontal skin reinforcement (Final reinforcement details are provided in Figures 6.26 and 6.27)

6.4.8 Step 8: Provide Necessary Anchorage for Ties

The reinforcement along the top and bottom chords of the global STM must be properly anchored at either end of the bent cap in accordance with Article 5.6.3.4.2 of the proposed STM specifications in Chapter 3 and Article 5.11.2 of AASHTO LRFD (2010). Continuity of the reinforcement over the bent cap length will be provided via longitudinal splices. Proper anchorage of the horizontal ledge reinforcement (proportioned via the local STM) must also be ensured.

The bottom chord reinforcement of the inverted-T must be fully developed at Nodes G and L. If straight bars are used, the required development length is:

$$l_d = \frac{1.25A_b f_y}{\sqrt{f'_c}} = \frac{1.25(1.56 \text{ in}^2)(60 \text{ ksi})}{\sqrt{5.0 \text{ ksi}}} = 52.3 \text{ in}$$

Adequate space is available for straight development between the interior face of each column and the exterior layer of longitudinal column reinforcement. The available length at Node G is illustrated in Figure 6.24.

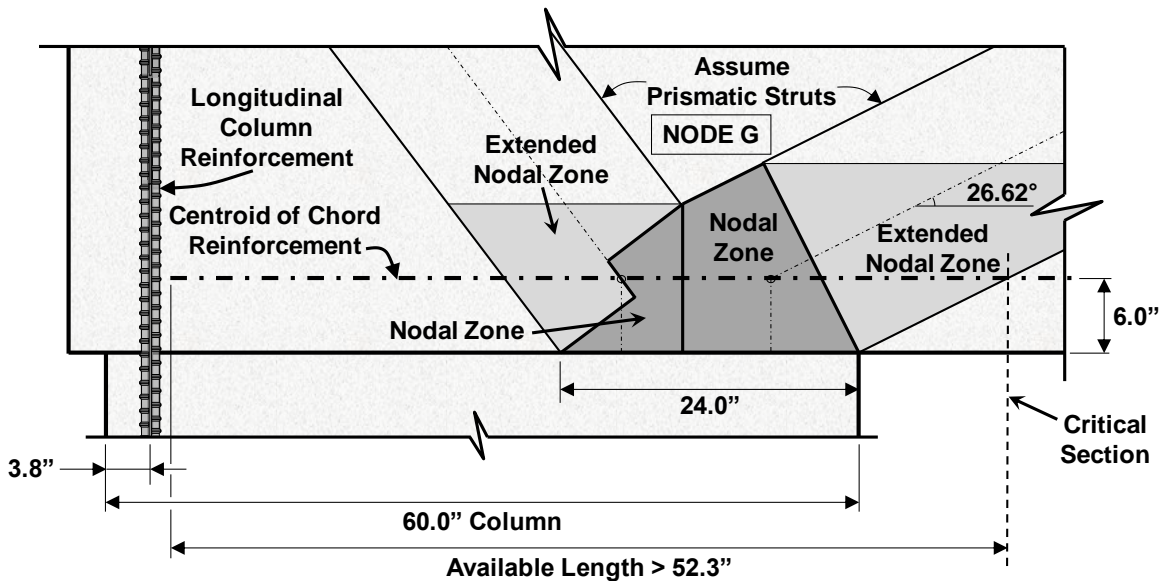


Figure 6.24: Anchorage of bottom chord reinforcement at Node G

Proper development of the longitudinal tie reinforcement at Nodes A and F was ensured during design of the curved-bar nodes. The bars along the top chord of the bent cap provided to satisfy the 22-ksi stress limit discussed in Section 6.4.9 (those provided in excess of the 5-#11 bars necessary to satisfy tie requirements) are anchored by providing a simple standard hook.

Lastly, anchorage of the ledge reinforcement (Tie $C_s F_s$ of the local STMs) must be checked. The top horizontal portion of the ledge reinforcement should be terminated in a 90-degree hook. The available development length at Nodes C_s and F_s of the local STM is measured from the location where the centroid of the bar enters the extended nodal zone (Figure 6.25).

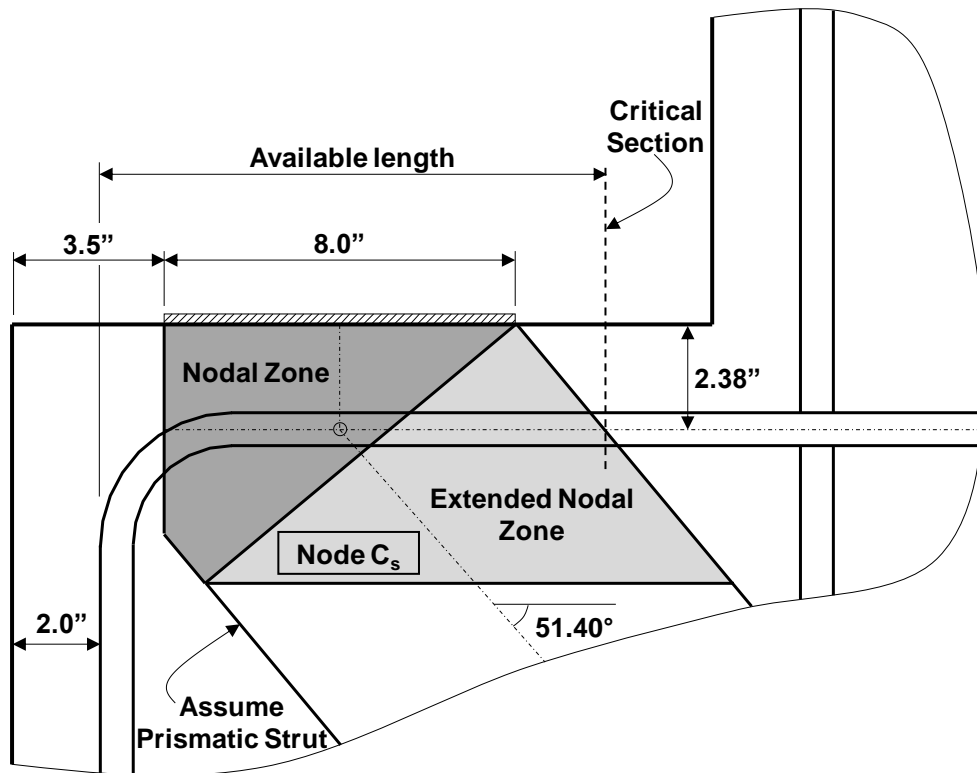


Figure 6.25: Anchorage of ledge reinforcement at Node C_s

The available length for the ledge reinforcement is:

$$\text{Available length} = 3.5 \text{ in} + 8.0 \text{ in} + \frac{2.38 \text{ in}}{\tan 51.40^\circ} - 2 \text{ in} = 11.4 \text{ in}$$

All the values within this calculation are shown in Figure 6.25. The required development length for a 90-degree hook on a #6 bar is:

$$l_{dh} = \frac{38.0d_b}{\sqrt{f'_c}} \cdot 0.7 = \frac{38.0(0.75 \text{ in})}{\sqrt{5.0 \text{ ksi}}} \cdot 0.7 = 8.9 \text{ in} < 11.4 \text{ in} \text{ OK}$$

Sufficient development length is available, and the reinforcement comprising Tie C_sF_s (of all three local STMs) is therefore adequately anchored with a 90-degree hook.

6.4.9 Step 9: Perform Other Necessary Checks

When designing inverted-T beams, the designer should ensure that all relevant provisions in AASHTO LRFD (2010) are satisfied. TxDOT's *Bridge Design Manual - LRFD* (2009) also includes other checks that must be considered.

The critical design provisions include those in Article 5.13.2.5 of AASHTO LRFD (2010) for beam ledges and those for interface shear transfer, distribution and spacing of reinforcement, detailing requirements for deep beams, and so forth. None of these provisions control the design of the bent cap featured within this example.

To minimize cracking, TxDOT requires that the longitudinal reinforcement stress be limited to 22 ksi when the AASHTO LRFD Service I load case is applied with dead load only. This requirement is satisfied if the bars needed for the STM design provisions are extended to the ends of the bent cap and properly anchored as shown in the final reinforcement details of Figure 6.26.

Lastly, a splice should be specified to provide continuity between the column longitudinal tension steel and the top chord reinforcement of the bent cap.

6.4.10 Step 10: Perform Shear Serviceability Check

To determine the likelihood of diagonal crack formation, the service level shear can be compared to the estimated diagonal cracking strength of the concrete. The

TxDOT Project 0-5253 expression for estimation of the diagonal cracking strength is repeated here for convenience (refer to Section 2.12):

$$V_{cr} = \left[6.5 - 3 \left(\frac{a}{d} \right) \right] \sqrt{f'_c} b_w d \quad (6.3)$$

but not greater than $5\sqrt{f'_c} b_w d$ nor less than $2\sqrt{f'_c} b_w d$

where:

- a = shear span (in.)
- d = effective depth of the member (in.)
- f'_c = specified compressive strength of concrete (psi)
- b_w = width of member's web (in.)

The AASHTO LRFD (2010) Service I load case is applied to the frame shown in Figure 6.7, assuming the self-weight is distributed along the length of the bent cap. An elastic analysis reveals that the maximum shear force occurs near the right end of the cap; the service level shear force at the interior face of the right column is 675.9 kips. The risk of service crack formation within the region between Beam Line 3 and the right column (Column B) should be checked. Considering the likelihood of diagonal cracking due to the stresses within Strut EL, the shear span a is taken as the horizontal distance between Beam Line 3 and Node L, or 59.9 inches. The effective depth, d , is taken as the distance from the bottom of the bent cap to the centroid of the top chord reinforcement, or 55.4 inches. The estimated diagonal cracking strength is:

$$\begin{aligned} V_{cr} &= \left[6.5 - 3 \left(\frac{59.9 \text{ in}}{55.4 \text{ in}} \right) \right] (\sqrt{5000 \text{ psi}}) (40 \text{ in}) (55.4 \text{ in}) \\ &= 510 \text{ kip} < 675.9 \text{ kip } \mathbf{NG} - \text{Expect diagonal cracks} \end{aligned}$$

This value is within the $5\sqrt{f'_c} b_w d$ and $2\sqrt{f'_c} b_w d$ limits. The check alerts the designer that diagonal cracking should be expected within the region near Column B.

Modifications to the bent cap geometry or the concrete strength can reduce the risk of service crack formation (refer to Section 2.12).

Another critical region of the bent cap is between the left column (Column A) and Beam Line 1. The maximum service shear force in this region occurs at the interior face of the left column and is equal to 388.6 kips. Due to the long shear span, a , between the applied beam load and the supporting column, the $2\sqrt{f'_c}b_wd$ limit controls, and the value of V_{cr} is:

$$\begin{aligned}V_{cr} &= 2\sqrt{f'_c}b_wd = 2\sqrt{5000 \text{ psi}}(40 \text{ in})(55.4 \text{ in}) \\ &= 313 \text{ kip} < 388.6 \text{ kip } \mathbf{NG} - \text{Expect diagonal cracks}\end{aligned}$$

The shear serviceability checks reveals that the designer should consider the risk of diagonal crack formation within both critical shear spans when full service loads are applied. This concern is further addressed for the inverted-T bent cap in Sections 7.6 and 7.7 of Example 3b.

The designer may wish to use the shear serviceability check during the preliminary design phase to initially size the structural member, ensuring that the chosen geometry limits the risk of diagonal cracking.

6.5 REINFORCEMENT LAYOUT

The reinforcement details for the load case considered in this design example are presented in Figures 6.26 and 6.27. Any reinforcement details not previously described within the example are consistent with standard TxDOT practice.

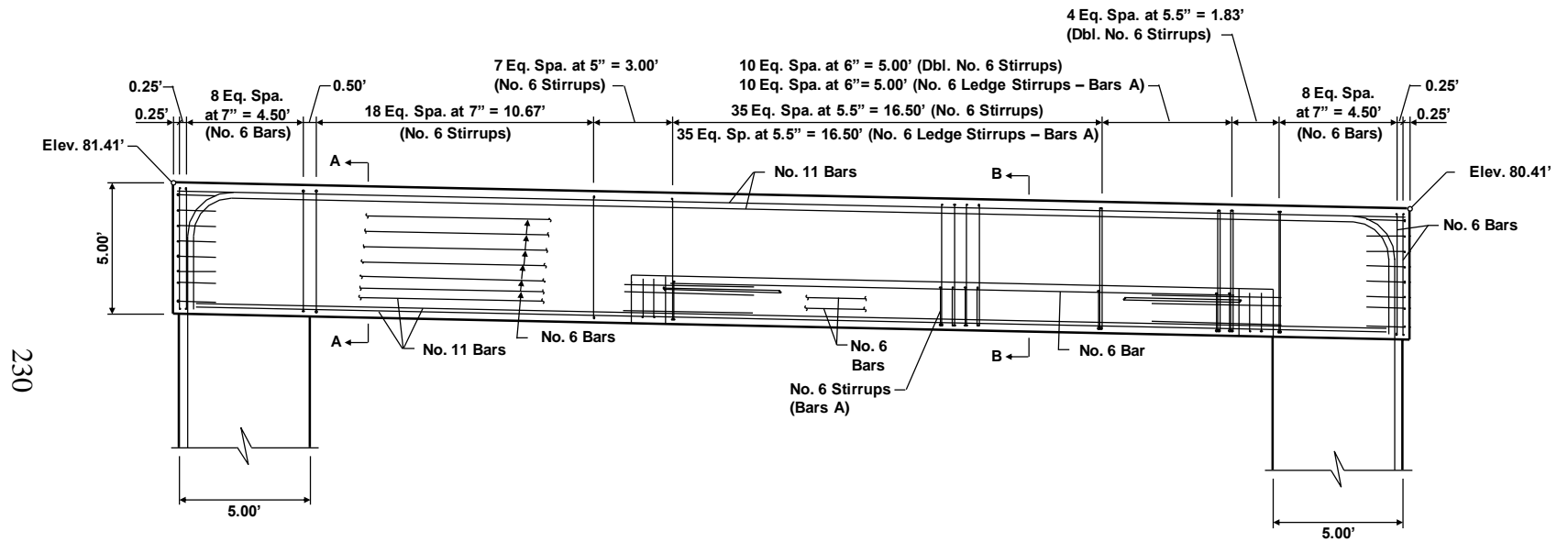
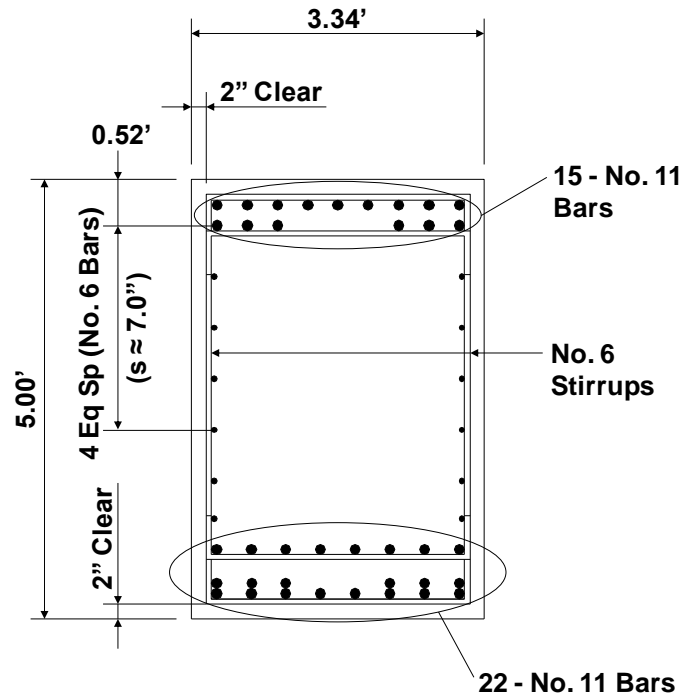
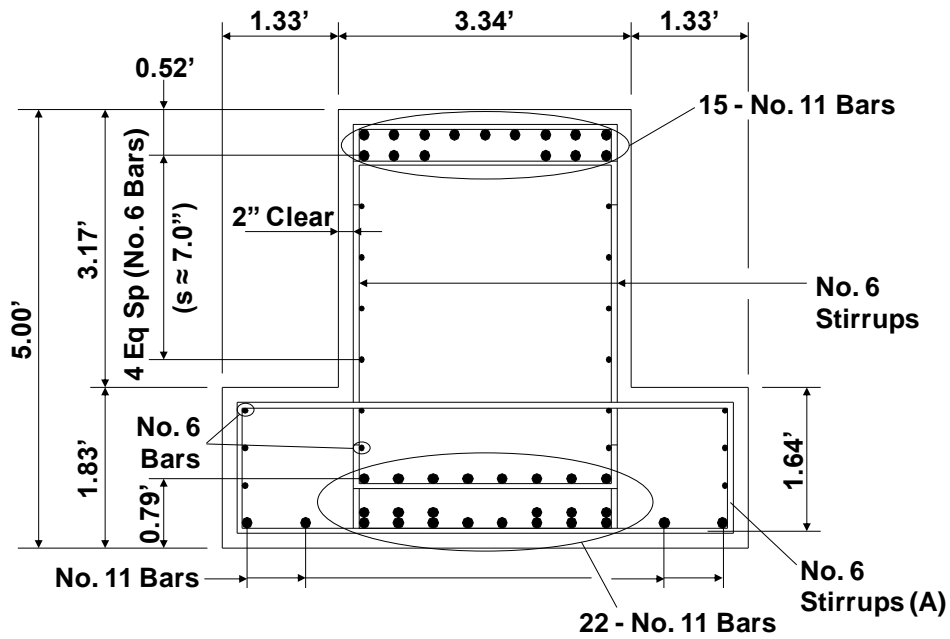


Figure 6.26: Reinforcement details – elevation (design per proposed STM specifications – moment frame case)



Section A-A



Section B-B

Figure 6.27: Reinforcement details – cross-sections (design per proposed STM specifications – moment frame case)

6.6 SUMMARY

The design of an inverted-T straddle bent cap was completed in accordance with the strut-and-tie model specifications of Chapter 3 and all relevant provisions of AASHTO LRFD (2010) and TxDOT's *Bridge Design Manual - LRFD* (2009). The substructure was designed to behave as a moment frame. The defining features and challenges of this design example are listed below:

- Modeling frame corners as full moment connections
- Determining D-region/B-region boundary forces from a moment frame analysis in order to calculate the member forces of the STM
- Developing local, or sectional, STMs to design the ledge of an inverted-T bent cap (essentially developing a three-dimensional STM)
- Detailing transverse ledge reinforcement using local STMs
- Detailing hanger reinforcement along an inverted-T ledge to transfer applied superstructure loads to the top chord of the global STM
- Designing curved-bar nodes at the outside of the frame corners (i.e. determining the required bend radius of the longitudinal bars)

Example 3b in Chapter 7 presents the design of the same inverted-T straddle bent cap assuming the cap is simply supported at the columns. The existing field structure, designed in accordance with the sectional design procedure of the AASHTO LRFD provisions, has experienced significant diagonal cracking. The observed serviceability behavior of the in-service bent cap will be discussed in Section 7.7.

Chapter 7. Example 3b: Inverted-T Straddle Bent Cap (Simply Supported)

7.1 SYNOPSIS

The inverted-T straddle bent was treated as a moment frame in Example 3a of Chapter 6. In order to illustrate the influence of the boundary conditions, the inverted-T bent cap is here assumed to be simply supported at each column. The basic principles of the previous example are followed here. Nevertheless, the geometry of the STM, its member forces, and the resulting reinforcement layout are significantly different than those of Example 3a.

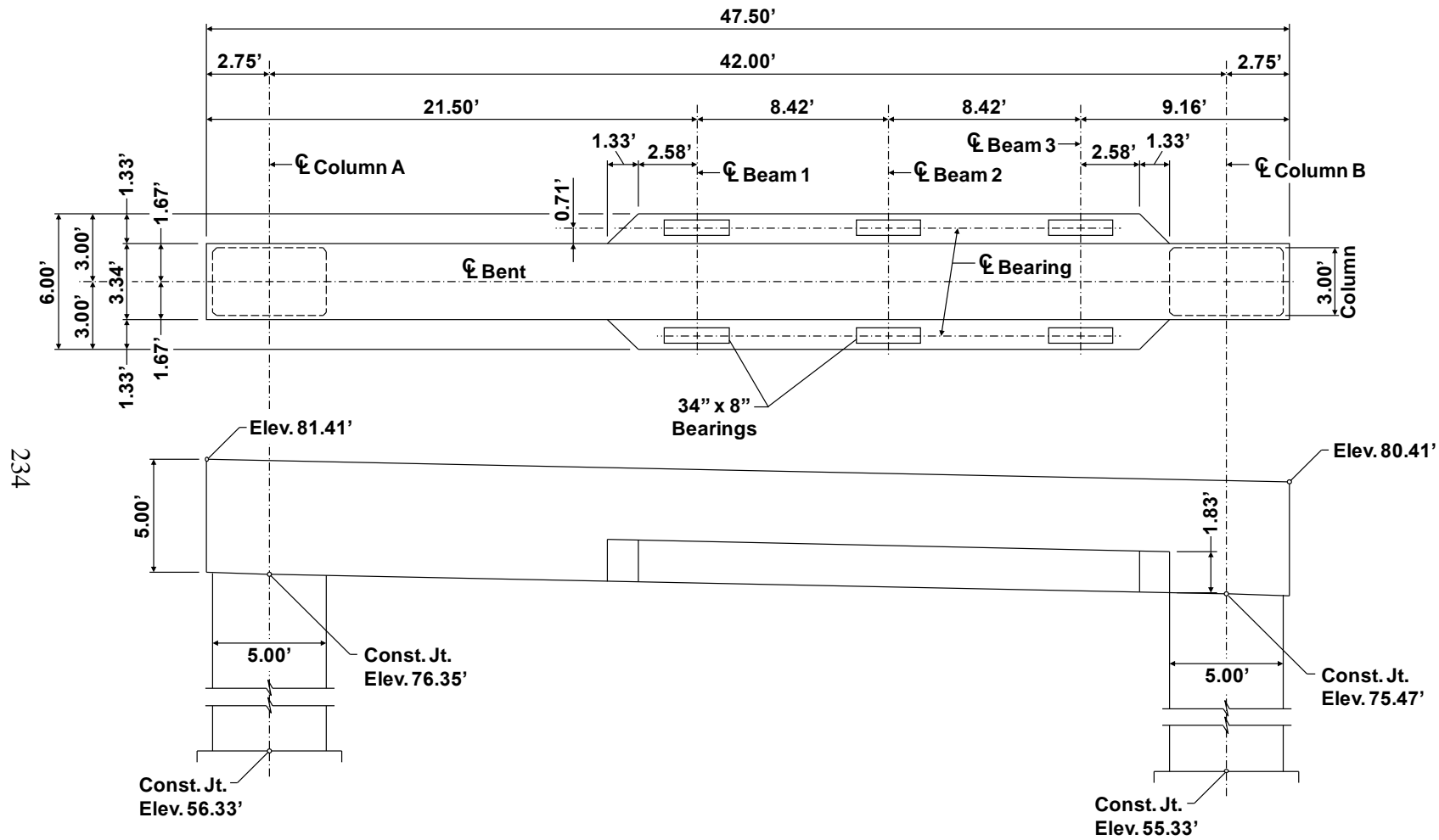
In the latter portion of this example, the moment frame (Example 3a) and simply supported (Example 3b) bent cap designs are compared with each other. The inverted-T bent cap is an existing field structure originally designed using sectional methods. The serviceability behavior of the existing bent cap is therefore discussed, and design improvements offered by the STM procedure and shear serviceability check are highlighted.

The reader is encouraged to review Example 3a prior to studying the current design example. Example 3a includes full disclosure of all details, some of which are not repeated here for the sake of brevity.

7.2 DESIGN TASK

7.2.1 Bent Cap Geometry

The geometry of the inverted-T straddle bent cap is described in Section 6.2.1 of Example 3a. Elevation and plan views of the bent cap are presented again in Figure 7.1 for convenience. The negligible cross slope is once again ignored during the design procedure.



234

Figure 7.1: Plan and elevation views of inverted-T bent cap

7.2.2 Determine the Loads

The load case for this design example is presented in Section 6.2.2 of Example 3a. The factored superstructure loads are repeated in Figure 7.2 for convenience. The tributary self-weight is once again distributed among the nodes of the STM. The global STM for the simply supported member (Figure 7.3) contains more nodes than that of the previous example, and the self-weight is distributed accordingly.

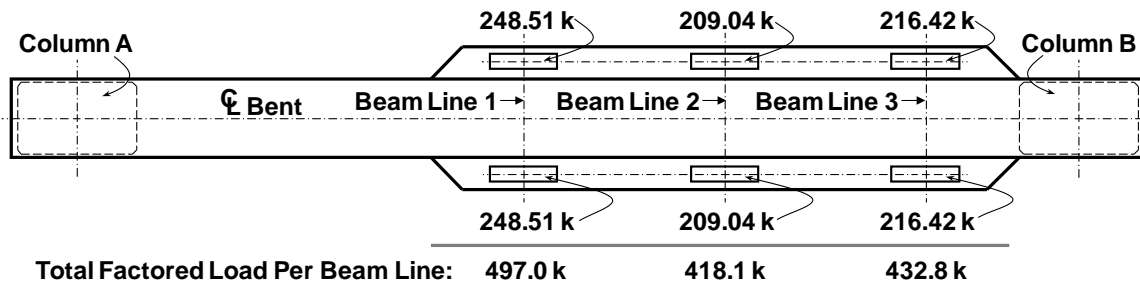


Figure 7.2: Factored superstructure loads acting on the bent cap

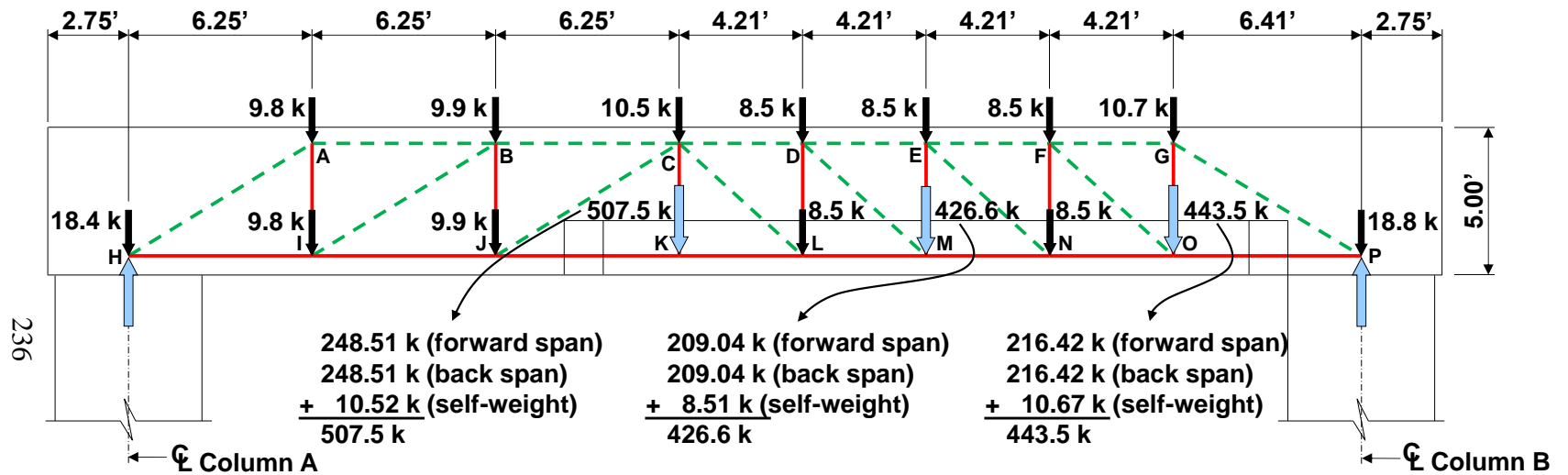


Figure 7.3: Factored loads acting on the global strut-and-tie model for the inverted-T bent cap (simply supported case)

7.2.3 Determine the Bearing Areas

Each of the trapezoidal box beams is supported on a bearing pad that is 34 inches by 8 inches. All of the bearing pads rest on concrete bearing seats, and the effect of the bearing seats on the stress applied to the top face of the bent cap is conservatively neglected. The size of the bearing pads does not control the design of the bent cap.

7.2.4 Material Properties

- Concrete: $f'_c = 5.0 \text{ ksi}$
- Reinforcement: $f_y = 60 \text{ ksi}$

The specified concrete compressive strength, f'_c , of the existing field structure is 3.6 ksi. An increased concrete strength is needed, however, to satisfy the nodal strength checks of Section 7.4.6. A strength of 5.0 ksi is consistent with that used in Example 3a, facilitating comparison of the two STM designs.

7.3 DESIGN PROCEDURE

Design of the simply supported inverted-T is analogous to that of the continuous inverted-T straddle bent with one exception. An overall analysis of the structural member is not necessary since the cap is simply supported. Analysis of the simply supported truss model provides the STM member forces as well as the column reactions. The steps for the design procedure are provided below:

- Step 1: Develop global strut-and-tie model
- Step 2: Develop local strut-and-tie models
- Step 3: Proportion longitudinal ties
- Step 4: Proportion hanger reinforcement/vertical ties
- Step 5: Proportion ledge reinforcement
- Step 6: Perform nodal strength checks
- Step 7: Proportion crack control reinforcement

- Step 8: Provide necessary anchorage for ties
- Step 9: Perform other necessary checks
- Step 10: Perform shear serviceability check

7.4 DESIGN CALCULATIONS

7.4.1 Step 1: Develop Global Strut-and-Tie Model

The global STM for the simply supported inverted-T bent cap is shown in Figure 7.4. The connection between each column and the bent cap is assumed to transfer vertical and horizontal forces only. In the absence of lateral forces, only a vertical reaction force exists at the centerline of each column. Bearing forces at the cap-to-column connection are therefore resisted by a single node, located above each column along the column centerline.

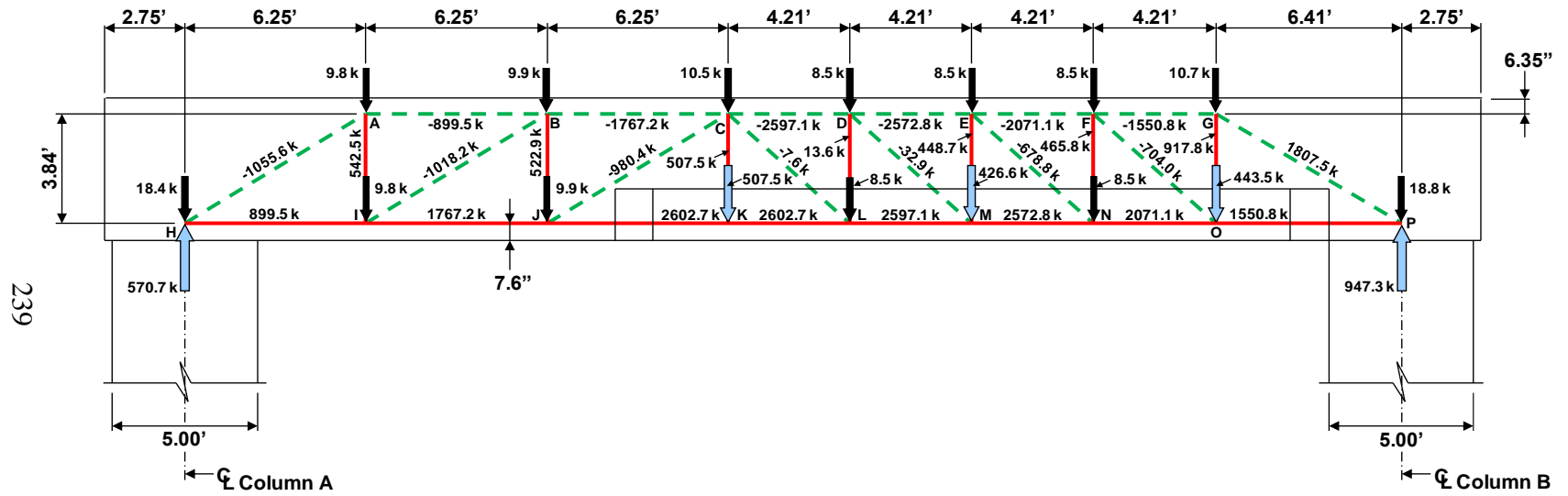


Figure 7.4: Global strut-and-tie model for the inverted-T bent cap (simply supported case)

Through a series of design iterations, the bottom chord of the STM is placed at the centroid of the longitudinal steel along the tension face of the bent cap. The maximum positive bending moment due to the applied loads is larger for the simply supported case than for the moment frame case (Example 3a). A greater amount of bottom chord reinforcement is therefore necessary, and the corresponding centroid of the reinforcement is farther from the bottom surface of the bent cap (in relation to Example 3a). As shown in Figure 7.4, the final location of the bottom chord is 7.6 inches from the bottom face of the cap.

The top chord of the global STM consists entirely of struts (positive moment exists along the length of the cap). For this reason, its position is not necessarily determined by the centroid of the longitudinal reinforcement along the top of the cap (refer to Example 3a). To achieve efficient use of the bent cap depth, the distance between the top and bottom chords of the STM (analogous to the moment arm, jd) and the width of the top chord struts (analogous to the rectangular compression stress block) should be optimized (Tjhin and Kuchma, 2002). In other words, the factored force acting on the back face of the most critical node located along the top chord should be nearly equal to its design strength (refer to Section 2.9.4 and Figure 2.17).

To optimize the STM, the critical section for flexure (i.e. the section with the largest force in the top chord) is first identified by analyzing the simply supported member. Applying the factored superstructure loads and the factored distributed self-weight to the bent cap reveals that the maximum positive moment occurs at Beam Line 1 ($M_{max} = 9972$ kip-ft, refer to Figure 7.5). Although the STM geometry has not yet been defined, the designer can know that all the nodes along the top chord will be CCT nodes (only one vertical tie joins at each node). To strengthen the back faces of the nodes along the top chord, 20-#11 bars are provided as compression reinforcement along the length of the bent cap. The centroid of the 20 bars will be located a distance d'_s of 4.9 inches from the top surface of the cap.

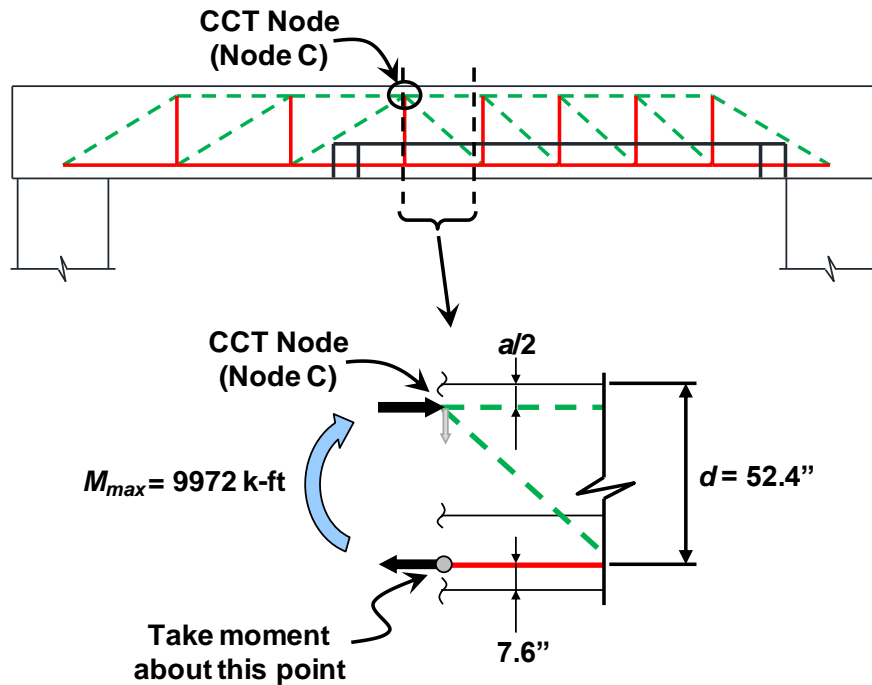


Figure 7.5: Determining the location of the top chord of the global STM

The equation below is used to determine the optimal position of the top chord, where a is the width of the top chord struts (i.e. $a/2$ is the distance from the top surface of the cap to the top chord of the STM).

$$M_{max} = \phi \left[\underbrace{\nu f'_c b_w a}_{\text{Concrete strength at the back face}} \underbrace{\left(d - \frac{a}{2} \right)}_{jd} + \underbrace{A_{st} f_y}_{\text{Steel contribution}} (d - d'_s) \right]$$

$$9972 \text{ kip-ft} = (0.7) \left[(0.7)(5.0 \text{ ksi})(40 \text{ in})a \left(52.4 \text{ in} - \frac{a}{2} \right) + (20)(1.56 \text{ in}^2)(60 \text{ ksi})(52.4 \text{ in} - 4.9 \text{ in}) \right]$$

Solving: $a = 12.70 \text{ in}$ and $a/2 = 6.35 \text{ in}$

The AASHTO LRFD (2010) resistance factor, ϕ , is taken as 0.7 for compression in strut-and-tie models. The concrete efficiency factor, ν , of 0.7 corresponds to the back face of

the CCT node at Beam Line 1 (Node C in Figure 7.4). The minimum width of the horizontal strut necessary to resist the top chord forces is 12.70 inches. The distance from the top surface of the bent cap to the top chord of the STM ($a/2$) is therefore 6.35 inches (see Figure 7.4).

Once the locations of the top and bottom chords are determined, vertical ties representing the hanger reinforcement within the stem of the bent are placed at the locations of the applied superstructure loads (Ties CK, EM, and GO in Figure 7.4). The proposed STM specifications of Chapter 3 state that the angle between a strut and a tie entering the same node should not be less than 25 degrees. To satisfy this requirement, additional vertical ties are necessary in four locations (Ties AI, BJ, DL, and FN). Diagonal struts are then positioned in each truss panel of the STM.

The final reinforcement layout within the stem of the bent cap is shown in Figure 7.16. Several iterations were necessary to ensure that (1) the centroids of the longitudinal reinforcement correspond with the locations assumed for the main tension and compression steel during the STM development and (2) the amount of compression reinforcement allows the nodal strength checks of the top chord to be satisfied. Engineering judgment should always be exercised in determining the necessity of additional design iterations.

The statically determinate truss, simply supported at Nodes H and P, is analyzed under the action of the beam loads (at Nodes K, M, and O) and the tributary self-weight (at each node). The truss analysis results in the internal member forces and external column reactions shown in Figure 7.4. Considering that the system is statically determinate, the column reactions obtained from the truss analysis are the same as those that would result from an analysis of the simply supported bent cap.

7.4.2 Step 2: Develop Local Strut-and-Tie Models

A local, or sectional, STM is developed at each beam line according to the methodology of Example 3a (refer to Section 6.4.2). Due to the minor shift of the bottom chord, the geometries of the local STMs are only slightly different than those of Example

3a. The STM for the section at Beam Line 1 is shown in Figure 7.6. Please note that the horizontal strut is located 7.6 inches from the bottom surface of the bent cap. The local STMs for the three beam lines are presented in Figure 7.7. All three STMs are geometrically identical.

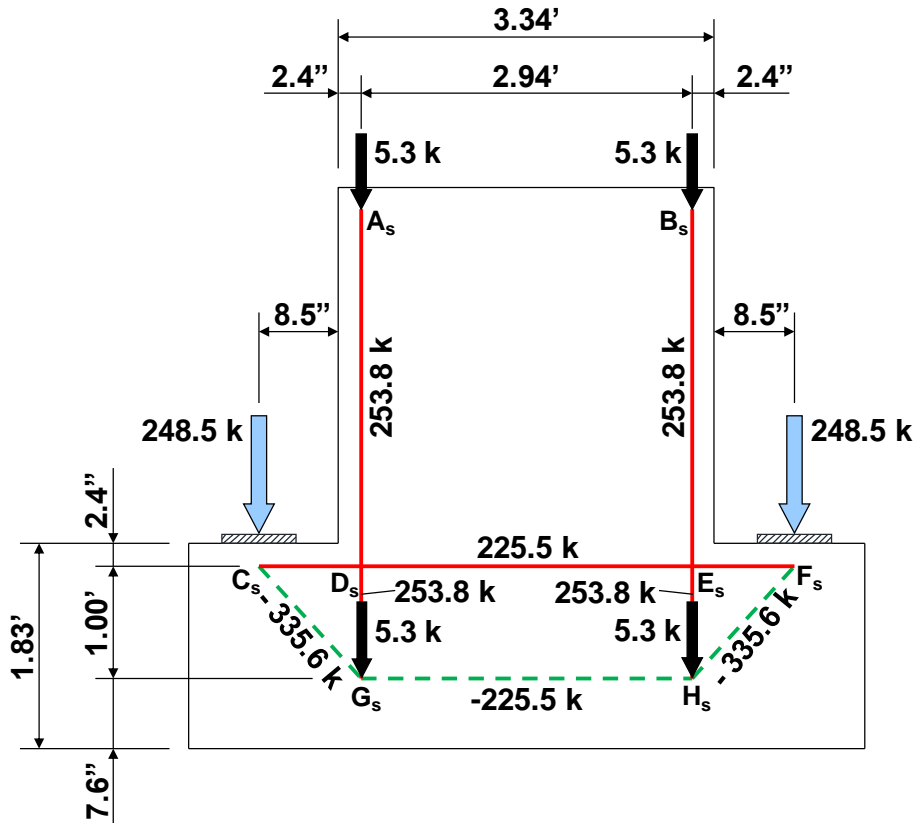


Figure 7.6: Local strut-and-tie model at Beam Line 1 (simply supported case)

To solve for the forces in the struts and ties, the concept of a single three-dimensional STM must be considered. Referring to Figure 7.7, the diagonal struts of the global STM impose forces on the vertical ties of the local STMs. The resulting forces in Ties A_sG_s and B_sH_s of each local STM should be equal to half the force in the corresponding vertical tie of the global STM. Satisfying equilibrium at each node of the local STMs results in the internal forces shown in Figure 7.7.

Comparing the three local STMs, the STM at Beam Line 1 governs the nodal strength checks and the design of the ledge reinforcement (Tie C_sF_s). The vertical ties

within the stem will be proportioned based on the global STM. Therefore, only the local STM at Beam Line 1 (Figure 7.6) will be used for the remainder of the design. The required spacing of the ledge reinforcement based on the STM at Beam Line 1 will be satisfied along the entire length of the ledge.

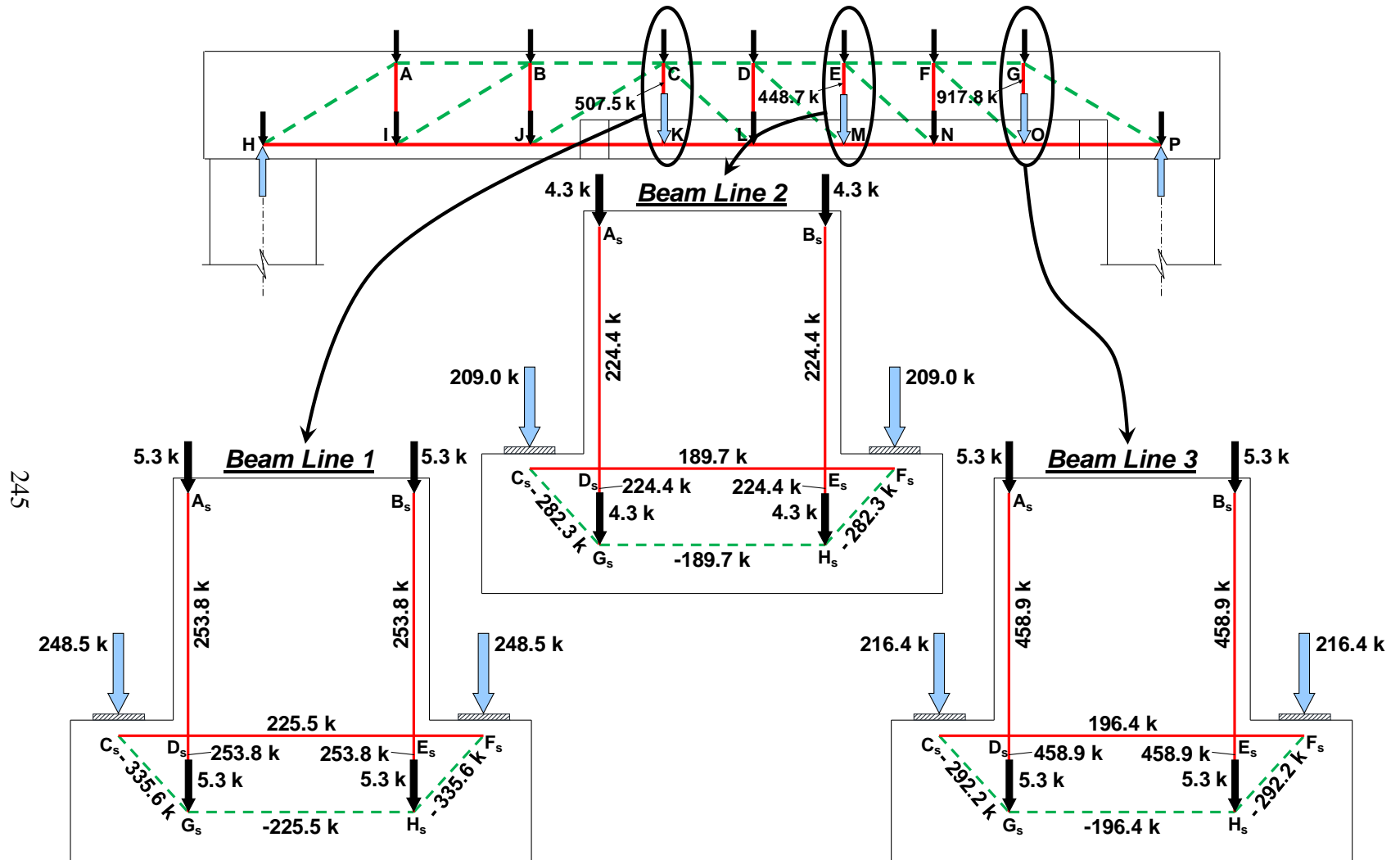


Figure 7.7: Comparing the local strut-and-tie models (simply supported case)

7.4.3 Step 3: Proportion Longitudinal Ties

Only the bottom chord reinforcement must be proportioned to satisfy longitudinal tension demands. A constant amount of longitudinal steel is provided along the full length of the cap for simplicity of design and construction.

Bottom Chord

Design of the bottom chord reinforcement is controlled by the force in Ties JK and KL. Using #11 bars, the reinforcement required for the bottom chord is:

$$\begin{aligned} \text{Factored Load:} & F_u = 2602.7 \text{ kip} \\ \text{Tie Capacity:} & \varphi \cdot f_y \cdot A_{st} = F_u \\ & (0.9)(60 \text{ ksi})A_{st} = 2602.7 \text{ kip} \\ & A_{st} = 48.20 \text{ in}^2 \end{aligned}$$

$$\text{Number of \#11 bars required: } 48.20 \text{ in}^2 / 1.56 \text{ in}^2 = 30.9 \text{ bars}$$

Use 32 - #11 bars

The top chord (compression) reinforcement is determined by the requirements of the nodal strength checks conducted at the compression face of the inverted-T (see Section 7.4.6).

7.4.4 Step 4: Proportion Hanger Reinforcement/Vertical Ties

The geometry of the node above each beam line (Nodes C, E, and G in Figure 7.4) is controlled by the width of the vertical hanger ties (Ties CK, EM, and GO). For this reason, the stirrups within the stem of the inverted-T are proportioned prior to conducting the nodal strength checks.

Due to the shallow height of the global STM (in comparison to that of Example 3a), more vertical ties are necessary to ensure that the angle between a strut and a tie entering the same node does not fall below 25 degrees (Figure 7.8). An additional truss panel is included between Beam Lines 1 and 2 and between Beam Lines 2 and 3 so that the diagonal struts are not excessively shallow. Similarly, a truss panel is added between Beam Line 1 and the left support (Column A). The addition of the ties will implicitly

increase the stirrup requirements of the simply supported case in relation to that of the moment frame case.

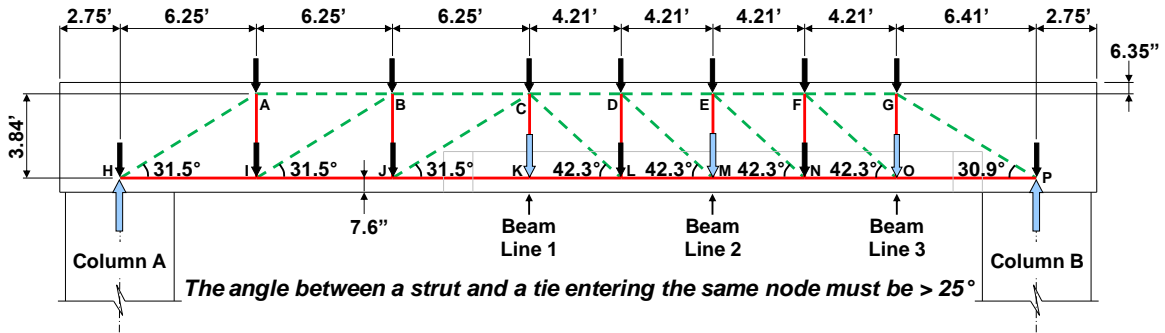


Figure 7.8: Diagonal strut inclinations (greater than 25 degrees)

The addition of the vertical ties along the ledge (Ties DL and FN), moreover, necessitates a different approach to proportioning the effective width of each hanger tie (Ties CK, EM, and GO). In Example 3a, the effective width of each vertical tie representing the hanger reinforcement was determined by using Article 5.13.2.5.5 of AASHTO LRFD (2010). For the current example, the width of each tie is taken as the smaller of the two adjacent truss panel lengths to ensure the assumed tie widths do not overlap. For example, the assumed width of Tie GO must not extend into the width of Tie FN. The width of Tie GO is therefore taken as the distance between Nodes F and G, or 4.21 feet. The stirrups for Tie GO can be distributed over a distance of $4.21 \text{ ft} \div 2$ on either side of the tie. The assumed width of each vertical tie located along the ledge of the inverted-T is illustrated in Figure 7.9. Please note that the use of the proportioning technique recommended by Wight and Parra-Montesinos (2003) would cause adjacent tie widths to overlap.

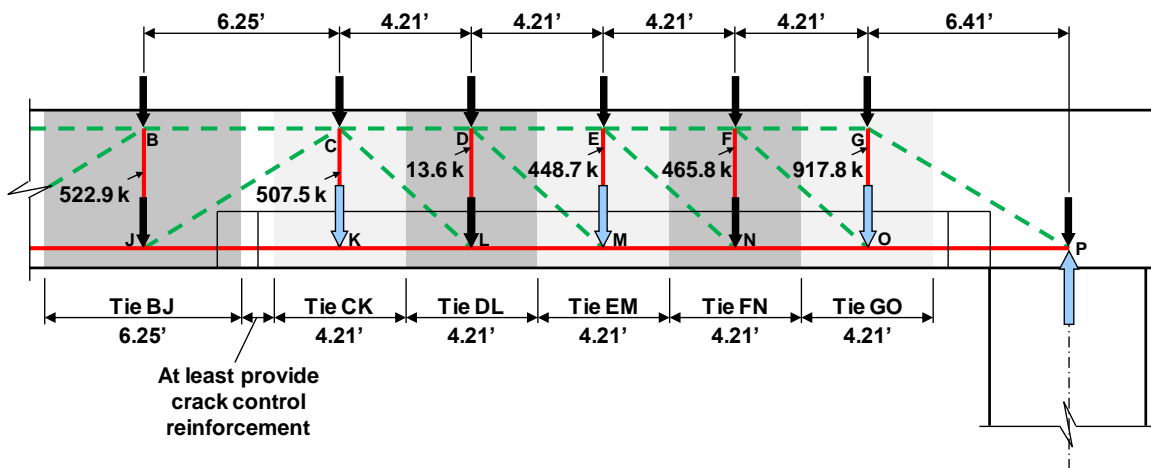


Figure 7.9: Vertical tie widths

Calculations will not be performed for each vertical tie in Figure 7.9. To simplify design and construction, the stirrup spacing required to carry the force in Tie CK will be conservatively used along the entire length of the ledge except for the region where a closer spacing is required for Tie GO. Due to the large force imposed over the limited width of Tie GO, it is the most critical vertical tie of the global STM and will therefore be portioned first. The required stirrup spacing for Tie CK will then be determined. Lastly, stirrups will be proportion within the shear span left of Beam Line 1.

Tie GO

To maintain consistency with the original design, two-legged #6 stirrups will be bundled together and spaced as necessary to resist the tie forces. The required spacing of the paired #6 stirrups is:

Factored Load:	$F_u = 917.8 \text{ kip}$
Tie Capacity:	$\phi \cdot f_y \cdot A_{st} = F_u$
	$(0.9)(60 \text{ ksi})A_{st} = 917.8 \text{ kip}$
	$A_{st} = 17.00 \text{ in}^2$

Number of double #6 stirrups required: $17.00 \text{ in}^2 / (4)(0.44 \text{ in}^2) = 9.66$ stirrups

$$l_a = 50.5 \text{ in} \quad s = 50.5 \text{ in} / 9.66 = 5.2 \text{ in}$$

Use 2 legs of double #6 stirrups with spacing less than 5.2 in.

Tie CK

Tie CK is the second most critical vertical tie. The required spacing of two-legged #6 stirrups is:

Factored Load:	$F_u = 507.5 \text{ kip}$
Tie Capacity:	$\phi \cdot f_y \cdot A_{st} = F_u$
	$(0.9)(60 \text{ ksi})A_{st} = 507.5 \text{ kip}$
	$A_{st} = 9.40 \text{ in}^2$

Number of #6 stirrups (2 legs) required: $9.40 \text{ in}^2 / (2)(0.44 \text{ in}^2) = 10.68$ stirrups

$$l_a = 50.5 \text{ in} \quad s = 50.5 \text{ in} / 10.68 = 4.7 \text{ in}$$

Use 2 legs of #6 stirrups with spacing less than 4.7 in.

Tie AI

The nodes at either end of Ties AI and BJ are smeared nodes. As with Tie BH of Example 3a, applying the proportioning technique recommended by Wight and Parra-Montesinos (2003) would cause adjacent tie widths to overlap. The width of both ties, therefore, is taken as the length of an adjacent truss panel ($l_a = 6.25$ feet, refer to Figure 7.9). Since the force in Tie AI is slightly larger (compared to Tie BJ), the stirrup spacing required for Tie AI will also be used over the width of Tie BJ. The required spacing is:

Factored Load:	$F_u = 542.5 \text{ kip}$
Tie Capacity:	$\phi \cdot f_y \cdot A_{st} = F_u$
	$(0.9)(60 \text{ ksi})A_{st} = 542.5 \text{ kip}$
	$A_{st} = 10.05 \text{ in}^2$

Number of #6 stirrups (2 legs) required: $10.05 \text{ in}^2 / (2)(0.44 \text{ in}^2) = 11.42$ stirrups

$$l_a = 75.0 \text{ in} \quad s = 75.0 \text{ in} / 11.42 = 6.6 \text{ in}$$

Use 2 legs of #6 stirrups with spacing less than 6.6 in.

7.4.5 Step 5: Proportion Ledge Reinforcement

The reinforcement required to carry the force in Tie C_sF_s of the local STM (Figure 7.6) is determined in a manner similar to that of Example 3a (refer to Section 6.4.5). The length over which the ledge reinforcement can be distributed is limited by the corresponding tie width of the hanger reinforcement determined in Section 7.4.4. The reinforcement carrying the force in Tie C_sF_s is therefore distributed over a length of 4.21 feet, or 50.5 inches (refer to Figure 7.9). The local STM at Beam Line 1 controls the ledge reinforcement design. The required spacing for #6 bars is:

$$\begin{aligned} \text{Factored Load:} \quad & F_u = 225.5 \text{ kip} \\ \text{Tie Capacity:} \quad & \phi \cdot f_y \cdot A_{st} = F_u \\ & (0.9)(60 \text{ ksi})A_{st} = 225.5 \text{ kip} \\ & A_{st} = 4.18 \text{ in}^2 \end{aligned}$$

Number of #6 bars required: $4.18 \text{ in}^2 / 0.44 \text{ in}^2 = 9.49$ bars

$$l_a = 50.5 \text{ in} \quad s = 50.5 \text{ in} / 9.49 = 5.3 \text{ in}$$

Use #6 bars with spacing less than 5.3 in.

The ledge reinforcement will be paired with the stirrups of the stem to satisfy this spacing requirement.

7.4.6 Step 6: Perform Nodal Strength Checks

Nodal strength checks for Nodes P, E, and C are demonstrated within this section. Many of the remaining nodes are smeared or can be deemed to have adequate strength by inspection. For Nodes E and C, a refined nodal geometry must be defined to accurately perform the strength checks. The refined geometries of both nodes are presented along with their respective strength calculations.

Node P (CCT)

Node P is shown in Figure 7.10; it is located directly above the right column of the bent. Due to a lack of moment transfer between the cap and column, the vertical reaction is assumed to be uniformly distributed over the bearing face of Node P (i.e. the total cross-sectional area of the column). The length of the bearing face is taken as the full width of the column, or 60.0 inches, as shown. The height of the back face is double the distance from the bottom of the bent cap to the centroid of the bottom chord reinforcement.

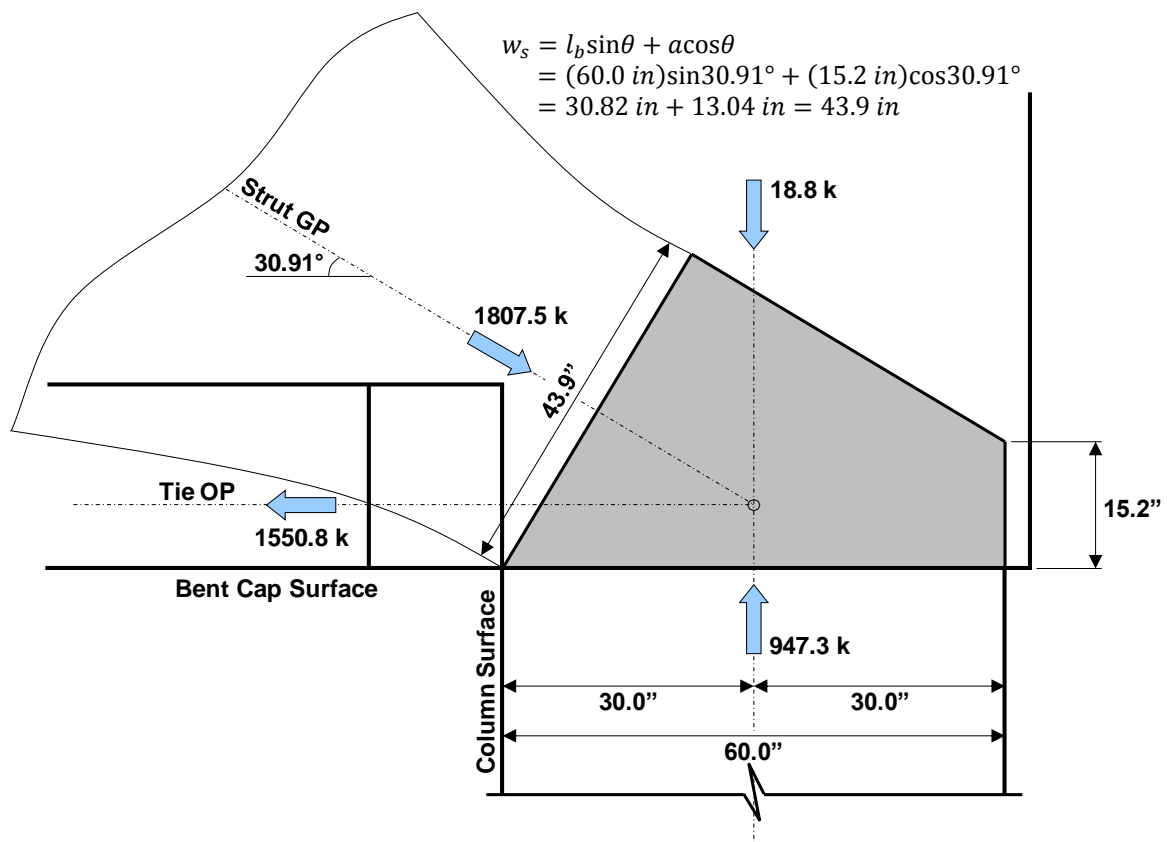


Figure 7.10: Node P (simply supported case)

The bent cap is slightly wider than the columns which support it. While the triaxial confinement of Node P could be considered, its effect would be slight and is ultimately unnecessary to satisfy the strength requirements.

Triaxial Confinement Factor: $m = 1$

BEARING FACE

$$\begin{aligned}\text{Factored Load:} & F_u = 947.3 \text{ kip} \\ \text{Efficiency:} & \nu = 0.7 \\ \text{Concrete Capacity:} & f_{cu} = m \cdot \nu \cdot f'_c = (1)(0.7)(5.0 \text{ ksi}) = 3.5 \text{ ksi} \\ & \varphi \cdot F_n = (0.7)(3.5 \text{ ksi})(60.0 \text{ in})(36 \text{ in}) \\ & = 5292 \text{ kip} > 947.3 \text{ kip} \textbf{OK}\end{aligned}$$

No direct compressive force acts on the back face; therefore, no strength check is necessary.

STRUT-TO-NODE INTERFACE

$$\begin{aligned}\text{Factored Load:} & F_u = 1807.5 \text{ kip} \\ \text{Efficiency:} & \nu = 0.85 - \frac{5.0 \text{ ksi}}{20 \text{ ksi}} = 0.6 \\ & \therefore \text{Use } \nu = 0.6 \\ \text{Concrete Capacity:} & f_{cu} = m \cdot \nu \cdot f'_c = (1)(0.6)(5.0 \text{ ksi}) = 3.0 \text{ ksi} \\ & \varphi \cdot F_n = (0.7)(3.0 \text{ ksi})(43.9 \text{ in})(36 \text{ in}) \\ & = 3319 \text{ kip} > 1807.5 \text{ kip} \textbf{OK}\end{aligned}$$

Therefore, the strength of Node P is sufficient to resist the applied forces.

Node H (CCT)

Node H is located directly above the left column. Comparing Node H to Node P reveals that Node H is not a critical node, and its strength is deemed sufficient by inspection.

Node E (CCT)

Node E is the CCT node located directly above Beam Line 2. Large compressive forces act along the top chord of the STM at the location of Node E, causing it to be one of the most highly stressed nodes. The length of the top face of Node E is assumed to be the same dimension as the width of Tie EM (previously determined in Section 7.4.4). The length of the top face is therefore 4.21 feet, or 50.5 inches. The height of the back face is taken as double the distance from the top surface of the bent cap to the top chord of the global STM. Since both Struts EF and EN enter Node E from the right, they are

resolved to form a strut 10.08° from the horizontal with a force of 2613.1 kips. The resulting nodal geometry and the forces acting on the node are shown in Figure 7.11.

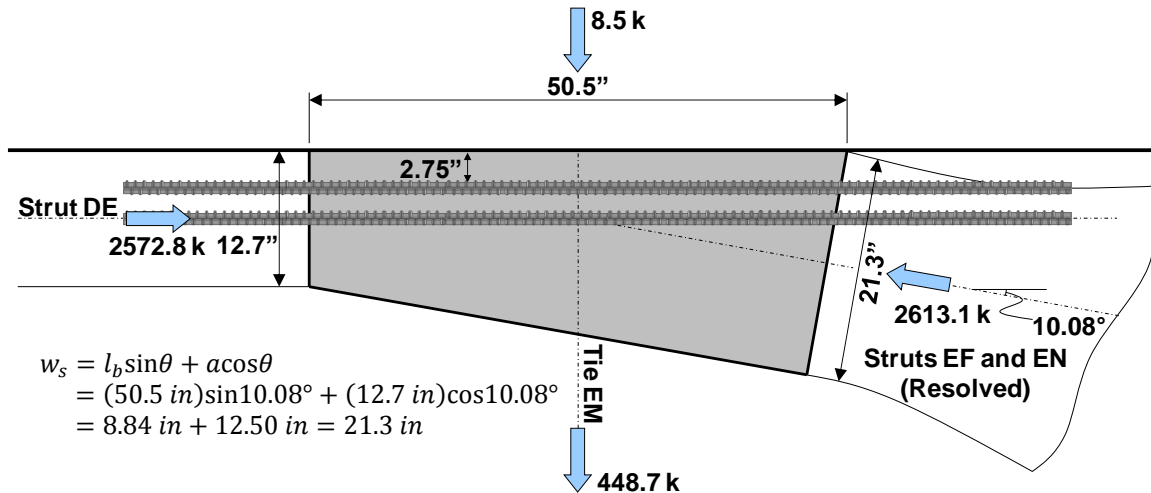


Figure 7.11: Node E – resolved struts (simply supported case)

Node E has no bearing surface; therefore, no bearing check is necessary. When determining the location of the top chord of the global STM in Section 7.4.1, 20-#11 bars were assumed to be sufficient to satisfy the back face checks. The contribution of the compression steel to the nodal strength is considered in the following calculations:

Triaxial Confinement Factor: $m = 1$

BACK FACE

Factored Load: $F_u = 2572.8 \text{ kip}$

Efficiency: $v = 0.7$

Concrete Capacity: $f_{cu} = m \cdot v \cdot f'_c = (1)(0.7)(5.0 \text{ ksi}) = 3.5 \text{ ksi}$

$$\phi \cdot F_n = (0.7)[(3.5 \text{ ksi})(12.7 \text{ in})(40 \text{ in}) + (31.2 \text{ in}^2)(60 \text{ ksi})]$$

$$= 2555.0 \text{ kip} < 2572.8 \text{ kip} \text{ OK}$$

$$\% \text{ Difference} = \left(\frac{2572.8 \text{ kip} - 2555.0 \text{ kip}}{2572.8 \text{ kip}} \right) (100) = 0.69\%$$

Although the strength check indicates that the back face does not have enough capacity to resist the applied stress, the shortfall is less than 2 percent. This small difference is negligible, and the strength of the back face is adequate.

STRUT-TO-NODE INTERFACE (Resolved struts)

$$\begin{aligned}\text{Factored Load:} & F_u = 2613.1 \text{ kip} \\ \text{Efficiency:} & v = 0.85 - 5.0 \text{ ksi} / 20 \text{ ksi} = 0.6 \\ & \therefore \text{Use } v = 0.6 \\ \text{Concrete Capacity:} & f_{cu} = m \cdot v \cdot f'_c = (1)(0.6)(5.0 \text{ ksi}) = 3.0 \text{ ksi} \\ & \varphi \cdot F_n = (0.7)(3.0 \text{ ksi})(21.3 \text{ in})(40 \text{ in}) \\ & = 1789 \text{ kip} < 2613.1 \text{ kip}\end{aligned}$$

The strength of the strut-to-node interface is significantly less than the demand imposed by the resolved forces of Struts EF and EN. The compression reinforcement is not parallel to the resolved strut, and its contribution to the nodal strength cannot therefore be considered. Referring to the original STM geometry of Figure 7.4, the force in the horizontal Strut EF is much greater than the force in the diagonal Strut EN. The compression reinforcement is expected to be active (to a great extent) in resisting the force imposed by Strut EF. A refined check of Node E can be performed to account for the effect of the compression steel. To perform the strength check, Struts EF and EN are not resolved but instead remain independent. The refined geometry of Node E is illustrated in Figure 7.12. The width of the nodal face at the confluence of Node E and Strut EN (referred to as the strut-to-node interface) is defined in the figure.

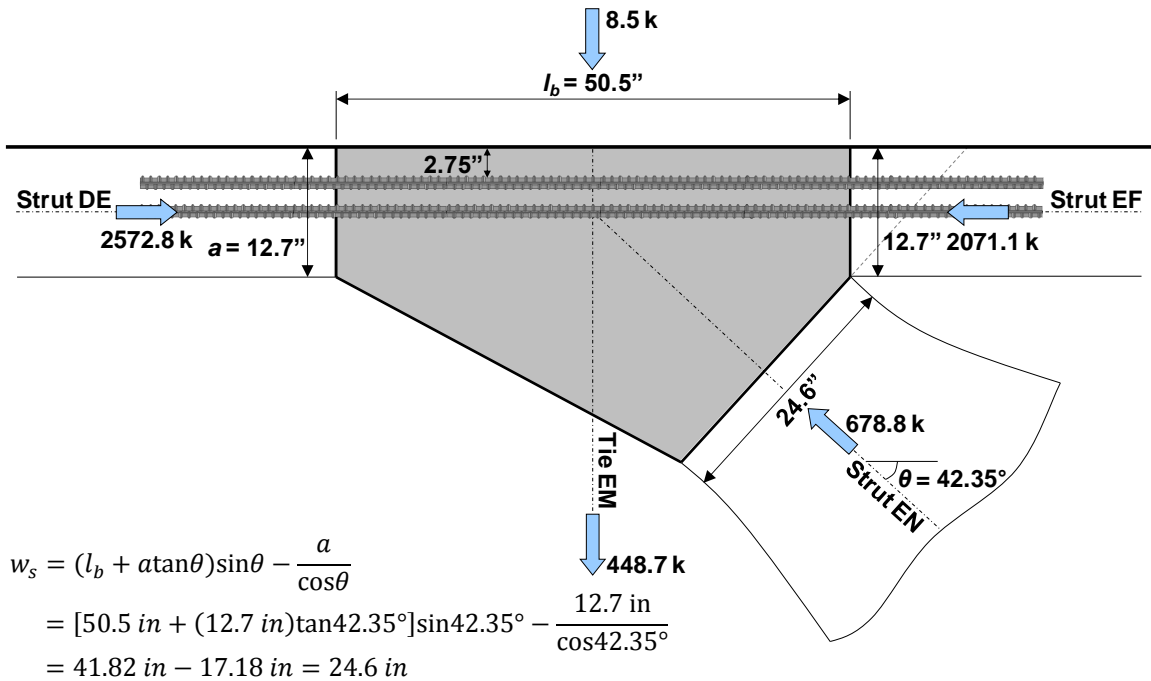


Figure 7.12: Node E – refined geometry (simply supported case)

The node in Figure 7.12 essentially has two back faces. The back face on the left was previously checked. The back face on the right has the same strength as the left back face, but the applied force is less. The right back face, therefore, has adequate strength. The strut-to-node interface is checked as follows:

STRUT-TO-NODE INTERFACE (Refined check)

Factored Load: $F_u = 678.8 \text{ kip}$

Efficiency: $v = 0.85 - 5.0 \text{ ksi} / 20 \text{ ksi} = 0.6$

\therefore Use $v = 0.6$

Concrete Capacity: $f_{cu} = m \cdot v \cdot f'_c = (1)(0.6)(5.0 \text{ ksi}) = 3.0 \text{ ksi}$

$$\varphi \cdot F_n = (0.7)(3.0 \text{ ksi})(24.6 \text{ in})(40 \text{ in})$$

$$= 2066 \text{ kip} > 678.8 \text{ kip} \text{ OK}$$

Therefore, the strength of Node E is sufficient to resist the applied forces.

When back face reinforcement is provided at a nodal region and a pair of struts enters the node from the same side (e.g. Node E), the strength of the node should first be checked by resolving adjacent struts (limiting scenario). If this check reveals that the

strength of the strut-to-node interface is insufficient, the refined nodal geometry can be defined. If the strut-to-node interface is still deficient, the initial design of the member should be revisited and changes to cross-sectional dimensions and/or material properties should be considered.

Node C (CCT)

Node C is located above Beam Line 1. Due to the large forces in Strut CJ and along the top chord of the STM, the node is identified as critical. The total length of the top face is the same dimension as the width of Tie CK, or 50.5 inches. The height of the back face is again taken as 12.7 inches. Node C will be subdivided into two parts to facilitate the nodal strength checks. Both nodal subdivisions are illustrated in Figure 7.13.

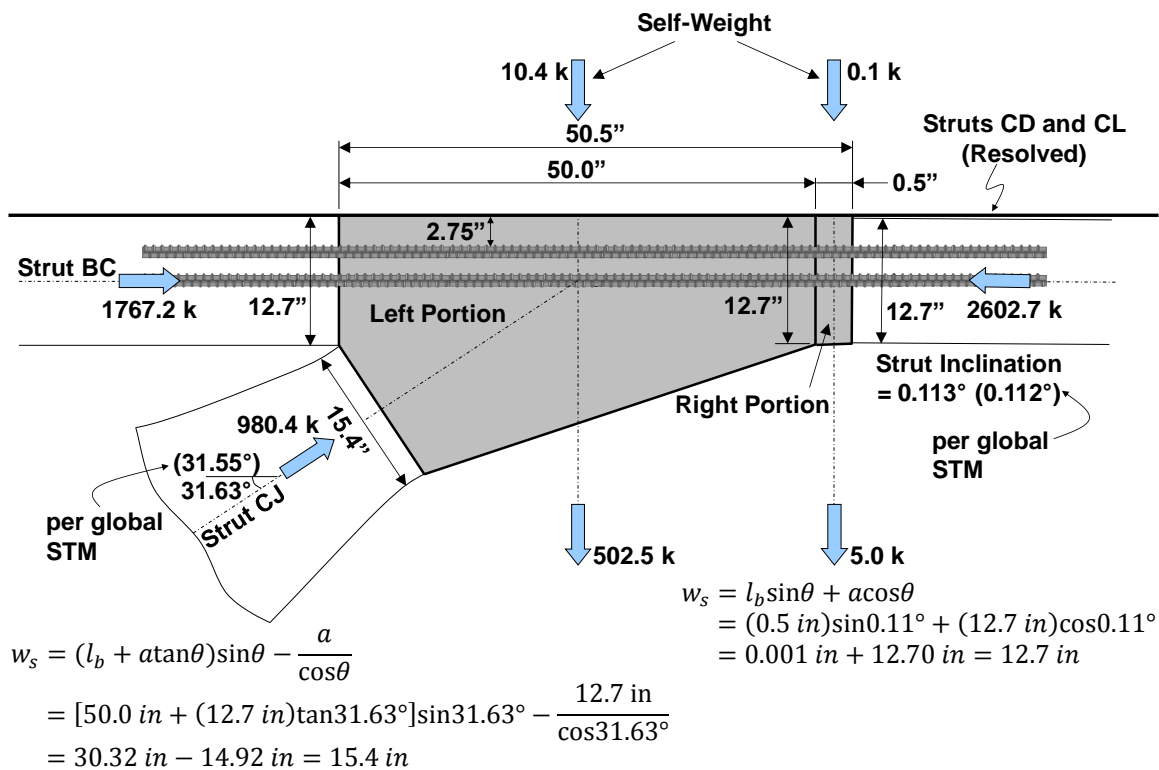


Figure 7.13: Node C (simply supported case)

The length of the top face for each nodal subdivision is based upon the magnitude of the vertical component of each diagonal strut entering the node in relation to the net vertical force from Tie CK and the applied self-weight. The length of each top face is:

$$\left[\frac{(980.4 \text{ kip}) \sin(31.55^\circ)}{507.5 \text{ kip} + 10.5 \text{ kip}} \right] (50.5 \text{ in}) = 50.0 \text{ in}$$

$$\left[\frac{(7.6 \text{ kip}) \sin(42.35^\circ)}{507.5 \text{ kip} + 10.5 \text{ kip}} \right] (50.5 \text{ in}) = 0.5 \text{ in}$$

where 31.55° and 42.35° are the inclinations of Struts CJ and CL, 507.5 kips is the force in Tie CK, and 10.5 kips is the total self-weight load applied at Node C. The 980.4-kip and 7.6-kip values are the forces in the diagonal struts (Struts CJ and CL, refer to Figure 7.4). The right nodal subdivision is very small compared to the left subdivision.

If Struts BC and CJ (entering the left side of Node C) are resolved together, the strut-to-node interface of the left portion of Node C is found to be deficient. The geometry of the left portion will therefore need to be refined. The width of the strut-to-node interface for this refined geometry is shown in Figure 7.13 ($w_s = 15.4 \text{ in.}$). The 31.63° inclination is the revised angle of Strut CJ due to the subdivision of Node C.

For the right portion of Node C, Struts CD and CL are resolved to form a strut with an inclination of 0.112° from the horizontal and a force of 2602.7 kips. A strut inclination of 0.113° is found when the subdivision of Node C is taken into account. The length of the corresponding strut-to-node interface is 12.7 inches (refer to the calculation in Figure 7.13). Due to the exceedingly slight inclination of the resolved strut, the strength check of this strut-to-node interface is virtually equivalent to the back face check. Therefore, the only necessary nodal strength checks for Node C are those related to the back face and the strut-to-node interface of the left portion of the node.

Node C – Left (CCT)

Triaxial Confinement Factor: $m = 1$

BACK FACE

Factored Load: $F_u = 2602.7 \text{ kip}$

Efficiency: $\nu = 0.7$

Concrete Capacity: $f_{cu} = m \cdot \nu \cdot f'_c = (1)(0.7)(5.0 \text{ ksi}) = 3.5 \text{ ksi}$

$$\begin{aligned}\phi \cdot F_n &= (0.7)[(3.5 \text{ ksi})(12.7 \text{ in})(40 \text{ in}) + (31.2 \text{ in}^2)(60 \text{ ksi})] \\ &= 2555.0 \text{ kip} < 2602.7 \text{ kip} \quad \mathbf{OK}\end{aligned}$$

$$\% \text{ Difference} = \left(\frac{2602.7 \text{ kip} - 2555.0 \text{ kip}}{2602.7 \text{ kip}} \right) (100) = 1.83\%$$

The deficiency of the back face is less than 2 percent. This small difference is negligible, and the strength of the back face is adequate. Please recall that the top chord of the global STM was positioned in a manner that causes the force on the back face of Node C to be approximately equal to its capacity (refer to Section 7.4.1).

STRUT-TO-NODE INTERFACE

Factored Load: $F_u = 980.4 \text{ kip}$

Efficiency: $\nu = 0.85 - \frac{5.0 \text{ ksi}}{20 \text{ ksi}} = 0.6$

\therefore Use $\nu = 0.6$

Concrete Capacity: $f_{cu} = m \cdot \nu \cdot f'_c = (1)(0.6)(5.0 \text{ ksi}) = 3.0 \text{ ksi}$

$$\begin{aligned}\phi \cdot F_n &= (0.7)(3.0 \text{ ksi})(15.4 \text{ in})(40 \text{ in}) \\ &= 1294 \text{ kip} > 980.4 \text{ kip} \quad \mathbf{OK}\end{aligned}$$

Therefore, the strength of Node C is sufficient to resist the applied forces.

Other Nodes

Nodes G, K, M, and O of the global STM (Figure 7.4) can be checked using the methods outlined here and in Example 3a. Nodes A, B, D, F, I, J, L, and N are all smeared nodes and do not need to be checked. The strength checks for Nodes C_s and F_s of the local STM at Beam Line 1 (Figure 7.6) are marginally different than the checks of the same nodes in Example 3a, and the nodes are deemed to have adequate strength by inspection (including the critical bearings at Beam Line 1). Nodes G_s and H_s of the local STM are smeared nodes and are not critical.

7.4.7 Step 7: Proportion Crack Control Reinforcement

The required crack control reinforcement of the current example is the same as that of Example 3a. If #6 stirrups with two legs are used as transverse reinforcement, the spacing should be no greater than 7.3 inches. Please recall that the stirrup spacing required for Tie CK (at Beam Line 1) will be provided along the entire length of the ledge except for the region where a closer spacing is required for Tie GO (at Beam Line 3). With this in mind, the reinforcement necessary to carry the forces in the vertical ties of the STM (refer to Section 7.4.4) governs the required stirrup spacing. The required spacing of the crack control reinforcement provisions, however, must be satisfied in regions outside of a vertical tie width (e.g. above the columns).

Finally, longitudinal skin reinforcement consisting of #6 bars should not be spaced more than 7.3 inches to satisfy the crack control reinforcement requirements.

Summary

- Use 2 legs of #6 stirrups with spacing less than 4.7 in. along the length of the ledge except for Tie GO
- Use 2 legs of double #6 stirrups with spacing less than 5.2 in. for Tie GO
- Pair the ledge stirrups with the stirrups in the stem along the entire length of the ledge
- Use 2 legs of #6 stirrups with spacing less than 6.6 in. for Ties AI and BJ
- Use 2 legs of #6 stirrups with spacing less than 7.3 in. along the remainder of the bent cap
- Use #6 bars with spacing less than 7.3 in. as horizontal skin reinforcement
(Final reinforcement details are provided in Figures 7.15 and 7.16)

7.4.8 Step 8: Provide Necessary Anchorage for Ties

The bottom chord reinforcement of the inverted-T bent cap must be properly anchored at Nodes H and P. Referring to the final reinforcement details of Figure 7.16, the bars in the uppermost layer of the tension reinforcement will have more than 12.0 inches of concrete cast below them (see Figure 7.14). According to Article 5.11.2.1.2 of

AASHTO LRFD (2010), the development length required for these bars will be 1.4 times longer than that required for the other longitudinal tension reinforcement. If straight bars are used, the required development length for the bars in the bottom four layers is:

$$l_d = \frac{1.25A_b f_y}{\sqrt{f'_c}} = \frac{1.25(1.56 \text{ in}^2)(60 \text{ ksi})}{\sqrt{5.0 \text{ ksi}}} = 52.3 \text{ in}$$

For the bars in the uppermost layer of the tension reinforcement, straight development length is:

$$l_d = \frac{1.25A_b f_y}{\sqrt{f'_c}} \cdot 1.4 = \frac{1.25(1.56 \text{ in}^2)(60 \text{ ksi})}{\sqrt{5.0 \text{ ksi}}} \cdot 1.4 = 73.3 \text{ in}$$

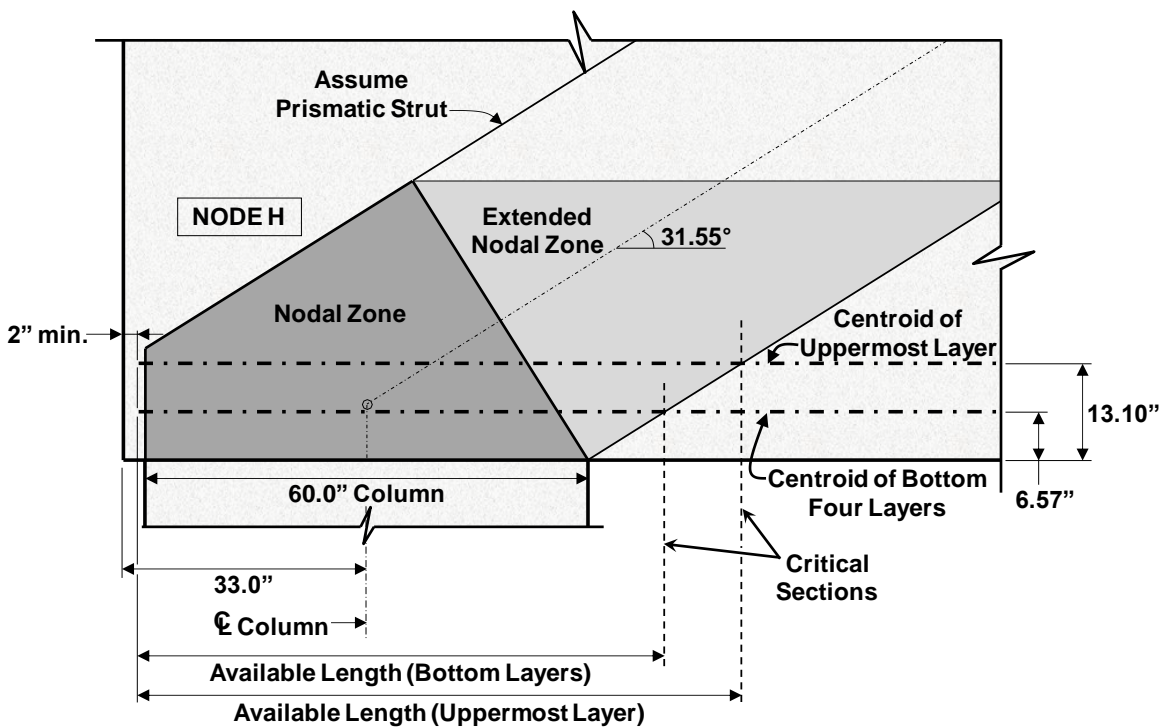


Figure 7.14: Anchorage of bottom chord reinforcement at Node H

The available length over which the bars can develop is measured from the point where the centroid of the reinforcement enters the extended nodal zone. Comparing the inclinations of Struts AH and GP, the available length at Node H will control the

anchorage design at the supports. The centroid of the bars in the bottom four layers of the tension reinforcement is 6.57 inches from the bottom surface of the bent cap (refer to Figure 7.14). The available length for these bars is:

$$\begin{aligned} \text{Available length} &= 33.0 \text{ in} + 60.0 \text{ in}/2 + 6.57 \text{ in}/\tan 31.55^\circ - 2 \text{ in} \\ &= 71.7 \text{ in} > 52.3 \text{ in} \textbf{OK} \end{aligned}$$

All the dimensional values within this calculation are shown in Figure 7.14. Enough length is available for straight development of the bottom four layers.

The centroid of the bars in the uppermost layer of longitudinal tension reinforcement is 13.10 inches from the bottom surface of the bent cap. The available length is:

$$\begin{aligned} \text{Available length} &= 33.0 \text{ in} + 60.0 \text{ in}/2 + 13.10 \text{ in}/\tan 31.55^\circ - 2 \text{ in} \\ &= 82.3 \text{ in} > 73.3 \text{ in} \textbf{OK} \end{aligned}$$

Therefore, enough length is available for straight development of the uppermost layer.

Proper anchorage of the compression reinforcement along the top of the bent cap is provided if the bars are extended to the ends of the member (while ensuring to provide adequate clear cover).

The anchorage of Tie C_sF_s of the local STM should also be checked. Comparing the inclination of Struts C_sG_s and F_sH_s (Figure 7.6) with the inclination of the same struts in Example 3a (Figure 6.9), a longer development length is available in the current design. Hooked anchorage of Tie C_sF_s was accommodated within the ledge of the moment frame case (Example 3a) and will therefore be accommodated within the current example (simply supported case).

7.4.9 Step 9: Perform Other Necessary Checks

All AASHTO LRFD (2010) requirements relevant to the design of an inverted-T beam should be satisfied alongside the STM provisions of Chapter 3. TxDOT's *Bridge Design Manual - LRFD* (2009) necessitates other checks that should be considered as

well. In specific reference to the TxDOT requirements, the longitudinal reinforcement stress should be limited to 22 ksi when the AASHTO LRFD Service I load case is applied with dead load only. Six additional #11 bars are provided along the bottom of the bent cap to satisfy this requirement. The final reinforcement layout in Figures 7.15 and 7.16 complies with all relevant provisions.

7.4.10 Step 10: Perform Shear Serviceability Check

The regions of the bent cap where diagonal cracks are most likely to form are (1) the region between the applied load at Beam Line 3 and the right column and (2) the long shear span between the left column and the load at Beam Line 1. Application of the AASHTO LRFD (2010) Service I load case indicates that the maximum shear force occurs at the right support (667.7 kips at the interior face of the right column). The effective depth, d , is here taken as the distance from the top of the bent cap to the centroid of the bottom chord reinforcement, or 52.4 inches. The most applicable shear span for the critical region near the right column lies between Nodes G and P (i.e. between Beam Line 3 and the centerline of Column B) and is 77.0 inches long. The estimated diagonal cracking strength is:

$$V_{cr} = \left[6.5 - 3 \left(\frac{77.0 \text{ in}}{52.4 \text{ in}} \right) \right] (\sqrt{5000 \text{ psi}}) (40 \text{ in}) (52.4 \text{ in})$$

$$= 310 \text{ kip} < 667.7 \text{ kip } \mathbf{NG} - \text{Expect diagonal cracks}$$

This value is within the $5\sqrt{f'_c}b_wd$ and $2\sqrt{f'_c}b_wd$ limits (refer to Section 2.12). The serviceability check reveals a significant risk of diagonal crack formation when full service loads are applied.

For the long shear span between the left column and Beam Line 1, the $2\sqrt{f'_c}b_wd$ limit controls the diagonal cracking strength estimate. The maximum service shear force in this region of the bent cap occurs at the interior face of the left column, and its magnitude is 396.9 kips. The value of V_{cr} is:

$$\begin{aligned} V_{cr} &= 2\sqrt{f'_c}b_wd = 2\sqrt{5000 \text{ psi}}(40 \text{ in})(52.4 \text{ in}) \\ &= 296 \text{ kip} < 396.9 \text{ kip } \mathbf{NG} - \text{Expect diagonal cracks} \end{aligned}$$

Again, the designer should be aware of the risk of diagonal crack formation and consider modifications to the design that will increase the diagonal cracking strength of the member.

7.5 REINFORCEMENT LAYOUT

The reinforcement details for the load case considered in this design example are presented in Figures 7.15 and 7.16. Any reinforcement details not previously described within the example are consistent with standard TxDOT practice.

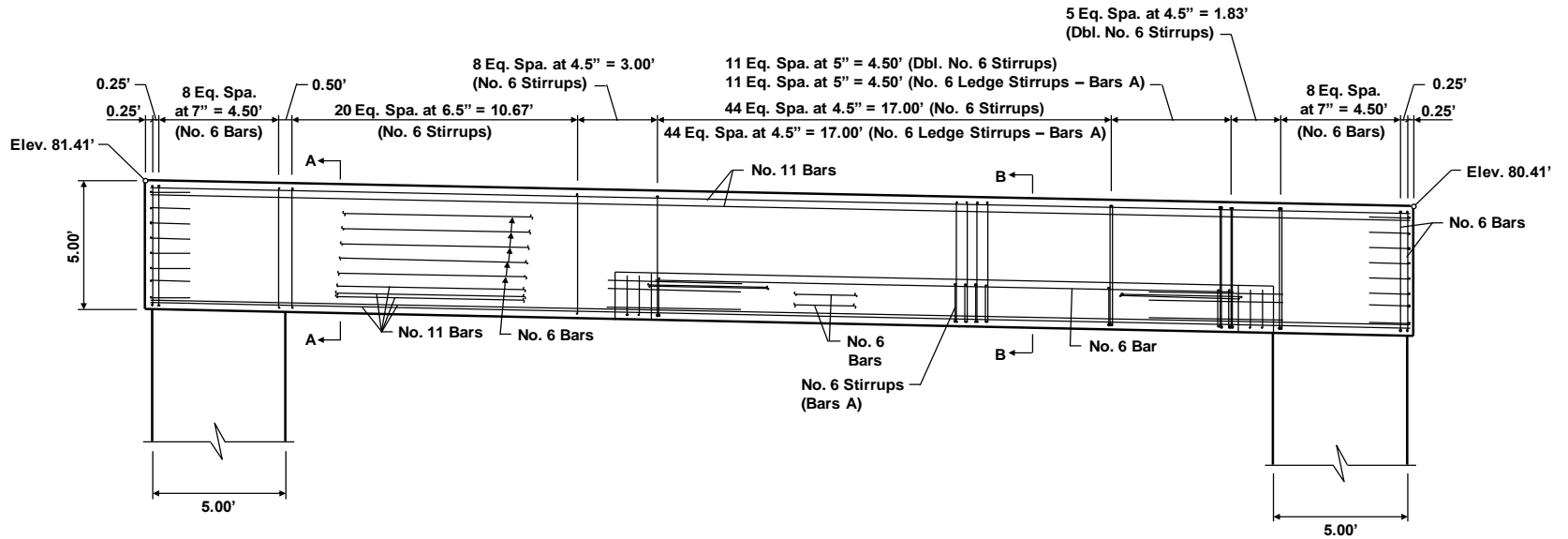


Figure 7.15: Reinforcement details – elevation (design per proposed STM specifications – simply supported)

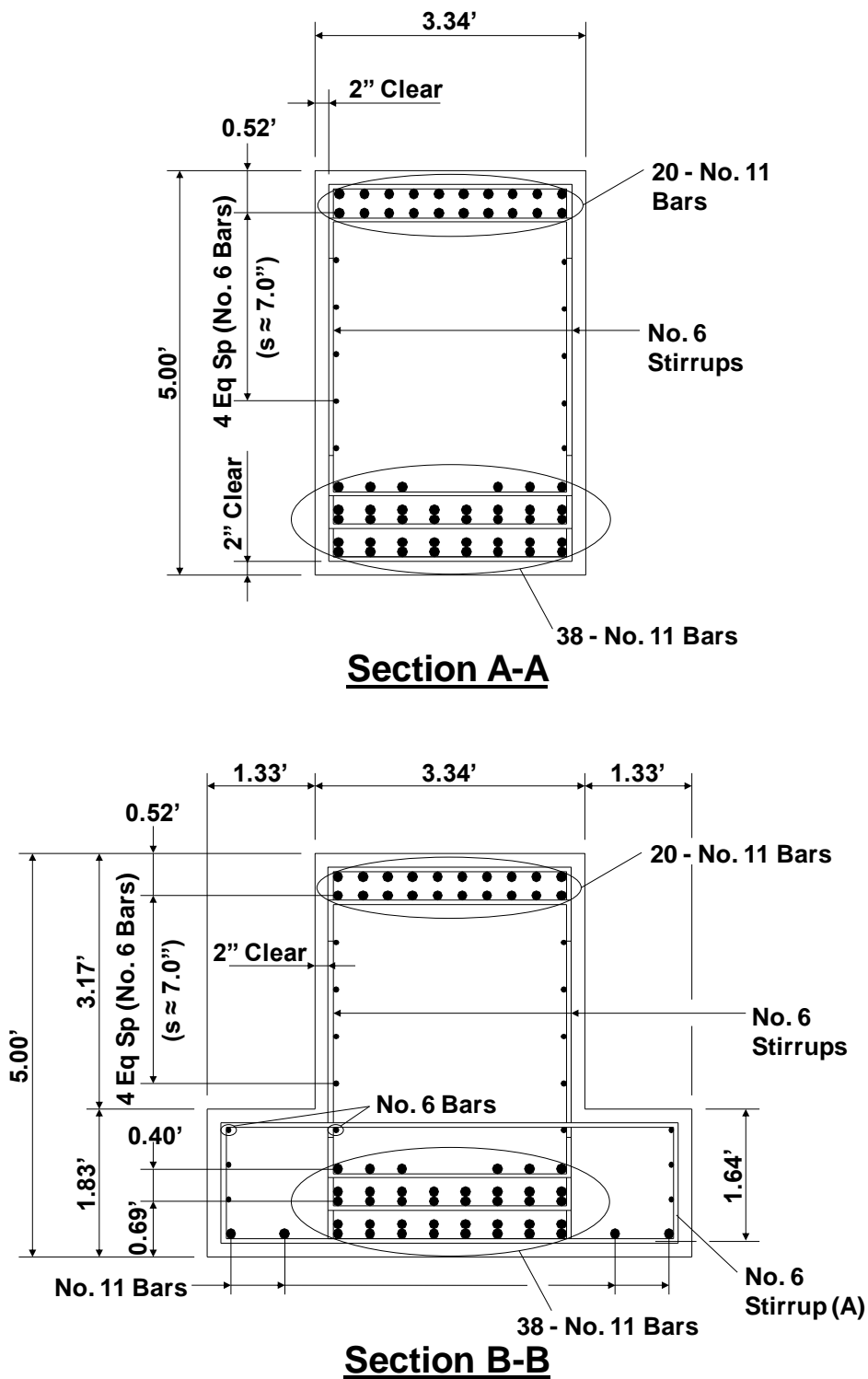


Figure 7.16: Reinforcement details – cross-sections (design per proposed STM specifications – simply supported case)

7.6 COMPARISON OF TWO STM DESIGNS – MOMENT FRAME AND SIMPLY SUPPORTED

The two designs, one assuming moment frame behavior and the other assuming simple supports at the columns, are compared in Table 7.1. Two main differences between the designs may be observed. First, the reinforcement details of the moment frame design implicitly allow for the flow of forces around the frame corners and permit moment to be transferred between the columns and the bent cap. During the design of the simply supported case, only vertical reactions were assumed to be transferred between the cap and the columns. Second, the design moment imposed at the midspan of the simply supported bent cap was significantly larger (compared to that of the continuous bent) and necessitated the use of more bottom chord reinforcement. Similarly, more compression reinforcement was needed to strengthen the back faces of the nodes along the top chord of the STM modeling the simply supported cap. (Although the number of longitudinal bars differs between the two designs, please note that the total static moment within the member is satisfied in both cases.) The number of stirrups provided in the stem along the length of the ledge also differs. The simply supported member contains a greater number of stirrups due to the reduced truss depth and the necessary addition of vertical ties to satisfy the 25-degree rule.

Table 7.1: Comparison of the two STM designs (moment frame versus simply supported)

	Moment Frame	Simply Supported
Beam-to-Column Connection	Full moment connection	Vertical reaction only
Bottom Chord Reinforcement (#11 Bars)	22 bars	38 bars
Top Chord Reinforcement (#11 Bars)	15 bars	20 bars
Stirrup Spacing along Ledge (#6 Stirrups)	$s = 5.5''$ (left) $s = 6''$ (right)	$s = 4.5''$ (left) $s = 5''$ (right)

The shear serviceability check also indicates possible differences in the behavior of the two designs when subjected to full service loads. The estimated diagonal cracking strength, V_{cr} , and the maximum service shear, V_{max} , for each critical region are summarized in Table 7.2. The formation of diagonal cracks is a possibility when the full service loads are applied to either the continuous or simply supported bent cap. However, design of the bridge substructure as a moment frame appears to reduce the possibility of diagonal cracking under service load levels (compare corresponding values of V_{max}/V_{cr} in Table 7.2 for both cases). In either case, the crack control reinforcement is provided to minimize the widths of cracks that may form.

For both designs, the size of the bent cap was found to be limiting. Considering the results of the shear serviceability check and the required amount of longitudinal reinforcement, resizing the bent cap may be the best solution for a more efficient and more serviceable design.

Table 7.2: Comparison of diagonal cracking strength to service shear (two STM designs)

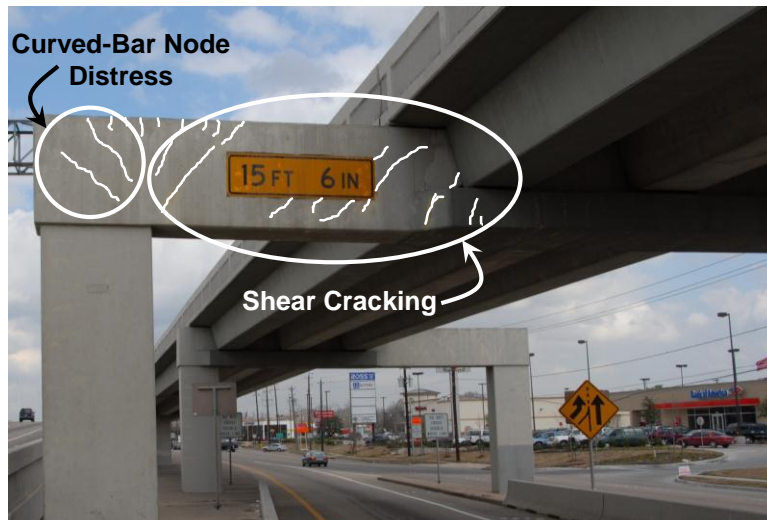
	Between Left Column and Beam Line 1		Between Right Column and Beam Line 3	
	Moment Frame	Simply Supported	Moment Frame	Simply Supported
V_{cr} (kips)	313	296	511	310
Maximum Shear Force, V_{max} (kips)	389	397	676	668
Ratio (V_{max}/V_{cr})	1.24	1.34	1.32	2.15

7.7 SERVICEABILITY BEHAVIOR OF EXISTING FIELD STRUCTURE

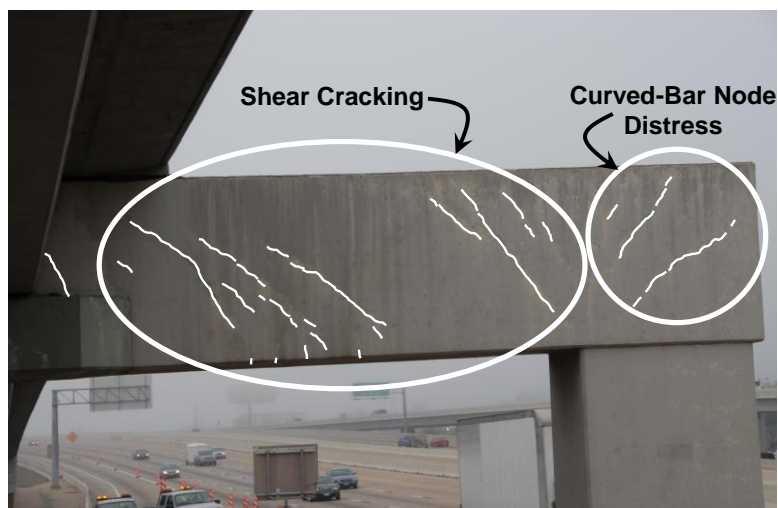
The inverted-T straddle bent cap presented in Examples 3a and 3b was previously designed by bridge engineers at TxDOT. The in-service structure was designed in accordance with the sectional design procedure of the AASHTO LRFD provisions. The

load case used for the STM design produces the largest shear force in the span between the left column (Column A) and Beam Line 1. The sectional design was completed under the assumption of continuous (moment frame) behavior. The geometry of the bent cap is the same for both the sectional and STM designs. The original specified compressive strength of the concrete, however, was increased from 3.6 ksi to 5.0 ksi to accommodate the controlling nodal strength checks.

Photographs of the field structure are presented in Figure 7.17. Significant diagonal crack formation can be observed. The shear serviceability check predicts the likelihood of diagonal cracking, suggesting that an increase in cross-sectional dimensions and/or the specified concrete compressive strength is necessary. Furthermore, the design of the curved-bar nodes located at the outside of the frame corners (refer to Section 6.4.6) indicated that a large bend radius is required for the longitudinal bars. Providing a smaller bend radius than required by the curved-bar node provisions likely contributed to the cracking observed at the outside of the frame corners in Figure 7.17.



(a)



(b)

Figure 7.17: Existing field structure (inverted-T straddle bent cap) – (a) Upstation; (b) Downstation

7.8 SUMMARY

The STM design of an inverted-T straddle bent cap was completed for one particular load case. The design assumed the bent cap was simply supported at the columns. The defining features and challenges of this design example (relative to Example 3a) are listed below:

- Developing a global STM that modeled an inverted-T bent cap as a simply supported member
- Defining a refined nodal geometry, allowing a more accurate strength check to be performed and the effect of compression steel to be considered

Following the STM design procedure, the moment frame design of the inverted-T (Example 3a) was compared with the simply supported design of the current example. Lastly, the serviceability behavior of the existing bent cap designed using sectional methods was discussed in relation to the requirements of the STM design.

Chapter 8. Example 4: Drilled-Shaft Footing

8.1 SYNOPSIS

The design of a deep drilled-shaft footing is presented for two unique load cases within this final example. The five-foot-thick footing supports a single column and is in turn supported by four drilled shafts. Research has shown that strut-and-tie modeling is appropriate for the design of such deep footings (Adebar et al., 1990; Cavers and Fenton, 2004; Park et al., 2008; Souza et al., 2009). The forces from the column flow to the four drilled shafts within a three-dimensional volume and necessitate the development of a three-dimensional STM. Attempts to streamline the design process through the use of a set of two-dimensional STMs may oversimplify the rather complex stress distribution within the footing and can lead to grossly unconservative specified amounts of reinforcement. The procedure to develop the three-dimensional STMs is clearly described and is intended to assist engineers with the development of STMs for other load cases that may be encountered.

There is an apparent lack of documented research on the STM design of deep pile caps or drilled-shaft footings, especially for load cases similar to those presented within this example. As a result, several design assumptions must be made through the course of this example. The broad design implications of the assumptions (in terms of safety and efficiency) are analyzed prior to implementation; the engineering judgments tend to err on the side of conservatism.

8.2 DESIGN TASK

8.2.1 Drilled-Shaft Footing Geometry

Elevation and plan views of the drilled-shaft footing geometry are shown in Figure 8.1. The five-foot-thick footing is 16 feet wide and 16 feet long. It supports a 7.50- by 6.25-foot rectangular column and is in turn supported by four drilled shafts, each 4.00 feet in diameter. The constants defined in Figure 8.1 will be used in future calculations.

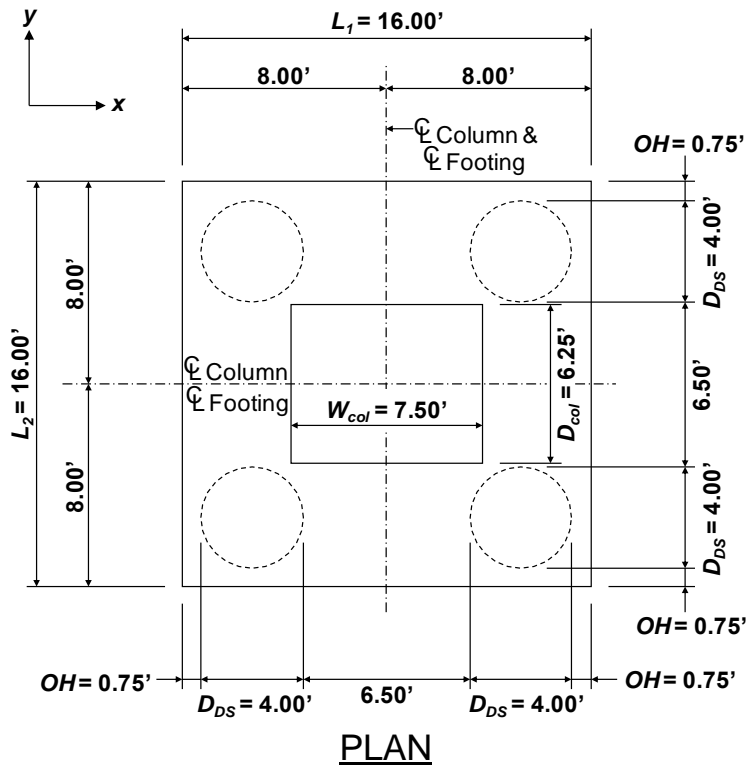
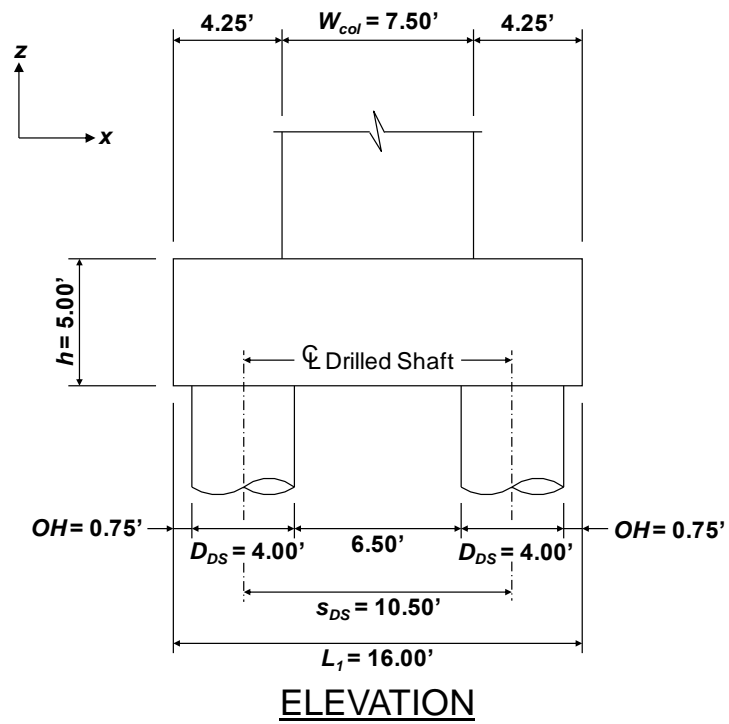


Figure 8.1: Plan and elevation views of drilled-shaft footing

8.2.2 First Load Case

In the first load case, the column is subjected to a combination of significant axial force and a moment about the strong axis (i.e. y-axis). When the load is transferred through the footing, all four of the drilled shafts will remain in compression. The factored load and moment for the first load case are shown in Figure 8.2.

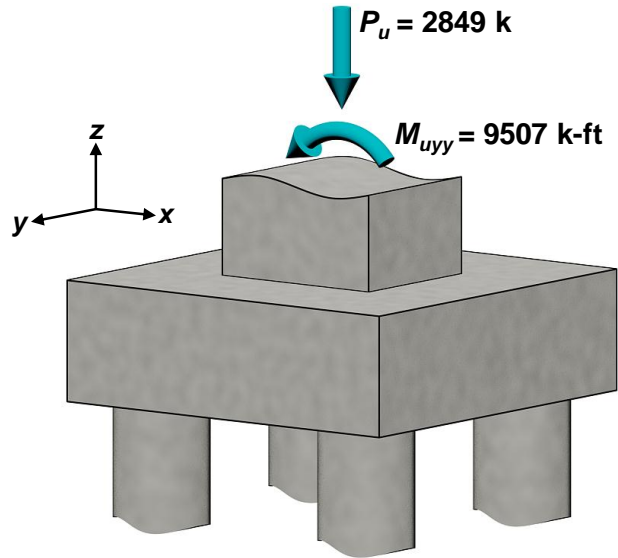


Figure 8.2: Factored load and moment of the first load case

8.2.3 Second Load Case

While the strong-axis moment demand on the column is similar, the magnitude of the axial force is less than half of that found in the first load case. The second load case results in tension within two of the four drilled shafts. The factored load and moment for the second load case are shown in Figure 8.3.

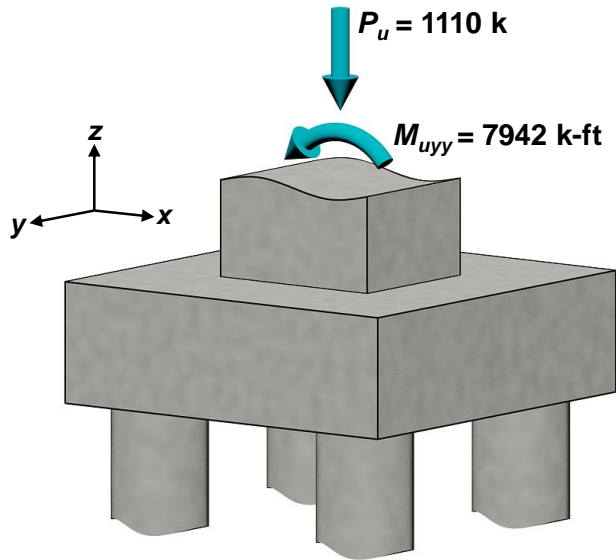


Figure 8.3: Factored load and moment of the second load case

This design example only considers the two load cases presented in Figures 8.2 and 8.3. Completion of the footing design is contingent on the consideration of all critical load cases.

8.2.4 Material Properties

- Concrete: $f'_c = 3.6 \text{ ksi}$
- Reinforcement: $f_y = 60 \text{ ksi}$

The material properties used within this design example meet TxDOT’s minimum specifications. TxDOT commonly specifies a concrete compressive strength, f'_c , of 3.6 ksi for drilled-shaft footings.

8.3 DESIGN PROCEDURE

Due to the close proximity of the column to each of the drilled shafts (relative to the footing depth), the footing is characterized as a D-region. In regards to the application of STM to pile caps and other three-dimensional D-regions, Park et al. (2008) state that there exists “a complex variation in straining not adequately captured by

sectional approaches.” The general STM procedure (refer to Section 2.3.3) has been adapted to the footing design, resulting in the steps listed below. The same design procedure will be followed for both load cases.

- Step 1: Determine the loads
- Step 2: Analyze structural component
- Step 3: Develop strut-and-tie model
- Step 4: Proportion ties
- Step 5: Perform strength checks
- Step 6: Proportion shrinkage and temperature reinforcement
- Step 7: Provide necessary anchorage for ties\

In the previous examples, the shear serviceability check typically concluded the STM design procedure. It should be noted that the diagonal cracking strength, V_{cr} , expression (refer to Section 2.12) was not calibrated for pile caps or deep footings and therefore does not apply to this three-dimensional problem. Provided that adequate clear cover is maintained, serviceability cracking of a pile cap or deep footing should not impact the performance of the member.

8.4 DESIGN CALCULATIONS (FIRST LOAD CASE)

8.4.1 Step 1: Determine the Loads

The forces imposed on the column will flow through the footing to each of the four drilled shafts. Please recall that strut-and-tie models (i.e. truss models) are incapable of resisting bending moments. In order to properly model the flow of forces through the footing, the axial force and bending moment (Figure 8.2) need to be redefined in terms of an equivalent force system (refer to Figure 8.4). The equivalent set of forces will be applied to the strut-and-tie model and, by definition, should produce the same axial load and moment as those shown in Figure 8.2. Since the applied forces flow through the footing to four drilled shafts, the equivalent set of forces should consist of four vertical

loads, each corresponding to a drilled-shaft reaction (each force in Figure 8.4(b) represents two of the loads that will be applied to the STM).

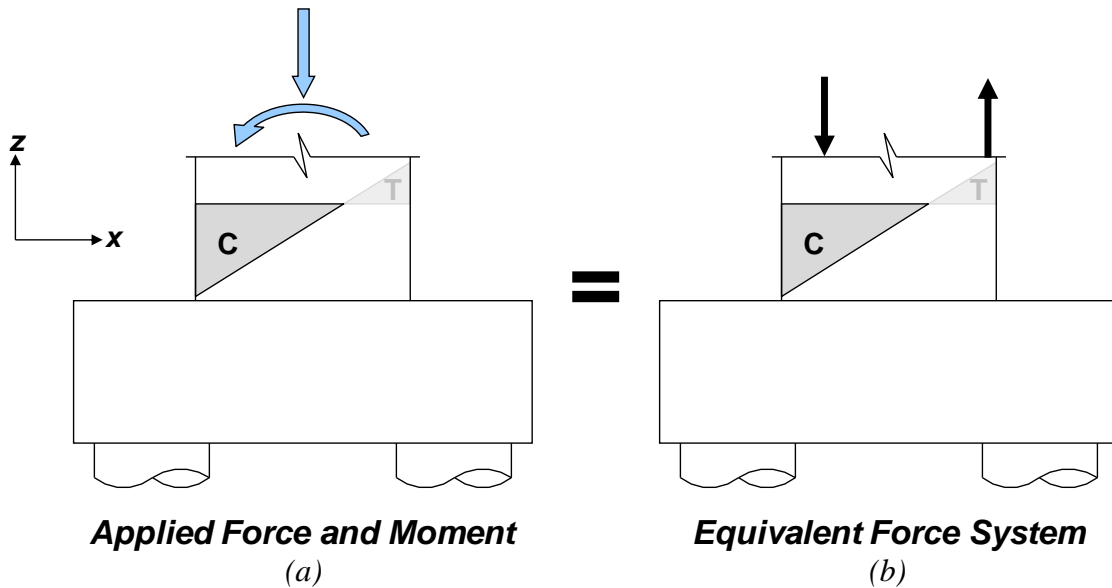


Figure 8.4: Developing an equivalent force system from the applied force and moment

To develop the equivalent force system, the elastic stress distribution over the column cross section is determined. The location of each of the four loads comprising the equivalent force system (relative to the column cross section) is then defined. Lastly, the magnitude of each force is calculated by establishing equilibrium.

The column cross section and corresponding linear stress distribution are illustrated in Figure 8.5. The positions of the four loads that comprise the equivalent force system are also shown in the column cross section. The two loads acting on the left are compressive (pushing downward on the footing), while the two loads acting on the right are tensile (pulling upward on the footing).

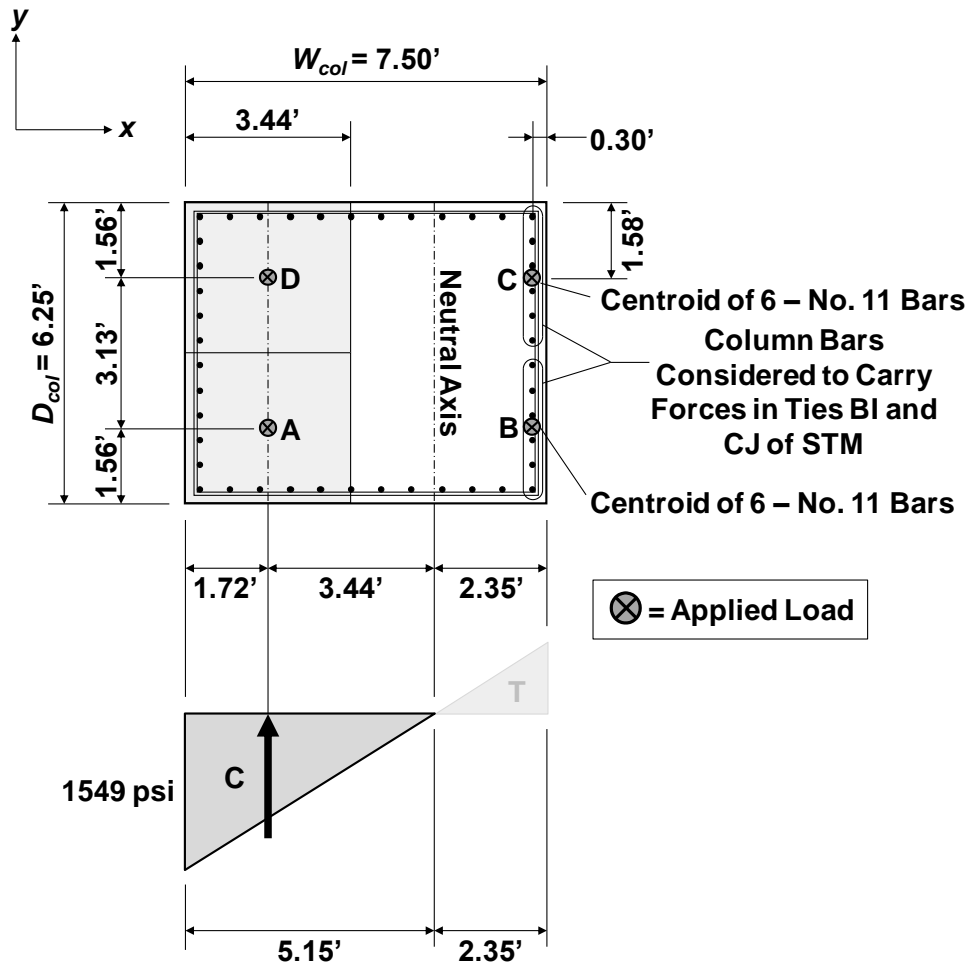


Figure 8.5: Linear stress distribution over the column cross section and the locations of the loads comprising the equivalent force system (first load case)

The locations of the two compressive forces are based on the linear stress diagram. The line of action for both forces coincides with the centroid of the compressive portion of the stress diagram, located 1.72 feet from the left face of the column. The compressive forces are transversely positioned at the quarter points of the column depth, D_{col} , or 1.56 feet from the top and bottom of the column section in Figure 8.5.

The longitudinal column steel configuration of Figure 8.5 (detailed in Figure 8.6 below) is an assumption. This reinforcement should be specified on the basis of the final column design, which is beyond the scope of this design example. The reinforcement on

the right face (or tension face) of the column will be most effective (relative to the bars elsewhere in the cross section) in resisting the tension due to the applied bending moment. The two tensile forces (which complete the equivalent force system) are therefore conservatively assumed to act at the centroid of this tension-face reinforcement, located 0.30 feet from the right face. Moreover, each of the tensile forces is transversely positioned at the centroid of either the lower or upper half of the selected column reinforcement. Each of the vertical ties (corresponding to the tensile forces) located beneath the column (Ties BI and CJ in Figure 8.8) therefore consists of six bars.

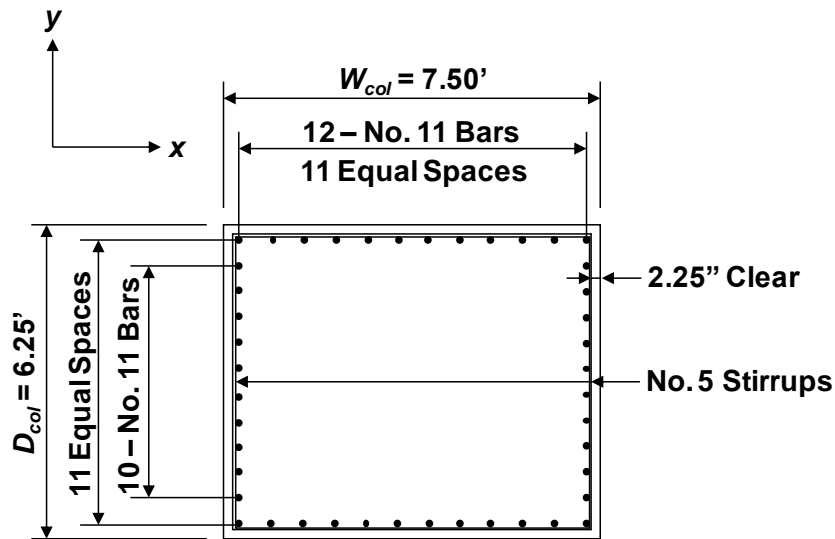


Figure 8.6: Assumed reinforcement layout of the column section

The magnitudes of the compressive and tensile forces are now determined so that the equivalent force system produces the same axial load, moment, and linear stress distribution as those respectively shown in Figures 8.2 and 8.5. This is accomplished by establishing equilibrium between the original and equivalent force systems. In the following equations, F_{Comp} is the total compressive force acting on the footing, or the sum of the loads acting at points A and D in Figure 8.5, and F_{Tens} is the total tensile force, or the sum of the loads acting at points B and C.

$$\begin{cases} F_{Comp} - F_{Tens} = P_u = 2849 \text{ kip} \\ F_{Comp} \left(\frac{7.50 \text{ ft}}{2} - 1.72 \text{ ft} \right) + F_{Tens} \left(\frac{7.50 \text{ ft}}{2} - 0.30 \text{ ft} \right) = M_{uyy} = 9507 \text{ k-ft} \end{cases}$$

$$\text{Solving: } F_{Comp} = 3527.1 \text{ kip} \quad F_{Tens} = 678.1 \text{ kip}$$

In the second equation, 7.50 ft is the value of W_{col} , and 1.72 ft and 0.30 ft are taken from Figure 8.5. The four loads acting on the STM from the column are then determined as follows:

$$F_A = F_D = \frac{F_{Comp}}{2} = 1763.6 \text{ kip (Compression)}$$

$$F_B = F_C = \frac{F_{Tens}}{2} = 339.1 \text{ kip (Tension)}$$

These forces are shown acting on the STM of Figure 8.8.

8.4.2 Step 2: Analyze Structural Component

The footing is now analyzed to determine the reaction forces. The reactions are assumed to act at the center of the 4-foot diameter drilled shafts (Figure 8.7). Since all four drilled shafts are equidistant from the column, the axial force is distributed evenly among the shafts (first term in the equations below). Moment equilibrium of the footing is enforced by the second term in each of the following equations.

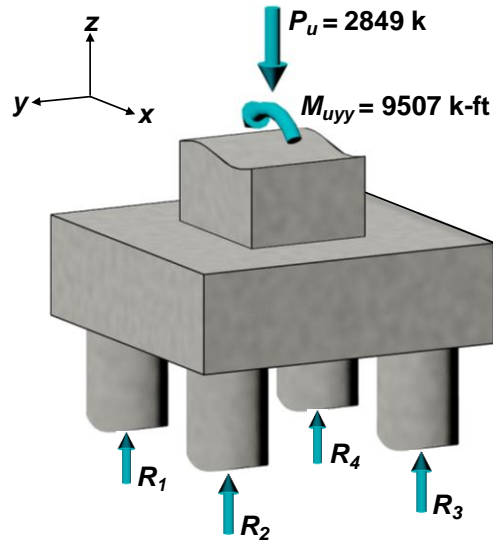


Figure 8.7: Applied loading and drilled-shaft reactions (first load case)

$$R_1 = R_4 = \frac{P_u}{4} + \frac{1}{2} \left(\frac{M_{uyy}}{s_{DS}} \right) = \frac{2849 \text{ kip}}{4} + \frac{1}{2} \left(\frac{9507 \text{ k-ft}}{10.50 \text{ ft}} \right) = 1165.0 \text{ kip (Compression)}$$

$$R_2 = R_3 = \frac{P_u}{4} - \frac{1}{2} \left(\frac{M_{uyy}}{s_{DS}} \right) = \frac{2849 \text{ kip}}{4} - \frac{1}{2} \left(\frac{9507 \text{ k-ft}}{10.50 \text{ ft}} \right) = 259.5 \text{ kip (Compression)}$$

The value of s_{DS} is shown in Figure 8.1. The four reactions are applied to the STM of Figure 8.8. Please note that all the drilled shafts are in compression.

8.4.3 Step 3: Develop Strut-and-Tie Model

The STM for the first load case is depicted in axonometric and plan views within Figures 8.8 and 8.9. Development of the three-dimensional STM was deemed successful if and only if (1) equilibrium was satisfied at every node and (2) the truss reactions (as determined from a linear elastic analysis of the truss model) were equivalent to the reactions of Section 8.4.2. The development of the STM is explained in detail within this section.

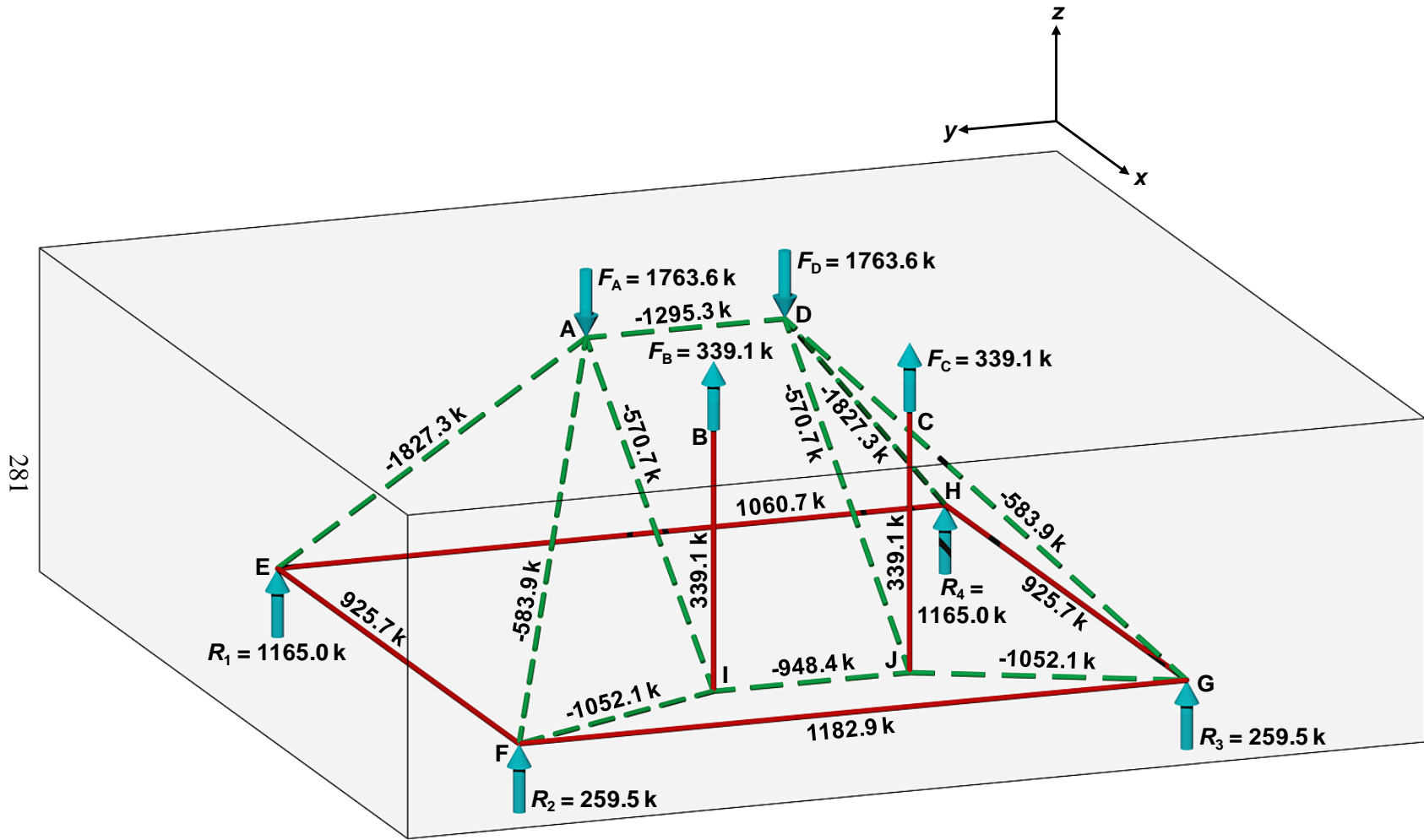


Figure 8.8: Strut-and-tie model for the drilled-shaft footing – axonometric view (first load case)

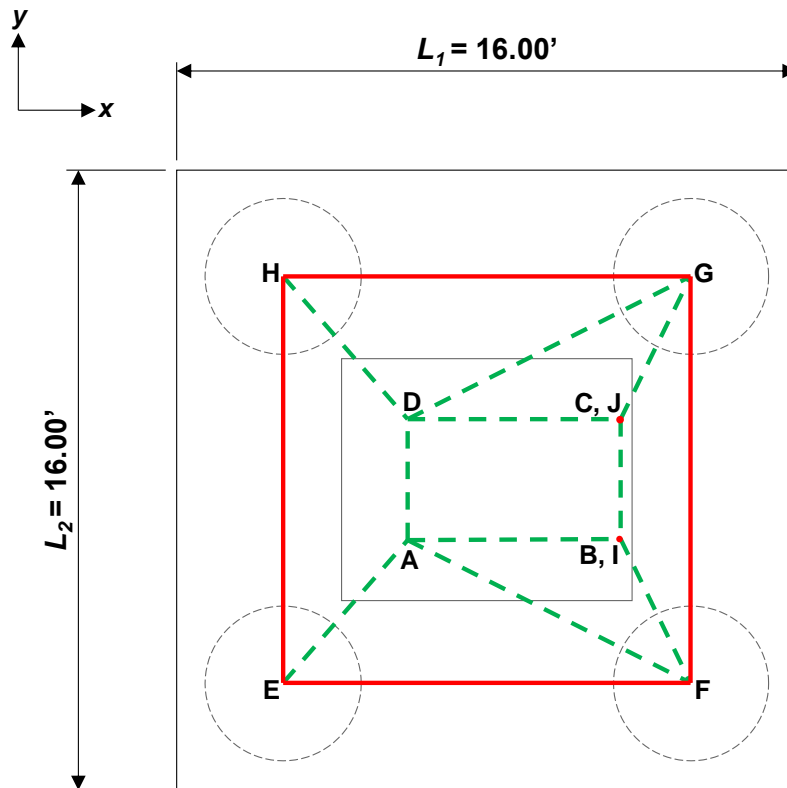


Figure 8.9: Strut-and-tie model for the drilled-shaft footing – plan view (first load case)

In order to successfully develop the three-dimensional STM, the designer must first determine (1) the lateral (x, y) location of each applied load and support reaction and (2) the vertical (z) position of the planes in which the upper and lower nodes of the STM lie. The lateral locations of the applied loads (relative to the column cross section) were previously determined in Section 8.4.1, and the reactions are assumed to act at the center of the circular shafts. The following discussion, therefore, centers on the vertical placement of the bottom ties and top strut (Strut AD).

The position of the bottom horizontal ties relative to the bottom surface of the footing will be defined first. These ties (Ties EF, FG, GH, and EH) represent the bottom mat of steel within the footing. Their location should therefore be based on the centroid of these bars. Four inches of clear cover will be provided from the bottom face of the footing to the first layer of the bottom mat reinforcement, as illustrated in Figure 8.10.

Assuming the same number of #11 bars will be used in both orthogonal directions, the centroid of the bottom mat will be located $4 \text{ in.} + 1.41 \text{ in.} = 5.4 \text{ in.}$ above the bottom face of the footing.

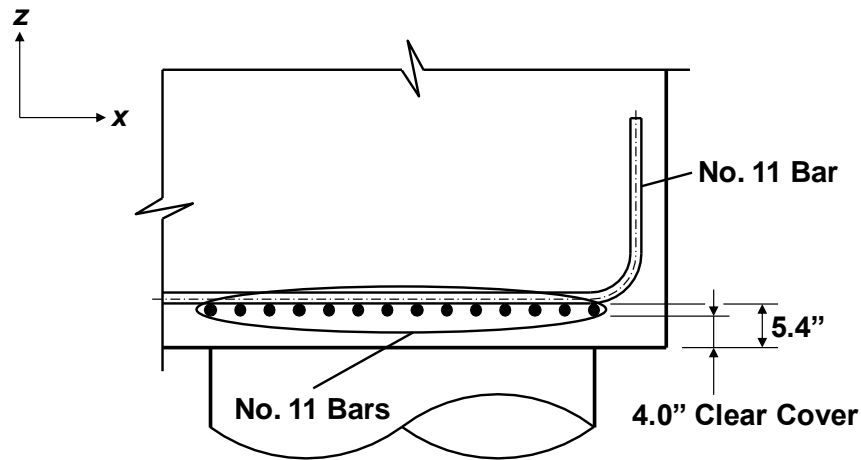


Figure 8.10: Determining the location of the bottom horizontal ties of the STM

The vertical position of the nodes (and intermediate strut) located directly beneath the column (Nodes A and D as well as Strut AD in Figure 8.8) must also be determined. The position of these nodes relative to the top surface of the footing is a value of high uncertainty, and further experimental research is needed to determine their actual location (Souza et al., 2009; Widiyanto and Bayrak, 2011; Windisch et al., 2010). The potential nodal positions, some of which have been recommended in the literature for the STM design of pile caps, are listed below and summarized in Figure 8.11.

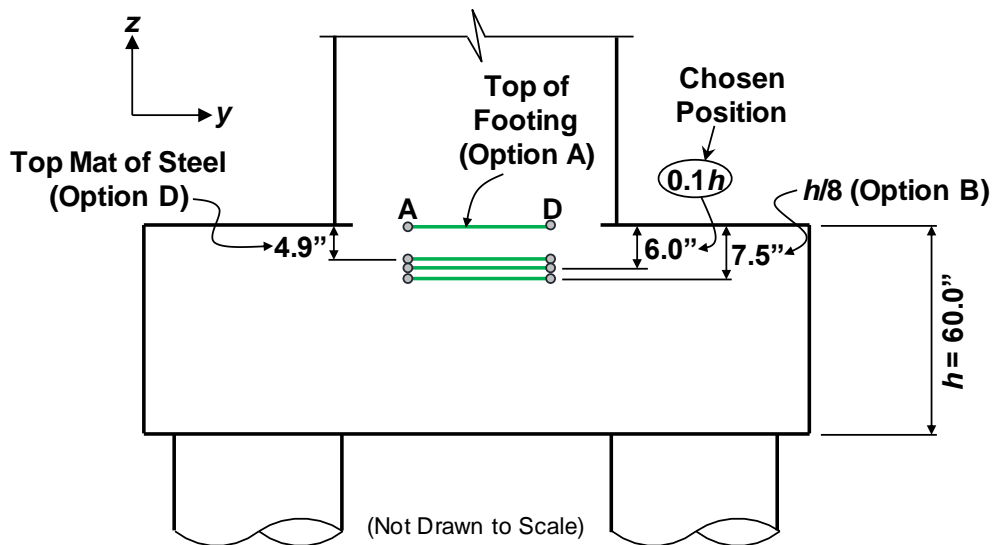


Figure 8.11: Potential positions of Nodes A and D (and Strut AD)

- Option A: Position the nodes at the top surface of the footing (Adebar, 2004; Adebar and Zhou, 1996) – If the nodes at the top of the STM are assumed to be located at the top surface of the footing (i.e. column-footing interface), effective triaxial confinement of these nodes cannot be guaranteed and more conservative estimates of the nodal strengths should therefore be used. (Please note that the strength check procedure introduced in Section 8.4.5 requires that all nodes be triaxially confined within the footing.) Furthermore, positioning the nodes at the top surface of the footing results in a large overall STM depth (analogous to a large flexural moment arm), and the approach, therefore, may potentially underestimate the bottom tie forces (relative to the other options listed below).
- Option B: Assume that the total depth of the horizontal strut under the column (Strut AD in Figure 8.8) is $h/4$, where h is the depth of the footing – The center of the strut, as well as Nodes A and D, would therefore be located a distance of $h/8$ from the top of the footing. This approach is recommended in Park et al. (2008) and Windisch et al. (2010). Both of these sources reference a suggestion made by Paulay and Priestley (1992) for the depth of the flexural compression zone of an

elastic column at a beam-column joint. Considering the nature of the current design, application of this option to the column-footing interface may not be accurate.

- Option C: Position the nodes based on the depth of the rectangular compression stress block as determined from a flexural (i.e. beam) analysis of the footing – The footing is an exceedingly deep member subjected to loads in close proximity to one another. The footing is therefore expected to exhibit complex D-region behavior that is in no way related to the behavior of a flexural member; application of flexural theory would be improper.
- Option D: Assume the nodes beneath the column coincide with the location of the top mat reinforcement – For the load case currently under consideration, the top mat of steel is necessary to satisfy requirements for shrinkage and temperature reinforcement. If horizontal ties existed within the STM near the top surface of the footing, placing the upper members of the STM at the centroid of the top mat reinforcement is viable. In fact, this methodology is used to develop the STM for the second load case (Figure 8.19). For the STM of Figure 8.8, however, there is no fundamental reason why the nodal locations must coincide with the reinforcement.

Each of the four options listed above has drawbacks that cannot be definitely resolved. Given the uncertainty related to this detail, the selected location of the nodes should result in a conservative design. It is important to consider that as the top nodes are moved further into the footing (1) the demands on, and requisite reinforcement for, the bottom horizontal ties will increase and (2) the reliability of the effects of triaxial confinement will increase. Considering these conditions, the nodes are placed at a distance of $0.1h$, or 6.0 inches, from the top surface of the footing (refer to Figure 8.11). This location is not significantly different from the position of the top mat of steel, offering consistency with the geometry of the STM that will be developed for the second load case. Although there is a high level of uncertainty regarding the nodal locations,

Widianto and Bayrak (2011) state that “it is believed...the final design outcome is not very sensitive to the exact location of the nodal zone underneath the column.”

To summarize, the distance from the bottom horizontal ties of the STM (Figure 8.8) to the bottom surface of the footing is 5.4 inches, and the distance of Nodes A and D from the top surface of the footing is assumed to be 6.0 inches. Therefore, the total height of the STM is $60.0 \text{ in.} - 5.4 \text{ in.} - 6.0 \text{ in.} = 48.6 \text{ in.}$

Further development of the three-dimensional STM is based upon (1) recognition of the most probable load paths (i.e. elastic flow of forces), (2) consideration of standard construction details, (3) a basic understanding of footing behavior, and (4) multiple sequences of trial-and-error to establish equilibrium. The logic underlying the development of the STM in Figure 8.8 is briefly outlined here for the benefit of the designer.

To begin, tensile forces acting at Nodes B and C will require vertical ties to pass through the depth of the footing (to Nodes I and J located along the bottom of the STM). Ties should almost always be oriented perpendicularly or parallel to the primary axes of the structural member; inclined reinforcement is rarely used in reinforced concrete construction. The tensile force in the vertical ties extending from Nodes B and C will be equilibrated at Nodes I and J by compressive stresses originating at Nodes A and D; these load paths are idealized as Struts AI and DJ. Moreover, Struts AE, AF, DG, and DH represent the flow of compressive stresses from Nodes A and D to the near supports (Nodes E and H) and far supports (Nodes F and G). Final equilibrium at Nodes A and D is established through the addition of Strut AD. The diagonal flow of compressive stresses to each of the drilled shafts (via Struts AE, AF, DG, and DH) will induce tension at the bottom of the footing; this is accommodated by the addition of Ties EF, FG, GH, and EH. The remaining horizontal struts are added near the bottom of the footing to establish lateral equilibrium at Nodes F, G, I, and J. As with all STMs, the angle between a strut and a tie entering the same node must not be less than 25 degrees (refer to Section 2.7.2). The STM in Figure 8.8 satisfies this requirement (the angle between Strut FI and Tie FG and the angle between Strut GJ and Tie FG are both 25.87 degrees).

While developing the STM, the designer should ensure that equilibrium can be achieved at each node of the truss model. In other words, enough truss members should join at each node so that equilibrium can be established in the x , y , and z directions. Furthermore, a symmetrical footing geometry and loading should result in a symmetrical strut-and-tie model.

Once the STM geometry is defined, the truss member forces and drilled-shaft reactions are determined from a linear elastic analysis of the completed STM. The reactions at the drilled shafts resulting from the truss analysis should be the same as those previously determined in Section 8.4.2, and equilibrium must be satisfied at each node. If equilibrium cannot be established, the STM must be revised.

The use of structural analysis software is recommended. The model can be easily modified within a software package and analyzed until a satisfactory STM is developed. As discussed in Section 2.7.2, multiple valid STMs may exist, and the designer should use engineering judgment to determine which model best represents the elastic flow of forces within the structural component. Another valid STM for the load case under consideration is shown in Figure 8.12. While it was possible to establish equilibrium, the STM does not accurately capture the direct flow of compressive stresses from Nodes A and D to each of the drilled shafts.

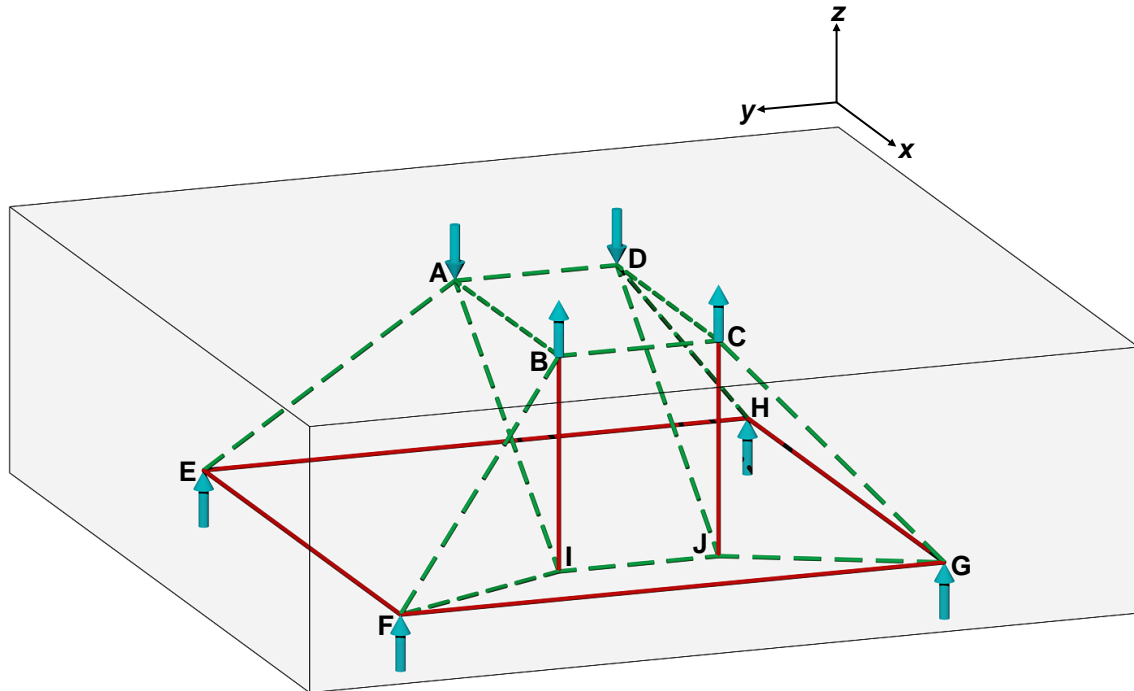


Figure 8.12: Alternative strut-and-tie model for the first load case

8.4.4 Step 4: Proportion Ties

The tie forces shown in Figure 8.8 are used to proportion the horizontal and vertical ties within the footing. The bottom mat reinforcement will be specified first, and as previously mentioned, #11 bars will be used.

Ties EF and GH

The forces in Ties EF and GH are equal due to the symmetry of the loading. The number of bars required for each tie is:

$$\begin{aligned}
 \text{Factored Load:} & & F_u &= 925.7 \text{ kip} \\
 \text{Tie Capacity:} & & \phi \cdot f_y \cdot A_{st} &= F_u \\
 & & (0.9)(60 \text{ ksi})A_{st} &= 925.7 \text{ kip} \\
 & & A_{st} &= 17.14 \text{ in}^2
 \end{aligned}$$

$$\text{Number of \#11 bars required: } 17.14 \text{ in}^2 / 1.56 \text{ in}^2 = 11.0 \text{ bars}$$

Use 11 - #11 bars

Ties FG and EH

In consideration of potential load reversal and constructability concerns, the reinforcement comprising Ties FG and EH will be based upon the controlling tie force. The force in Tie FG supersedes that of Tie EH, and the required reinforcement is:

$$\begin{aligned} \text{Factored Load:} & \quad F_u = 1182.9 \text{ kip} \\ \text{Tie Capacity:} & \quad \varphi \cdot f_y \cdot A_{st} = F_u \\ & \quad (0.9)(60 \text{ ksi})A_{st} = 1182.9 \text{ kip} \\ & \quad A_{st} = 21.91 \text{ in}^2 \end{aligned}$$

$$\text{Number of \#11 bars required: } 21.91 \text{ in}^2 / 1.56 \text{ in}^2 = 14.0 \text{ bars}$$

Use 14 - #11 bars

TxDOT's *Bridge Design Manual - LRFD* (2009) states that "[t]he tension tie reinforcement must be close enough to the drilled shaft to be considered in the truss analysis. Therefore, the tension tie reinforcement must be within a 45 degree distribution angle." In the current example, the tie reinforcement along the bottom of the footing will be concentrated directly over the drilled shafts in order to simplify the design. The length over which the reinforcement could be spaced and the actual reinforcement configuration are shown in Figure 8.13.

Please recall that the position of the bottom horizontal ties of the STM coincides with the bottom mat reinforcement, assuming the same number of bars is provided in both orthogonal directions. Although the specified reinforcement in each direction differs slightly (11 bars versus 14 bars), the discrepancy between the actual centroid of the bars and the position of the horizontal ties is negligible.

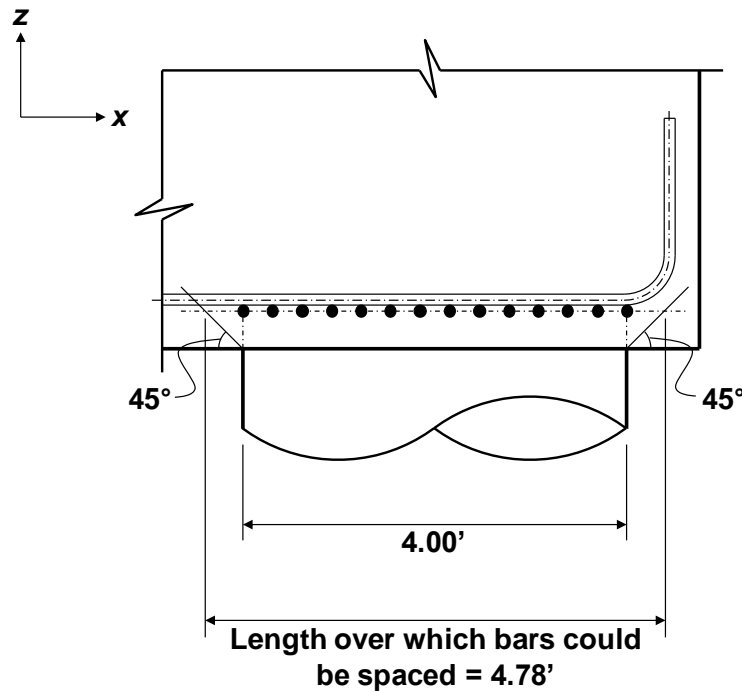


Figure 8.13: Spacing of bottom mat reinforcement

Ties BI and CJ

Next, the reinforcement requirements for Ties BI and CJ are determined. The forces in these ties are equal, and the amount of reinforcement required for each tie is:

Factored Load: $F_u = 339.1 \text{ kip}$
 Tie Capacity: $\phi \cdot f_y \cdot A_{st} = F_u$
 $(0.9)(60 \text{ ksi})A_{st} = 339.1 \text{ kip}$
 $A_{st} = 6.28 \text{ in}^2$

Number of #11 bars required: $6.28 \text{ in}^2 / 1.56 \text{ in}^2 = 4.0 \text{ bars}$

Use 4 - #11 bars (6 - #11 bars are provided)

The reinforcement along the column face (12-#11 bars as specified in Section 8.4.1) will be extended into the footing (through a lap splice) and should satisfy the requirements of Ties BI and CJ.

8.4.5 Step 5: Perform Strength Checks

The nodal regions within a three-dimensional STM have very complex geometries that complicate the strength checks. Although some attempts have been made to approximate nodal geometries within three-dimensional STMs (Klein, 2002; Martin and Sanders, 2007; Mitchell et al., 2004), the value of precisely defining the geometries of such complicated nodal regions is limited. A simplified procedure will therefore be recommended to ensure the strengths of the nodes within three-dimensional STMs are adequate.

A simplified nodal strength check procedure was developed on the basis of a literature search regarding the STM design of pile caps and deep footings. The results of the literature review are briefly summarized within the following points. It should be noted that the review was generally inconclusive; additional research is needed to refine the STM design procedure for pile caps and deep footings.

- Widianto and Bayrak (2011): The authors present the STM design of a column footing supported on H-piles. In lieu of conducting strength checks at each singular node, the strengths of all nodal regions were deemed sufficient by limiting the bearing stress imposed by the piles and column pedestal to $0.85f'_c$. The bearing stress limit was based on recommendations made within the Concrete Design Handbook (2005) of the Cement Association of Canada (CAC). The authors also make special note of the likelihood for superior nodal confinement (i.e. enhanced concrete compressive strength) within large, three-dimensional structures.
- Schlaich et al. (1987): The authors suggest that bearing stress limitations, when accompanied by proper reinforcement detailing, are sufficient to ensure adequate nodal strengths (f_{cd} is the concrete compressive design strength in the excerpt below):

Since singular nodes are bottlenecks of the stresses, it can be assumed that an entire D-region is safe, if the pressure under the most heavily loaded bearing

plate or anchor plate is less than $0.6 f_{cd}$ (or in unusual cases $0.4 f_{cd}$) and if all significant tensile forces are resisted by reinforcement and further if sufficient development lengths are provided for the reinforcement.

- Adebar et al. (1990): The authors conclude that “[t]he maximum bearing stress is a good indicator of the likelihood of a strut splitting failure...To prevent shear failures, the maximum bearing stress on deep pile caps should be limited to about $1.0f'_c$.” It should be noted that the recommendation of Adebar et al. (1990) was made with limited experimental verification.
- Souza et al. (2009): The authors reveal that the $1.0f'_c$ bearing stress limit proposed by Adebar et al. (1990) is not valid for all ranges of the shear span-to-depth ratio. If the shear span-to-depth ratio is limited to 1.0, the authors suggest that a limiting bearing stress of $1.0f'_c$ will normally result in ductile failures.
- Adebar and Zhou (1996): The authors recommend combining the concept of a bearing stress limit with traditional provisions for one-way and two-way shear design. The proposed maximum bearing stress limit depends on the confinement and aspect ratio (height-to-width ratio) of the compression strut entering the node under consideration. The initial pile cap depth is based on application of the one-way and two-way shear design procedures, and the reinforcement is specified according to an STM analysis. Potential concerns for this design method are addressed in Park et al. (2008) and Cavers and Fenton (2004).
- Park et al. (2008): As part of the research conducted by Park et al. (2008), the design approach recommended by Adebar and Zhou (1996) was compared to an experimental database of 116 pile cap tests. Although the approach did not overpredict any of the specimens’ strengths, the authors conclude that the bearing capacity requirement yields unconservative strength estimates for many pile caps that were reported to have failed in shear (rather than longitudinal yielding of the primary ties). Therefore, the nodal bearing stress limit “is not a good indicator for pile cap strengths.”

Additional discussions regarding the application of strut-and-tie modeling to pile caps are included within Cavers and Fenton (2004) and Adebar (2004); neither reference provides the insight necessary to complete the footing design. Despite the inconclusive nature of the literature review, two important observations should be noted:

1. Pile cap and deep footing researchers are reluctant to recommend STM design procedures that require determination of the three-dimensional nodal geometries. It is recognized that such an approach would be overly cumbersome.
2. A majority of the references recommend a design philosophy that includes a bearing stress checks and proper reinforcement detailing. The primary uncertainty related to the approach is rooted in the inability to accurately define a bearing stress limitation; a problem that will only be reconciled with additional tests.

The recommendation of a conservative approach to the STM design of pile caps and deep footings is appropriate given the uncertainty noted above. Future experimental results will enable refinement of the recommendations in terms of both safety and efficiency.

In consideration of the former observations, the guidelines outlined here will forgo determination of the three-dimensional nodal geometries in favor of a conservative bearing stress limitation. The stress limitation ensures the strengths of all nodal faces within the STM are adequate. The nodal strength check guidelines for pile caps and footings are:

- Position all nodes within the confines of the footing or pile cap. In particular, the nodes directly under a column should not be placed at the column-footing interface.
- Limit the compressive bearing stress on the footing or pile cap to $\nu f'_c$, where ν is the concrete efficiency factor defined in the STM specifications of Chapter 3. This limitation is conservative in regards to the recommendations made in the literature.

- Neglect the triaxial confinement factor, m , for added conservatism. More testing is needed to verify the benefits of triaxial confinement in deep footings and pile caps.

Referring to the STM shown in Figure 8.8, the critical bearing stresses occur at Nodes A and D and Nodes E and H. The strengths of these bearing faces are checked below according to the proposed procedure.

Nodes E and H (CTT) – Bearing Check

The forces and bearing areas at both Nodes E and H are the same and, therefore, only necessitate one check. The bearing area of a 4-foot diameter drilled shaft is:

$$\text{Bearing Area: } A_{cn} = \frac{\pi}{4} D_{DS}^2 = \frac{\pi}{4} (48.0 \text{ in})^2 = 1809.6 \text{ in}^2$$

Nodes E and H are CTT nodes, and the corresponding concrete efficiency factor, ν , is determined to be 0.65 (see calculation below). The bearing strength check for Nodes E and H is performed as follows:

BEARING AT NODES E AND H

Factored Load:	$F_u = 1165.0 \text{ kip}$
Efficiency:	$\nu = 0.85 - \frac{3.6 \text{ ksi}}{20 \text{ ksi}} = 0.67 > 0.65$
	$\therefore \text{ Use } \nu = 0.65$
Concrete Capacity:	$f_{cu} = m \cdot \nu \cdot f'_c = (1)(0.65)(3.6 \text{ ksi}) = 2.34 \text{ ksi}$
	$\phi \cdot F_n = (0.7)(2.34 \text{ ksi})(1809.6 \text{ in}^2)$
	$= 2964 \text{ kip} > 1165.0 \text{ kip} \text{ OK}$

Therefore, the bearing strength of Nodes E and H satisfy the proposed strength check procedure.

Nodes A and D (CCC) – Bearing Check

The loads and bearing areas are the same for both Nodes A and D. The locations of the loads as illustrated in Figure 8.5 are assumed to be at the center of the bearing

areas. Therefore, the bearing area for each node, as indicated by the shaded regions on the column section in Figure 8.5, is:

$$\text{Bearing Area: } A_{cn} = (3.44 \text{ ft}) \left(\frac{6.25 \text{ ft}}{2} \right) = 10.74 \text{ ft}^2 = 1546.4 \text{ in}^2$$

Nodes A and D are CCC nodes, and the strengths of their bearing faces are determined as follows:

BEARING AT NODES A AND D

Factored Load:	$F_u = 1763.6 \text{ kip}$
Efficiency:	$\nu = 0.85$
Concrete Capacity:	$f_{cu} = m \cdot \nu \cdot f'_c = (1)(0.85)(3.6 \text{ ksi}) = 3.06 \text{ ksi}$
	$\varphi \cdot F_n = (0.7)(3.06 \text{ ksi})(1546.4 \text{ in}^2)$
	$= 3312 \text{ kip} > 1763.6 \text{ kip} \text{ OK}$

Therefore, the bearing strength of Nodes A and D satisfy the proposed procedure.

Since the strengths of all the bearing areas of the footing satisfy the proposed strength check procedure, all nodal strengths within the STM are adequate to resist the applied loads.

8.4.6 Step 6: Proportion Shrinkage and Temperature Reinforcement

Although the crack control reinforcement requirements of the proposed STM specifications (see Chapter 3) do not apply to footings (consistent with current AASHTO LRFD provisions), shrinkage and temperature reinforcement in accordance with Article 5.10.8 of AASHTO LRFD (2010) should be provided. The following expression defines the reinforcement necessary (per foot) in both orthogonal directions on each face of the footing:

$$A_s \geq \frac{1.30bh}{2(b+h)f_y} \tag{8.1}$$

$$0.11 \leq A_s \leq 0.60$$

where A_s is the area of reinforcement on each face and in each direction with units of $\text{in.}^2/\text{ft}$, and b and h are the least width and thickness of the component section, respectively, with units of inches. For the drilled-shaft footing, the value of b is 16 feet, or 192 inches, and the value of h is 5 feet, or 60 inches. Therefore, the required shrinkage and temperature reinforcement for the footing is:

$$A_s \geq \frac{1.30bh}{2(b+h)f_y} = \frac{1.30(192 \text{ in})(60 \text{ in})}{2(192 \text{ in} + 60 \text{ in})(60 \text{ ksi})} = 0.50 \text{ in}^2/\text{ft}$$

To satisfy this requirement, #7 bars will be provided in both directions along each face of the footing except for the bottom face, where #11 bars will be evenly spaced between the drilled shafts. Article 5.10.8 also states that the spacing between the bars used as shrinkage and temperature reinforcement shall not exceed 12 inches for footings with a thickness greater than 18 inches. The area of the reinforcement provided (A_b for #7 bars = 0.60 in.^2 and A_b for #11 bars = 1.56 in.^2) is greater than that required per linear foot (0.50 in.^2); therefore, the maximum spacing requirement controls the design. With the exception of the bottom face (featuring #11 bars), #7 bars will be spaced at approximately 12 inches in both orthogonal directions. (Final reinforcement details are provided in Section 8.6.)

8.4.7 Step 7: Provide Necessary Anchorage for Ties

Ties EF, FG, GH, and EH

Each tie must be fully developed at the point where the centroid of the reinforcement exits the extended nodal zone. Anchorage of the ties representing the bottom mat reinforcement (Ties EF, FG, GH, and EH) will be considered first. The complex geometries of the nodes and extended nodal regions remain undefined; determination of the available development length is therefore impossible. A conservative assumption will be made in lieu of the standard approach. First, the circular drilled shafts are idealized as square shafts of the same cross-sectional area. The dimension of each square area, l_b , is:

$$\text{Drilled Shaft Cross-Sectional Area} = \frac{\pi}{4} D_{DS}^2 = \frac{\pi}{4} (48.0 \text{ in})^2 = 1809.6 \text{ in}^2$$

$$l_b = \sqrt{1809.6 \text{ in}^2} = 42.5 \text{ in}$$

The critical section for development of the bottom ties is assumed to correspond with the interior edge of the equivalent square shafts (refer to Figure 8.14). Therefore, the available development length for each of the bottom ties is:

$$\begin{aligned} \text{Available length} &= OH + D_{DS}/2 + l_b/2 - 3 \text{ in} \\ &= 9.0 \text{ in} + 48.0 \text{ in}/2 + 42.5 \text{ in}/2 - 3 \text{ in} = 51.3 \text{ in} \end{aligned}$$

All the dimensional values within this calculation are shown in Figure 8.14.

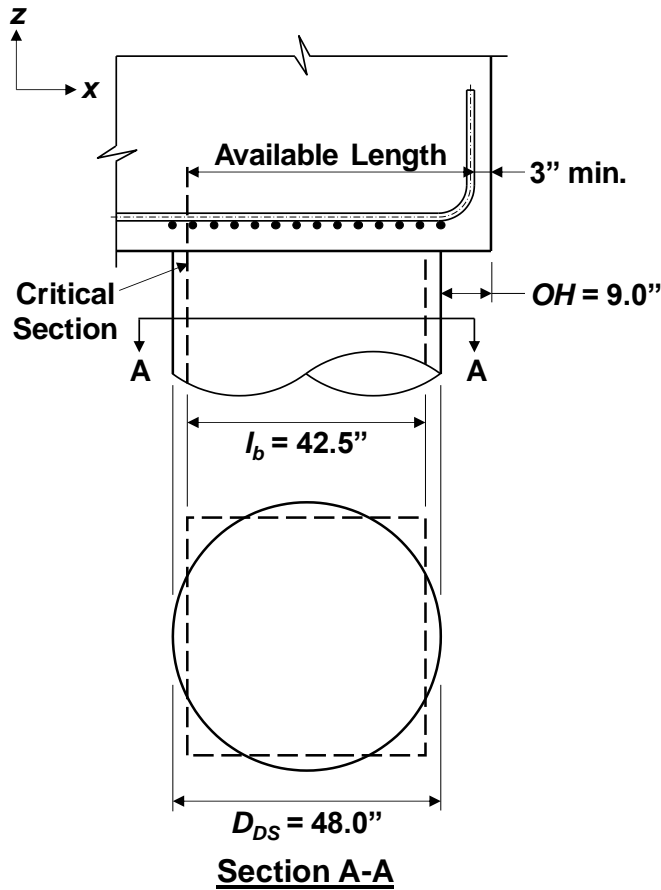


Figure 8.14: Anchorage of bottom mat reinforcement

From Article 5.11.2.1 of AASHTO LRFD (2010), the required development length for straight #11 bars is:

$$l_d = \frac{1.25A_b f_y}{\sqrt{f'_c}} = \frac{1.25(1.56 \text{ in}^2)(60 \text{ ksi})}{\sqrt{3.6 \text{ ksi}}} = 61.7 \text{ in} > 51.3 \text{ in } \mathbf{NG}$$

Since the available length is not adequate for the development of straight bars, 90-degree hooks will be used. From Article 5.11.2.4 of AASHTO LRFD (2010), the development length for a hooked bar is:

$$l_{dh} = \frac{38.0d_b}{\sqrt{f'_c}} \cdot 0.7 = \frac{38.0(1.41 \text{ in})}{\sqrt{3.6 \text{ ksi}}} \cdot 0.7 = 19.8 \text{ in} < 48.5 \text{ in } \mathbf{OK}$$

All reinforcement assumed to carry the forces in Ties EF, FG, GH, and EH will be hooked, as shown in Figures 8.26 and 8.28 of Section 8.6.

Ties BI and CJ

The vertical Ties BI and CJ consist of reinforcing bars extending from the column into the footing (through a lap splice). Standard TxDOT practice specifies the use of 90-degree hooks to anchor the tie bars. As previously calculated, the development length for hooked #11 bars is 19.8 inches. The tie reinforcement should be fully developed at the point where the centroid of the bars exits the extended nodal zones of Nodes I and J. The depth of the extended nodal regions (created by the smearing of Struts AI and DJ at Nodes I and J), however, cannot be defined; both Nodes I and J are smeared nodes with no bearing plates or geometric boundaries to define their geometries. The available development length is therefore unknown (see Figure 8.15). Considering TxDOT’s long-term successful practice of using hooks to anchor column bars within deep footings, 90-degree hooks are specified in the current design. Due to potential load reversal and constructability concerns, hooked anchorage will be provided for all the longitudinal column bars extending into the footing, as shown in the final reinforcement details of Figure 8.25.

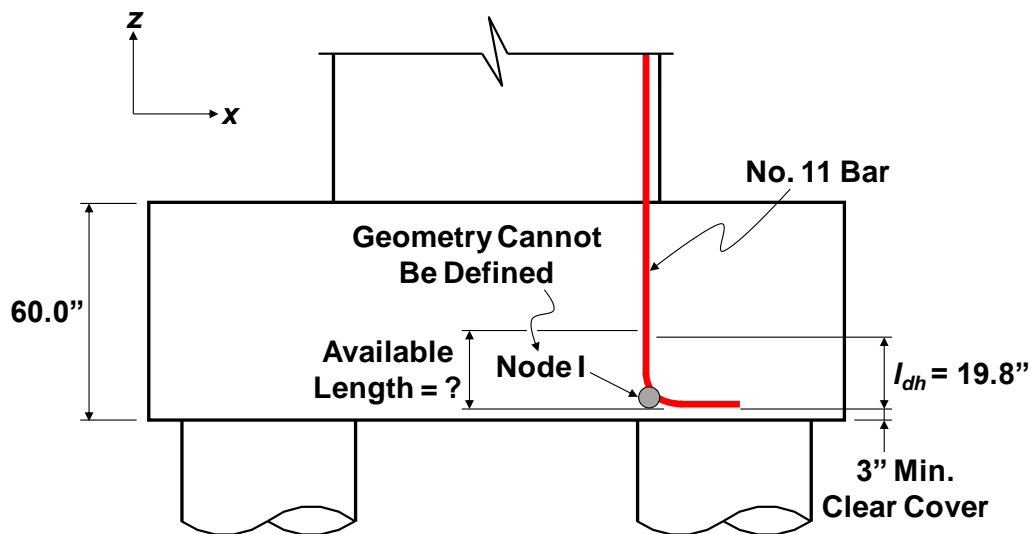


Figure 8.15: Anchorage of vertical ties – unknown available length

8.5 DESIGN CALCULATIONS (SECOND LOAD CASE)

The STM design procedure completed for the first load case is now followed for the second load case. Many of the same techniques previously introduced are used below. Any differences between the designs for the first and second load cases will be highlighted.

8.5.1 Step 1: Determine the Loads

The depiction of the second load case is repeated in Figure 8.16 for convenience. The axial force and moment acting on the column need to be redefined in terms of an equivalent force system that will be applied to the STM. The process is analogous to that outlined for the first load case in Section 8.4.1.

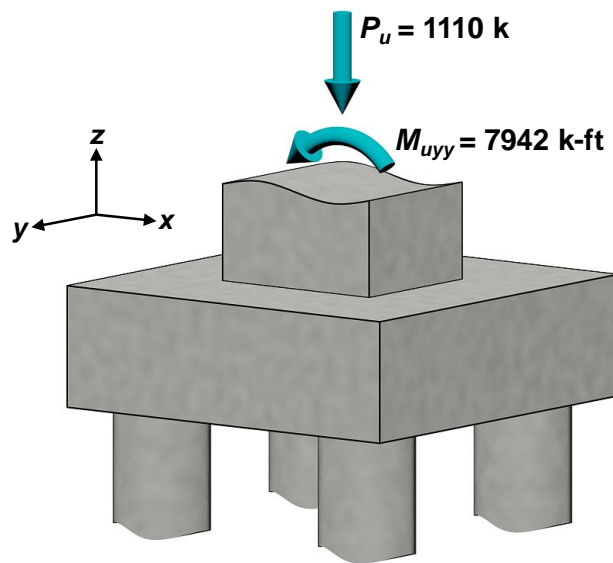


Figure 8.16: Factored load and moment of the second load case

The linear stress distribution resulting from application of the factored axial force and moment is shown in Figure 8.17. The equivalent force system once again consists of four vertical forces (two compressive and two tensile) which correspond to the four reactions at the drilled shafts. The compressive (downward) forces act at the compressive stress resultant of the linear stress diagram. More specifically, the compressive forces act at a distance of 1.47 feet from the left face of the column and one-quarter of the column

$$\begin{cases} F_{Comp} - F_{Tens} = P_u = 1110 \text{ kip} \\ F_{Comp} \left(\frac{7.50 \text{ ft}}{2} - 1.47 \text{ ft} \right) + F_{Tens} \left(\frac{7.50 \text{ ft}}{2} - 0.30 \text{ ft} \right) = M_{uyy} = 7942 \text{ k-ft} \end{cases}$$

$$\text{Solving: } F_{Comp} = 2053.5 \text{ kip} \quad F_{Tens} = 943.5 \text{ kip}$$

Within the equations, F_{Comp} is the sum of the two compressive forces acting at points A and D and F_{Tens} is the sum of the tensile forces acting at points B and C. The four loads acting on the STM are then determined as follows:

$$F_A = F_D = \frac{F_{Comp}}{2} = 1026.8 \text{ kip (Compression)}$$

$$F_B = F_C = \frac{F_{Tens}}{2} = 471.8 \text{ kip (Tension)}$$

These forces are shown acting on the STM of Figure 8.19.

8.5.2 Step 2: Analyze Structural Component

The drilled-shaft reaction forces are calculated next. The reactions are assumed to act at the center of the 4-foot diameter shafts (Figure 8.18) and are obtained from overall equilibrium of the drilled-shaft footing under the applied loads.

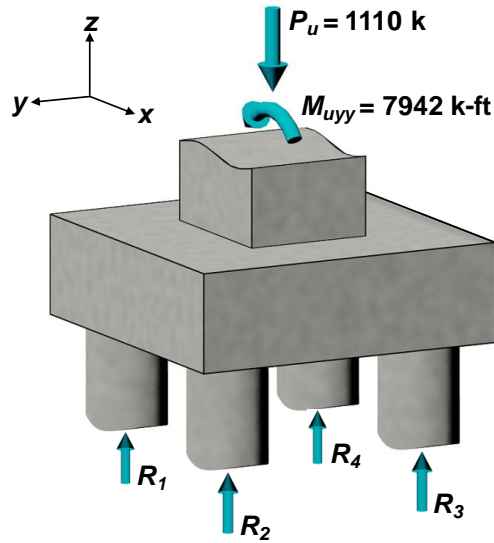


Figure 8.18: Applied loading and drilled-shaft reactions (second load case)

$$R_1 = R_4 = \frac{P_u}{4} + \frac{1}{2} \left(\frac{M_{uyy}}{s_{DS}} \right) = \frac{1110 \text{ kip}}{4} + \frac{1}{2} \left(\frac{7942 \text{ k-ft}}{10.50 \text{ ft}} \right) = 655.7 \text{ kip (Compression)}$$

$$R_2 = R_3 = \frac{P_u}{4} - \frac{1}{2} \left(\frac{M_{uyy}}{s_{DS}} \right) = \frac{1110 \text{ kip}}{4} - \frac{1}{2} \left(\frac{7942 \text{ k-ft}}{10.50 \text{ ft}} \right) = -100.7 \text{ kip (Tension)}$$

The four reactions are shown acting on the STM of Figure 8.19. It is important to note that two of the four drilled shafts are put into tension under the application of the design loads. For this reason, the final STM corresponding to the second load case is significantly different from that of the first load case.

8.5.3 Step 3: Develop Strut-and-Tie Model

The STM corresponding to the second load case is shown in Figure 8.19. Development of the STM for this unique load case is based on the same methodology described in Section 8.4.3.

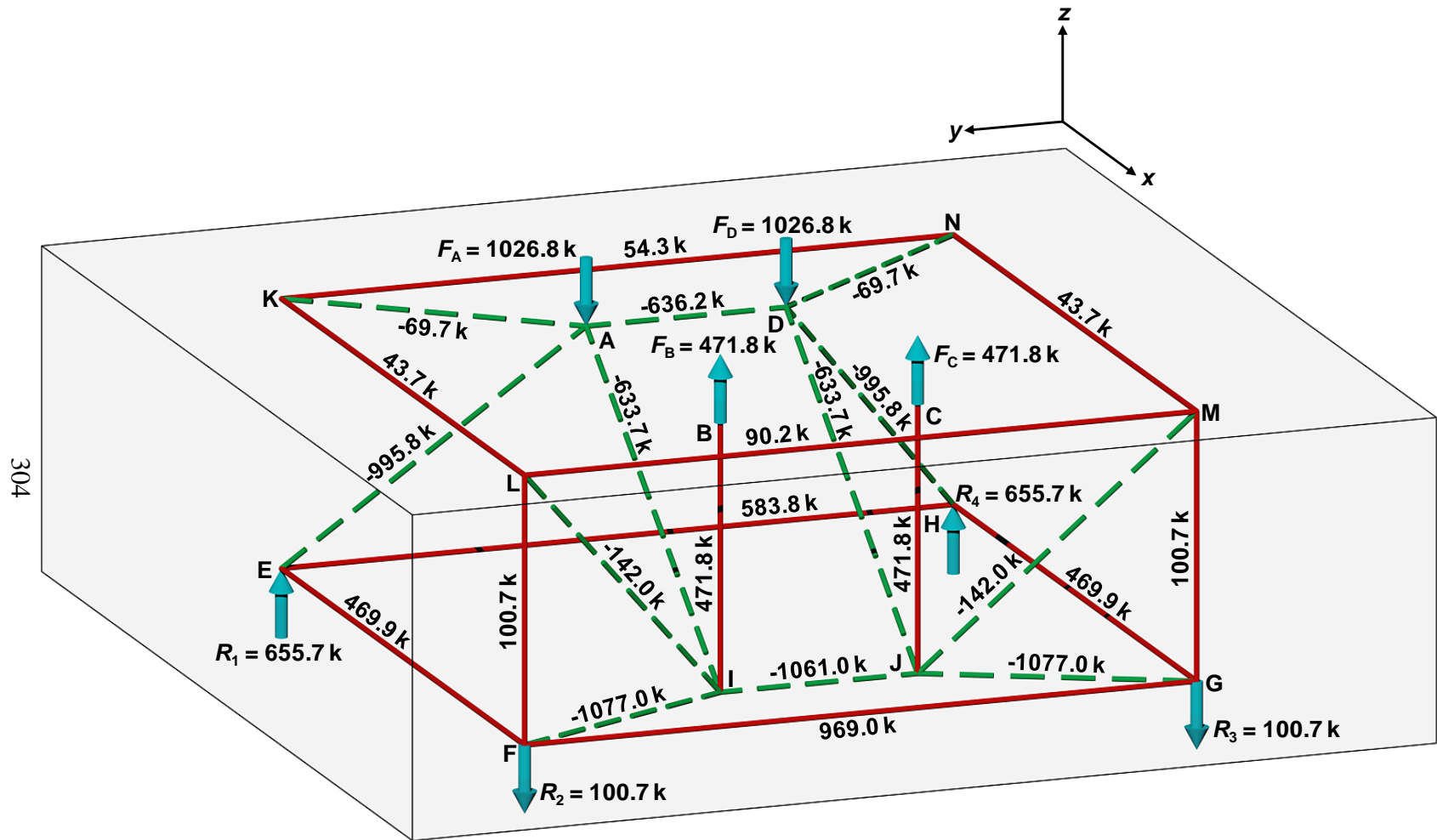


Figure 8.19: Strut-and-tie model for the drilled-shaft footing – axonometric view (second load case)

Prior to placement of the individual struts and ties, the vertical position of the upper and lower nodes of the STM should be determined. The lower ties of the STM (Ties EF, FG, GH, and EH) coincide with the bottom mat reinforcement. The distance from the bottom surface of the footing to the centroid of the bottom mat (including both orthogonal layers of reinforcement) is the same as that determined for the first load case: 5.4 inches. In addition, a set of horizontal ties (Ties KL, LM, MN, and KN) will be needed near the top surface of the footing to represent the tension generated by the large overturning moment. The fact that two of the drilled shafts are in tension indicate the need for these ties and corresponding top mat reinforcement, as explained below. The top horizontal ties of the STM should correspond to the centroid of the top mat reinforcement that the ties represent. The top mat will consist of two orthogonal layers of #7 bars. An equal number of bars will be used within each layer and a clear cover of 4 inches measured from the top surface of the footing will be provided. Referring to Figure 8.20, the centroid of the top mat will be located $4 \text{ in.} + 0.875 \text{ in.} = 4.9 \text{ in.}$ below the top surface of the footing. The total height of the STM is therefore $60.0 \text{ in.} - 5.4 \text{ in.} - 4.9 \text{ in.} = 49.7 \text{ in.}$

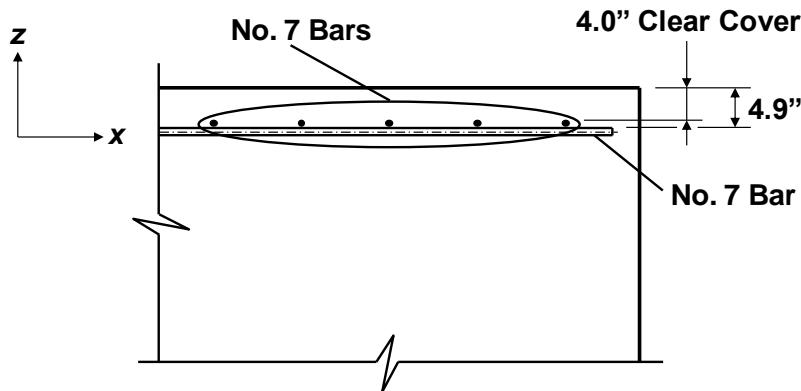


Figure 8.20: Determining the location of the top horizontal ties of the STM (second load case)

Further development of the STM should trace the most intuitive load path, and equilibrium should be established at each node along the way. The tensile forces acting at Nodes B and C again require vertical Ties BI and CJ to transfer loads through the

footing depth. Similarly, two additional vertical ties (Ties FL and GM) are needed to resist the tensile reaction forces of the two drilled shafts at Nodes F and G. In other words, Ties FL and GM are required to properly anchor the shafts to the footing. Considering Figure 8.19, Ties BI and FL together resemble a non-contact lap splice. Compressive stresses will therefore develop between Nodes I and L, idealized as the diagonal Strut IL. The forces in Ties CJ and GM similarly require a strut to transfer force between Nodes J and M. Vertical equilibrium at Node I and J will be satisfied by compressive stresses originating at Nodes A and D, represented by Struts AI and DJ. Compressive stresses from the forces imposed at Nodes A and D will also flow to the nearest supports at Node E and H; these load paths are idealized as Struts AE and DH. These two struts satisfy vertical equilibrium at Node E and H. Due to these compressive stresses flowing diagonally to the drilled shafts, tensile stresses develop across the bottom of the footing. These stresses are carried by Ties EF, FG, GH, and EH. In a similar manner, the diagonal Struts IL and JM connecting the vertical ties induce tension at the top of footing; this requires the addition of Ties KL, LM, MN, and KN. Please note that Nodes K and N are located directly above the drilled shaft reactions at Nodes E and H. The remaining horizontal struts near both the top and bottom of the footing are added to satisfy equilibrium at Nodes A and D and Nodes I and J, respectively. Again, the strut-and-tie model is ensured to comply with the 25-degree rule regarding the angle between a strut and a tie entering the same node.

The STM is analyzed in the same manner as the STM for the first load case. A linear elastic analysis of the model should result in the same reaction forces as those determined in Section 8.5.2. A trial-and-error approach may be necessary to develop an STM that satisfies equilibrium at each node and best models the elastic flow of forces through the footing. An analysis of the truss model results in the member forces shown in Figure 8.19.

8.5.4 Step 4: Proportion Ties

Forces within the STMs of the first and second load cases (Figures 8.8 and 8.19, respectively) should be compared to identify the controlled design scenarios. The bottom tie forces (Ties EF, FG, GH, and EH) within the first load case control, and the design of those ties will not be revisited. In contrast, the vertical tie forces (Ties BI and CJ) of the second load case are most critical; a redesign is presented below. The remaining ties within the STM are unique to the second load case (Ties FL, GM, KL, LM, MN, and KN); reinforcement should be provided to carry the forces in these ties.

The top mat reinforcement will be proportioned first. Comparing the four ties along the top of the STM, Tie LM carries the largest force and is considered below.

Tie LM

Using #7 bars for the top mat of steel, the reinforcement requirement for Tie LM is:

$$\begin{aligned} \text{Factored Load:} & \quad F_u = 90.2 \text{ kip} \\ \text{Tie Capacity:} & \quad \varphi \cdot f_y \cdot A_{st} = F_u \\ & \quad (0.9)(60 \text{ ksi})A_{st} = 90.2 \text{ kip} \\ & \quad A_{st} = 1.67 \text{ in}^2 \end{aligned}$$

$$\text{Number of \#7 bars required: } 1.67 \text{ in}^2 / 0.60 \text{ in}^2 = 2.8 \text{ bars}$$

Use 3 - #7 bars

The shrinkage and temperature reinforcement defined in Section 8.4.6 is capable of carrying the force in Tie LM. The bars considered to be included in these ties are those located directly above the drilled shafts. At a spacing of about 11 inches, 4-#7 bars are located above each shaft (refer to Figure 8.21). The number of bars available to carry the tension in Tie LM exceeds the reinforcement requirements; use of the shrinkage and temperature reinforcement is sufficient.

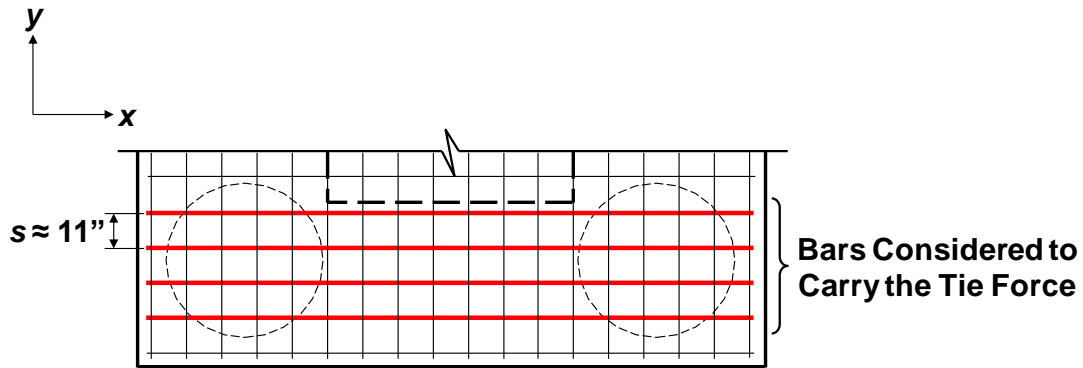


Figure 8.21: Shrinkage and temperature reinforcement considered to carry the tie force

Considering that Tie LM carries the largest force compared to the other horizontal ties along the top of the STM, the required shrinkage and temperature reinforcement is also adequate to carry the forces in the remaining horizontal ties (Ties KL, MN, and KN).

Ties BI and CJ

Next, the reinforcement requirement for the ties extending from the tension face of the column (Ties BI and CJ) is revisited; the tie forces of the second load case supersede those of the first load case. Considering the force in either Tie BI or CJ, the required number of bars is:

Factored Load:	$F_u = 471.8 \text{ kip}$
Tie Capacity:	$\phi \cdot f_y \cdot A_{st} = F_u$
	$(0.9)(60 \text{ ksi})A_{st} = 471.8 \text{ kip}$
	$A_{st} = 8.74 \text{ in}^2$

Number of #11 bars required: $8.74 \text{ in}^2 / 1.56 \text{ in}^2 = 5.6 \text{ bars}$

Use 6 - #11 bars (6 - #11 bars are provided)

When extended into the footing, the longitudinal reinforcement specified within the column is adequate to carry the forces in Ties BI and CJ.

Ties FL and GM

Lastly, the reinforcement requirements for Ties FL and GM are defined. These ties represent the bars which anchor the drilled shafts to the footing. The assumed layout of the longitudinal reinforcement within the drilled shafts (typical of standard construction) is shown in Figure 8.22.

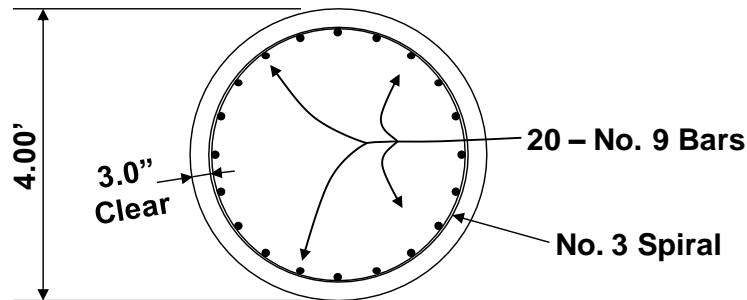


Figure 8.22: Assumed reinforcement layout of the drilled shafts

Drilled shafts commonly feature #9 bars as longitudinal reinforcement. The longitudinal reinforcement of the drilled shafts at Nodes F and G will be extended into the footing to satisfy the requirements of Ties FL and GM. The reinforcement requirement is determined as follows:

$$\begin{aligned} \text{Factored Load:} & F_u = 100.7 \text{ kip} \\ \text{Tie Capacity:} & \varphi \cdot f_y \cdot A_{st} = F_u \\ & (0.9)(60 \text{ ksi})A_{st} = 100.7 \text{ kip} \\ & A_{st} = 1.86 \text{ in}^2 \end{aligned}$$

$$\text{Number of \#9 bars required: } 1.86 \text{ in}^2 / 1.00 \text{ in}^2 = 1.9 \text{ bars}$$

Use 2 - #9 bars

All of the longitudinal bars within the drilled shafts will be extended into the footing. However, the longitudinal reinforcement must be properly anchored at Nodes L and M in order to credibly contribute to the resistance of the tensile forces of Ties FL and GM. A minimum of 2-#9 bars will therefore be anchored at Nodes L and M; refer to Section 8.5.7 for further details.

8.5.5 Step 5: Perform Strength Checks

Due to the complicated and largely unknown nodal geometries within a three-dimensional STM, a simplified nodal strength check procedure was introduced in Section 8.4.5. The proposed procedure ensures all nodes within the STM have sufficient strength by limiting the bearing stress to a conservative level. Comparing the STMs of the first and second load cases (Figures 8.8 and 8.19), the compressive forces bearing on the footing are greater for the first load case. Therefore, the bearing strength checks for the second load case do not govern the design, and no further strength checks are required.

8.5.6 Step 6: Proportion Shrinkage and Temperature Reinforcement

The necessary shrinkage and temperature reinforcement for the footing was specified in Section 8.4.6.

8.5.7 Step 7: Provide Necessary Anchorage for Ties

Proper anchorage of the bottom mat reinforcement (Ties EF, FG, GH, and EH) and the vertical Ties BI and CJ was discussed in Section 8.4.7. These ties are properly anchored with the use of 90-degree hooks. Anchorage of the ties unique to the STM of the second load case (Figure 8.19), the top mat reinforcement (Ties KL, LM, MN, and KN) as well as the vertical Ties FL and GM, is detailed below.

Ties KL, LM, MN, and KN

The horizontal ties along the top of the STM must be properly anchored at Nodes K, L, M, and N. These four nodes are smeared nodes with no boundaries that clearly define their geometries. The diagonal struts (Struts AK, DN, IL, and JM) that connect at the four nodes will create large extended nodal zones. At each node, the tie reinforcement must be fully developed at the point where the centroid of the bars exits the extended nodal zone. The critical development section of the tie bars is conservatively assumed to be the same as the critical section for the bottom horizontal ties of the STM: the bars should be developed at the point directly above the interior edge of the equivalent square drilled shafts (refer to Section 8.4.7). The available development

length is therefore the same as the available length of the ties along the bottom of the STM, or 51.3 inches (see Figure 8.23).

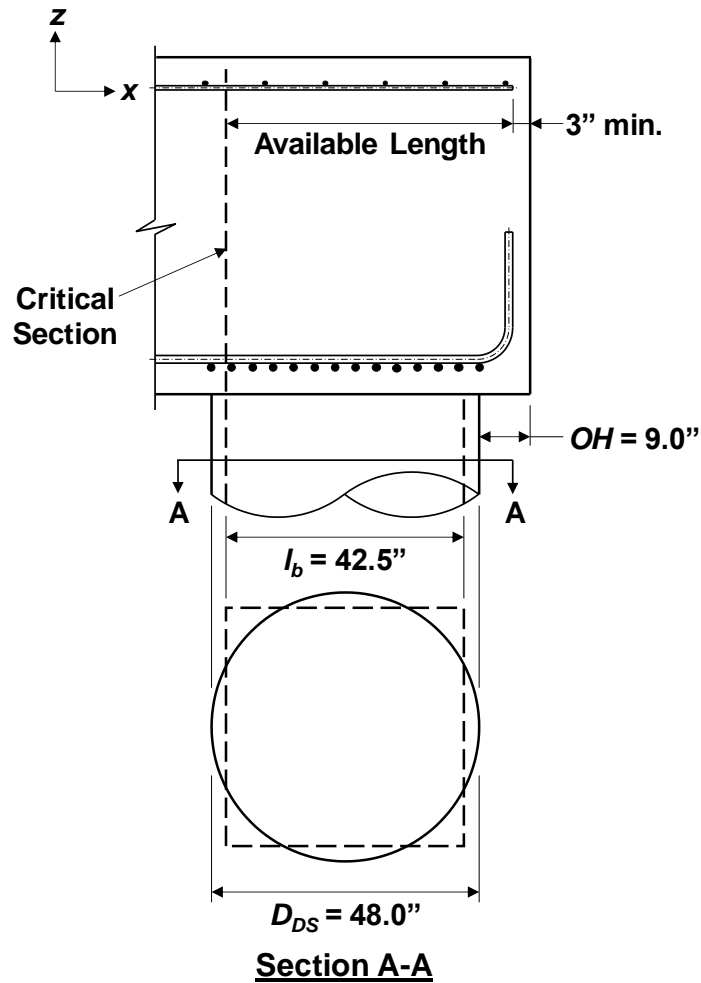


Figure 8.23: Anchorage of top mat reinforcement

The required development length for straight #7 bars is:

$$l_d = \frac{1.25A_b f_y}{\sqrt{f'_c}} \cdot 1.4 \cdot 0.8 = \frac{1.25(0.60 \text{ in}^2)(60 \text{ ksi})}{\sqrt{3.6 \text{ ksi}}} \cdot 1.4 \cdot 0.8 = 26.6 \text{ in} < 51.3 \text{ in } \mathbf{OK}$$

Therefore, proper anchorage is provided if the bars are extended to the end of the footing leaving 3 inches of clear cover.

Ties FL and GM

Ties FL and GM must be properly anchored at Nodes L and M. Please recall that Ties FL and GM each require two #9 bars to carry the tensile forces (refer to Section 8.5.4). At least two bars extending into the footing from each drilled shaft should therefore be properly anchored at Nodes L and M.

Considering TxDOT design practice, the tie bars will be anchored by using 180-hooks. The required development length of the #9 bars is:

$$l_{dh} = \frac{38.0d_b}{\sqrt{f'_c}} \cdot 0.7 = \frac{38.0(1.128 \text{ in})}{\sqrt{3.6 \text{ ksi}}} \cdot 0.7 = 15.8 \text{ in}$$

Similar to Nodes I and J, Node L and M are smeared nodes, and the available development length for Ties FL and GM cannot be determined. Considering the success of past TxDOT designs, the tie bars will be anchored at Nodes L and M by using 180-hooks. Four of the 20-#9 bars extending into the footing from each drilled-shaft will be anchored at the nodes, as shown in Figure 8.24. The bars of all four drilled shafts will be anchored in this manner in consideration of potential load reversal and constructability concerns.

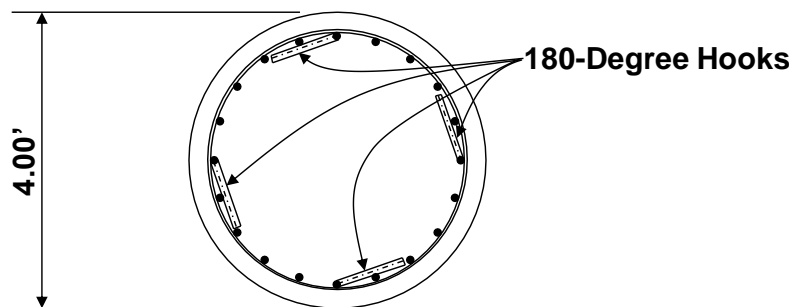


Figure 8.24: Anchorage of Ties FL and GM (drilled-shaft reinforcement)

8.6 REINFORCEMENT LAYOUT

The reinforcement details developed for the two load cases are shown in Figures 8.25 through 8.31. The reinforcement details are presented in seven unique views for the sake of clarity.

Anchorage details of the vertical ties within the STMs are presented in Figure 8.25. Hooked bars are provided to anchor the drilled-shaft and column reinforcement. Elevation views of the footing are provided in Figures 8.26 and 8.27. The main reinforcement within the footing is shown in Figure 8.26, while the required shrinkage and temperature reinforcement are depicted in Figure 8.27. These figures do not include the drilled-shaft reinforcement other than the hooked bars comprising the vertical ties that anchor the shafts. Section A-A denoted in Figures 8.26 and 8.27 is presented in Figures 8.28 and 8.29 and reveal the layout of the main reinforcement and the shrinkage and temperature reinforcement, respectively. Finally, plan views of the footing are shown in Figures 8.30 and 8.31. The top mat reinforcement within the footing is illustrated in Figure 8.30, and the bottom mat reinforcement is depicted in Figure 8.31.

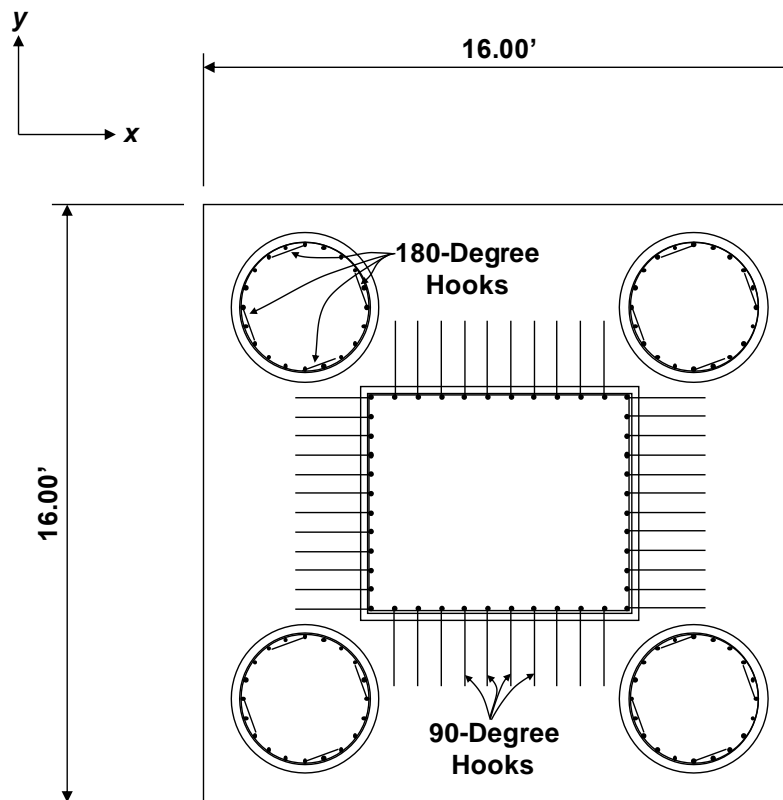


Figure 8.25: Reinforcement details – anchorage of vertical ties

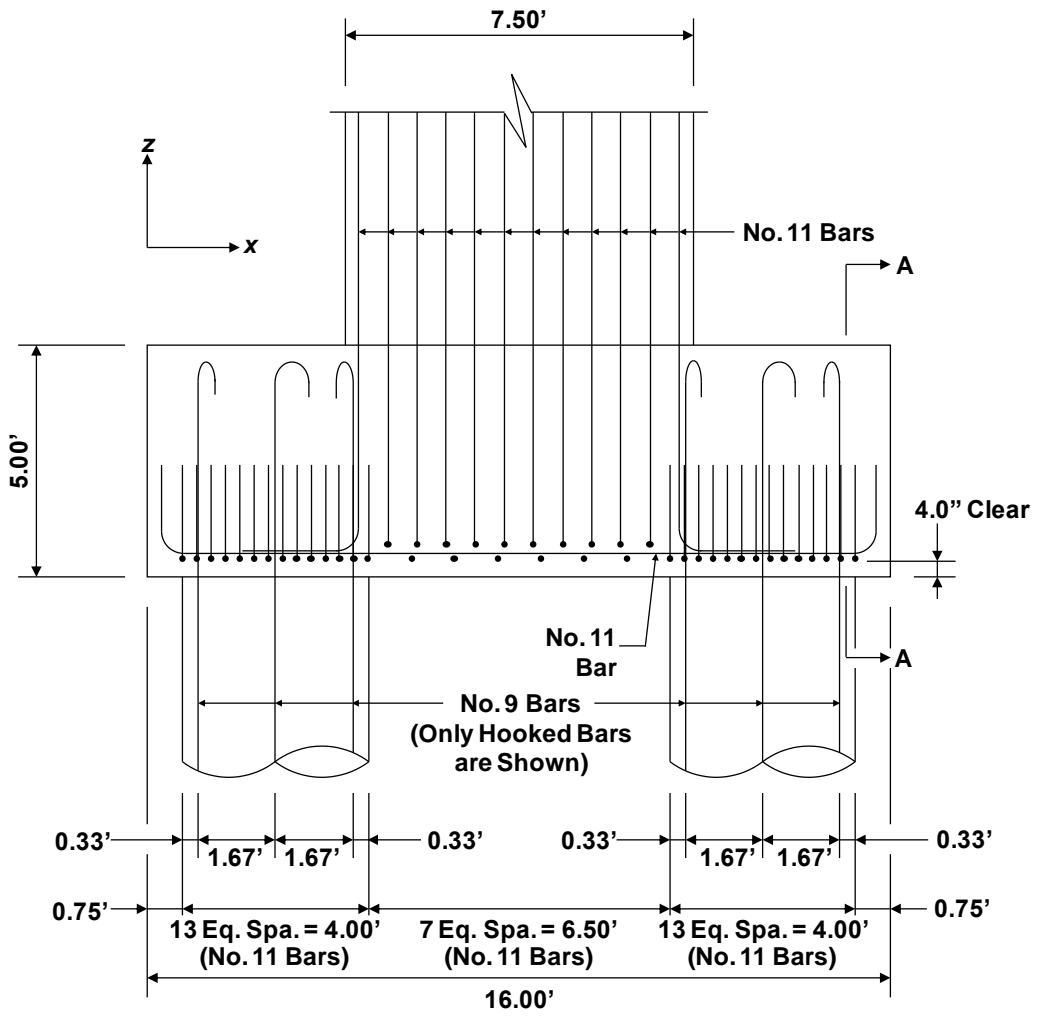


Figure 8.26: Reinforcement details – elevation view (main reinforcement)

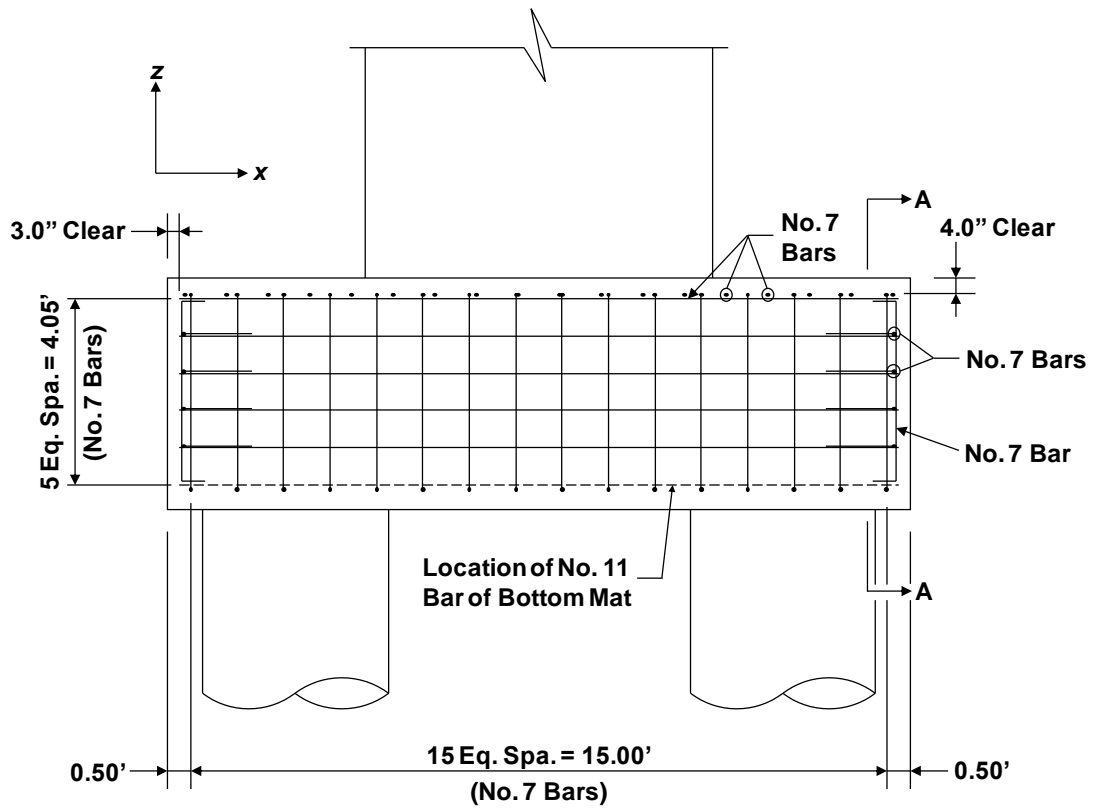


Figure 8.27: Reinforcement details – elevation view (shrinkage and temperature reinforcement)

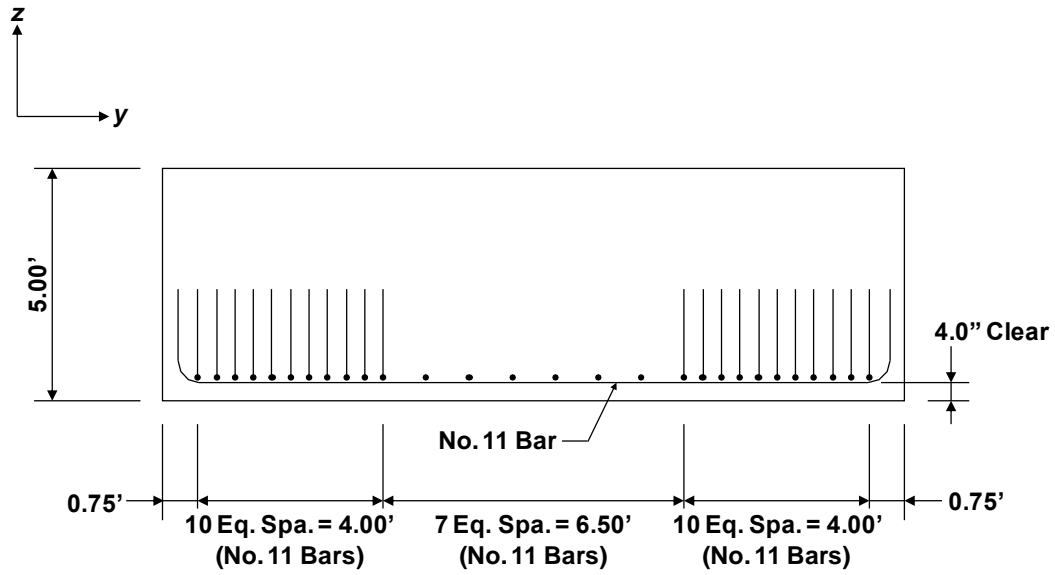


Figure 8.28: Reinforcement details – Section A-A (main reinforcement)

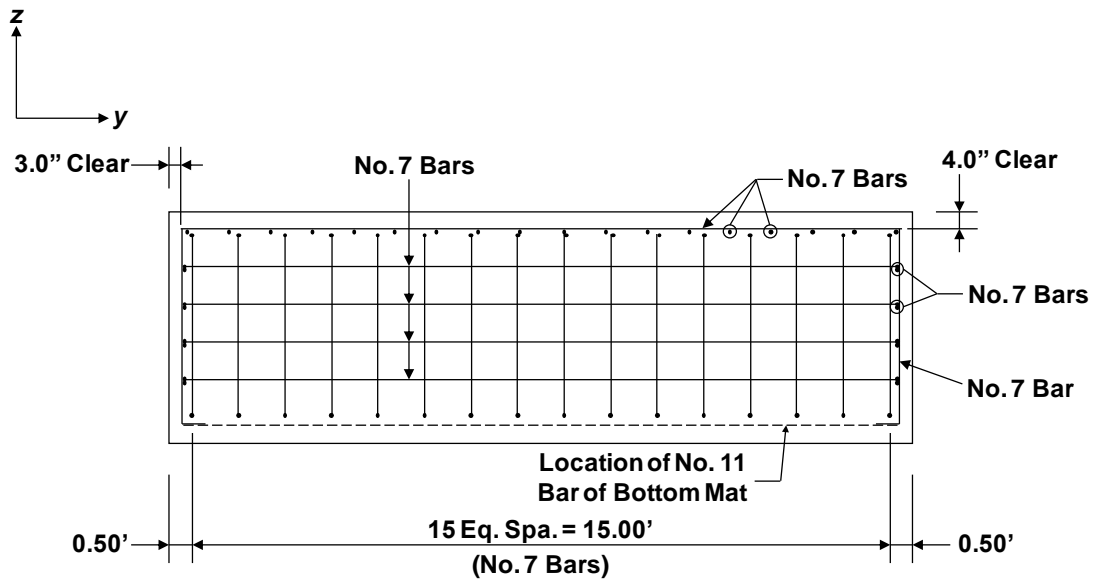


Figure 8.29: Reinforcement details – Section A-A (shrinkage and temperature reinforcement)

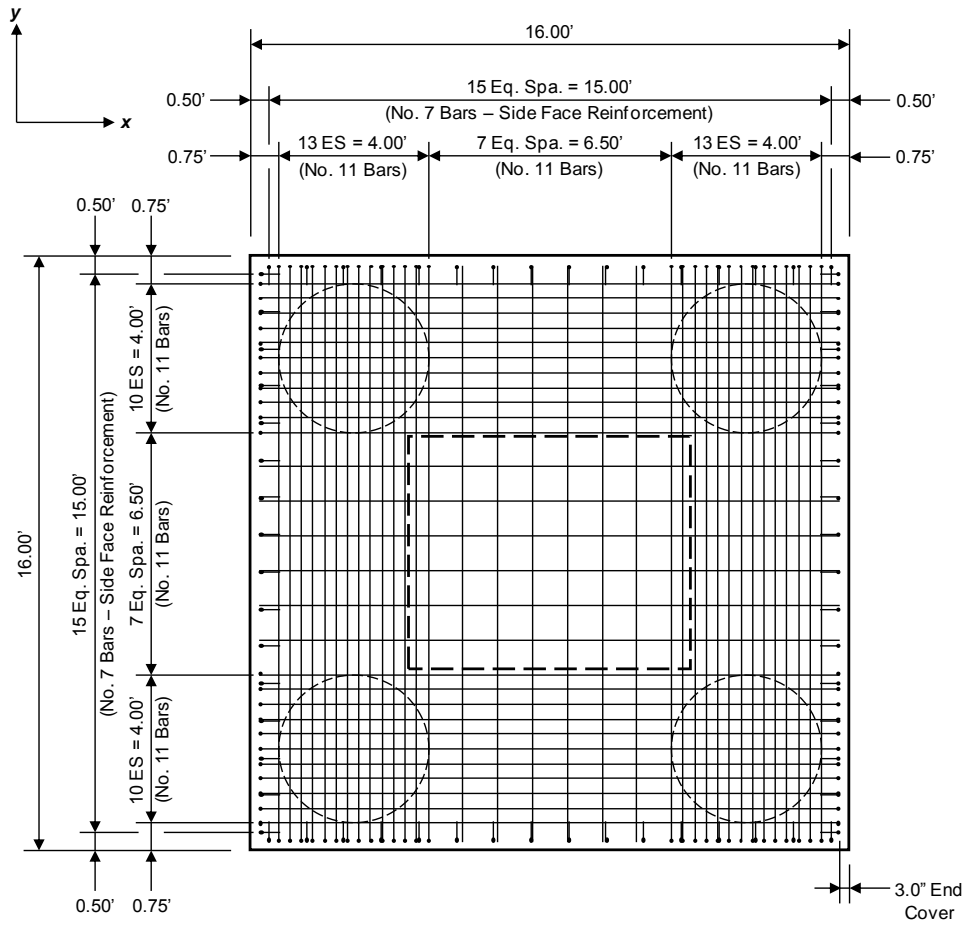


Figure 8.30: Reinforcement details – plan view (bottom mat reinforcement)

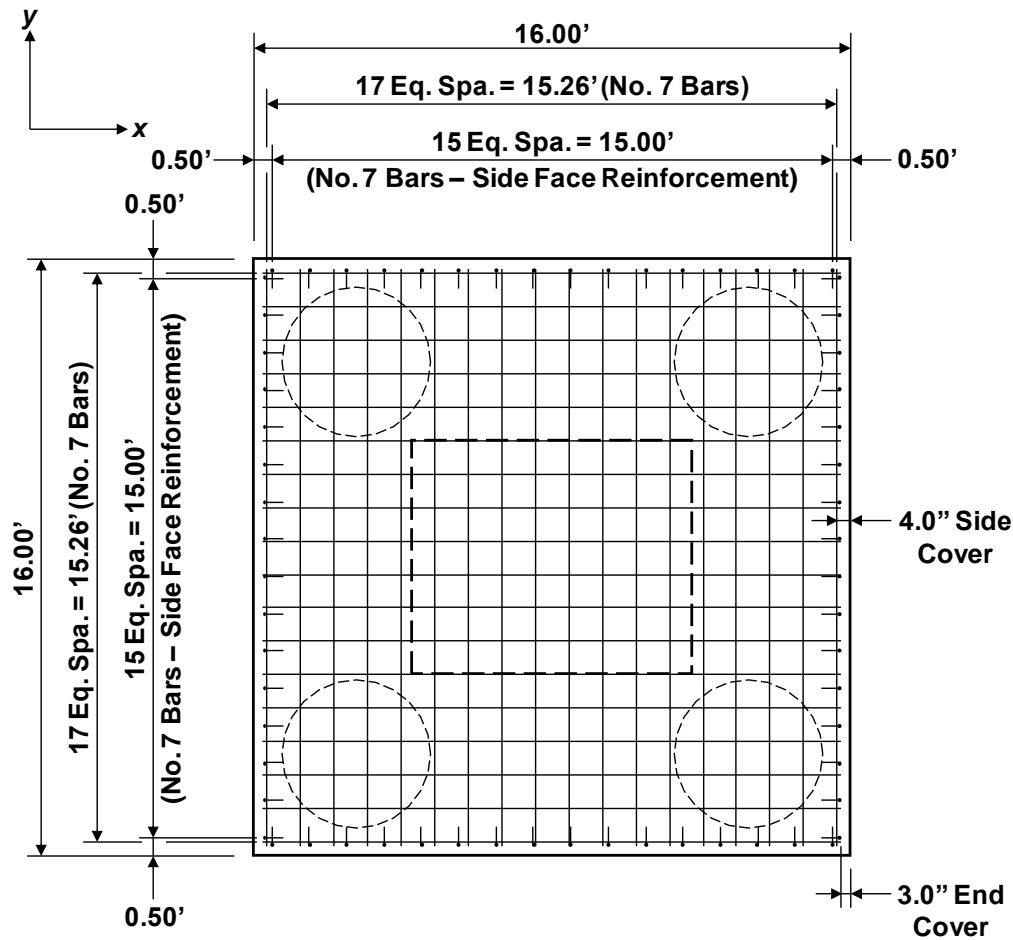


Figure 8.31: Reinforcement details – plan view (top mat reinforcement)

8.7 SUMMARY

The design of a drilled-shaft footing was completed in accordance with the strut-and-tie model design specifications of Chapter 3. Conservative design assumptions were made when necessary on the basis of literature reviews. Two load cases were considered, one resulting in all the drilled shafts being in compression and the other causing two of the drilled shafts to be in tension. The defining features and challenges of this design example are listed below:

- Defining an equivalent force system that produces the same effect as the axial load and moment applied to the column

- Developing three-dimensional STMs to idealize the complex flow of forces through a deep footing
- Determining the location of the nodes along the top of the three-dimensional STMs
- Developing a conservative strength check procedure (based on bearing stress limits) that forgoes determination of three-dimensional nodal geometries
- Defining critical sections for development of tie bars within the three-dimensional geometry of the footing

Chapter 9. Summary and Concluding Remarks

9.1 SUMMARY

Strut-and-tie modeling is an invaluable tool for the design of D-regions within reinforced concrete bridge components. It is a versatile method with applications ranging from the design of a simple five-column continuous bent cap (Example 1) to the detailing of a very complex (three-dimensional) drilled-shaft footing (Example 4). As presented within this guidebook, implementation of the proposed strut-and-tie modeling specifications is simpler and more accurate than application of the STM provisions of the current and previous versions of the *AASHTO LRFD Bridge Design Specifications*. The guidelines and design examples contained within this document are intended to aid in the practical application and widespread use of strut-and-tie modeling in reinforced concrete bridge design.

To familiarize designers with the STM design process, the theoretical background of strut-and-tie modeling was presented alongside an outline of common design tasks in Chapter 2. Strut-and-tie modeling specifications developed over the course of TxDOT Project 0-5253 (D-Region Strength and Serviceability Design) and the current implementation project (TxDOT Project 5-5253-01: Strut-and-Tie Model Design Examples for Bridges) were subsequently presented in Chapter 3. Within Chapters 4 through 8, five STM design examples were presented to demonstrate the use of the new specifications. The unique features of each design example are briefly described here:

- Example 1: Five-Column Bent Cap of a Skewed Bridge (Chapter 4) – This design example served as an introduction to the application of strut-and-tie modeling. Challenges were introduced by the bridge’s skew and complicated loading pattern. These issues were resolved, and a simple, realistic strut-and-tie model was developed. A clear procedure for defining relatively complicated nodal geometries was also presented.

- Example 2: Cantilever Bent Cap (Chapter 5) – An STM was developed to model the flow of forces around a frame corner subjected to closing loads. This was accomplished, in part, through the design of a curved-bar node at the outside of the frame corner. The curved-bar node recommendations, included within the STM specifications of Chapter 3, were used for proper detailing of the bend region within the frame corner reinforcement.
- Example 3a: Inverted-T Straddle Bent Cap (Moment Frame) (Chapter 6) – The inverted-T bent cap was modeled as a component within a moment frame. Moment transfer between the bent cap and the supporting columns was enforced through proper development of the global STM. Bottom-chord (ledge) loading of the inverted-T bent cap also required the use of local STMs to model the flow of forces through the bent cap cross section. Ledge and hanger reinforcement were proportioned on the basis of local STMs and a global STM, respectively.
- Example 3b: Inverted-T Straddle Bent Cap (Simply Supported) (Chapter 7) – The inverted-T bent cap introduced in Example 3a was designed as a simply supported member. The reinforcement layouts for both the moment frame case and the simply supported case were compared to illustrate the influence of boundary condition assumptions.
- Example 4: Drilled-Shaft Footing (Chapter 8) – A three-dimensional STM was developed to properly model the flow of forces through a deep drilled-shaft footing. Two unique load cases were considered. Brief literature reviews were conducted during the course of the example in an attempt to minimize design uncertainties and maximize design efficiency. Due to the unique nature of the STM application and a lack of guidance in the literature, it was necessary to make a number of conservative design assumptions.

These design examples are intended to assist bridge engineers with the implementation of the proposed STM specifications. Application of the STM methods

presented here can and should be extended to design scenarios that may exist outside the scope of this document.

9.2 CONCLUDING REMARKS

Numerous recommendations and tips for implementation of the STM specifications were offered within the design examples of Chapters 4 through 8. The nine fundamental steps of the STM procedure (refer back to Chapter 2) are summarized below for the benefit of the designer.

1. Separate B- and D- regions:
 - The interface between a D-region and a B-region is assumed to be located one member depth away from a load or geometric discontinuity. A linear distribution of strains can be assumed at this interface. See Examples 2, 3a, and 4.
2. Define load case:
 - In order to develop a reasonable STM, loads that act in very close proximity to one another may need to be resolved. See Examples 1 and 2.
 - For accuracy, the self-weight of the structural component should be distributed among the nodes of the STM. See Examples 1, 2, 3a, and 3b.
3. Analyze structural component:
 - At the interface between a D-region and a B-region, the internal force and moment should be converted into an equivalent force system that can be applied to the STM. Moments cannot be applied to the truss model at the D-region/B-region interface. See Examples 2, 3a, and 4.
 - At a D-region/B-region interface, the tie along the tension face of the member as well as the tensile force of the equivalent force system should coincide with the centroid of the corresponding reinforcement. See Examples 2, 3a, and 4.

4. Develop strut-and-tie model:
 - The STM must satisfy internal equilibrium (at each node) and external equilibrium (with all reaction and boundary forces). See all examples.
 - The STM featuring the fewest and shortest ties is typically the most efficient and realistic model for the particular structural component and load case under consideration. See Examples 1, 2, 3a, and 3b.
 - The angle between a strut and tie entering the same node must not be less than 25 degrees. See all examples.
5. Proportion ties:
 - The longitudinal ties of the STM should coincide with the centroid of the reinforcing bars carrying the tie force. See all examples.
6. Perform nodal strength checks:
 - Special attention should be placed on defining the correct geometry of the nodes to ensure accurate strength calculations. See Examples 1, 2, 3a, and 3b.
 - The bond forces from reinforcement anchored at a CCT or CTT nodal region need not be applied as a direct force to the back face of the node. See Examples 1, 2, 3a, and 3b.
7. Proportion crack control reinforcement:
 - The importance of providing the required crack control reinforcement cannot be overemphasized. In addition to minimizing crack widths, this reinforcement aids in the redistribution of stresses within the structural member. See Examples 1, 2, 3a, and 3b.
8. Provide necessary anchorage for ties:
 - The ability of the forces to follow the assumed load paths of the STM is heavily dependent upon proper detailing of the reinforcement. Proper anchorage of the bars at each node cannot be overemphasized. See all examples.

9. Perform shear serviceability check:

- The shear serviceability check estimates the likelihood of diagonal crack formation under the application of service loads. The designer may wish to utilize the shear serviceability check during the preliminary design phase as a means of initially sizing the structural element. See Examples 1, 2, 3a, and 3b.

STM is a powerful design tool when implemented properly. The STM examples address most, but not all, of the most common design challenges. When unique design challenges are encountered, the designer should make reasonable, conservative assumptions, referring to recommendations and research in the literature if necessary.

The current implementation project demonstrated the applicability of the proposed STM specifications to the design of actual bridge components. Review of the design examples should equip engineers with the tools necessary to extend the application of strut-and-tie modeling to all facets of reinforced concrete bridge design.

References

- AASHTO LRFD 2008 *Interim Revisions, Bridge Design Specifications, 4th ed., 2007*. American Association of State Highway and Transportation Officials, Washington, D.C., 2008.
- AASHTO LRFD *Bridge Design Specifications, 5th ed., 2010*. American Association of State Highway and Transportation Officials, Washington, D.C., 2010.
- ACI Committee 318 (2008): *Building Code Requirements for Structural Concrete (ACI 318-08) and Commentary*. American Concrete Institute, Farmington Hills, MI, 2008.
- Adebar, Perry. "Discussion of 'An evaluation of pile cap design methods in accordance with the Canadian design standard'." *Canadian Journal of Civil Engineering* 31.6 (2004): 1123-126.
- Adebar, Perry, Daniel Kuchma, and Michael P. Collins. "Strut-and-Tie Models for the Design of Pile Caps: An Experimental Study." *ACI Structural Journal* 87.1 (1990): 81-92.
- Adebar, Perry, and Luke (Zongyu) Zhou. "Design of Deep Pile Caps by Strut-and-Tie Models." *ACI Structural Journal* 93.4 (1996): 437-48.
- Ashour, Ashraf, and Keun-Hyeok Yang. "Application of Plasticity Theory to Reinforced Concrete Deep Beams." Proc. of Morley Symposium on Concrete Plasticity and Its Application, University of Cambridge, Cambridge, UK, 23 July 2007, pp. 11-26.
- Bergmeister, K., J. E. Breen, J. O. Jirsa, and M. E. Kreger. *Detailing for Structural Concrete*. Rep. no. 1127-3F. Center for Transportation Research, The University of Texas at Austin, 1993.
- Birrcher, David, Robin Tuchscherer, Matt Huizinga, Oguzhan Bayrak, Sharon Wood, and James Jirsa. *Strength and Serviceability Design of Reinforced Concrete Deep Beams*. Rep. no. 0-5253-1. Center for Transportation Research, The University of Texas at Austin, 2009.
- Bridge Standards*. "Elastomeric Bearing and Bearing Seat Details: Prestr Conc U-Beams." Texas Department of Transportation, July 2006. <<ftp://ftp.dot.state.tx.us/pub/txdot-info/cmd/cserve/standard/bridge/ubstde02.pdf>>.

- Bridge Standards*. “Elastomeric Bearing and Girder End Details: Prestr Concrete I-Girders.” Texas Department of Transportation, June 2007. <ftp://ftp.dot.state.tx.us/pub/txdot-info/cmd/cserve/standard/bridge/igebste1.pdf>.
- Brown, Michael D, Cameron L. Sankovich, Oguzhan Bayrak, James O. Jirsa, John E. Breen, and Sharon L. Wood. *Design for Shear in Reinforced Concrete Using Strut-and-Tie Models*. Rep. no. 0-4371-2. Center for Transportation Research, The University of Texas at Austin, 2006.
- CAC: *Concrete Design Handbook*. 3rd Ed. Ottawa: Cement Association of Canada, 2005.
- Cavers, William, and Gordon A. Fenton. “An evaluation of pile cap design methods in accordance with the Canadian design standard.” *Canadian Journal of Civil Engineering* 31.1 (2004): 109-19.
- Clark, A. P. “Diagonal Tension in Reinforced Concrete Beams.” *ACI Journal* 48.10 (1951): 145-56.
- Collins, M. P., and D. Mitchell. *Prestressed Concrete Structures*. Englewood Cliffs, NJ: Prentice Hall, 1991, 766 pp.
- de Paiva, H. A. R., and C. P. Siess. “Strength and Behavior of Deep Beams in Shear.” *ASCE Journal of the Structural Division* 91.5 (1965): 19-41.
- fib, Practitioners' Guide to Finite Element Modelling of Reinforced Concrete Structures: State-of-art Report*. Lausanne, Switzerland: International Federation for Structural Concrete, 2008, 344 pp.
- fib, Structural Concrete: Textbook on Behaviour, Design and Performance*. Vol. 2. Lausanne, Switzerland: International Federation for Structural Concrete, 1999, 324 pp.
- fib, Structural Concrete: Textbook on Behaviour, Design and Performance*. Vol. 3. Lausanne, Switzerland: International Federation for Structural Concrete, 1999, 292 pp.
- Klein, Gary J. “Curved-Bar Nodes.” *Concrete International* 30.9 (Sept. 2008): 42-47.
- Klein, Gary J. “Example 7: Dapped-end Double-tee Beam with Curved-bar Nodes.” *SP-273 Further Examples for the Design of Structural Concrete with Strut-and-Tie Models*. Ed. Karl-Heinz Reineck and Lawrence C. Novak. Farmington Hills, Michigan: American Concrete Institute, 2011, 288 pp.

- Klein, Gary J. "Example 9: Pile Cap." *SP-208 Examples for the Design of Structural Concrete with Strut-and-Tie Models*. Ed. Karl-Heinz Reineck. Farmington Hills, Michigan: American Concrete Institute, 2002, 250 pp.
- Kong, F. K., P. J. Robins, and D. F. Cole. "Web Reinforcement Effects on Deep Beams." *ACI Journal* 67.12 (1970): 1010-18.
- Kuchma, Daniel, Sukit Yindeesuk, Thomas Nagle, Jason Hart, and Heui Hwang Lee. "Experimental Validation of Strut-and-Tie Method for Complex Regions." *ACI Structural Journal* 105.5 (2008): 578-89.
- Kuchma, D., S. Yindeesuk, and T. Tjhin. "Example 10: Large Propped Cantilever Beam with Opening." *SP-273 Further Examples for the Design of Structural Concrete with Strut-and-Tie Models*. Ed. Karl-Heinz Reineck and Lawrence C. Novak. Farmington Hills, Michigan: American Concrete Institute, 2011, 288 pp.
- Leu, Liang-Jenq, Chang-Wei Huang, Chuin-Shan Chen, and Ying-Po Liao. "Strut-and-Tie Design Methodology for Three-Dimensional Reinforced Concrete Structures." *ASCE Journal of Structural Engineering* 132.6 (2006): 929-38.
- MacGregor, J. G., and J. K. Wight. *Reinforced Concrete: Mechanics and Design*. 4th Ed. Upper Saddle River, NJ: Pearson Prentice Hall, 2005, 1132 pp.
- Martin, T. Barney, and David H. Sanders. *Verification and Implementation of Strut-and-Tie Model in LRFD Bridge Design Specifications*. NCHRP Project 20-07, Task 217, 2007.
- Mitchell, Denis, Michael P. Collins, Shrinivas B. Bhide, and Basile G. Rabbat. *AASHTO LRFD Strut-and-Tie Model Design Examples*. Skokie, Illinois: Portland Cement Association, 2004, 76 pp.
- Moody, K. G., I. M. Viest, R. C. Elstner, and E. Hognestad. "Shear Strength of Reinforced Concrete Beams: Part 1 – Tests of Simple Beams." *ACI Journal* 51.12 (1954): 317-32.
- Park, JungWoong, Daniel Kuchma, and Rafael Souza. "Strength predictions of pile caps by a strut-and-tie model approach." *Canadian Journal of Civil Engineering* 35.12 (2008): 1399-413.
- Paulay, T., and Priestley, M. J. N. *Seismic Design of Reinforced Concrete and Masonry Buildings*. New York: John Wiley and Sons, 1992, 768 pp.

- Rogowsky, D. M., J. G. MacGregor, and S. Y. Ong. "Tests of Reinforced Concrete Deep Beams." *ACI Journal* 83.4 (1986): 614-23.
- Schlaich, Jörg, Kurt Schäfer, and Mattias Jennewein. "Toward a Consistent Design of Structural Concrete." *PCI Journal* 32.3 (1987): 75-150.
- Souza, Rafael, Daniel Kuchma, JungWoong Park, and Túlio Bittencourt. "Adaptable Strut-and-Tie Model for Design and Verification of Four-Pile Caps." *ACI Structural Journal* 106.2 (2009): 142-50.
- Texas Department of Transportation Bridge Design Manual - LRFD*. Revised May 2009. Texas Department of Transportation, 2009. <<http://onlinemanuals.txdot.gov/txdotmanuals/lrf/lrf.pdf>>.
- Thompson, M. K., A. L. Ledesma, J. O. Jirsa, J. E. Breen, and R. E. Klinger. *Anchorage Behavior of Headed Reinforcement, Part A: Lap Splices, Part B: Design Provisions and Summary*. Rep. no. 0-1855-3. Center for Transportation Research, The University of Texas at Austin, 2003a.
- Thompson, M. K., M. J. Young, J. O. Jirsa, J. E. Breen, and R. E. Klinger. *Anchorage of Headed Reinforcement in CCT Nodes*. Rep. no. 0-1855-2. Center for Transportation Research, The University of Texas at Austin, 2003b.
- Tjhin, Tjen N., and Daniel A. Kuchma. "Example 1b: Alternative design for the non-slender beam (deep beam)." *SP-208 Examples for the Design of Structural Concrete with Strut-and-Tie Models*. Ed. Karl-Heinz Reineck. Farmington Hills, Michigan: American Concrete Institute, 2002, 250 pp.
- Widianto, and Oguzhan Bayrak. "Example 11: Deep Pile Cap with Tension Piles." *SP-273 Further Examples for the Design of Structural Concrete with Strut-and-Tie Models*. Ed. Karl-Heinz Reineck and Lawrence C. Novak. Farmington Hills, Michigan: American Concrete Institute, 2011, 288 pp.
- Wight, J.K., and G.J. Parra-Montesinos. "Strut-and-Tie Model for Deep Beam Design: A Practical Exercise Using Appendix A of the 2002 ACI Building Code." *Concrete International* 25.5 (May 2003): 63-70.
- Windisch, Andor, Rafael Souza, Daniel Kuchma, JungWoong Park, and Túlio Bittencourt. Discussion of "Adaptable Strut-and-Tie Model for Design and Verification of Four-Pile Caps." *ACI Structural Journal* 107.1 (2010): 119-20.

Vita

Christopher Scott Williams was born and raised in West Frankfort, Illinois. He graduated from Frankfort Community High School in 2005 and then enrolled at Southern Illinois University Carbondale, receiving a Bachelor of Science in Civil Engineering in May 2009. During the same year, he began his graduate studies at The University of Texas at Austin and became a research assistant at the Phil. M. Ferguson Structural Engineering Laboratory. He earned a Master of Science in Engineering in December 2011 and will continue his studies at The University of Texas at Austin, pursuing a Doctor of Philosophy degree.

Permanent address and email: 8653 Knox Road
West Frankfort, IL 62896
chrisw05@utexas.edu

This thesis was typed by the author.